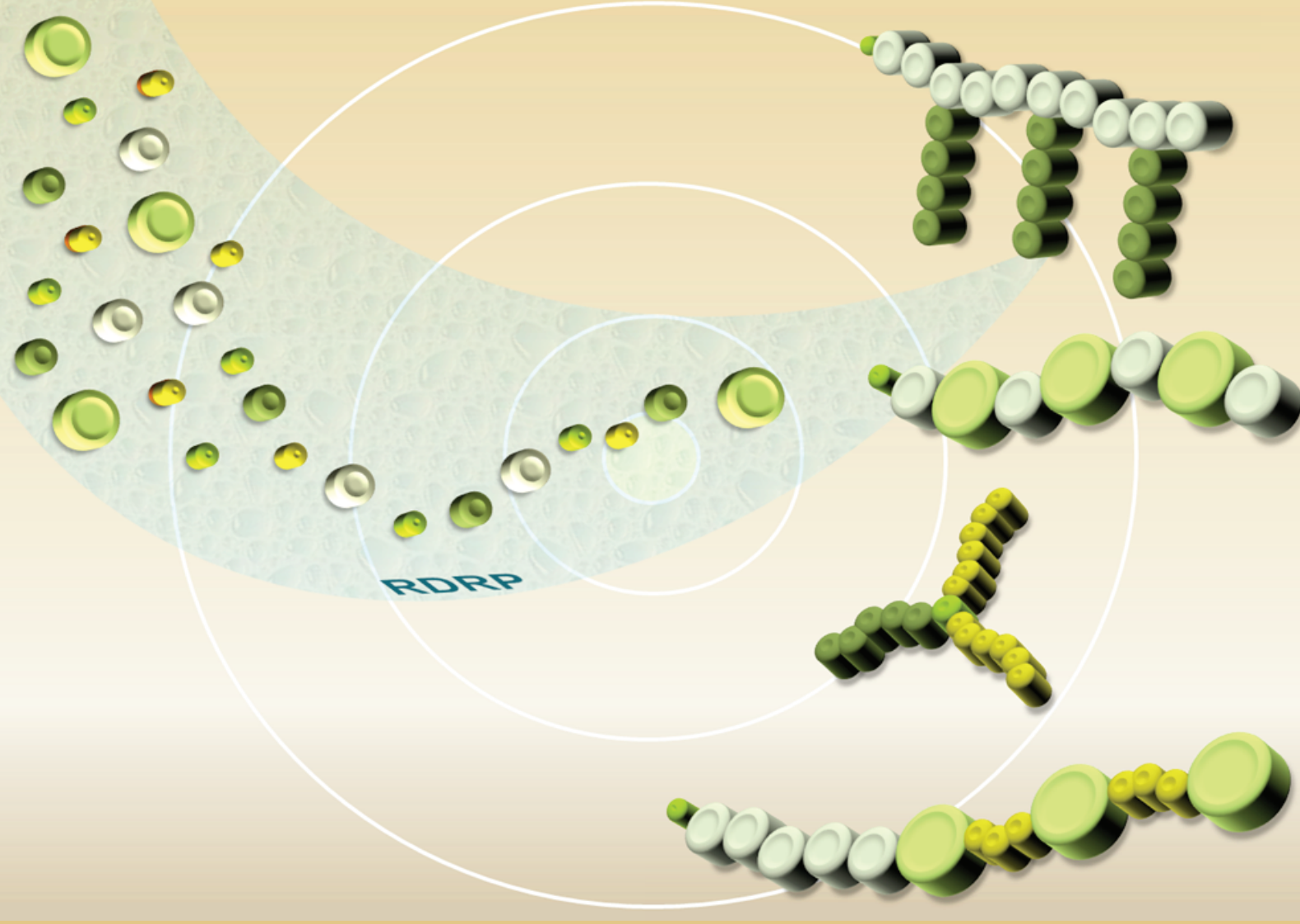

Patrícia Vitorino Mendonça

METAL-CATALYZED REVERSIBLE DEACTIVATION RADICAL POLYMERIZATION: MECHANISTIC STUDIES AND APPLICATION ON THE DESIGN OF POLYMER DRUGS

Tese de doutoramento em Engenharia Química, orientada por Professor Doutor Jorge Fernando Jordão Coelho e Professor Doutor Anatoliy V Popov e apresentada ao Departamento de Engenharia Química/Faculdade de Ciências e Tecnologia da Universidade de Coimbra

Fevereiro de 2015

· U C ·

UNIVERSIDADE DE COIMBRA

Patrícia Vitorino Mendonça

Metal-catalyzed reversible deactivation radical polymerization: mechanistic studies and application on the design of polymer drugs

Thesis submitted to the Faculty of Sciences and Technology of the University of Coimbra, to obtain the Degree of Doctor in Chemical Engineering

Coimbra
2015

UNIVERSIDADE DE COIMBRA

Patrícia Vitorino Mendonça

Metal-catalyzed reversible deactivation radical polymerization: mechanistic studies and application on the design of polymer drugs

Thesis submitted to the Faculty of Sciences and Technology of the University of Coimbra, to obtain the Degree of Doctor in Chemical Engineering

Advisors:

Prof. Dr. Jorge Fernando Jordão Coelho

Prof. Dr. Anatoliy V. Popov

Host institutions

University of Coimbra

University of Pennsylvania

Carnegie Mellon University

Financing

Portuguese Foundation for Science and Technology (FCT)

Doctoral degree grant: SFRH/BD/69152/2010

Coimbra

2015

· U C ·

UNIVERSIDADE DE COIMBRA


POPH
QUALIFICAR É CRESCER.


QREN
QUADRO
DE REFERÊNCIA
ESTRATÉGICO
NACIONAL
PORTUGAL 2007.2013


GOVERNO DA REPÚBLICA
PORTUGUESA


UNIÃO EUROPEIA
Fundo Social Europeu

Everybody is a genius. But if you judge a fish by its ability to climb a tree, it will live its whole life believing that it is stupid.

Albert Einstein

Acknowledgments

Sinto-me uma felizarda por ter tido o privilégio de estar rodeada de excelentes pessoas que contribuiram de diversas formas para o sucesso deste trabalho de doutoramento e para o meu desenvolvimento pessoal e profissional. Quero fazer um agradecimento especial a todas elas!

Ao Jorge Coelho, meu orientador desde sempre, que me tem vindo a aturar ao longo de todos estes anos e que tem sido um exemplo de dedicação e gosto pelo trabalho que desenvolvemos. Agradeço por nos ter lançado nesta aventura, quando ainda pouco se falava de RDRP no grupo, e por ter acreditado e confiado em mim. Agradeço também toda a ajuda prestada, todo o conhecimento transmitido e o facto de me ter proporcionado duas incríveis experiências nos Estados Unidos. Sem dúvida que contribuiram imenso para o meu desenvolvimento.

Ao Professor Arménio Serra, por estar sempre disposto a ajudar em qualquer situação.

À Professora Maria João Moreno, designada por mim como "uma anjo caído do céu", por ter aparecido na altura exacta, por me ter recebido com enorme simpatia e por ter permitido que parte do Capítulo 8 da tese existisse. Quero agradecer a disponibilidade que demonstrou na deslocação a Espanha para realizar os testes de ITC, o interesse pelo trabalho, as horas de discussão dos resultados e por ter disponibilizado o seu HPLC.

À Doutora Cláudia Silva e ao Professor Sérgio Simões, da Bluepharma, por me terem dado a oportunidade de colaborar com eles. Obrigada por toda a disponibilidade que tiveram para reunir e pelo interesse demonstrado pelo projecto.

Ao Tamaz Guliashvili, uma mente brilhante, pela simpatia, por todas as discussões de trabalho e por partilhar o seu conhecimento.

Ao Tolya (Anatoliy Popov), por me orientar neste trabalho e por se mostrar sempre interessado. Quero agradecer pela preocupação que teve e pelo apoio que prestou durante o período em que estudei em Filadélfia. Foi, sem dúvida, um segundo pai para mim!

Ao Jim Delikatny, Sean e Mike pela simpatia com que me receberam no seu grupo de investigação. Obrigada por todos os momentos de boa disposição. Jamais irei esquecer as famosas e descontraídas reuniões de grupo!

Ao Professor Krzysztof Matyjaszewski, pela gentileza de me ter recebido no seu grupo de investigação e na sua casa. Foi uma experiência que nunca pensei ser possível e confesso que até me faltam as palavras para conseguir descrever o que sinto. Fico grata por ter tido a oportunidade de aprender com os melhores! O agradecimento extende-se à sua esposa, que é um amor de pessoa, e me fez sentir parte da família!

A todos os membros do grupo do Professor Krzysztof Matyjaszewski, pela simpatia com que me receberam e pelos momentos de diversão proporcionados, que fizeram com que a minha integração fosse muito rápida e fácil. Quero agradecer especialmente ao pessoal do mini grupo de mecanismos, ao Dominik Konkolewicz e ao Saadyah Averick por toda ajuda na discussão do trabalho e pelo interesse demonstrado.

Ao Polymer Research Group, em especial ao pessoal do laboratório B37, pelo bom ambiente de trabalho criado e pelas discussões de resultados durante o nosso duro processo de desenvolvimento de novos sistemas de RDRP.

À Filipa Dins e à Ana Carreira, pela amizade e por todos os jantares, lanches, almoços e saídas, que nos permitiram descontrair e divertir, mesmo quando o trabalho de doutoramento de cada uma não corria da melhor forma.

À Joana Góis, companheira de viagem nas duas estadias nos Estados Unidos. Quero agradecer por todo o apoio, amizade e aventuras que vivemos que, sem dúvida, fizeram com que essas temporadas no estrangeiro se tenham tornado em experiências inesquecíveis.

Ao Departamento de Engenharia Química e a todos os seus funcionários, pelas condições proporcionadas.

À Fundação para a Ciência e Tecnologia, pelo finacioamento deste trabalho.

A **todos** os meus amigos, por fazerem parte da minha vida e por a tornarem ainda mais rica e interessante! Tenho que fazer um especial agradecimento à Telma e à Ana por terem estado mais próximas na questão do doutoramento e pelas fantásticas sessões de psicoterapia!

Ao Paulo, por fazer parte da minha vida e por me ajudar a crescer todos os dias. "And it´s always you and me always and forever."

À minha "grande e gorda" família, por ser espectacular. Adoro todas as nossas reuniões e o carinho e amor que partilhamos. Vocês são os maiores!

Aos meus pais, por me apoiarem incondicionalmente, por partilharem a sua experiência e por me permitirem ter tido sempre as melhores condições ao longo da minha vida.

À Mia, por ter aparecido na minha vida numa altura em que estava a precisar de uma motivação extra para terminar o trabalho. O seu amor incondicional ajudou-me a sorrir e a relativizar os problemas. A partir daí, tudo melhorou!

Abstract

The aim of this work was the development of new ecofriendly metal-catalyzed reversible deactivation radical polymerization (RDRP) methods for monomers with potential to be applied in the biomedical field. It was also a goal to prepare new polymeric structures to act as bile acids sequestrants (BAS) using the RDRP developed methods, as a proof-of-concept.

There has been an intense debate on the literature regarding the metal-catalyzed RDRP mechanism, being the two proposed mechanisms the single electron transfer living radical polymerization (SET-LRP) and the supplemental activator and reducing agent atom transfer radical polymerization (SARA ATRP). Therefore, the initial part of the work intended to contribute to the understanding of the real polymerization mechanism, which is a key factor for the development of new catalytic systems. The ratio of ligand/soluble copper was evaluated during the Cu(0)-catalyzed RDRP of methyl acrylate (MA) and the results suggested that the polymerization is governed by the proposed SARA ATRP mechanism.

One of the major limitations of the ATRP techniques is the use of metal catalyst, which can contaminate the final product or difficult the purification procedure. The strategy followed in this work aimed the reduction of the amount of soluble catalyst used to mediate the polymerizations as well as the use of alternative solvents that could be less harmful that the ones described in the literature for the monomers selected in this work. Several parameters, such as concentration of soluble catalyst, solvent mixture composition and polymerization temperature, among others were evaluated during the development of the new RDRP systems.

The investigation of new catalytic systems started with the study of the Fe(0)/$CuBr_2$/Me_6TREN-catalyzed (Me_6TREN: tris[2-(dimethylamino)ethyl]amine) SARA ATRP of the hydrophobic model monomer methyl acrylate (MA) in an ecofriendly solvent mixtures (ethanol/water) near room temperature (30 °C). The stringent control over both linear and star-shaped poly(methyl acrylate) (PMA) molecular weight was possible using only a residual amount of soluble copper catalyst (50 ppm). The Fe(0)/$CuBr_2$/Me_6TREN-catalyzed SARA ATRP method was also extended to the

polymerization of styrene (Sty), showing good results in respect to polymers dispersity (*Đ* ≈ 1.2) and maximum monomer conversion achieved (≈ 75%). In addition, both azide and alkyne–polystyrene (PS), which could participate in further reactions to produce complex polymeric structures, were prepared.

The work continued with the selection of three cationic hydrophilic monomers ((3-acrylamidopropyl)trimethylammonium chloride (AMPTMA), 2-aminoethyl methacrylate hydrochloride (AMA) and *N*-(3-acrylamidopropyl)methacrylamide hydrochloride) (APMA), with relevance considering the BAS application, and the development of different RDRP methods. The controlled polymerization of AMPTMA was achieved by Cu(0)/$CuCl_2$/Me_6TREN-catalyzed SARA ATRP in aqueous medium or ethanol/water mixtures, at room temperature, and the concentration of soluble copper used was ten times lower than the one reported in the literature using other ATRP systems. Poly-APMTPMA-based hydrophilic block copolymers were also prepared to prove the "livingness" of the polymer and the possibility to create unique materials. A new activators regenerated by electron transfer (ARGET) ATRP method was developed for the polymerization of the AMA, which is a challenging monomer due to its acidic character. The polymerizations were catalyzed by $CuBr_2$/TPMA complexes (TPMA: tris(2-pyridylmethyl)amine), in combination with small amounts of ascorbic acid fed into the system, and were conducted in aqueous medium or isopropanol/water mixtures near room temperature (35 °C). This new method allowed, for the first time, the preparation of poly-AMA with high chain-end functionality. This result was attributed to the residual occurrence of termination side reactions, due to the low concentration of soluble copper used. The last hydrophilic monomer investigated was the functional APMA. Unfortunately, due to the nature of monomer/radical it was not possible to develop a suitable ATRP-based system for the polymerization of this monomer, as every attempt resulted in uncontrolled reactions. Therefore, an alternative RDRP method, namely reversible addition-fragmentation chain transfer radical polymerization (RAFT) was investigated and used for the preparation of both alkyne-terminated and azide-terminated poly-APMA, which could participate in further "click" chemistry reactions. The reaction mixture composition was found to influence the control over the polymers dispersity, when using chain transfer agents with different aliphatic chain lengths.

The last part of the work was dedicated to the design of new macromolecules, with potential to act as BAS, using the previously developed Cu(0)/$CuBr_2$/Me_6TREN-catalyzed SARA ATRP method in ethanol/water mixtures. Controlled PAMPTMA-based hydrogels and amphiphilic PMA-*b*-PAMPMTA star block copolymers were prepared and tested in the equilibrium binding of sodium cholate (NaCA), used as bile salt model molecule. The results suggested that the interaction of the polymers with NaCA micelles is stronger than with NaCA unimers. It was also proved the possibility to fine-tune the binding parameters of the star block copolymers-based BAS through the control over the molecular weight and composition of the block copolymers. Finally, the PAMPTMA-based hydrogels revealed to be promising materials for BAS applications, with binding parameters similar to the most effective commercial BAS available (Colesevelam hydrochloride).

Resumo

O principal objectivo deste trabalho consistiu no desenvolvimento de novas técnicas de polimerização radicalar por desactivação reversivel (RDRP) catalisada por metais, mais ecológicos do que os existentes, para a polimerização de monómeros com interesse para aplicações biomédicas. Como prova de conceito, este trabalho teve também como objectivo a preparação de novas estruturas poliméricas, para utilização como sequestradores de ácidos biliares (BAS), recorrendo aos métodos RDRP desenvolvidos.

O mecnaismo que rege a RDRP catalisada por metais tem sido alvo de um intenso debate na literatura, existindo a proposta de dois mecanismos distintos: polimerização radicalar viva por transferência de electrão (SET-LRP) e polimerização radicalar por transferência de átomo com activador suplementar e agente redutor (SARA ATRP). Na fase inicial do trabalho pretendeu-se contribuir para a compreensão do mecanismo da polimerização referida, por ser um factor crucial para o desenvolvimento de novos sistemas catalíticos. O rácio ligante/cobre solúvel foi avaliado durante a polimerização do acrilato de metilo (MA) por RDRP catalisada por Cu(0) e os resultados sugeriram que a polimerização é governada pelo mecanismo de SARA ATRP proposto.

Uma das maiores limitações da técnica de ATRP prende-se com o uso de catalisadores metálicos, que podem contaminar o produto final ou dificultar o processo de purificação do mesmo. A estratégia seguida neste trabalho visou a redução da quantidade de catalisador solúvel usada para a mediação da polimerização, bem como a utilização de solventes menos nocivos que os actualmente descritos na literatura para os monómeros seleccionados neste projecto. Parâmetros como, por exemplo, a concentração de catalisador solúvel, a composição do solvente de reacção e a temperatura de polimerização, foram avaliados durante o desenvolvimento dos novos sistemas RDRP.

A investigação de novos sistemas catalíticos teve início com o estudo da polimerização do monómero hidrofóbico modelo MA por SARA ATRP, catalisada por Fe(0)/$CuBr_2$/Me_6TREN (Me_6TREN: tris[2-(dimetilamino)etil]amina), usando uma mistura de solventes verdes (água/etanol) a 30 °C. O sistema permitiu controlar o peso molecular do poli(acrilato de metilo) (PMA), linear e estrela, usando apenas uma concentração residual de cobre solúvel (50 ppm) como catalisador. A gama de aplicação do referido sistema de polimerização foi posteriormente extendida à polimerização do

estireno (Sty), demonstrando bons resultados relativamente à distribuição de pesos moleculares ($Đ \approx 1.2$) e à conversão máxima de monómero atingida (≈ 75%). Adicionamelmente, o sistema de SARA ATRP permitiu preparar poliestireno com terminais azida ou alcino, que podem ser usados em reacções de pós-polimerização para a criação de estruturas poliméricas complexas.

O trabalho prosseguiu com a selecção de três monómeros hidrofílicos catiónicos com relevância para a aplicação como BAS (cloreto de (3-acrilamidopropil)trimetil amónio (AMPTMA); hidrocloreto de 2-aminoetil metacrilato (AMA) e hidrocloreto de *N*-(3-acrilamidopropil)metacrilamida (APMA)), bem como com o desenvolvimento de diferentes métodos de RDRP para a polimerização dos mesmos. A polimerização controlada do AMPTMA foi conseguida através de SARA ATRP, catalisada por Cu(0)/$CuCl_2$/Me_6TREN, em água ou misturas etanol/água. As recções foram realizadas à temperatura ambiente e a concentração de cobre solúvel usada foi dez vezes menor do que a reportada na literatura para a polimerização do AMPTMA utilizando outros sistemas de ATRP. O "carácter vivo" do polímero, bem como a possibilidade de criar materiais com características únicas, foram demontrados através da síntese de copolímeros de bloco hidrofílicos. Um novo sistema de activadores regenerados por transferência de electrão (ARGET) ATRP foi desenvolvido para a polimerização do AMA, o qual é considerado um monómero difícil de polimerizar por ATRP devido ao seu carácter ácido. As polimerizações foram catalisadas por complexos $CuBr_2$/TPMA (TPMA: tris(2-piridilmetil)amina), em combinação com uma pequena quantidade de ácido ascórbico adicionado de forma controlada à reacção, e realizadas em água ou misturas isopropanol/água a 35 °C. Este novo método permitiu, pela primeira vez, a preparação de PAMA com elevada funcionalidade. Este resultado foi explicado pela diminuição da ocorrência de reacções secundárias de terminação, devido à baixa concentração de cobre utilizado. O último monómero hidrofílico estudado foi o APMA. Infelizmente, devido à natureza do monómero/radical, não foi possível desenvolver um sistema de ATRP apropriado para a sua polimerização. Todas as tentativas realizadas deram origem a reacções não controladas. Em alternativa, a técnica RDRP polimerização radicalar por transferência de cadeia reversível por adição-fragmentação (RAFT) foi utilizada para a preparação de poli-APMA com terminais azida e alcino, capazes de participar em reacções de "click chemistry". Foi demonstrado que o peso molecular dos

polímeros foi influenciado pela composição da mistura de solventes, quando foram utilizados agentes de transferência de cadeia com segmentos alifáticos de diferentes comprimentos.

A última parte do trabalho centrou-se na síntese de novos candidatos a BAS usando o método de SARA ATRP desenvolvido anteriormente, catalisado por Cu(0)/$CuBr_2$/Me_6TREN, em misturas etanol/água. Hidrogéis de base PAMPTMA e copolímeros anfifílicos de bloco PMA-*b*-PAMPMTA em forma de estrela foram sintetizados e testados na ligação ao sal de sódio do ácido cólico (NaCA), utilizado como molécula modelo de sal biliar. Os resultados sugeriram que a interacção entre o polímero e micelas de NaCA é mais forte do que a ligação com NaCA em forma de unímeros. Foi também demonstrada a possibilidade de ajustar as propriedades dos BAS baseados nos copolímeros em estrela, através do controlo do peso molecular e composição dos mesmos. Finalmente, os parâmetros de ligação obtidos para os hidrogéis de base PAMPTMA foram semelhantes aos do BAS comercial mais eficiente (Colesevelam hydrochloride), revelando-se assim, materiais bastante promissores para a referida aplicação.

List of publications

Papers published from the research work presented in this thesis:

Guliashvili T., **Mendonça P. V.**, Serra A. C., Popov A. V., Coelho J. F. J., "Copper Mediated Living Radical Polymerization in Polar Solvents: Insight into Some Relevant Mechanistic Aspects", *Chemistry – A European Journal*, 2012, 18, (15), 4607-4612 (Chapter 2).

Carlos M. R. Abreu, **Patrícia V. Mendonça**, Arménio C. Serra, Jorge F. J. Coelho, Anatoliy V. Popov, and Tamaz Guliashvil, "Accelerated Ambient-Temperature ATRP of Methyl Acrylate in Alcohol–Water Solutions with a Mixed Transition-Metal Catalyst System", *Macromolecular Chemistry and Physics*, 2012, 213, (16), 1677-1687 (Chapter 3).

Nuno Rocha, **Patrícia V. Mendonça**, Joana P. Mendes, Pedro N. Simões, Anatoliy V. Popov, Tamaz Guliashvili, Arménio C. Serra, and Jorge F. J. Coelho,"Facile synthesis of well-defined telechelic alkyne-terminated polystyrene in polar media using ATRP with mixed Fe/Cu transition metal catalyst", *Macromolecular Chemistry and Physics*, 2013, 214, 76−84 (Chapter 4).

Patrícia V. Mendonça, Arménio C. Serra, Cláudia L. Silva, Sérgio Simões, and Jorge F.J. Coelho, "Polymeric bile acid sequestrants—Synthesis using conventional methods and new approaches based on "controlled"/living radical polymerization", *Progress in Polymer Science*, 2013, 38, 445–461 (part of Chapter 1).

Patrícia V. Mendonça, Arménio C. Serra, Anatoliy V. Popov, Tamaz Guliashvili and Jorge F.J. Coelho, "Efficient RAFT polymerization of N-(3-aminopropyl)methacrylamide hydrochloride using unprotected "clickable" chain transfer agents", *Reactive and Functional Polymers*, 2014, 81, 1–7 (Chapter 7).

Patrícia V. Mendonça, Dominik Konkolewicz, Saadyah E. Averick, Arménio C. Serra, Anatoliy V. Popov, Tamaz Guliashvili, Krzysztof Matyjaszewski and Jorge F. J. Coelho, "Synthesis of cationic poly((3-acrylamidopropyl) trimethylammonium chloride) by SARA ATRP in ecofriendly solvent mixtures", *Polymer Chemistry*, 2014, 5, 5829-5836 (Chapter 5).

Patrícia V. Mendonça, Saadyah E. Averick, Dominik Konkolewicz, Arménio C. Serra, Anatoliy V. Popov, Tamaz Guliashvili, Krzysztof Matyjaszewski and Jorge F. J. Coelho, "Straightforward ARGET ATRP for the Synthesis of Primary Amine Polymethacrylate with Improved Chain-End Functionality under Mild Reaction Conditions", *Macromolecules*, 2014, 47 (14), 4615–4621 (Chapter 6).

Papers published from the collaboration in other projects during the PhD program:

Carlos M. R. Abreu, **Patrícia V. Mendonça**, Arménio C. Serra, Jorge F. J. Coelho, Anatoliy V. Popov, Ganna Gryn'ova, Michelle L. Coote, and Tamaz Guliashvili, "Reversible Addition–Fragmentation Chain Transfer Polymerization of Vinyl Chloride", *Macromolecules*, 2012, 45 (5), 2200–2208.

Carlos M. R. Abreu, **Patrícia V. Mendonça**, Arménio C. Serra, Anatoliy V. Popov, Krzysztof Matyjaszewski, Tamaz Guliashvili, and Jorge F. J. Coelho, "Inorganic Sulfites: Efficient Reducing Agents and Supplemental Activators for Atom Transfer Radical Polymerization", *ACS Macro Letters*, 2012, 1, 1308–1311.

Fonseca AC, Ferreira P, Cordeiro RA, **Mendonça PV**, Góis JR, Gil MH, Coelho JFJ, "Drug delivery systems for predictive medicine: polymers as tools for advanced applications", in "New Strategies to Advance Pre/Diabetes Care: Integrative Approach by PPPM", Advances in Predictive, Preventive and Personalised Medicine, Vol. 3, Springer, 2013.

Nuno Rocha, **Patrícia Mendonça**, Joana Góis, Rosemeyre Cordeiro, Ana Fonseca, Tamaz Guliashvili, Krzysztof Matyjaszewski, Arménio Serra and Jorge Coelho, "The Importance of Controlled/Living Radical Polymerization Techniques in the Design of Tailor Made Nanoparticles for DSS" , in "Advances in Predictive, Preventive and Personalised Medicine", Volume 4, pp 315-357, Springer, 2013.

Dominik Konkolewicz, Pawel Krys, Joana R. Góis, **Patrícia V. Mendonça**, Mingjiang Zhong, Yu Wang, Armando Gennaro, Abdirisak A. Isse, Marco Fantin, and Krzysztof Matyjaszewski, "Aqueous RDRP in the Presence of Cu^0: The Exceptional Activity of Cu^I Confirms the SARA ATRP Mechanism", *Macromolecules*, 2014, 47 (2), 560–570.

Joana P. Mendes, Fábio Branco, Carlos Abreu, **Patrícia V. Mendonça**, Anatoliy V. Popov, Tamaz Guliashvili, Arménio C. Serra and Jorge F. J. Coelho, "Synergistic effect of 1-butyl-3-methylimidazolium hexafluorophosphate and DMSO in the SARA ATRP at room temperature affording very fast reactions and polymers with very low dispersity", *ACS Macro Letters*, 2014, 3 (6), 544–547.

Joana P. Mendes, Fábio Branco, Carlos M. R. Abreu, **Patrícia V. Mendonça**, Arménio C. Serra, Anatoliy V. Popov, Tamaz Guliashvili and Jorge F. J. Coelho, "Sulfolane: an Efficient and Universal Solvent for Copper-Mediated Atom Transfer Radical (co)Polymerization of Acrylates, Methacrylates, Styrene, and Vinyl Chloride", *ACS Macro Letters*, 2014, *3* (9), 858–861.

Thesis outline

This project was designed based on the encouraging results obtained during my Master program in Industrial Applications of Polymers, in which a new supplemental activator and reducing agent atom transfer radical polymerization (SARA ATRP) technique was developed for the controlled polymerization of methyl acrylate (MA), methyl methacrylate (MMA) and styrene (Sty). From there, the logical pathway to follow was the understanding of the mechanism behind the polymerization, which remains a subject of intense debate in the literature, as well as to develop new ecofriendly ATRP systems for the polymerization of different monomer families. Additionally, to prove the potential of the ATRP systems developed in this work, new polymeric bile acid sequestrants (BAS) were prepared. Concerning the goals described, the Chapter 1 of this document provides a literature review covering both the reversible deactivation radical polymerization (RDRP) field, with especial focus on metal-catalyzed techniques, and the methods available for the synthesis of polymeric BAS.

The first part of the experimental work (Chapter 2) was dedicated to the kinetic studies performed on the metallic Cu(0)-catalyzed RDRP model polymerization of MA in dimethylsulfoxide (DMSO) at 30 °C, as a tool to provide insights about the polymerization mechanism. By determining the copper (I)/ligand (catalytic complex) ratio during the polymerization, it was possible to conclude that the polymerization was governed by the SARA ATRP proposed mechanism.

Current research trend in ATRP methods is focused on the development of ecofriendly systems, meaning the use of smaller amounts of toxic metal catalyst and less harmful solvents. This is critically important considering the preparation of polymers for biomedical applications. In this work, MA (Chapter 3) and Sty (Chapter 4) were used as hydrophobic model monomers for the development of new SARA ATRP systems that allowed the synthesis of functional polymers using low concentrations of soluble copper catalyst in combination with the biocompatible iron catalyst. Notable improvements were achieved in the controlled polymerization of MA with the use of ecofriendly ethanol/water mixtures as the reaction solvent, instead of the traditional DMSO, near room temperature. The SARA ATRP technique was also extended to the polymerization of hydrophilic cationic (3-acrylamidopropyl)trimethylammonium chloride (AMPTMA)

and to the preparation of AMPTMA-based block copolymers at room temperature (Chapter 5). Very promising results were obtained for controlled polymerizations in water, which is often a problematic solvent for ATRP systems.

Continuing the development of ecofriendly ATRP systems for different monomer families, the challenging acidic monomer 2-aminoethyl methacrylate hydrochloride (AMA) was studied. Chapter 6 describes a new activators regenerated by electron transfer (ARGET) ATRP system for the synthesis of poly-AMA in aqueous medium or alcohol/water mixtures near room temperature. For the first time, it was possible to prepare well-defined AMA-based block copolymers using AMA as the first block, by using ATRP techniques, due to the low concentration of catalyst used. Willing to expand range of application of ATRP to other acidic monomers, the controlled polymerization of the biorelevant *N*-(3-acrylamidopropyl)methacrylamide hydrochloride) (APMA) was investigated. Several attempts of implementing ATRP-based systems to the polymerization of APMA failed to control both the molecular weight and dispersity (*Đ*). Alternatively, new functional poly-APMA homopolymers (azide and alkyne functionalities) were polymerized using reversible addition-fragmentation chain transfer radical polymerization (RAFT) (Chapter 7). The synthesized polymers proved to be able to participate in "click" chemistry reactions and thus, can be useful for the preparation of complex polymeric structures for biomedical applications.

Chapter 8 describes the preparation of a new generation of polymeric BAS, based on amphiphilic PMA-*b*-PAMPTMA star block copolymers and PAMPTMA-based cationic hydrogels, by the previously developed ecofriendly SARA ATRP method. These controlled materials revealed to be promising BAS candidates in the binding of sodium cholate used as the bile salt model molecule.

Finally, Chapter 9 presents the main conclusions from this work, along with suggestions for future work.

List of acronyms

AMA	2-Aminoethyl methacrylate hydrochloride
APMA	*N*-(3-Aminopropyl)methacrylamide hydrochloride
AMPTMA	(3-Acrylamidopropyl)trimethylammonium chloride
AGET	Activators generated by electron transfer
ARGET	Activators regenerated by electron transfer
AscA	Ascorbic acid
ATRA	Atom transfer radical addition
ATRP	Atom transfer radical polymerization
*t*BA	*tert*-Butyl acrylate
BAS	Bile acids sequestrants
BDDA	1,4 Butanediol diacrylate
bpy	2,2'-Bipyridine
4f-BiB	Pentaerythritol tetrakis(2-bromoisobutyrate)
6f-BiB	Dipentaerythritol hexakis(2-bromoisobutyrate)
dn/dc	Refractive Index Increment
CLRP	Controlled/living radical polymerization
DHB	2,5-Dihydroxybenzoic acid
DMF	Dimethylformamide
DMSO	Dimethyl sulfoxide
DP	Degree of polymerization
DT	Degenerative transfer
DV	Differential viscometer
eATRP	Electrochemically mediated atom transfer radical polymerization
EBiB	Ethyl α-bromoisobutyrate
ECP	Ethyl 2-chloropropionate
EtOH	Ethanol

FDA	Food and Drug Administration
FRP	Free radical polymerization
FTIR-ATR	Fourier transform infrared attenuated total reflection
GI	Gastrointestinal
HABA	2-(4-Hydroxyphenylazo)benzoic acid
HBiB	2-hydroxyethyl α-bromoisobutyrate
HPLC	High performance liquid chromatography
ICAR	Initiators for continuous activator regeneration
IUPAC	International Union of Pure and Applied Chemistry
IPA	Isopropanol
LALLS	Low-angle laser-light scattering
LRP	Living radical polymerization
MALDI-TOF	Matrix assisted laser desorption/ionization time-of-flight mass
MA	Methyl acrylate
MMA	Methyl methacrylate
Me_6TREN	Tris[2-(dimethylamino)ethyl]amine)
NaCA	Cholic acid sodium salt (sodium cholate)
NIPAAm	*N*-isopropylacrylamide
NMP	Nitroxide mediated polymerization
NMR	Nuclear magnetic resonance
OEOA	Oligo(ethylene oxide) methyl ether acrylate
OEOMA	Oligo(ethylene oxide) methyl ether methacrylate
OSET	outer sphere electron transfer process
PRE	Persistent radical effect
PMA	Poly(methyl acrylate)
PAMA	Poly(2-aminoethyl methacrylate hydrochloride)
PAPMA	Poly(*N*-(3-aminopropyl)methacrylamide hydrochloride)
PAMPTMA	Poly((3-acrylamidopropyl)trimethylammonium chloride)

PEG	Poly(ethylene glycol)
PVC	Poly(vinyl chloride)
PgBiB	Propargyl α-bromoisobutyrate
PgOH	Propargyl alcohol
PNIPAAm	Poly(*N*-isopropylacrylamide)
PMDETA	*N*,*N*,*N*′,*N*′′,*N*′′-Pentamethyldiethylenetriamine
POEOA	Poly(ethylene glycol) methyl ether acrylate
POEOMA	Poly(ethylene glycol) methyl ether methacrylate
ppm	Parts per million
PS	Polystyrene
PTFE	Polytetrafluoroethylene
RALLS	Right-angle laser-light scattering
RAFT	Reversible addition-fragmentation chain transfer
RDRP	Reversible deactivation radical polymerization
RI	Refractive index
SARA	Supplemental activator and reducing agent
SET	Single-electron transfer
SEC	Size exclusion chromatography
SFRP	Stable free radical polymerization
SGF	Simulated gastric fluid
SIF	Simulated intestinal fluid
Sty	Styrene
UV-Vis	Ultraviolet-visible
TEA	Triethylamine
TEMPO	2,2,6,6-Tetramethylpiperidinyl-1-oxy
TEGDA	Tetra(ethylene glycol) diacrylate
THF	Tetrahydrofuran
TMS	Tetramethylsilane

TPMA	Tris(pyridin-2-ylmethyl)amine
TREN	Tris(2-aminoethyl)amine

Nomenclature

$Đ$	Dispersity
M_n^{NMR}	Number-average molecular mass determined by NMR spectroscopy
M_n^{SEC}	Number-average molecular mass determined by SEC
M_n^{th}	Theoretical number-average molecular mass
M_w	Theoretical mass-average molecular mass
k_p^{app}	Apparent rate constant of propagation
k_a	Activation rate constant
k_d	Deactivation rate constant
k_{disp}	Disproportionation rate constante
k_{comp}	Comproportionation rate constante
K_{ATRP}	ATRP equilibrium constant
T	Temperature

Contents

List of figures

List of schemes

List of tables

Motivation, targets and research significance

The strong need for polymers with well-defined architecture, composition, molecular weight and chain-end functionality has definitively shifted the attention of the scientific community to the use of reversible deactivation radical polymerization (RDRP) methods. Metal-catalyzed RDRP, covering both single electron transfer living radical polymerization (SET-LRP) and atom transfer radical polymerization (ATRP) techniques, is considered one of the most robust and versatile available methods, considering the range of polymerizable monomers and relatively mild conditions required for polymerizations. However, the use of a metal catalyst, which can contaminate the final product, is one of the limitations of this method. This issue, along with the possible use of harmful organic solvents can hamper the implementation of metal-catalyzed RDRP processes at a large scale. Considering both environmental issues and the industrial viability of metal-catalyzed RDRP, this project aimed the development of new catalytic systems, able to employ "green" solvents and low concentration of metal catalysts, for the polymerization of different monomer families. At the same time, it was intended to contribute to the understanding of the metal-catalyzed RDRP reaction mechanism, which has been the subject of intense debate in the literature during the past decade. It was expected that the goals set for this project could potentiate the expansion of the range of application of the metal-catalyzed RDRP as well as enhance the possibility of future large scale implementation.

The main feature of RDRP methods is the ability to allow the control over the structure, morphology and functionality of polymers. As a proof-of-concept, this project aimed the preparation of new polymeric bile acids sequestrants (BAS) candidates that can be used for hypercholesteremia treatment. High blood cholesterol level is the leading cause of coronary heart disease, which is a health problem that affects millions of people around the world, especially in industrialized countries. Usually this disorder is controlled by statins, which act directly in the cholesterol synthesis process, or by BAS with action limited to the gastrointestinal (GI) tract. For this reason BAS administration is preferable over statins, since it can prevent systemic toxicity and long-term complications associated to the later, such as liver dysfunction. However, currently the main disadvantages of BAS are their low efficiency and poor patient compliance in comparison with statins. The use

of RDRP to synthesize tailor-made polymeric drugs could lead to materials with improved properties, which is of outstanding relevance since they will be able to compete in the pharmaceutical market. Therefore, it is expected that this work could have an important social impact, contributing to enhance the patient's life quality.

Chapter 1

Literature review

Part of this chapter, regarding the bile acids sequestrants subject, is published in: ***Patrícia V. Mendonça****, Arménio C. Serra, Cláudia L. Silva, Sérgio Simões, and Jorge F.J. Coelho, "Polymeric bile acid sequestrants—synthesis using conventional methods and new approaches based on "controlled"/living radical polymerization", Progress in Polymer Science, 38, (2013), 445–461.*

1.1. Fundamentals on free radical polymerization - commercial limitations and new way towards "controlled" polymers

Polymeric materials, usually known as plastics, are present in almost every areas of human life, such as: electronics, automobile, packaging, construction and medicine. The most used polymers are low density polyethylene, poly(vinyl chloride) (PVC), polystyrene (PS), polyacrylates and polyacrylamides, being 50% of their consumption produced by free radical polymerization (FRP).[1] This technique have been largely used in the industry due to several important features, such as: tolerance to impurities and monomer functionality; relatively easy implementation at industrial scale; compatibility with aqueous systems; possibility to carry the polymerizations using different technologies (e.g., solution, emulsion and bulk)[2, 3] and good reproducibility of the products properties.[4]

Regarding the reaction mechanism, FRP proceeds via three basic steps:[2, 5] initiation; propagation and termination. In a first stage, the conventional initiator is decomposed (e.g., thermal decomposition, photochemical homolytic cleavage of covalent bonds or decomposition by a redox process)[6] leading to the formation of species known as radicals. Subsequently, monomer units are added to the propagating chains every 1 ms of reaction.[5] Propagation follows a first-order kinetics, with respect to propagating radicals concentration, and the lifetime of an active polymer chain is in average near 1 s.[5] In the final stage of the polymerization, propagating radical chains terminate via combination or disproportionation, forming polymers with dead chain-ends. In FRP there is no possibility of controlling the polymers structure or molecular weight due to both the short time between each monomer addition and the existence of termination reactions. In addition to these aspects, during the polymerization, some chain transfer reactions between a propagating radical chain and other chemical species (monomer, polymer or transfer agent) may occur due to the high reactivity of radicals.[3] As a result, polymers produced by FRP present high dispersity values ($Đ = M_w/M_n$), typically $Đ > 2$, and the preparation of copolymers with controlled compositions is almost impossible.[2] Also, it is not possible to control the architecture or functionality of the polymers, which are known to have great influence on the properties of the final products. These limitations restrict the increase of

the commercial applications of some materials prepared by FRP, since there are specialized areas that require, for instance, tailor-made polymers with specific architectures and functionalities, such as the biomedical field (e.g., drug delivery systems).

Over the decades, many research efforts have been made to achieve control over the polymer structures and molecular weight aiming to create new materials with advanced properties. On this matter, the concept of "living polymerization" came up for the first time in 1956 by Michel Szwarc's research group with an anionic polymerization process that allowed the preparation of copolymers with controlled compositions.[7, 8] Despite the absence of termination reactions, which enabled the control over the polymerization, the experimental conditions were very severe (e.g., very low temperature) and not easily scaled for industrial production, as FRP processes.[9] Other limitations of this technique were associated to its intolerance to some monomer functionalities, to the presence of impurities or oxygen[3] and the need for high purity monomers and solvents.[4] Due to the interesting properties exhibited by the different polymer architectures (e.g., star shaped) synthesized by anionic polymerization, other different techniques have been developed in an attempt to adequate living polymerization to industrial processes, namely: cationic polymerization; ring opening metathesis polymerization; Ziegler-Natta polymerization and reversible deactivation radical polymerization (RDRP).[5] From the above mentioned techniques, RDRP has received a remarkable attention by the scientific community, as it combines the flexibility and mild experimental conditions, similar to those of FRP, with the precise control over polymers characteristics, comparable to ionic polymerization.[10] Despite of being produced at a low scale, commercial materials prepared by RDRP are already a reality in different areas like automotive paints, health care, coatings and electronics among others.[4]

1.2. Fundamentals on reversible deactivation radical polymerization

RDRP is a group of polymerization techniques that rely on the same basic principle: keep the radicals concentration very low during the polymerization by means of an equilibrium between active (propagating radicals) and dormant species that have no activity (Scheme 1.1).[3] In opposition to FRP, in RDRP systems the initiation is very fast compared to

propagation. Therefore, the initiator species are activated at low monomer conversions and the polymer chains start to grow roughly at the same time.[5, 11] The propagation step is similar to that of FRP, with addition of monomer units to the propagating radicals. However, due to the equilibrium between active and dormant species, the life of a propagating radical in RDRP can be extended to hours, in opposition to FRP (lifetime of propagating radical ≈ 1 s).[3] Every 0.1-10 ms, propagating radicals are reversibly deactivated, which decreases about 90% the probability of radical termination reactions in comparison with FRP systems and opens the possibility of controlling the polymers molecular weight. Nevertheless, termination reactions may also occur in RDRP systems. However, since the total number of chains is much greater than in FRP, the effect of termination could be negligible. Additionally, the rate of termination per chain and the rate of chain transfer to monomer per chain are much lower in RDRP. As the result of the simultaneous growth of all chains and the absence of chain transfer reactions, the number of propagating polymer chains during the polymerization is constant. Therefore, a linear increase of the polymers molecular weight with monomer conversion is expected. In addition, polymers prepared by RDRP present active chain-ends ("livingness"), which can be reinitiated with further monomer supply to form, for instance, block copolymers.

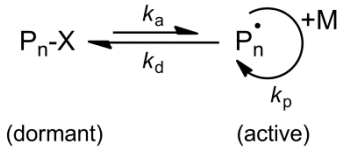

Scheme 1.1. General dormant-active species equilibrium in RDRP.

The terminology of the concept behind RDRP has been changing during the past decade. Firstly, due to the so-called "living" character of the polymers obtained by RDRP, the method was first coined as living radical polymerization (LRP). However, with further developments in the area, not only "living" polymers could be prepared, but controlled polymeric structures and narrow molecular weight distributions could be achieved ($Đ$ < 1.5). Due to this fact, a new term was proposed to describe the LRP method - controlled/living radical polymerization (CLRP). However, the term "controlled" did not address which phenomenon was being controlled (e.g., transfer, termination, end groups, etc.)[12] and, for that reason, some authors did not adopted the CLRP concept. A discussion about the right nomenclature of "living" radical systems was opened in 2000, on a special

issue of the Journal of Polymer Science, Part A: Polymer Chemistry.[13] According to the International Union of Pure and Applied Chemistry (IUPAC) recommendation, a living polymerization was "a chain polymerization from which irreversible chain transfer and irreversible chain termination (deactivation) are absent".[12] This fact did not imply control over, for instance, molecular weight and molecular weight distribution. Control over such parameters is only possible if the initiator is completely consumed in the beginning of the reaction and the exchange reactions between dormant species and active species are at least as fast as propagation.[9] The most recent update from the IUPAC concerning this issue was reported in 2010 and it recommends the use of the term "reversible deactivation radical polymerization" (RDRP) to describe polymerizations "in which certain additives react reversibly with the radicals, thus enabling the reactions to take on much of the character of living polymerizations, even though some termination inevitably takes place".[14]

To sum up, RDRP systems can be identified by four main key criteria:[11]

- Internal first-order kinetics with respect to monomer;
- Linear growth of the degree of polymerization ($DP = [M]_0/[I]_0$; M: monomer; I: initiator) with monomer conversion;
- Narrow molecular weight distribution ($1 < Đ < 1.5$);
- Long-lived polymer chains.

Nevertheless, the evaluation of the system has to be done carefully since the verification of an isolated criterion could lead to wrong interpretations. For instance, constant number of propagating radicals (first criterion in the list above) can also be observed for FRP, under steady-state conditions. This feature by itself does not guarantee the living character of the system. It is always necessary to ensure the presence of active chain-ends, which can be done by nuclear magnetic resonance (NMR) analysis, and prove the "livingness" of the chains, by doing a reinitiating experiment.

1.3. Description of the reversible deactivation radical polymerization techniques

As referred in the previous section, one of the RDRP bases is the dynamic equilibrium between active and dormant species (Scheme 1.1), which maintains the concentration of radicals very low during the polymerization. To accomplish that, there are two main strategies available: (i) reversible activation/deactivation of radicals or (ii) reversible chain transfer (degenerative transfer process).[5] Several RDRP techniques based on different strategies have been developed over the years, being the three main ones the atom transfer radical polymerization (ATRP), the stable free radical polymerization (SFRP) and the reversible addition-fragmentation chain transfer (RAFT).

In processes based on reversible activation/deactivation of radicals, such as ATRP or SFRP, the propagating radicals are formed by an atom exchange in the activation step. For this reason, the use of a conventional radical initiator is not required in this type of RDRP systems. During polymerization, the dynamic equilibrium is maintained by a kinetic phenomenon called "persistent radical effect" (PRE), which strongly induces a shift towards dormant species. In the first stages of polymerization some radical-radical termination occurs leading to the accumulation of deactivator species over the reaction time (can be radical or metal complex in higher valence state depending on the system),[5] which cannot propagate or self-terminate.[15] By this mean, the amount of propagating radicals will be very low in comparison to the deactivator species, which will be "persistent" during the polymerization. Therefore, the equilibrium is shifted towards dormant species since radicals will most likely react with persistent species forming dormant species than react with themselves terminating (see Scheme 1.2 for example).

In what concerns techniques like RAFT or (reverse) iodine transfer polymerization ITP/RITP, the equilibrium between active and dormant species is regulated by a reversible exchange of an unstable end-group between the two species. This degenerative chain transfer mechanism can be done by direct end-group (or atom) exchange or addition-fragmentation with unsaturated methacrylate oligomers or dithioesters (see Scheme 1.4 for example).[5, 11] In this type of polymerization, the radicals are formed by the decomposition of conventional free radical initiators like in FRP. Therefore, the

reaction proceeds with slow initiation and fast termination with a steady state of propagating radicals. However, as a regular RDRP system, control over molecular weight and polymer structure can be achieved since the constant rate of chain transfer between the active radicals and dormant species is higher than the constant rate of propagation ($k_{ex}/k_p > 1$).[5] The quality of the control achieved in the degenerative processes is strongly dependent on the chain transfer agent structure and its suitability to the monomer that is being polymerized.

1.3.1. Atom transfer radical polymerization

The ATRP method involves the use of an alkyl halide initiator and a metal catalyst/ligand complex which mediates the dynamic equilibrium (Scheme 1.2). The polymerization starts with fast initiation via abstraction of the halogen atom (X) from the initiator by the metal catalyst/ligand complex in the lower oxidation state ($M_t^nX_m/L$). The radicals formed in this stage can propagate by monomer addition and/or be deactivated by the higher valence state metal/ligand complex (also formed in the initiation step) leading to dormant species (P_n–X). The dynamic equilibrium is regulated by a redox equilibrium, in which the halogen atom is transferred between the transition metal catalyst/ligand complex ($M_t^nX_m/L$ or $M_t^{n+1}X_{m+1}/L$) and the propagating radicals ($P_n^{\bullet}$).[10] The accumulation of the higher valence state metal/ligand complex during polymerization (see PRE in section 1.3) shifts the equilibrium towards the dormant species, providing good control over polymers molecular weight.[16]

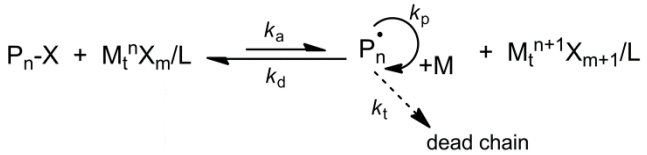

Scheme 1.2. General mechanism of ATRP.

ATRP has been the most extensively studied and applied RDRP technique for the polymerization of different monomer families, such as acrylonitrile, (meth)acrylates, styrenes and water soluble monomers,[2, 11] due to its versatility and an easy access to the required reagents (usually commercially available).[15] For the precise control over the polymerization it is necessary to adjust the metal catalyst/ligand complex nature to a

given monomer.[5] The ligand plays an important role since it regulates the activity of the metal catalyst through stabilization and its solubility in the reaction solvent. Transition metal catalysts, such as copper, iron or ruthenium have been employed in ATRP systems in conjugation with nitrogen-containing ligands.[10] The main disadvantages of this technique are associated with the need of catalyst removal after the polymerization and the fact that most acidic monomers have to be protected, to avoid catalyst poisoning, in order to be polymerized.[5] ATRP belongs to the class of metal-catalyzed RDRP techniques, which is the subject of this work. Therefore, more details about the technique are provided in section 1.4.

1.3.2. Stable free radical polymerization

In SFRP, a stable radical ($X^{\bullet}$) is used to activate dormant species and reversibly couple with active propagating radicals ($P_n^{\bullet}$) (Scheme 1.3). The stable radical plays the role of persistent radical deactivator, in a similar way as the metal/ligand complex in the higher valence state does in ATRP. Therefore, in order to properly mediate the polymerization, the stable radical should not react with itself neither with monomer, to avoid the formation of new chains, and should not contribute to other side reactions.[5] By contrast with ARTP, in SFRP the initiation is induced by a synthesized unimolecular alkoxyamine initiator or, alternatively, by a conventional initiator combined with a nitroxide radical.[10]

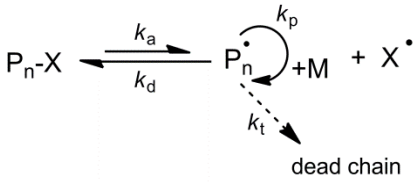

Scheme 1.3. General mechanism of SFRP.

Usually, SFRP reactions require higher temperatures than other RDRP techniques, which turns very difficult the use of this method for the polymerization of non-conjugated monomers.[10] The use of SFRP started with the polymerization of styrene in the presence of 2,2,6,6-tetramethylpiperidinyl-1-oxy (TEMPO) at 120 °C.[17] Despite the good control over the PS molecular weight, the method proved to be inefficient for the homopolymerization of other monomers due to the low equilibrium constant ($K_{eq} = k_a/k_d$) that shifted the equilibrium towards dormant species.[9] In the case of PS, the reaction

could be controlled due to thermal self-initiating events (at the reaction temperature) of styrene forming radicals and thus, lowering the amount of TEMPO in the system.[5] In order to expand the range of polymerizable monomers, different derivatives of TEMPO were designed and synthesized (Figure 1.1) showing successful results on the polymerization of acrylamides, dienes and acrylates, at lower temperature than the original nitroxide mediator.[11]

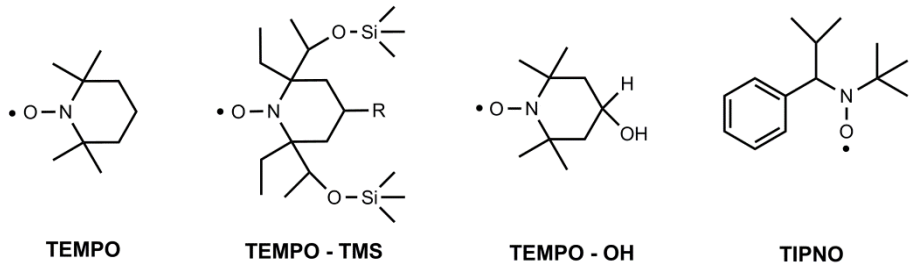

Figure 1.1. TEMPO and TEMPO derivatives commonly used in SFRP reactions.

Due to their high efficacy, nitroxide radicals are often employed in SFRP reactions and, for that reason, the technique is commonly referred in the literature as nitroxide mediated polymerization (NMP).[11] However, other stable radicals such as dithiocarbamates, organometallic species, acyclic nitroxides, trityl and benzhydryl derivatives and triazolinyl radicals are effectively used in SFRP.[9] This area of research has been focused on the synthesis of styrenic and acrylic polymers and on the development of new nitroxides that can be both used at lower reaction temperature and provide faster reactions.[2, 18]

1.3.3. Reversible addition-fragmentation chain transfer

RAFT polymerizations are regulated by a reversibly degenerative transfer of a leaving group (R) between a propagating polymer chain and a chain transfer agent, via addition-fragmentation. Mechanistically, the RAFT polymerization proceeds in three different steps. In the initiation, a conventional radical initiator (e.g., azobisisobutyronitrile) is decomposed and reacted with monomer units to give the primary propagating radicals (Scheme 1.4 (a)). These primary propagating radicals will then react with the chain transfer agent in a pre-polymerization equilibrium forming a polymeric transfer agent (Scheme 1.4 (b)).[9] Subsequently, the leaving group (R) of the polymeric transfer agent,

which is a radical specie, forms new chains that will add monomer units or reversible exchange with dormant species (polymeric transfer agent) (Scheme 1.4 (c)), in the main RAFT equilibrium.[11] Due to the nature of the mechanism, it is clear that RAFT polymerizations produce some amount of dead polymer chains. However, these can be neglected when compared to the number of "living" polymer chain. Therefore, well-controlled polymerizations can also be achieved by RAFT polymerization.

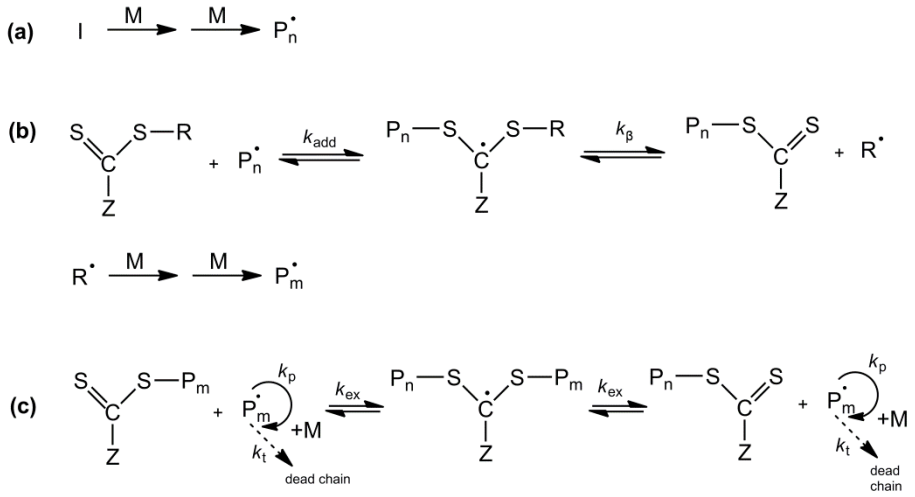

Scheme 1.4. General mechanism of the RAFT polymerization: (a) initiation; (b) pre-equilibrium and (c) main RAFT equilibrium.

The selection of the chain transfer agent is the most critical aspect to allow the control over the polymers molecular weight, molecular weight distribution and molecular architecture. On this matter, the leaving group must present good capacity to hemolytic cleavage from the transfer agent and must be able to be reinitiated in the radical form. In addition, the chain transfer agent must be quickly consumed and the rate of exchange must be higher than the rate of propagation ($k_{ex} > k_p$).[19] Common transfer agents used in RAFT include dithioesters, dithiocarbamates, trithiocarbonates, xanthates and thiocarbonylthio compounds.[5] Information about the nature of both R and Z groups most adequate for the polymerization of different monomers can be found in review articles.[5, 19]

RAFT is one of the most successful RDRP techniques since it enables the polymerization of a broad range of monomers and, in many cases, using relatively mild reaction conditions.[9] However, the main disadvantages of this technique include a significant retardation in polymerizations of low molecular weight polymers, the complexity of the

synthesis of some RAFT agents, the high cost of the commercially available RAFT agents and the gel effect observed at high monomer conversion. The research trend on RAFT systems is mainly focused on temperature decrease, preparation of new materials and understanding of the effect of the RAFT agent structure on the living features of the polymerization.[19]

1.4. Metal-catalyzed reversible deactivation radical polymerization – brief history

The term "metal-catalyzed RDRP" can be used to identify the RDRP methods that use metal catalysts to mediate the polymerization (e.g., ATRP). The first reports on this method were published independently by two research groups, Sawamoto´s and Matyjaszewski´s, in 1995.[16, 20] Sawamoto and co-workers used organometallic complexes of Ru(II) as effective catalysts to mediate controlled polymerizations and coined this method as "transition metal-catalyzed living radical polymerization",[20] while Matyjaszewski was able to obtain living polymers using Cu(I) as catalyst. Despite using a transition metal catalyst, the author named the technique as "Atom Transfer Radical Polymerization", assuming that the reaction mechanism was similar to the well-known organic chemistry reaction "atom transfer radical addition" (ATRA).[5] After these two pioneer reports, important scientific research efforts were made in order to expand the range of application of the ATRP reactions. The research was based on the development of new metal catalyst/ligand complexes and initiators, synthesis of well-defined and complex polymers architectures and the application of the technique in aqueous-phase systems.[21] An important milestone was achieved in 1997 with the use of the industrially attractive metallic copper (Cu(0)), as an efficient reducing agent for ATRP reactions.[22] Later, in 2006, Percec's group reinvestigated the use of Cu(0) as catalyst in the controlled polymerization of acrylates, methacrylates and vinyl chloride at room temperature.[23] However, the authors proposed a new term for the technique, named "single-electron transfer living radical polymerization" (SET-LRP), believing that the reaction mechanism was different from the initial proposed for ATRP. This work presented a crucial point in the history of metal-catalyzed RDRP techniques since it started a vast discussion aiming to address the real reaction mechanism behind the technique. Some authors adopted the

nomenclature ATRP or SET-LRP to define copper-catalyzed RDRP reactions, while others chose to simple call them metal-catalyzed RDRP meaning, as mentioned before, that the polymerization is catalyzed by metal compounds and presents "living" features. Fundamental studies on this field are very important since they will certainly lead to the development of powerful catalysts for a vast range of monomers and to the adaptation of the reaction conditions for large scale production.

1.4.1. Atom transfer radical polymerization fundamentals

ATRA is an organic chemistry reaction widely used for the addition of an alkyl halide (RX) to an alkene (Y) forming a 1:1 adduct (RXY), which can be catalyzed by metal species (Scheme 1.5).[24] Mechanistically, the reaction starts with the abstraction of the halogen atom (X) from the alkyl halide species by a metal catalyst in a lower oxidation state, forming an active radical ($R^{\bullet}$) and a metal in a higher oxidation state, which is coordinated with appropriate ligands. This step is conducted by an inner sphere process, involving the homolytic dissociation of the C-X bond.[25] Then the alkene molecule reacts with the active radical, which is subsequently deactivated leading to the adduct and the initial higher oxidation state transition metal complex.[9] Usually, a stable adduct can be produced in high yield with proper selection of alkyl halide and alkene molecules.[26]

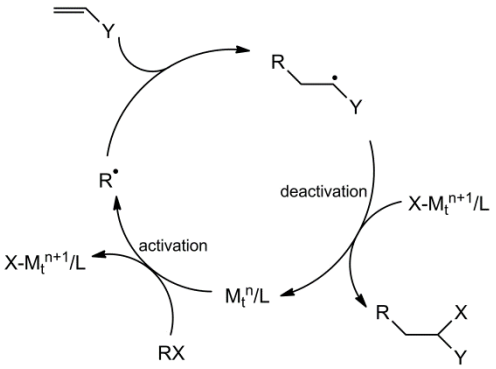

Scheme 1.5. General mechanism of ATRA.

Based on the ATRA mechanism, the ATRP concept was developed by selecting halogenated initiators which could react with vinyl monomer units (multiple additions of units) in the presence of suitable metal catalyst complexes. This process lead to a polymerization where the polymers molecular weight increased linearly with monomer conversion and the polymers molecular weight distribution was narrow.[24] One

requirement is that ideally the activation-addition-deactivation cycle should only be repeated until monomer is vanished, if radical species formed before and after monomer addition have similar reactivity.[26] Taking into account the mechanism of ATRA, it is known that the rate of ATRP reactions could be enhanced by the increasing of the reaction temperature since the inner sphere electron transfer mechanism is based on the covalent linkage between the two redox species. It is also expected that the catalyst has to be employed in high amounts (typically 0.1-1 mol% relative to the monomer)[27] to compensate the higher valence state complex ($M_t^{n+1}X_{m+1}/L$) irreversible accumulation in the system, due to the occurrence of radical termination reactions (see PRE in section 1.3). These conditions represent important drawbacks of the original ATRP technique since they turn very difficult the implementation of an industrial scale process due to the high cost of the catalytic systems and the need to remove the metal from the polymer matrix after the polymerization. Another mechanistic limitation of ATRP reported by Matyjaszewski[28] is that the technique could not be used to polymerize non-conjugated monomers. The dynamic equilibrium could not be achieved since those monomers have a very low K_{ATRP} ($K_{ATRP} = k_a/k_d$) and thus generate very stable dormant species (see Scheme 1.2). This assumption was supported by the comparison of K_{ATRP} values for conjugated and non-conjugated monomers, using different catalytic systems.[28]

As previously mentioned, the equilibrium between the activation process and the deactivation process is the key factor to achieve controlled polymerizations. Therefore, the value of the rate constants of activation (k_a), deactivation (k_d) and their ratio (K_{ARTP}) play a critical role in the control over the polymers dispersity and in the rate of polymerization (Equations 1.1 and 1.2).

$$Đ = \frac{M_w}{M_n} = 1 + \left(\frac{[RX]_0 \, k_p}{k_d \left[M_t^{n+1} X_{m+1} / L \right]} \right) \left(\frac{2}{\text{conv.}} - 1 \right) \qquad \textbf{(Equation 1.1)}$$

$$R_p = k_p [M] \left[P_n^{\bullet} \right] = k_p K_{ATRP} [RX] \frac{\left[M_t^n X_m / L \right]}{\left[M_t^{n+1} X_{m+1} / L \right]} \qquad \textbf{(Equation 1.2)}$$

Ideally, both k_a and k_d values should be high enough to afford a reasonable polymerization rate and a good control, while K_{ATRP} should be as low as possible ($k_a \ll k_d$) to keep a low concentration of radicals, diminishing bimolecular termination. Therefore, in order to successfully polymerize different monomers by ATRP, it is necessary to consider several reaction parameters, such as reaction temperature, initiator structure, solvent, ligand and metal catalyst, which have influence on both k_a[29] and k_d[30, 31] values.

Initiator structure

Alkyl halides (RX), where X is a (pseudo)halogen, are commonly used as initiators for ATRP (Figure 1.2). The reactivity of the initiator, which depends on both the structure of the alkyl chain and the halogen atom, is an important parameter that must be considered according the choice of monomer to polymerize.[32] In ideal conditions, the rate of activation should be at least as high as the rate of propagation. In addition, to perform successful ATRP reactions, the halide (X) must be transferred between the catalytic complex and the growing polymer chains in a fast and selective way. Initiators containing either bromine or chlorine have proved to allow for better control over the polymers dispersity.[33] Information on the influence of several initiators on the rate of activation during ATRP is available in the literature.[31, 34]

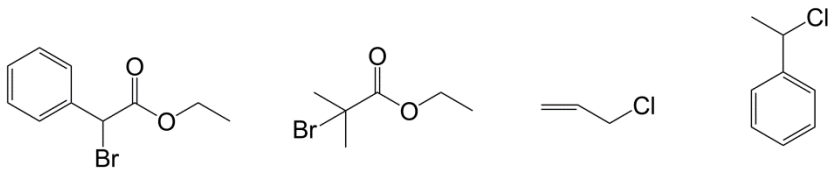

Figure 1.2. Examples of initiators used in ATRP reactions.

There is a vast library of initiators that can be used for ATRP. Interestingly, it is possible to prepare functional polymers by simply using an ATRP initiator with the desired functionality (e.g., azide). In addition, commercially available polymers such as poly(ethylene glycol) (PEG) can be modified and used as macroinitiators for ATRP, in order to prepare unique block copolymers.[35]

Solvents

There is a wide range of both polar and non-polar solvents that can be used for ATRP. When choosing the solvent for homogenous polymerizations, it is usually necessary to ensure that the monomer, the polymer and the catalytic complex are soluble, in order to achieve controlled polymerizations. In addition, one has to be aware that the control of the reaction can be also affected by the polarity of the solvent, as this parameter influences both k_a and k_d.[30, 36-38] Typically, more polar solvents provide faster and less controlled polymerizations, due to the increase of k_a and decrease of k_d. Despite this available information, systematic studies on the effect of the solvent on the ATRP control are scarce.[39]

Considering both environmental issues and industrial viability of ATRP, "green" solvents are the preferable ones to be used. On this matter, it is commonly accepted that the most environmentally friendly and inexpensive solvent is water. Controlled ATRP in aqueous heterogeneous medium, by emulsion, miniemulsion or suspension, has already been reported.[11] However, homogeneous ATRP using water as the solvent, has been proven very challenging due to the occurrence of side reactions that lead to partial catalyst deactivation and ultimately, poor control over the polymers molecular weight. In the past few years, remarkable achievements were made with aqueous controlled polymerizations of different hydrophilic monomers by ATRP variations techniques[40-42] (see details of the techniques in section 1.4.2). Successful ATRP reactions using other "green" solvents, such as supercritical carbon dioxide[43] and ionic liquids,[44] have also been reported.

Transition metal complexes

As already pointed out, metal catalysts mediate ATRP reactions through electron transfer by changing their oxidation state. In the activation of alkyl halides, the metal catalyst is oxidized by abstraction of the halogen atom, whereas in the deactivation of propagating radicals the metal catalyst is reduced by releasing the capping agent. Therefore, efficient metal catalysts must have high association constant to halide ions (halidophilicity), should be able to form two valence states with one valence difference and the coordination sphere of the metal should be able to embrace the halogen atom.[21, 24] Considering these features, the most suitable catalysts to be used are the transition metals such as copper,

iron, ruthenium, nickel and cobalt among others. In the majority of the cases the metal catalyst has to be coordinated with an appropriated ligand in order to enhance its reactivity and selectivity.[45] Cocatalysts that accelerate the catalytic cycle (activation/deactivation) are often used as additives. Some of these species include reducing agents, free radical initiators, halogen sources and amines.[20] Fundamental studies on catalyst complexes design are based on the combination of metals and ligands for the polymerization of selected monomer structures, taking into account several catalyst requirements: should control the polymerization at low concentration; should be easily removed from the reaction medium (or recycled); should provide good control over the polymer molecular weight; should be applicable to a wide range of monomers and functionalities and preference is given to abundant, safe and inexpensive metals.[20, 21] Information on the influence of the activity of different metal catalysts on the polymerization kinetics of different monomers can be found in several publications.[29, 31, 46, 47]

Due to its properties such as high activity, easily handling and accessible price, copper has been one of the most extensively studied catalysts for ATRP.[20] Usually, to achieve high catalytic efficiency, copper should be coordinated with nitrogen-based ligands (Figure 1.3).[33] The major drawbacks associated are the toxicity of the copper complexes, their intense color and sometimes the high amount required to achieve well controlled polymerizations.[16] Iron is another relevant metal that has been largely investigated, in combination with different types of ligands, such as both nitrogen-based and phosphorus-based ones among others, for the mediation of ATRP reactions.

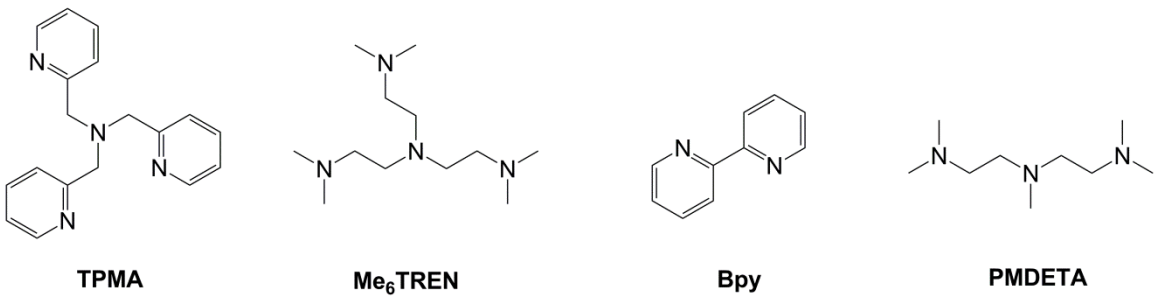

Figure 1.3. Examples of nitrogen-based ligands used in ATRP reactions.

Regarding the current concerns with the environment, iron is a preferable catalyst for ATRP since it is inexpensive, abundant, biocompatible and non-toxic. However, iron complexes present some limitations when compared with copper, namely sensitivity to functional groups, lower control efficiency in block copolymerization and narrower range of polymerizable monomers. Besides copper and iron, other metal catalyst such as, ruthenium and nickel among others, have been successfully employed in ATRP reactions. There are numerous research works dealing with the use of different catalysts for ATRP reactions, which are covered by extensive reviews.[20, 33]

The contamination of the final product with the catalysts is a serious concern when producing polymers via ATRP. The homogeneous metal catalysts can co-precipitate with the polymers, affecting their function and being toxic depending on the concentration.[48] Therefore, research efforts are focused on the discovery of more active species, as well as on the removing/recycling or reducing the catalyst amounts used in ATRP reactions in order to decrease/avoid post-polymerization purification processes, which can increase the cost of the polymers production. On this matter, several approaches have been used to easily remove catalysts namely: (i) supported catalysts,[49] in which the metals are attached to an insoluble supporting material in order to facilitate the catalyst removal; (ii) use of ligands to precipitate,[50] which consists of isomerized compounds that have different solubility in the reaction solvent, depending on the isomerized form, and thus can be precipitated after the reaction and (iii) use of fluorous biphasic systems[51] or ionic liquids[44] as the reaction solvents. A review about the catalyst separation in metal-catalyzed RDRP is available.[48] Alternatively, several ATRP variation techniques that allow the use of low concentrations of metal catalyst have been developed, and those will be presented in the upcoming section.

1.4.2. Atom transfer radical polymerization variations

Matyjaszewski's group has been extensively investigating the ATRP technique in order to develop new systems that could provide mild reaction conditions and use low amounts of metal catalyst, while maintaining a precise control over the polymers dispersity. This strategy aims to extend the range of application of the ATRP as well as to potentiate the implementation of the technique at an industrial scale. On this matter, great efforts have

been made by developing several ATRP variation techniques (Scheme 1.6), which could be effective in the presence of very low concentration of metal catalyst (1-100 parts per million (ppm) relative to the monomer concentration). The first approach was based on the activators generated by electron transfer (AGET) technique, which employed reducing agents in combination with Cu(II) species to prepare *in situ* the Cu(I) activator species.[52] Considering that in ATRP the rate of polymerization is not regulated by the total amount of catalyst used but by the ratio of activator to deactivator species (see Equation 1.2 in section 1.4.1), it was possible to adjust the AGET procedure in order to continuously regenerate the Cu(I) activator species during the reaction. This was accomplished by the creation of the activators regenerated by electron transfer (ARGET) technique,[53, 54] in which the copper catalyst could be used in very low concentration since the accumulated deactivating species ($Cu(II)X_2/L$) were continuously being reduced to regenerate the Cu(I)X/L activator species.[20, 27] The direct use of Cu(II) is another advantage of ARGET, since the metal in this valence state is more stable and more preferable in catalyst handling than Cu(I) used in normal ATRP systems.[20]

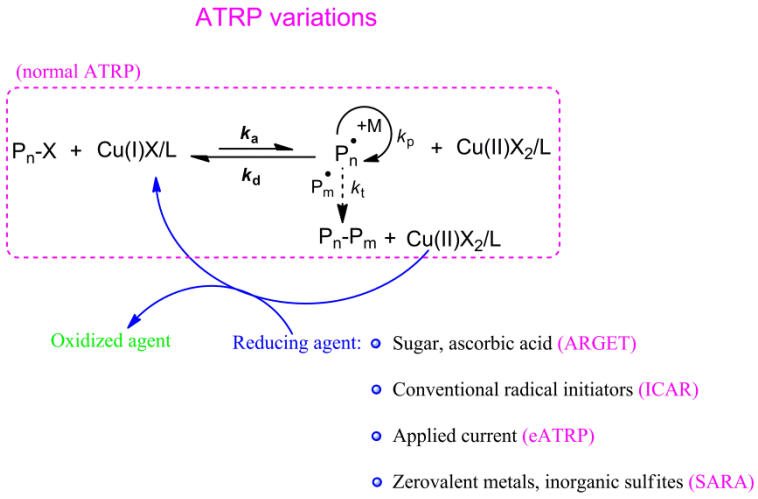

Scheme 1.6. Scheme of the different ATRP variation techniques.

Besides reducing agents, common radical initiators (e.g., azo compounds) can be used to continuously generate free radicals, which will also reduce the accumulated $Cu(II)X_2/L$ species, in the initiators for continuous activator regeneration (ICAR) technique.[53] However, the main drawback of this technique is the generation of new chains during the process, that is not appropriate for the synthesis of well-defined block copolymers.[5] Electrochemically mediated ATRP (eATRP) is one of the most recent and ecofriendly

ATRP variations, which operates via ellectrochemical (re)generation of the activator species.[55, 56] In this case, several parameters, such as applied current or potential, can be used to mediate the polymerization by manipulating the valence state of the metal catalysts. Recent research lead to the development of the later ATRP variation, named supplemental activator and reducing agent (SARA) ATRP, in which multiple compounds can be used to act not only as reducing agents, to regenerate the Cu(I)X/L activator species, but can also participate in a supplemental activation of the dormant species.[57, 58] This method has gained increasing attention since it can employ zerovalent metals to mediate the polymerization, which can be easily removed from the reaction medium.[58-60] In addition, Food and Drug Administration (FDA) approved inorganic sulfites can be also effectively used as SARA agents.[61-63]

As previously mentioned, along with the decrease of the catalyst concentration, the use of less harmful reaction solvents and lower reaction temperatures has been also a research trend on the ATRP field. The work presented in this thesis aimed to contribute to the development of new ecofriendly ATRP systems as well as for the expansion of the technique to different monomer families (Chapters 3 to 6).

1.4.3. Single electron transfer living radical polymerization fundamentals

The SET-LRP technique was developed by Percec´s research group.[23, 64-68] The discovery of the LRP of vinyl chloride initiated by iodoform and catalyzed by Cu(0)/TREN (TREN: tris(2-aminoethyl)amine), lead to the suggestion of a putative mechanism for that polymerization (Scheme 1.7),[65] that later became known as SET-LRP. However, further investigations on the reaction mechanism revealed that Cu(II)(TREN)X_2 (X = Cl, Br or I) did not terminate either reversibly or irreversibly the polymer chain growth. Additionally, the reversible termination step occurred only via degenerative iodine-exchange between the growing PVC-radical and iodoform or dormant PVC-I species.[69] Thus, the copper-catalyst was not regenerated completely due to the stability of Cu(II)(TREN)X_2.

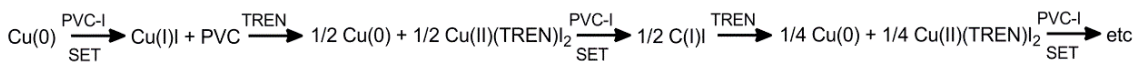

Scheme 1.7. Putative mechanism for the polymerization of vinyl chloride initiated by iodoform and catalyzed by Cu(0)/TREN.

As evident from Scheme 1.7, only half of Cu(0)-catalyst was regenerated after each SET-oxidation and TREN-mediated disproportionation steps. Control over the polymers molecular weight was provided by degenerative transfer. Therefore, Cu(0)/TREN-catalyzed LRP of vinyl chloride occurred via a competitive mechanism,[66] which was later called (outer sphere) single electron transfer/degenerative transfer-mediated living radical polymerization (SETDT-LRP). Understanding that the reversible termination step was not Cu(II)-mediated but included only degenerative iodine transfer had led to the development of the non-transition metal-catalyzed SETDT-LRP of vinyl chloride and acrylates initiated by iodo-derivatives and catalyzed by one-electron reductants ($Na_2S_2O_4$ or thiourea dioxide).[70-75] To regenerate copper-catalyst quantitatively instead of TREN ligand, which forms too stable inactive complexes with Cu(II)X_2, its permethylated derivative Me_6TREN (Me_6TREN: tris[2-(dimethylamino)ethyl]amine) was applied. Cu(II)X_2/Me_6TREN complex can be distorted, reacting with growing polymer chains and thus providing reversible termination. On the other hand, the use of bromo-initiators instead of iodo-ones, allowed to avoid degenerative transfer and formation of probable chemically unstable Cu(II)X_2/Me_6TREN, which can evolve free iodine. This technique was called SET-LRP (Scheme 1.8) and was successfully applied for the controlled polymerization of vinyl chloride and (meth)acrylates at room temperature.[23]

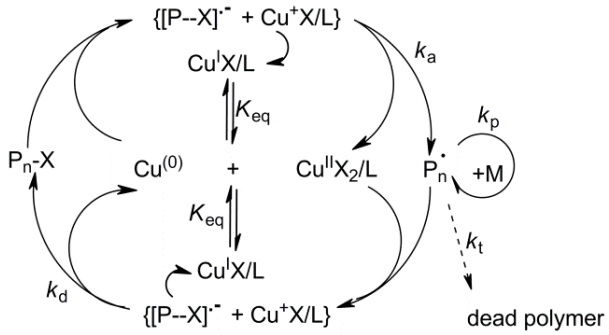

Scheme 1.8. SET-LRP proposed mechanism.

According to the authors assumptions, the proposed SET-LRP mechanism relies on an outer sphere electron transfer, in which Cu(0) acts as electron donor and the halide initiator and dormant species act as the electron acceptors (Scheme 1.8).[23] This process involves the formation of a radical-anion intermediate from the alkyl halide initiator and its stepwise decomposition via "heterolytic" cleavage of C-X (X: halogen) bond. The generated Cu(I)X/L species instantaneously disproportionate into Cu(0) and Cu(II)X_2/L,

in the presence of specific ligand and solvent in certain conditions,[76] leading to the regeneration of the Cu(0) activator and the generation of the Cu(II)X_2/L deactivator complex (autocatalytic system). In this case, the polymerization mechanism does not rely on the PRE as ATRP does, since the deactivator (Cu(II)X_2/L) is assumed to be formed by the decomposition of Cu(I)X/L species and does not accumulate in the system. In addition, the Cu(I)X/L complex (activator in ATRP) is considered to be just a precursor, since the disproportionation reaction is believed to be instantaneous. The so-called "nascent" Cu(0) is used to generate propagating radicals and, due to its high reactivity, very small amounts (ppm) of catalyst lead to fast and controlled reactions.

SET-LRP has been applied with great success since it is compatible with a broad range of functional monomers, both conjugated and non-conjugated monomers, homogenous and heterogeneous conditions, promotes fast reactions with very low occurrence of termination reactions and enables the preparation of very high molecular weight polymers (M_n > 1 000 000) at room temperature.[23, 77, 78]

1.4.4. Debate on the Cu(0)-catalyzed RDRP mechanism: SET-LRP *vs* SARA ATRP

As mentioned in the previous sections, SARA ATRP and SET-LRP are two metal-catalyzed RDRP techniques in which Cu(0) can be used in the beginning of the polymerization, to mediate the RDRP equilibrium, however governed by distinct mechanistic assumptions. Scheme 1.9 summarizes the main differences between the two polymerization mechanisms, which are essentially based on the activation, deactivation, comproportionation and disproportionation reactions.

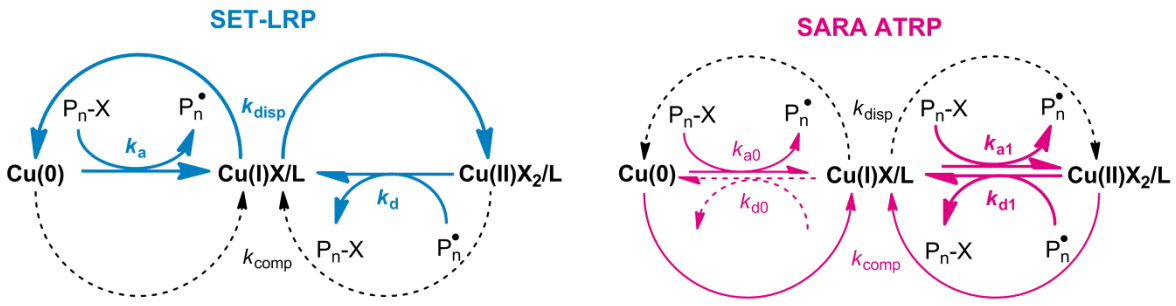

Scheme 1.9. Main differences between SET-LRP and SARA ATRP reaction mechanisms. Bold lines represent dominating reactions, thin solid lines represent contributing reactions and dashed lines represent negligible reactions.

In the SET-LRP it is assumed that the activation of alkyl halides (dormant species) is exclusively performed by Cu(0), through an outer-sphere process, whereas the Cu(I)X/L complex produced during the activation step instantly disproportionates.[23] Alternatively, the SARA ATRP mechanism is based on the activation of alkyl halides mainly by Cu(I)X/L complexes, through an inner-sphere process.[79] In addition, there are contributing reactions, such as the slow activation of alkyl halides by Cu(0) and comproportionation of $Cu(II)X_2$/L with Cu(0), which compensates the loss of Cu(I)X/L complexes due to the low occurrence of termination reaction.[40] Both techniques acknowledge that the deactivation is done by $Cu(II)X_2$/L complexes. These two different standpoints have aroused many discussion topics in the scientific community, mainly centered in the role of Cu(0) during the reaction, the mechanism of activation of alkyl halides and the extent of disproportionation of the *in situ* formed Cu(I)X/L species.[80, 81]

Arguments opposing ATRP

Percec has been the main opponent of the ATRP theory and thus, many of the studies are intended to prove that the formation of radicals species on copper-catalyzed RDRP is achieved by extremely active Cu(0) species. The reported work on Cu(0)-catalyzed polymerization of vinyl chloride at room temperature in water brought the first evidences that the reaction could not be mediated by inner-sphere electron transfer.[23] Some experimental conditions used were not in agreement with those proposed for the ATRP mechanism, namely the polymerization of non-conjugated monomers such as vinyl chloride and the use of non-stoichiometric amounts of metal catalyst (case of normal ATRP).[28] In addition, Percec proved that the polarity of the solvent has great impact on the polymerization rate which can be expected from an outer sphere transfer based process, due to the formation of an anion-radical intermediate, as the author proposed for the SET-LRP mechanism.[23]

Arguments opposing SET-LRP

The proposed mechanism of SET-LRP is based on the disproportionation of Cu(I)X/L, which is known to be dependent on the polarity of the polymerization media and on the ligand concentration.[82] Percec and co-workers reported studies on the disproportionation of Cu(I)Br coordinated with Me_6TREN complexes in different solvents and showed that

when the [Me_6TREN]/[Cu(I)Br] ratio is lower than the unit, there is an extent of disproportionation leading to the formation of Cu(0).[82] However, the results obtained using dimethylsulfoxide (DMSO) as a solvent were measured after 60 min, period time during which a regular SET-LRP of MA in the same conditions could lead to complete monomer conversion.[23] Therefore, the presence of Cu(I)Br/ Me_6TREN complex during those 60 min could not be ruled out. In addition, for [Me_6TREN]/[Cu(I)Br] ratios equal or greater than 2, the diproportionation was suppressed allowing Cu(I)Br/Me_6TREN complex to exist in the solvent.[82]

The equilibrium between Cu(0)-Cu(I)X/L-Cu(II)X_2/L-RX was also studied by Matyjaszewski's group.[80] The authors determined the activation barriers of activation/deactivation and disproportionation/comproportionation (Scheme 1.10) and found that comproportionation of Cu(0) with Cu(II)X_2/L to form Cu(I)X/L was slow but dominant in all solvents tested. As result of this study, Matyjaszewski suggested that the mechanism of polymerization using Cu(0) as a catalyst was similar to the ARGET ATRP process*, with dormant species being activated by the inner sphere transfer process. Theoretical and experimental work about the mechanism of C-Br bond reductive cleavage in alkyl halide species, commonly used as SET-LRP and ATRP initiators, were reported by Isse and co-workers.[25] The results suggested that the "heterolytic" decomposition mode is not possible for the studied initiators under outer sphere electron transfer conditions, rejecting the proposed SET-LRP mechanism for the activation of dormant species.

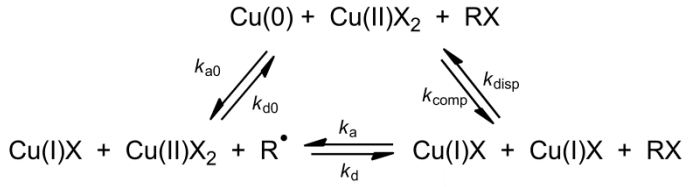

Scheme 1.10. Cu(0)-Cu(I)X/L-Cu(II)X_2/L-RX equilibrium steps.

* The concept of SARA ATRP was later introduced when the authors recognized the direct activation of alkyl halides by Cu(0) (supplemental activator) as well as the comproportionation (reducing agent) events during the polymerization.[58]

Due to the importance of the subject, during the course of this PhD project, many advances were made regarding the study of the metal-catalyzed RDRP mechanism.[78, 83-90] In addition, Chapter 2 of this thesis presents relevant work on the determination of the extent of disproportionation under real polymerization conditions. The debate on the Cu(0)-catalyzed RDRP was recently covered in two comprehensive reviews which suggested that the polymerization is ruled by the proposed SARA ATRP mechanism.[81, 83] Nevertheless, some authors still adopt the SET-LRP terminology. Taking into account the results obtained in this project, as well as the literature available, the metal-catalyzed RDRP method will be referred as ATRP (including ATRP variations) in the subsequent chapters.

1.5. Controlled polymer structures/functionalities by RDRP and their applications

With the appearance of the RDRP techniques, many different polymeric materials with complex architectures were developed.[10] As the "living" polymers present active chain-ends, a wide range of well-defined block copolymers with several compositions can be easily synthesized (Figure 1.4). The preparation of different polymeric structures could be accomplish by using only RDRP techniques, the combination of the later with other chemical synthesis methods, such as "click" chemistry,[91] or by the modification of commercially available polymers (e.g., PEG) that can be turned into RDRP macroinitiators/macro-chain transfer agents.[92] Using these strategies, it is possible to tailor the properties of some materials in order to expand their range of application. Graft copolymers can nowadays be synthesized by RDRP with a controlled number of branches per branch point and defined branch point spacing.[93] Besides the control over the copolymers composition, RDRP is useful to prepare functionalized polymers with branched architectures, such as: star-shaped, denditric/hyperbranched and networks among others (Figure 1.4). Branched polymers can be prepared by recurring to multivinyl crosslinkers, multifunctional initiators or coupling agents. These approaches avoid multistep reactions required to prepare those polymer structures by stepwise organic chemistry methods. Due to the "infinite" number of possible combinations of the mentioned agents, it is possible to obtain materials with the same polymers but

completely different properties by simply changing the order of monomer addition during the polymerization. Moreover, desired functionalities can be introduced in telechelic† polymers, which are commonly used as block units for the preparation of branched polymers.[94] More information on functional polymers by RDRP can be found in an extensive review by Matyjaszewski.[95]

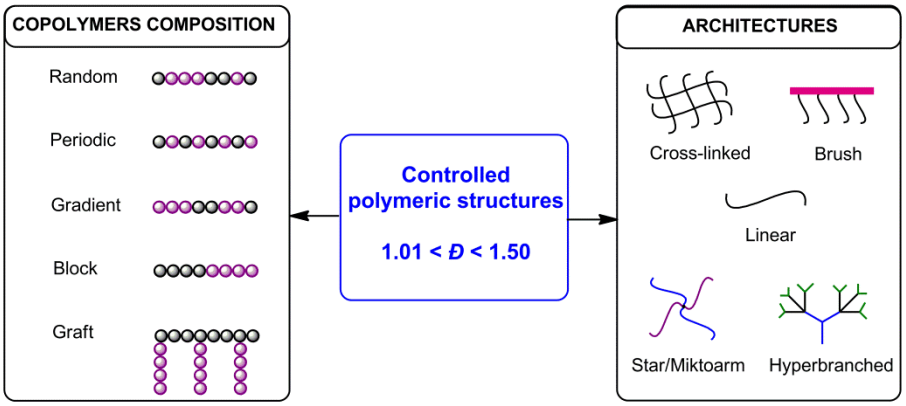

Figure 1.4. General topology and composition of polymers produced by RDRP.

The modifications of both polymer structure and functionality allow the design of a myriad of new materials with targeted properties for specific applications. Therefore, high performance materials produced by RDRP can be applied in a wide range of segments, such as surfactants, lubricants, dispersants, coatings, paints, adhesives, thermoplastic elastomers, biomaterials, membranes and electronic materials among others.[2, 3, 10] Especially, the use of RDRP to prepare tailor-made materials for biomedical applications has been extensively investigated,[96] mainly for the development of both delivery systems[97, 98] and polymer-protein conjugates (bioconjugates).[99] There is also a less-explored but very interesting class of polymers, polymers with intrinsic therapeutic activity (polymer drugs), which have been showing promising results for the treatment of several health conditions.[100-102] However, the main limitations concerning the use of these polymers as effective therapeutics are based on the lack of control over their properties due to the use of conventional polymerization techniques and/or problems related to the proper functionalization of the synthesized polymers. In order to prepare reliable and effective therapeutic products, it is necessary to ensure, among other aspects, that the

† A polymer can be considered to be telechelic if it contains end-groups that react selectively to give a bond with another molecule.[94]

materials present homogenous properties. Therefore, the use of RDRP techniques could provide an excellent basis for the design of new polymer drugs, with enhanced performance.

1.6. Introduction on polymeric bile acids sequestrants

The use of polymeric materials in both the pharmaceutical and the medical fields has received great attention during recent years due to their distinctive physico-chemical characteristics, such as their biocompatibility and their appropriate mechanical properties. Polymers have been used for a wide range of applications in the biomedical area, namely in drug delivery systems, as components of artificial organs, in the delivery of antibodies and in medical devices, among others.[100]

Recent progress in this field has led to the development of a new class of drugs, namely polymer therapeutics,[101] which can be divided in two major types according to the polymer function. These include polymers used as vehicles for targeted drug delivery and polymers with intrinsic therapeutic activity.[103] Examples of polymer therapeutics are polymer-drug combinations (pro-drugs), bioconjugates and polymers with sequestration properties.[104]

The use of polymers that act as active pharmaceutical ingredients is of great interest and offers considerable potential since they present some advantages in comparison to small molecule drugs. These advantages include long-term safety profiles, lower toxicity, the capacity to recognize and to bind molecular components and their polyvalence (raising the possibility of multiple interactions with the disease species).[103] Furthermore, the structure of the polymers can be designed and functionalized with many different pendant molecules, leading to materials with different biological activities than those of conventional drugs. In addition, the action of these polymers can be limited to the gastrointestinal (GI) tract, since their high molecular weight prevents their absorption into the systemic circulation.[100] Therefore, polymers can be used to selectively bind and remove detrimental molecules from the GI tract as well as to eliminate viruses, toxins and bacteria. These polymers properties constitute an advantage in treatments in which systemic exposure of the drug is undesirable.[105] Through the manipulation of the polymer

structure and the incorporation of appropriate functional groups, it is possible to develop polymer therapeutics with high selectivity and potency towards specific molecules, also known as polymer sequestrants.[102] In recent years, different polymer sequestrants have been developed to bind and to remove species that cause diseases, such as phosphate ions (renal diseases), potassium ions (hyperkalemia), iron salts/complexes (iron overload disorders) and toxins,[106] among others.[100, 103] Some of these polymer therapeutics are currently available, exhibiting and providing healing benefits at acceptable therapeutic doses.[104] Particular interest is devoted to the use of this approach to create materials that have the ability to sequester bile acid molecules, the so-called bile acids sequestrants (BAS).

BAS have an important application in the control of the blood cholesterol level, a major cardiovascular disease risk factor, which is a leading cause of death, an increasing source of morbidity and a major factor in disability and ill-health, especially in the industrialized countries.[107] Commonly, cholesterol lowering drugs are based on statins or cholesterol absorption inhibitors, which rely on a different treatment strategy than BAS.[105, 108] Statins act directly on the cholesterol synthesis by inhibiting the HMG-CoA reductase (rate-controlling enzyme in the cholesterol production process), while cholesterol absorption inhibitors have the ability to reduce the intestinal absorption of dietary and biliary cholesterol at the level of the brush border of the intestine. On the other hand, BAS operate in an indirect way by capturing bile acids in the small intestine, which causes an organism response that leads to cholesterol consumption and, ultimately, to the reduction of the blood-cholesterol level. Due to their mechanism of action, BAS present some advantages in comparison to other therapies. For instance, statins therapy (the first line of treatment) is not advised for pregnant women, nursing mothers and patients with significant hepatic dysfunction.[100, 109] Moreover, in about 10% of patients, long-term complications can arise such as liver dysfunction and musculoskeletal symptoms.[109] These are the most common reasons for statins discontinuation.[100] Thus, it is of utmost importance that new and more efficient BAS are developed for patients that cannot use statins or must take high statin doses. However, the presence of such polymeric therapeutics in the market is very limited at present.

1.7. Bile acids and cholesterol homeostasis

Bile acids are cholesterol based amphiphilic molecules produced in the liver. They act as biological surfactants aiding food digestion and absorption of lipids in the GI tract.[104] In addition, bile acids control several metabolic processes such as the breakdown of both glucose and triglycerides and, principally, the control of cholesterol homeostasis.[110]

Cholesterol is excreted from the body through the bile as free cholesterol or in the form of bile acids, after a conversion process.[111] Nearly 50% of the cholesterol catabolism is governed by its conversion into bile acids.[110, 112] The first reaction of this process is catalyzed by the hepatic microsomal cholesterol 7α-hydroxylase, leading to the formation of the primary bile acids, (cholic acid and chenodeoxycholic acid in humans). The second step is based on the conversion of the primary bile acids into deoxycholic acid and lithocholic acid (secondary bile acids), by the action of the intestinal bacteria flora.[110, 111] The bile acids present in the bile consist largely of 30-40% of cholic acid, 30-40% of chenodeoxycholic acid, 20-25% of deoxycholic acid and 1-2% of lithocholic acid (Figure 1.5).[111] Bile acids are synthesized in the parenchymal cells (hepatocytes) of the liver and are stored in the gall bladder, that releases the bile through the bile duct into the GI lumen, upon ingestion of a meal.[105] Subsequently, the bile acids enter into the intestine lumen, to aid food digestion, being the most part, further reabsorbed by the distal ileum, returning to the liver via portal circulation. This process is known as the enterohepatic cycle (Figure 1.6).[110]

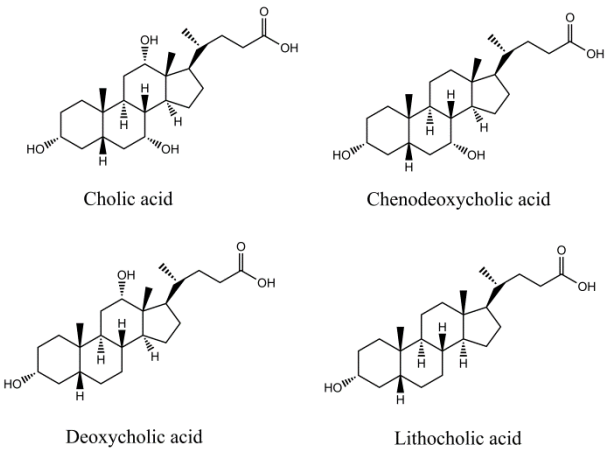

Figure 1.5. Chemical structures of bile acids.

In this cycle, there is a small amount (nearly 5%) of bile acids that can be lost through feces excretion. This loss is compensated by the synthesis of new bile acids in the liver. The mixture of bile acids present in the body is very complex since they are commonly conjugated with the amino acids taurine or glycine, (ratio of taurine/glycine = 1/3).[113, 114] The pKa of bile acids is between 2 and 5 and so, under the conditions that prevail in the small intestine (pH = 7.0-9.0), these molecules are in their ionized form (also called bile salts).[115]

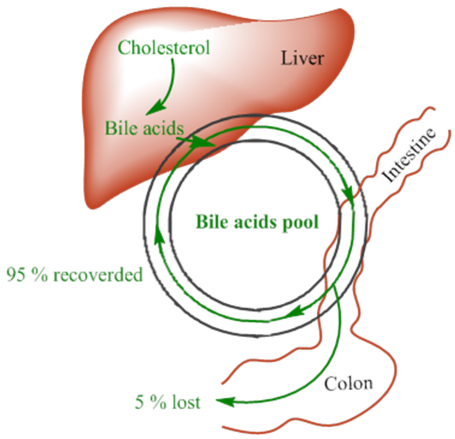

Figure 1.6. Illustration of the enterohepatic cycle.

1.8. Bile acid sequestrants – features and mechanism of action

Hypercholesteremia is one of the most important risk factors for coronary heart disease, a health issue that affects millions of people around the world, especially in the developed countries. As previously mentioned, BAS can be used as cholesterol reducing agents without having the problems associated with the long-term systemic exposure like statins.

Usually, BAS are cationic polymeric hydrogels that bind the negatively charged bile salts in the small intestine, avoiding their reabsorption, and causing fecal bile acid excretion. This loss of bile salts induces the conversion of cholesterol into bile within the liver, which promotes an increase in low density lipoprotein receptors and the increased clearance of low density lipoprotein cholesterol from the circulation system.[116] BAS bind bile salts mainly by both electrostatic interactions and hydrophobic interactions.[104, 117] The chemical structure of bile acids is represented by a hydrophobic core (steroid skeleton) and a hydrophilic anionic segment. For this reason, an efficient BAS must have

positive charges within its structure and a maximized hydrophobicity, while maintaining sufficient hydrophilicity to provide appropriate swelling characteristics in physiologic environment. Also, an appropriate density of cationic charges is required to ensure the occurrence of electrostatic interactions (the primary interactions of the binding process) with anionic bile salts.[118] For this purpose, the use of synthetic methods that result in the creation of polymers that possess appropriate controlled structure, architecture and functionality is of extreme importance.

Additionally, BAS have shown benefits beyond controlling high cholesterol levels. One of the most significant is the ability to reduce the fasting blood glucose and to decrease hemoglobin A1c in diabetic patients. Although the mechanism of action is not completely clear,[108] it is expected that these polymer therapeutics may also have a very important role in the treatment of hypercholesterolemic patients that present type II diabetes.

1.9. Commercial bile acid sequestrants available

BAS have been used for about thirty years[116] to decrease cholesterol blood levels in humans. Scientific research has led to the development of several products,[119-122] however exhibiting lower clinical efficacy compared to statins. Three examples that are approved by FDA for hypercholesterolemia treatment and are on the US market are (a) Cholestyramine, (b) Colestipol and (c) Colesevelam hydrochloride (Table 1.1 and Figure 1.7).[112, 123] Two other BAS compositions are commercially available, including (d) Colextran in Spain and Italy and (e) Colestilan (also known as Colestimide) in Japan[124, 125] (Table 1.1 and Figure 1.7).

Cholestyramine and Colestipol are the two first generation products of BAS. In the case of Cholestyramine, the binding capacity towards bile acid molecules was recognized only after its commercialization as an anion exchange resin.[117] Cholestyramine is a cationic hydrogel based on PS, partly crosslinked with divinylbenzene (2%), with molecular weights greater than 10^6 and swelling ratios of approximately 2.5 g/g (amount of water uptake per gram of dry polymer).[117, 126] This product can be prepared by the chloromethylation of the polymer, followed by quaternization of the hydrogel with trimethylamine, (4 meq of cationic groups per gram of dry polymer).[127] Colestipol is a

condensation polymer produced by the step-growth polymerization of diethylenetriamine and epichlorohydrin and is commercialized as its hydrochloride salt (Figure 1.7 (b)). Due to the type of functional groups present in the Colestipol structure (secondary and tertiary amines), the efficacy of this BAS is more dependent on the pH of the medium than is the Cholestyramine, which has a permanent positively charged quaternary ammonium ion. However, with regard to the pH of the small intestine, most of the secondary amines and tertiary amines that have a pKa value in the range from 9-10[128] should be ionized.

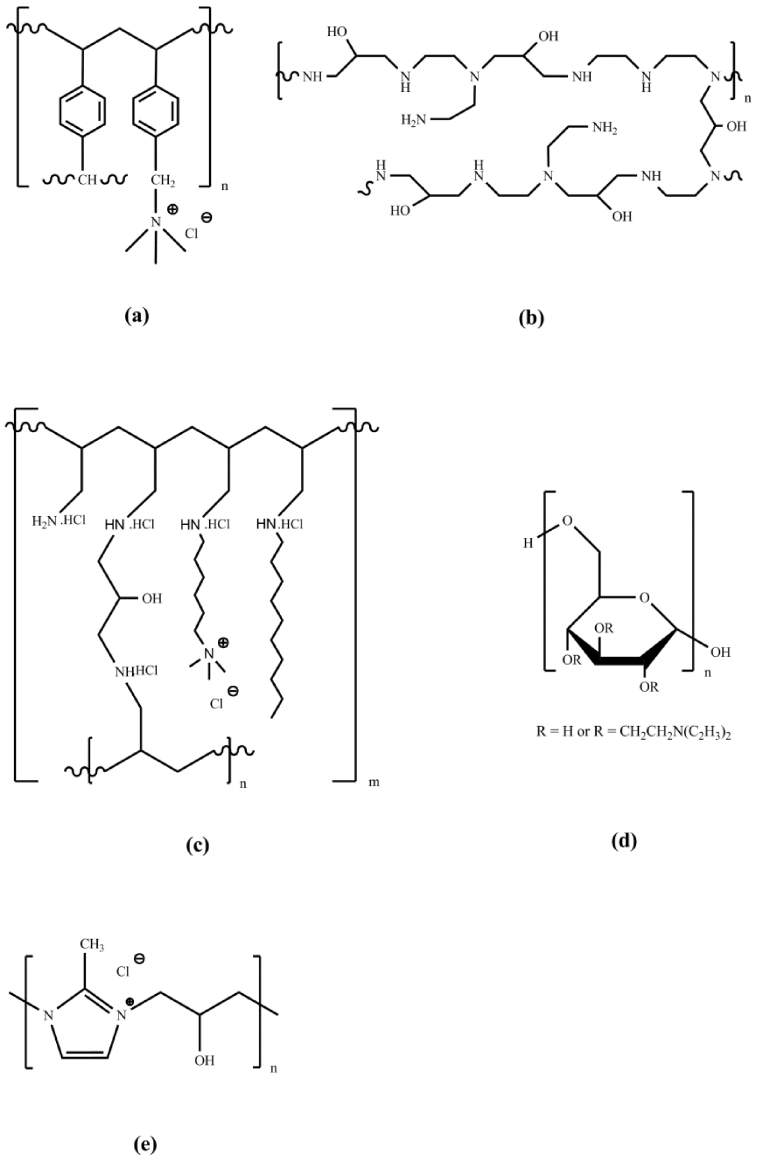

Figure 1.7. Chemical structures of the commercially available BAS: (a) Cholestyramine; (b) Colestipol; (c) Colesevelam hydrochloride; (d) Colextran and (e) Colestilan.

Despite the differences in their molecular structures, Cholestyramine and Colestipol present the same order of clinical efficacy. As an example, the Cholestyramine binding capacity has been reported as being 1.8-2.2 g of sodium glycocholate per gram of dry polymer (Table 1.1).[125] Cholestyramine and Colestipol bind and remove preferentially dihydroxy bile acids from the GI tract.[116] Since the liver produces a mixture of dihydroxy and trihydroxy bile acids and only the dihydroxy ones are removed significantly, the trihydroxy acids content in the bile acids pool increases over the time. This fact leads inevitably to a decrease in both the Cholestyramine and Colestipol efficacy. In fact, the low binding capacity towards trihydroxy acids is the main reason for the low efficacy of both Cholestyramine and Colestipol.[129] Adverse effects that have been reported involving these two BAS are related to their complexation with fat-soluble vitamins, a decrease in the absorption of some other drugs and to GI distress (e.g., dyspepsia, nausea and constipation).[116] In addition, these BAS present poor patient compliance and the need to be administered in high doses; usually it is necessary to take 16-24 g/day to reduce the cholesterol level by 20%.[118] Part of this inefficiency is also due to the competition between the BAS and the active bile acids reuptake transporter system of the GI tract.[105] In order to overcome this limitation, it was necessary to create BAS molecules with a greater binding strength and affinity towards bile acids.

Colextran, a modified dextran, is an ion exchange resin that exhibits some efficacy in reducing total cholesterol blood levels as well as reducing triglyceridemia in patients presenting with type II and type IV hypercholesterolemia.[117]

The second generation of BAS, represented by both Colesevelam hydrochloride and Colestilan, was specifically designed to have a greater affinity for the binding of bile acids leading to fewer side effects.[118, 130] Colesevelam was approved by the FDA in 2000 for the treatment of hypercholesterolemia, either as a monotherapy, or in combination with statins. Since then, Colesevelam has been approved by the FDA for treatments, as an adjunct to diet, exercise, and other antidiabetic drugs, to improve glycemic control in patients with type II diabetes. Another clinical indication is the treatment of familial hypercholesterolemia in boys and in postmenarchal girls, in the age ranging from 10 to 17 years, as a monotherapy or in combination with a statin.

Table 1.1. Commercially available BAS.

BAS	Approval date	Brand name	Molecular name	Binding capacity (g of bile acid/g of polymer) polymer)	Therapeutic dose (g/day)	Reference
Cholestyramine	1973 (FDA)	Questran® Efensol® Prevalite® Ipocol® Vasosan® Quantalan®	Poly(styrenebenzyltrimethylamoniumchloride)	1.8-2.2 g [a]	12-24	116, 125
Colestipol	1977 (FDA)	Colestid® Lestid® Cholestabyl®	*N*'-(2-aminoethyl)-*N*-[2-(2-aminoethylamino)ethyl]ethane-1,2-diamine 2-(chloromethyl)oxirane hydrochloride	0.5-0.7 g [a]	5-30	116, 125
Colextran	1985 (Spain)	Dexide® Pulsar® Rationale®	Diethylaminoethyl-dextran hydrochloride	[b]	2-3	125
Colestilan	1999 (Japan)	Cholebine®	2-Methylimidazole polymer with 1-chloro-2,3-epoxypropane	2.3 g [c] 2.4 g [d]	3	125, 131
Colesevelam hydrochloride	2000 (FDA)	Welchol® Cholestagel®	Allylamine polymer with 1-chloro-2,3-epoxypropane, [6-(allylamino)-hexyl]trimethylammonium chloride and *N*-allyldecylamine, hydrochloride.	[b]	3.8-4.4	125

[a] Determined for sodium glycocholate; [b] Not available in the literature; [c] Determined for sodium cholate in water at 37 °C; [d] Determined for sodium deoxycholate in water at 37 °C

The chemical structure of Colesevelam is substantially different from those of the first generation BAS since it includes spaced long hydrophobic chains, with protonated primary amines. At the intestine environment pH, these structures establish electrostatic interactions with the bile acids molecules and the quaternary amines stabilize the hydrogel.[116, 132] Additionally, the crosslinked epichlorohydrin-based structure reduces the possibility of systemic absorption while decreasing the interactions with the GI tract lining. In comparison with Cholestyramine and Colestipol, Colesevelam hydrochloride exhibits less side effects, these mainly being minimal constipation and GI irritation,[133, 134] due to its improved water retaining characteristics that create a soft, gelatinous-like material.[132] Another important feature is related to the dose decrease to 2-16 g/day.[116] *In vivo* experiments (using hamsters) have shown that Colesevelam is three times more efficient than conventional BAS in the sequestration of bile acids. Due to its structure, Colesevelam has affinity to both dihydroxy and trihydroxy bile acids which enhances the clinical efficacy in long-term treatments.[132]

Colestilan (Figure 1.7 (e)) is a BAS that has imidazolium salt units, derived from the crosslinking reaction between poly(2-methylimidazole) and epichlorohydrin. Its clinical pharmacological effects are similar to those exhibited by Cholestyramine, at approximately one quarter of the dose.[131] *In vitro* adsorption studies have been used to demonstrate the superior binding capacity of Colestilan when compared with Cholestyramine, probably related to the 1.6 times greater ion exchange capacity[131] and a higher swelling capacity in water, making the binding sites more accessible to the bile salts. It has also been shown that in comparison with Cholestyramine, Colestilan has a lower rate of adsorption to other drugs.[135] Even though, Colestilan exhibits a greater affinity towards bile salts than cholesthyramine, a steric hindrance effect that is due to the hydroxyl group on the steroid ring, seems to be a serious limiting factor for the adsorption of bile salts by this polymeric therapeutic molecular system.

Despite the advantages of the second generation of BAS that have been identified, such as improved efficacy, better tolerance, reduced side effects and reduced drug interactions, further developments in the BAS synthesis field are still needed in order to enhance the specificity of the polymers towards bile salts. By this means, it should be possible to reduce common undesirable side effects (e.g., stomach distress), to enhance the

therapeutic efficacy of the polymer therapeutics, to reduce the therapeutic dose and to improve the patient compliance.

1.10. Bile acid sequestrants functional – polymers and synthesis routes

Over the last decade, different materials have been tested, both *in vivo* and *in vitro*, for their binding of bile salts. These include dietary fibers, anti-acids, charcoal and various polymers.[136] Due to their properties (e.g., their high molecular weight and their multiple functionalities) polymeric materials are the most widely studied materials for this application. Cationic hydrogels (with epichlorohydrin as the crosslinking agent) based on (meth)acrylates, vinyl polymers, allyl polymers, poly(meth)acrylamides and polyethers are the most common used polymeric structures. Also, polymers based on PS backbones (as a hydrophobic segment), containing amine/ammonium pendant groups (as a cationic, hydrophilic segment) have been employed (Figure 1.8).[100, 104, 105] The cationic groups ensure the occurrence of electrostatic interactions with the ionized bile salts, the more efficient being usually based on the ammonium group.[113, 137] Other cationic groups, such as guanidinium have been tested showing poorer results.[137] The polymers hydrophobic segments are used to attract the steroid skeleton of bile salts.

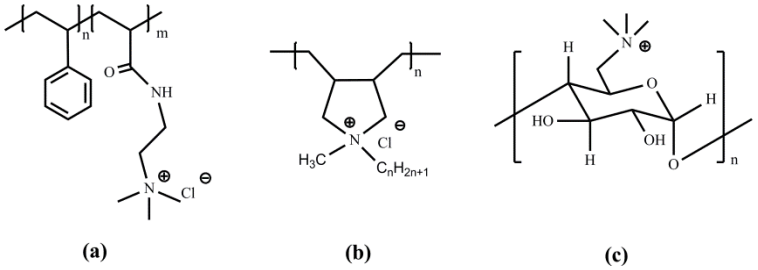

Figure 1.8. Chemical structures of representative BAS reported in the literature: (a) PS-*b*-poly(*N*,*N*,*N*-trimethylammoniumethylene acrylamide chloride);[138] (b) *N*-alkyl-*N*-methyldiallylammonium salt ;[118] (c) quaternized amino methylan.[113]

The design and synthesis strategies of BAS are based on these two types of interactions (electrostatic and hydrophobic), requiring a balance between the charged groups and the hydrophobic segments in order to achieve the maximum binding capacity. It is also necessary to take into account the competing desorbing forces that are present in the GI tract and the time limiting factor for the bile salts binding (the small intestine transit time

for pharmaceutical dosages is 3 ± 1h).[113] Therefore, an efficient polymeric BAS must exhibit a high binding capacity (number of binding sites) and a high binding strength (force required to separate the bile salts from the BAS) as well as selectivity towards bile acid molecules.[118] Other key factors in the design of BAS are the polymers backbone flexibility (needed to provide the appropriate swelling properties) and the relative position of the cationic groups (needed to prevent intra-polymeric interactions).[139]

In vitro studies that are related to monitoring binding mechanisms are usually performed through the use of isotherms of sorption.[117] BAS polymer samples are kept in contact with bile salts (individual or combination) solutions at a constant temperature and a constant pH. In general, the equilibrium concentration of bile salts is measured by high performance liquid chromatography (HPLC)-related techniques that allow the rapid separation and quantification of the compounds.[114] *In vivo* studies, normally with hamsters as the animal model, are also used and can give more realistic results, since it is difficult to mimic intestinal physiological conditions in the laboratory. The results obtained from the binding experiments are of extreme importance since they can provide relevant information with respect to the design of molecular structures with suitable properties that are essential to afford efficient BAS materials.

1.10.1. Biopolymeric materials

Fibers constitute an important part of the daily diet of humans, corresponding to polymer-based carbohydrate materials that are resistant to the digestion process, including both soluble fibers and insoluble fibers.[140, 141] These biopolymeric materials have been shown to be capable of binding bile salts both *in vitro*[140-146] and *in vivo*.[147-149] The advantages of its consumption to human health are amply claimed.[150, 151] However, studies in humans have shown that the extent of cholesterol level reduction that is due to fiber consumption, can be very limited.[152, 153] Several studies have been used to prove the ability of different types of food to bind bile acids, these foods having a binding capacity that is substantially lower than that of Cholestyramine.[154-157] Moreover, the binding activity of dietary fiber products has also been determined for bile acids that are in a glycoconjugated form.[158] The enzymatic modification of dietary fibers and/or their chemical modification can lead to an improvement of the binding capacity,[159] as can a simple transformation of food,

such as the steam cooking.[160, 161] The bile acids binding capacity of both water soluble and water insoluble dietary fibers can be predicted by a simplified model developed by Zacherl and co-authors. This model correlates the binding capacity with the fiber viscosity after digestion.[162] It was shown that an increased viscosity of the fiber-containing medium leads to an increase of the binding capacity towards bile salts. However, this correlation was not verified when the viscosity of oat fiber-based slurries was intentionally diminished, showing that the binding mechanism could also be regulated by other interactions, such as hydrophobic interactions. Besides bile acids removal, other effects such as the inhibition of the intestinal absorption[163] or the increased excretion[164-166] of cholesterol can be also promoted by these fibers.

Other types of biopolymers, including polysaccharides, have been used as starting materials to produce BAS due to their biocompatibility, low toxicity, hydrophilicity[126] and the presence of hydroxyl groups that can be easily functionalized. β-Cyclodextrin is an oligosaccharide composed by seven glucose units linked in a cyclic structure and it has been reported to produce hypolipidemic and hypocholesterolemic effects in animals.[112] The mechanism of action of these polymers involves the absorption of lipids and the increase of fecal excretion. Zhu's research group has synthesized crosslinked aminated β-cyclodextrin polymers with a degree of crosslinking ranging from 14 to 20%.[167] Both the hydrophobic cavity and the hydrophilic exterior segments available in the polymer structure facilitated the binding of the bile salts, by the creation of inclusion complexes. The size of the cavity was found to be an important parameter since the binding capacity was lower towards more hydrophilic bile acids (higher content of hydroxyl groups in the structure) due to steric hindrance. Functionalization of the polymers was achieved by introducing alkylammonium groups through tosylation, followed by treatment with trimethylamine. However, the reaction presented low efficiencies (1 functional group per 5 units of β-cyclodextrin). The binding capacity of the prepared materials was evaluated in the presence of bile salts with different hydrophobic characters, in a temperature range of 10-50 °C. Despite the low degree of functionalization, the authors found that the presence of the quaternary ammonium groups in the polymer structure enhanced their binding capacity, suggesting that electrostatic interactions play an important role in the complexation process. However, this component became of less relevance when the temperature increased.[167] Also, an increase in the degree of crosslinking of the hydrogels

led to a decrease in their binding capacity, since the β-cyclodextrin cavity was less available for the interactions. The maximum binding capacity of the functionalized β-cyclodextrin was close to 0.3 mmol/g (mmol of bile salt/g of dry polymer).

Dextran hydrogels modified with alkylammonium groups have been used to study the extent of correlation between the hydrophobic character of BAS networks and their binding capacity.[126, 139, 168] In the study, dextran spherical particles (molecular weight of 70 000) or linear dextran (molecular weight of 30 000) were crosslinked with epichlorohydrin and functionalized with *N,N*-dimethyl-*N*-alkyl ammonium chloride groups, with an extent of functionalization of approximately 20%. This value corresponds to a defined balance between the repulsive electrostatic forces and the hydrophobic interactions. The degree of crosslinking was optimized to afford hydrogels that were able to take up 3-4 g of water, at equilibrium, per gram of dry polymer.[169] By varying the alkyl chain length, the authors showed that the binding process could be regulated by different mechanisms depending on the hydrophobic character of the BAS network.[139] For alkyl chains longer than the equivalent of a C_4 chain sequence, the sequestration of bile salts took place by mixed micelle formation, with predominance of the hydrophobic interactions between the polymer and the steroid skeleton of the bile salts. For shorter chain lengths, the binding process was found to be regulated by the electrostatic interactions between the ammonium groups and the anionic bile salts. In these hydrogels, hydrophobic interactions seem to play a very important role in the bile salts sequestration, originating materials with higher binding capacity than that shown by the commercial Cholestyramine.

Lee and co-workers investigated the competitive binding of bile salts by modified methylans (polysaccharides with molecular weight higher than 100 000),[113] in order to simulate the intestinal environment. The polymers exhibited higher binding capacities than the commercial Cholestyramine. However, these materials presented the same limitation exhibited by conventional BAS, which is the poor affinity towards trihydroxy bile salts in comparison to the more hydrophobic dihydroxy ones. This result emphasizes the importance of hydrophobic interactions in the bile salts sequestration process.

Chitosan is a glucosamine-based polymer derived from the deacetylation of chitin and it can be considered an interesting starting polymer for the preparation of BAS. This biopolymer is not digestible by humans and presents good biocompatibility and safety. Chitosan was first tried in the deacetylated form in animal studies and proved to have good hypocholesterolemic action, to an extent that was comparable with that of Cholestyramine.[170-174] Zhou and co-authors studied several samples of chitosan with different molecular weights and degrees of deacetylation in order to establish a possible correlation between the properties of the polymers and their binding capacity.[174] However, under the experimental conditions used, it was not possible to establish any relationship that could predict the polymers efficiency as BAS. In comparison to the Cholestyramine binding capacity, chitosan hydrolysates (molecular weight between 5 000 and 20 000)[175] as well as chitosan modified by quaternization of the amino groups,[176] provided materials with greater efficiency. This biopolymer was also modified so that it contained diethylaminoethyl groups in its structure, giving rise to a material that possessed higher sequestration capacity, especially for deoxycholate.[177] Another interesting and successful approach is the use of organic acid salts of chitosan.[178, 179] In this case, the absorption of bile salts occurred by ionic exchange with the displacement of the anion of the acid.

1.10.2. Synthetic polymers

In an attempt to design the appropriate polymer structure for an efficient BAS and to understand their binding mechanism with bile salts, many authors have used synthetic polymers with different functionalities and structures.[138, 180, 181]

One strategy that is commonly followed for the preparation of polymeric BAS is the modification of commercial BAS polymer backbones, such as polyamines (similar structures of Colestipol and Colesevelam).[168] Figuly and co-workers have reported the synthesis of 61 different poly(alkylamine)-based polymer networks, prepared by the reaction of several (di)amines with dihalo compounds or diepoxides, in different solvents/mixtures.[182] The swelling capacity of the hydrogels increased with the increase of both polarity and polymers flexibility and with the decrease of the degree of crosslinking. Preliminary *in vitro* binding experiments with methyl cholate were used to

demonstrate that the hydrogels formed by diamines and α,ω-dibromoalkanes were more efficient than Cholestyramine. Considering the main structure of Cholestyramine (PS crosslinked with divinylbenzene), Zhang and colleagues reported an innovative approach to the BAS synthesis. The new methodology was based on the bio-conjugation of the polymer with the bile acid molecules.[181] Bile acids have been either attached to polymer backbones or chemically modified in order to produce polymerizable compounds for different biomedical applications.[183] Particles of PS crosslinked with divinylbenzene, with several diameters, were synthesized with 0-15% of the chloromethylene groups being quaternized by the aminated derivatives of cholic acid. The rest were quaternized as ammonium groups using triethylamine. Despite the low degree of functionalization, the authors suggested that the use of bile acid molecules as part of the polymer structure would lead to an enhanced binding capacity due to van der Waals interactions and/or hydrogen bonding interactions between the nearest-neighbors (Figure 1.9).[181]

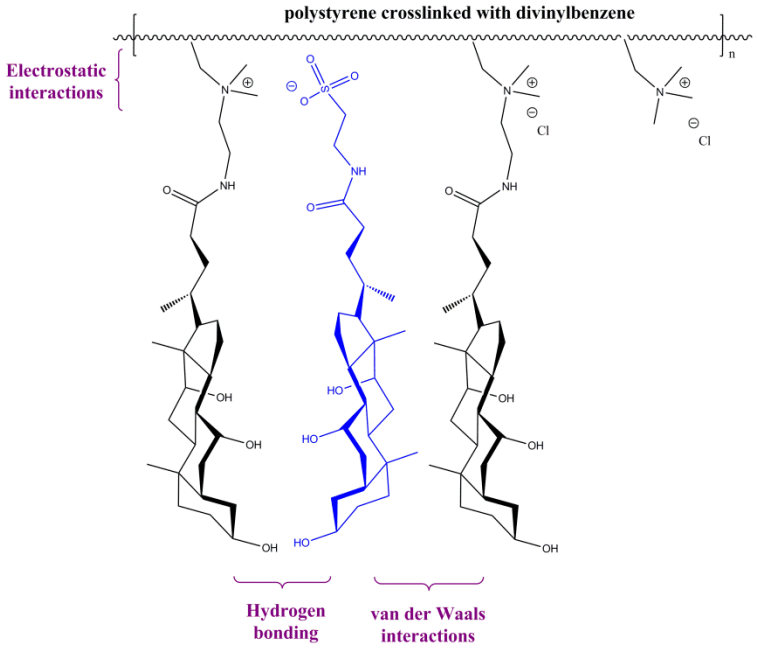

Figure 1.9. Binding mechanism between bioconjugated based BAS and bile salts (blue), proposed by Zhang and co-workers.[181]

Both the binding capacity of the prepared BAS and the rate of release of bile salts were evaluated in the presence of sodium taurocholate by ultraviolet (UV) spectroscopy. The capacity to bind taurocholate ions increased as the content of the tertiary amine derivative of cholic acid in the polymer matrix increased. The kinetics of the taurocholate ions

release process indicated that, besides the film diffusion process, the diffusion of ions within the polymer matrix (particle diffusion) played an important role in the kinetic behavior.[181]

As an alternative structure to BAS networks, Cameron and co-workers prepared new amphiphilic diblock copolymers.[138, 184] These polymers contained both hydrophobic segments and hydrophilic segments and could self-assemble in the presence of selective solvents, creating diverse nanostructures. Such structures present a great surface area, which is able to provide a large number of binding sites for the bile salts. Also, the solutions of these amphiphilic structures, in comparison with those of the common polymer networks, possess lower viscosities which can be seen as an advantage considering the patient compliance (fewer side effects such as constipation). The polymer studied was based on PS (hydrophobic segment) and polyacrylamide (hydrophilic segment), functionalized with trimethylammonium methylene chloride.[138] The size and morphology of the micelles was influenced by several parameters, such as the molecular weight distribution of the block copolymers, the temperature, the ionic strength and the pH. By varying the degree of polymerization of the block copolymers segments, the authors were able to prepare BAS with different structures such as small spheres (≈ 20 nm), large micelles (> 100 nm), vesicles and lamellae shapes, each one confirmed by scanning electron microscopy and transmission electron microscopy analyses. The molecular weight of the polymers was controlled using anionic polymerization, which enabled the synthesis of well-defined block copolymers with $Đ \approx 1.1$.[138] The authors obtained promising results, with micelles showing good stability and an ability to bind sodium glycocholate in sorption experiments. However, the experimental steps involved in the polymerization and purification of the amphiphilic block copolymers required complex and time-consuming procedures. Another important issue is the functionalization (amidation) step that required optimized. The major advantages and disadvantages of the functionalization (amidation) step were explored using three different strategies: (i) direct reaction between the ester group and an amine or an aluminium amide; (ii) hydrolysis of the ester groups to form carboxylic acids, followed by conversion into the corresponding acid chloride and reaction with an amine and (iii) hydrolysis of the ester groups to form carboxylic acids, followed by carbodiimide coupling to an amine.[184] Considering the complexity of the experimental conditions, the degree of functionalization achieved and

the solubility of the produced polymers, together with issues related to reactivity and steric hindrance, the carbodiimide coupling route was the pathway that showed the greatest potential. The same research group prepared a series of amine-functionalized polymers, based on polyether backbones, in different solvents.[185] Poly(epichlorohydrin) with molecular weight of 700 000 was chemically modified with different low molecular weight amines, followed by crosslinking and alkylation to produce amphiphilic hydrogels. In a similar way, poly(2-chloroethyl vinyl ether) was produced by cationic polymerization and used as a backbone to create the final amine-functionalized cationic hydrogel. The introduction of desired functionalities in the polymers structure allowed the preparation of BAS with higher binding capacities towards bile salts compared to those of both commercially available Cholestyramine and Colestipol. However, the synthetic routes used required demanding experimental conditions, such as either a very high temperature or a very low temperature (e.g., -70 °C in cationic polymerization), long reaction times and the need for careful optimization of the poly(epichlorohydrin) modification step.[185]

Some of the polymer modifications described so far require time-consuming and complex experimental steps[113] and present a low efficiency of functionalization.[167] However for the proper design of new BAS one must consider not only the final properties of the polymer, but also the method of synthesis. There is a need to establish relatively simple, but highly efficient and less expensive ways to prepare these materials. This is a critical issue in the development of new products that could have commercial impact and relevance. An easier and somewhat novel strategy was developed for the preparation of BAS based on ammonium cyclic structures along the polymer backbone.[118] Such cationic hydrogels were prepared by cyclopolymerization using *N*-substituted diallylammonium monomers (modified methyl diallylamine) followed by the reaction with crosslinking monomers. A series of BAS with distinct hydrophilic properties were obtained by using different alkyl substituent groups in the methyl diallylamine modification step, as well as several crosslinking monomers in the final step of the reaction process (Figure 1.10). The performance of these materials was monitored and evaluated by studying their aqueous swelling properties and by the use of *in vivo* bile salts sequestration experiments. Their strong binding capacity and their enhanced swelling properties were attributed to the more flexible hydrogels based on hydrophilic crosslinkers. Concerning the hydrophobic

interactions, the authors proved that the BAS efficacy is not linearly dependent on the number of hydrophobic chains.[118] Therefore, an optimum density of hydrophobic segments is required in order to maximize the binding capacity of the hydrogels.

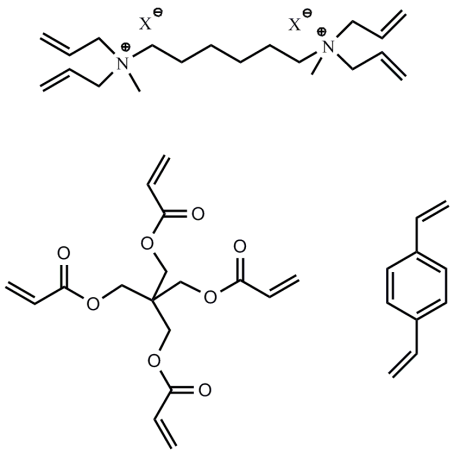

Figure 1.10. Representative crosslinkers used in the BAS synthesis.[118]

Besides the chemical modification of polymer backbones, new strategies based on molecular imprinting have been proposed, showing interesting results with respect to the preparation of more effective BAS.[186-188] Using this technique, functional monomers are connected to a polymer backbone in the presence of template molecules. The functional groups or chemical structures present in the monomer must be able to interact with the template molecules in order to create a pre-polymerization complex.[189] The type of interactions (covalent or non-covalent interactions) established in the formation of the pre-polymerization complex is the main difference between the two different molecular imprinting techniques, as reported in the literature[189] (Figure 1.11). Subsequently, after the polymerization in the presence of a crosslinking monomer and a solvent, the template molecules are removed from the polymer, leaving specific cavities. This step can occur by chemical cleavage, in the case of covalent interaction with the pre-polymerization complex, or by solvent extraction via diffusion, when the template molecules are non-covalently bonded to the functional monomer. For this reason, non-covalent systems are the most widely used, even though their efficacy is less than that of covalent systems. Molecular imprinting has been used in other biomedical applications for the preparation of appropriate polymer structures, in trying to mimic natural recognition systems,[189, 190] and for the synthesis of hydrogel matrixes for drug delivery systems. Imprinted hydrogels, with their highly flexible polymer chains, which were believed to produce less

efficient imprinted materials due to the high mobility of the created cavities, have been developed showing promising results.[191] Concerning these features, molecular imprinting could be also attractive for the preparation of BAS. In addition, the process provides a tailor-made component (the desired receptor), it is not expensive and does not require complex syntheses.[192] The use of bile acids as template molecules creates artificial recognition cavities in the BAS hydrogel. These could contribute to the enhancement of the binding forces during the bile salts sequestration process. This is the key factor to allow the BAS polymers to be able to compete with the desorbing forces present in the GI tract and, at the same time, preserve the bile salts that are entrapped in the hydrogels matrix. Huval and co-workers proposed for the first time the synthesis of BAS by the non-covalent molecular imprinting technique (Figure 1.11).[180] This strategy was intended to enhance the BAS binding capacity by creating complementary binding sites for both the bile salts shape and the carboxylic groups present in the structure. Different polymer networks based on poly(allylammonium chloride) crosslinked with epichlorohydrin, were prepared in the presence of the sodium cholate as the template. The sequestration capacity of the materials was tested in both *in vitro* experiments and *in vivo* experiments. Cholic acid-imprinted polymer networks showed a higher binding capacity towards bile salts, in both tests, in comparison to a control polymer hydrogel without template.[180] Moreover, the binding capacity increased with the increase in the cholic acid template content used for the imprinting, reaching 1.97 mmol/g (mmol bile salt/g dry polymer). These results show that the molecular imprinting technique could be useful for the preparation of BAS with enhanced binding capacity, since all of the polymer networks were prepared with the same cationic charge density (equivalent electrostatic interactions) and degree of crosslinking. These additional pieces of evidence to support the binding mechanism suggest that, besides being influenced by both electrostatic interactions and hydrophobic interactions, the binding process can also be influenced by the shape-selective fitting of steroidal skeletons into complementary cavities, at least in the initial stage. After an initial binding of small amounts of the bile salts by the imprinted BAS, the hydrophobic character of the aggregates increases, leading to stable structures that provide more affinity towards new bile salts molecules.[180] Similar results were obtained by Wang and colleagues[187] using a hybrid molecular imprinting approach. This hybrid method joins the major advantage of covalent molecular imprinting, which is the clear structure of the

guest-binding site, with fast guest binding, that is characteristic of the non-covalent molecular imprinting method. The polymers were synthesized by covalent molecular imprinting, while the guest binding occurred by non-covalent interactions, which is characteristic of the non-covalent molecular imprinting technique.[192]

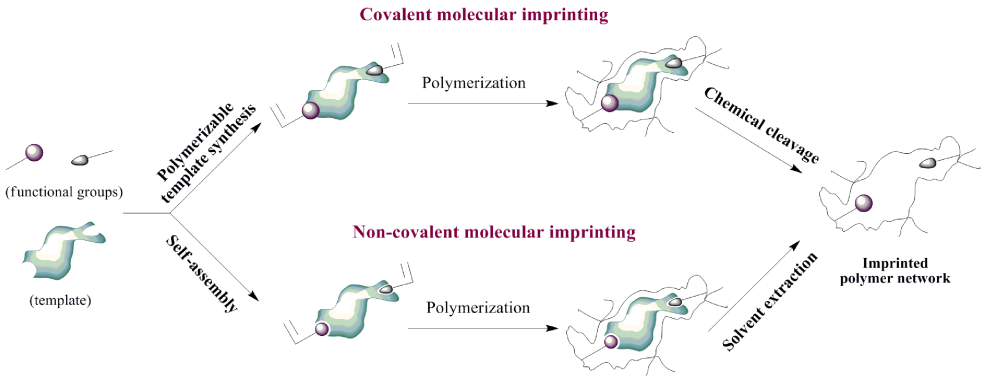

Figure 1.11. Polymer molecular imprinting strategies.

Imprinted polymer networks have been synthesized by the free radical polymerization of a cholic acid-containing monomer, followed by crosslinking with ethylene glycol dimethacrylate.[187] The cholic acid complementary cavities were created by polymer hydrolysis (template cleavage), achieving only 45% of template removal efficiency. This step of chemical cleavage is somehow limiting since it is not possible to achieve high degrees of hydrolysis in crosslinked polymers because of the steric hindrance,[187] which restricts the number of specific interaction sites presented in the imprinted BAS. Nevertheless, the imprinted polymer networks prepared exhibited a nearly seven fold higher binding capacity towards both cholic acid and deoxycholic acid, in comparison to the binding capacity of the control sample (without the template). Besides the complementary cavities created in the hydrogel matrix, it was assumed that the entrapped molecules favored the binding process, since the binding capacity of the hydrogels was higher than the number of cavity sites. This observation arises from the cooperative effect of the bile salts molecules, that have a tendency to self-aggregate in aqueous media at high concentrations.[180] This result is extremely important and could provide useful information for further BAS developments. In the same work,[187] different polar solvents and non-polar solvents were tested as imprinting solvent. It was found that this self-aggregating parameter influenced the properties of the final hydrogels and ultimately influenced their binding capacity, showing that the use of non-polar solvents was

preferable. Imprinted materials showed better results when their polymerization took place in solvents that could mimic the final medium of the application.[193] BAS are intended to work in aqueous media, such as the intestine environment. However, this solvent was not tested in the identified study. Water has some limitations when used for the imprinting strategy, since it can prevent hydrogen bonding between the template and the monomer. By this means, the capacity of recognition of the hydrogels could be compromised. Despite the good results indicated by early reports on molecular imprinting, recent studies on the application of this technique to the synthesis of new BAS have shown that this approach could not be useful in some circumstances. Yañez and co-workers[188] have reported a computational modeling study of imprinted polymer networks based on different functional acrylic monomers that possessed affinity towards cholic acid, with a cholic acid/functional monomer molar ratio of 1/4. Several monomers commonly used in the preparation of BAS polymers were chosen and their binding energy with cholic acid molecules was estimated using computational modeling. After this screening, the authors selected three monomers, each one with a different binding affinity towards cholic acid, to assess experimentally their results with respect to the preparation of BAS imprinted hydrogels and their binding capacity towards sodium cholate. The results were in agreement with the theoretical predictions and suggested that the molecular imprinting technique is not so effective for polymers that already present high affinity towards the template molecules. It seems that in polymeric BAS, this technique can only provide initial affinity towards bile salts molecules, being the main binding mechanism regulated by both electrostatic interactions and hydrophobic interactions. This information is very relevant since it helps one to rule out some alternative possible synthetic approaches to the development of new BAS materials. Another parameter studied by the authors[188] was the influence of the polymer degree of crosslinking on the binding capacity. The results are consistent with the findings of reports presented in the literature,[169] suggesting that there is an optimal degree of crosslinking that allows the targeted molecules to diffuse through the polymer matrix and reach the binding sites, while maintaining the polymer swelling characteristics. The ideal level of crosslinking with respect to maximizing the BAS efficacy is dependent on the polymer structure and on the molecular size of the targeted bile salts molecules. This study showed that computational modeling can be a very helpful tool in the design of new

BAS, since it enables the screening of potential monomers to be used, taking into to account their ability to bind bile salts. This reduces the need to rely on time-consuming synthesis procedures and characterization tests in the search for new monomers that would be suitable for the preparation of new BAS.

Despite the recent progress in the synthesis of polymeric BAS, only a few products have been able to enter pre-clinical development stages and subsequent human clinical trials. More research is required to create ideal structures that can be more selective towards bile salts, especially the more hydrophilic examples as the case of the trihydroxy bile salts. However, the studies reported in the literature provide important information concerning the variables that have to be taken into account for the BAS design:

- Cationic groups: positive charges along the polymer structure ensure the occurrence of electrostatic interactions, which are the primary mechanism of the binding process involving ionized bile acids;
- Hydrophobic chain length: longer aliphatic chains ensure the occurrence of hydrophobic interactions with the steroid skeletons of bile salts during the binding process;
- Degree of crosslinking and polymer backbone flexibility: lower crosslinking densities and flexible polymer backbones lead to enhanced swelling properties and typically higher binding capacity;
- Polymers shape: the use of appropriate polymer structures that can complement the bile salts architecture can favor the binding process.

It is noteworthy that these variables have to be adjusted on the basis of the nature of the polymers used in the synthesis of the BAS.

1.11. References

1. Colombani, D., Chain-growth control in free radical polymerization. *Prog. Polym. Sci.* **1997,** 22, (8), 1649-1720.

2. Moad, G.; Rizzardo, E.; Thang, S. H., Toward living radical polymerization. *Acc. Chem. Res.* **2008,** 41, (9), 1133-1142.

3. Zetterlund, P. B.; Kagawa, Y.; Okubo, M., Controlled/living radical polymerization in dispersed systems. *Chem. Rev.* **2008,** 108, (9), 3747-3794.

4. Destarac, M., Controlled Radical Polymerization: Industrial Stakes, Obstacles and Achievements. *Macromol. React. Eng.* **2010,** 4, (3-4), 165-179.

5. Braunecker, W. A.; Matyjaszewski, K., Controlled/living radical polymerization: Features, developments, and perspectives. *Prog. Polym. Sci.* **2007,** 32, (1), 93-146.

6. Yamada, B.; Zetterlund, P. B., General chemistry of radical polymerization. In *Hanbook of radical polymerization*, Matyjaszewski, K.; Davis, T. P., Eds. John Wiley & Sons, Inc.: 2002.

7. Szwarc, M., Living polymers. *Nature* **1956,** 178, (4543), 1168-1169.

8. Szwarc, M.; Levy, M.; Milkovich, R., Polymerization initiated by electron transfer monomer - A new method of formation of block polymers. *J. Am. Chem. Soc.* **1956,** 78, (11), 2656-2657.

9. Matyjaszewski, K., General Concepts and History of Living Radical Polymerization. In *Handbook of radical polymerization*, Matyjaszewski, K.; Davis, T. P., Eds. John Wiley & Sons, Inc.: 2002; pp 361-406.

10. Cunningham, M. F., Controlled/living radical polymerization in aqueous dispersed systems. *Prog. Polym. Sci.* **2008,** 33, (4), 365-398.

11. Qiu, J.; Charleux, B.; Matyjaszewski, K., Controlled/living radical polymerization in aqueous media: homogeneous and heterogeneous systems. *Prog. Polym. Sci.* **2001,** 26, (10), 2083-2134.

12. Penczek, S., Terminology of kinetics, thermodynamics, and mechanisms of polymerization. *J. Polym. Sci., Part A: Polym. Chem.* **2002,** 40, (11), 1665-1676.

13. Percec, V.; Tirrell, D. A., Living or controlled? *J. Polym. Sci., Part A: Polym. Chem.* **2000,** 38, (10), 1705-1705.

14. Jenkins, A. D.; Jones, R. G.; Moad, G., Terminology for reversible-deactivation radical polymerization previously called "controlled" radical or "living" radical polymerization (IUPAC Recommendations 2010). *Pure Appl. Chem.* **2010,** 82, (2), 483-491.

15. Ayres, N., Atom Transfer Radical Polymerization: A Robust and Versatile Route for Polymer Synthesis. *Polym. Rev.* **2011,** 51, (2), 138-162.

16. Mueller, L.; Matyjaszewski, K., Reducing Copper Concentration in Polymers Prepared via Atom Transfer Radical Polymerization. *Macromol. React. Eng.* **2010,** 4, (3-4), 180-185.

17. Veregin, R. P. N.; Georges, M. K.; Kazmaier, P. M.; Hamer, G. K., Free-radicalpolymerizations for narrow polidispersity resins - electron-spin-resonance studies of the kinetics and mechanism. *Macromolecules* **1993,** 26, (20), 5316-5320.

18. Grubbs, R. B., Nitroxide-Mediated Radical Polymerization: Limitations and Versatility. *Polym. Rev.* **2011,** 51, (2), 104-137.

19. Barner-Kowollik, C.; Blinco, J. P.; Destarac, M.; Thurecht, K. J.; Perrier, S., Reversible Addition Fragmentation Chain Transfer (RAFT) Polymerization: Mechanism, Process and Applications. In *Encyclopedia of Radicals in Chemistry, Biology and Materials*, John Wiley & Sons, Ltd: 2012.

20. Ouchi, M.; Terashima, T.; Sawamoto, M., Transition Metal-Catalyzed Living Radical Polymerization: Toward Perfection in Catalysis and Precision Polymer Synthesis. *Chem. Rev.* **2009,** 109, (11), 4963-5050.

21. Ouchi, M.; Terashima, T.; Sawamoto, M., Precision Control of Radical Polymerization via Transition Metal Catalysis: From Dormant Species to Designed Catalysts for Precision Functional Polymers. *Acc. Chem. Res.* **2008,** 41, (9), 1120-1132.

22. Matyjaszewski, K.; Coca, S.; Gaynor, S. G.; Wei, M.; Woodworth, B. E., Zerovalent Metals in Controlled/"Living" Radical Polymerization. *Macromolecules* **1997,** 30, (23), 7348-7350.

23. Percec, V.; Guliashvili, T.; Ladislaw, J. S.; Wistrand, A.; Stjerndahl, A.; Sienkowska, M. J.; Monteiro, M. J.; Sahoo, S., Ultrafast synthesis of ultrahigh molar mass polymers by metal-catalyzed living radical polymerization of acrylates, methacrylates, and vinyl chloride mediated by SET at 25 degrees C. *J. Am. Chem. Soc.* **2006,** 128, (43), 14156-14165.

24. Matyjaszewski, K.; Xia, J., Atom Transfer Radical Polymerization. *Chem. Rev.* **2001,** 101, (9), 2921-2990.

25. Isse, A. A.; Gennaro, A.; Lin, C. Y.; Hodgson, J. L.; Coote, M. L.; Guliashvili, T., Mechanism of Carbon−Halogen Bond Reductive Cleavage in Activated Alkyl Halide Initiators Relevant to Living Radical Polymerization: Theoretical and Experimental Study. *J. Am. Chem. Soc.* **2011,** 133, (16), 6254-6264.

26. Matyjaszewski, K., From atom transfer radical addition to atom transfer radical polymerization. *Current Organic Chemistry* **2002,** 6, (2), 67-82.

27. Pintauer, T.; Matyjaszewski, K., Atom transfer radical addition and polymerization reactions catalyzed by ppm amounts of copper complexes. *Chem. Soc. Rev,* **2008,** 37, (6), 1087-1097.

28. Queffelec, J.; Gaynor, S. G.; Matyjaszewski, K., Optimization of atom transfer radical polymerization using Cu(I)/tris(2-(dimethylamino)ethyl)amine as a catalyst. *Macromolecules* **2000,** 33, (23), 8629-8639.

29. Tang, W.; Matyjaszewski, K., Effect of Ligand Structure on Activation Rate Constants in ATRP. *Macromolecules* **2006,** 39, (15), 4953-4959.

30. Matyjaszewski, K.; Paik, H.-j.; Zhou, P.; Diamanti, S. J., Determination of Activation and Deactivation Rate Constants of Model Compounds in Atom Transfer Radical Polymerization1. *Macromolecules* **2001,** 34, (15), 5125-5131.

31. Tang, W.; Kwak, Y.; Braunecker, W.; Tsarevsky, N. V.; Coote, M. L.; Matyjaszewski, K., Understanding Atom Transfer Radical Polymerization: Effect of Ligand and Initiator Structures on the Equilibrium Constants. *J. Am. Chem. Soc.* **2008,** 130, (32), 10702-10713.

32. Matyjaszewski, K., Atom Transfer Radical Polymerization (ATRP): Current Status and Future Perspectives. *Macromolecules* **2012,** 45, (10), 4015-4039.

33. di Lena, F.; Matyjaszewski, K., Transition metal catalysts for controlled radical polymerization. *Prog. Polym. Sci.* **2010,** 35, (8), 959-1021.

34. Tang, W.; Matyjaszewski, K., Effects of Initiator Structure on Activation Rate Constants in ATRP. *Macromolecules* **2007,** 40, (6), 1858-1863.

35. Wei, H.; Perrier, S.; Dehn, S.; Ravarian, R.; Dehghani, F., One-pot ATRP synthesis of a triple hydrophilic block copolymer with dual LCSTs and its thermo-induced association behavior. *Soft Matter* **2012,** 8, (37), 9526-9528.

36. Nanda, A. K.; Matyjaszewski, K., Effect of [bpy]/[Cu(I)] Ratio, Solvent, Counterion, and Alkyl Bromides on the Activation Rate Constants in Atom Transfer Radical Polymerization. *Macromolecules* **2003,** 36, (3), 599-604.

37. Nanda, A. K.; Matyjaszewski, K., Effect of [PMDETA]/[Cu(I)] Ratio, Monomer, Solvent, Counterion, Ligand, and Alkyl Bromide on the Activation Rate Constants in Atom Transfer Radical Polymerization. *Macromolecules* **2003,** 36, (5), 1487-1493.

38. Bergenudd, H.; Coullerez, G.; Jonsson, M.; Malmström, E., Solvent Effects on ATRP of Oligo(ethylene glycol) Methacrylate. Exploring the Limits of Control. *Macromolecules* **2009,** 42, (9), 3302-3308.

39. Horn, M.; Matyjaszewski, K., Solvent Effects on the Activation Rate Constant in Atom Transfer Radical Polymerization. *Macromolecules* **2013,** 46, (9), 3350-3357.

40. Konkolewicz, D.; Krys, P.; Góis, J. R.; Mendonça, P. V.; Zhong, M.; Wang, Y.; Gennaro, A.; Isse, A. A.; Fantin, M.; Matyjaszewski, K., Aqueous RDRP in the Presence of Cu0: The Exceptional Activity of CuI Confirms the SARA ATRP Mechanism. *Macromolecules* **2014,** 47, (2), 560-570.

41. Konkolewicz, D.; Magenau, A. J. D.; Averick, S. E.; Simakova, A.; He, H.; Matyjaszewski, K., ICAR ATRP with ppm Cu Catalyst in Water. *Macromolecules* **2012,** 45, (11), 4461-4468.

42. Simakova, A.; Averick, S. E.; Konkolewicz, D.; Matyjaszewski, K., Aqueous ARGET ATRP. *Macromolecules* **2012,** 45, (16), 6371-6379.

43. Xia, J.; Johnson, T.; Gaynor, S. G.; Matyjaszewski, K.; DeSimone, J., Atom Transfer Radical Polymerization in Supercritical Carbon Dioxide. *Macromolecules* **1999,** 32, (15), 4802-4805.

44. Xiao, G. L.; Zhang, H. B.; Hong, X. L.; Zhang, G. Y.; Zhou, X. H.; Xia, B. L., Atom transfer radical polymerization of methyl methacrylate in a novel ionic liquid and recycling of the catalyst. *J. Appl. Polym. Sci.* **2008,** 108, (6), 3683-3689.

45. Kamigaito, M., Recent developments in metal-catalyzed living radical polymerization. *Polymer Journal* **2011,** 43, (2), 105-120.

46. Tsarevsky, N. V.; Braunecker, W. A.; Vacca, A.; Gans, P.; Matyjaszewski, K., Competitive Equilibria in Atom Transfer Radical Polymerization. *Macromol. Symp.* **2007,** 248, (1), 60-70.

47. Tsarevsky, N. V.; Matyjaszewski, K., "Green" Atom Transfer Radical Polymerization: From Process Design to Preparation of Well-Defined Environmentally Friendly Polymeric Materials. *Chem. Rev.* **2007,** 107, (6), 2270-2299.

48. Shen, Y. Q.; Tang, H. D.; Ding, S. J., Catalyst separation in atom transfer radical polymerization. *Prog. Polym. Sci.* **2004,** 29, (10), 1053-1078.

49. Faucher, S.; Zhu, S. P., Fundamentals and development of high-efficiency supported catalyst systems for atom transfer radical polymerization. *J. Polym. Sci., Part A: Polym. Chem.* **2007,** 45, (4), 553-565.

50. Honigfort, M. E.; Brittain, W. J.; Bosanac, T.; Wilcox, C. S., Use of Precipitons for Copper Removal in Atom Transfer Radical Polymerization. *Macromolecules* **2002,** 35, (13), 4849-4851.

51. Haddleton, D. M.; Jackson, S. G.; Bon, S. A. F., Copper(I)-mediated living radical polymerization under fluorous biphasic conditions. *J. Am. Chem. Soc.* **2000,** 122, (7), 1542-1543.

52. Jakubowski, W.; Matyjaszewski, K., Activator Generated by Electron Transfer for Atom Transfer Radical Polymerization. *Macromolecules* **2005,** 38, (10), 4139-4146.

53. Matyjaszewski, K.; Jakubowski, W.; Min, K.; Tang, W.; Huang, J.; Braunecker, W. A.; Tsarevsky, N. V., Diminishing catalyst concentration in atom transfer radical polymerization with reducing agents. *Proc. Natl. Acad. Sci. U. S. A.* **2006,** 103, (42), 15309-15314.

54. Jakubowski, W.; Matyjaszewski, K., Activators Regenerated by Electron Transfer for Atom-Transfer Radical Polymerization of (Meth)acrylates and Related Block Copolymers. *Angew. Chem. Int. Ed.* **2006,** 45, (27), 4482-4486.

55. Magenau, A. J. D.; Bortolamei, N.; Frick, E.; Park, S.; Gennaro, A.; Matyjaszewski, K., Investigation of Electrochemically Mediated Atom Transfer Radical Polymerization. *Macromolecules* **2013,** 46, (11), 4346-4353.

56. Magenau, A. J. D.; Strandwitz, N. C.; Gennaro, A.; Matyjaszewski, K., Electrochemically Mediated Atom Transfer Radical Polymerization. *Science* **2011,** 332, (6025), 81-84.

57. Mendonça, P. V.; Serra, A. C.; Coelho, J. F. J.; Popov, A. V.; Guliashvili, T., Ambient temperature rapid ATRP of methyl acrylate, methyl methacrylate and styrene in polar solvents with mixed transition metal catalyst system. *Eur. Polym. J.* **2011,** 47, (7), 1460-1466.

58. Zhang, Y.; Wang, Y.; Matyjaszewski, K., ATRP of Methyl Acrylate with Metallic Zinc, Magnesium, and Iron as Reducing Agents and Supplemental Activators. *Macromolecules* **2011,** 44, (4), 683-685.

59. Mendonca, P. V.; Serra, A. C.; Coelho, J. F. J.; Popov, A. V.; Guliashvili, T., Ambient temperature rapid ATRP of methyl acrylate, methyl methacrylate and styrene in polar solvents with mixed transition metal catalyst system. *Eur. Polym. J.* **2011,** 47, (7), 7-7.

60. Cordeiro, R. A.; Rocha, N.; Mendes, J. P.; Matyjaszewski, K.; Guliashvili, T.; Serra, A. C.; Coelho, J. F. J., Synthesis of well-defined poly(2-(dimethylamino)ethyl methacrylate) under mild conditions and its co-polymers with cholesterol and PEG using Fe(0)/Cu(ii) based SARA ATRP. *Polym. Chem.* **2013,** 4, (10), 3088-3097.

61. Abreu, C. M. R.; Mendonça, P. V.; Serra, A. C.; Popov, A. V.; Matyjaszewski, K.; Guliashvili, T.; Coelho, J. F. J., Inorganic Sulfites: Efficient Reducing Agents and Supplemental Activators for Atom Transfer Radical Polymerization. *ACS Macro Lett.* **2012,** 1, (11), 1308-1311.

62. Abreu, C. M. R.; Serra, A. C.; Popov, A. V.; Matyjaszewski, K.; Guliashvili, T.; Coelho, J. F. J., Ambient temperature rapid SARA ATRP of acrylates and methacrylates in alcohol-water solutions mediated by a mixed sulfite/Cu(ii)Br2 catalytic system. *Polym. Chem.* **2013,** 4, (23), 5629-5636.

63. Mendes, J. P.; Branco, F.; Abreu, C. M. R.; Mendonça, P. V.; Popov, A. V.; Guliashvili, T.; Serra, A. C.; Coelho, J. F. J., Synergistic Effect of 1-Butyl-3-methylimidazolium Hexafluorophosphate and DMSO in the SARA ATRP at Room Temperature Affording Very Fast Reactions and Polymers with Very Low Dispersity. *ACS Macro Lett.* **2014,** 3, (6), 544-547.

64. Asandei, A. D.; Percec, V., From metal-catalyzed radical telomerization to MetalCatalyzed radical polymerization of vinyl chloride: Toward living radical polymerization of vinyl chloride. *J. Polym. Sci., Part A: Polym. Chem.* **2001,** 39, (19), 3392-3418.

65. Percec, V.; Popov, A. V.; Ramirez-Castillo, E.; Monteiro, M.; Barboiu, B.; Weichold, O.; Asandei, A. D.; Mitchell, C. M., Aqueous room temperature metal-catalyzed living radical polymerization of vinyl chloride. *J. Am. Chem. Soc.* **2002,** 124, (18), 4940-4941.

66. Percec, V.; Popov, A. V.; Ramirez-Castillo, E.; Weichold, O., Living radical polymerization of vinyl chloride initiated with iodoform and catalyzed by nascent Cu0/tris(2-aminoethyl)amine or polyethyleneimine in water at 25 °C proceeds by a new competing pathways mechanism. *J. Polym. Sci., Part A: Polym. Chem.* **2003,** 41, (21), 3283-3299.

67. Percec, V.; Guliashvili, T.; Popov, A. V., Ultrafast synthesis of poly(methyl acrylate) and poly(methyl acrylate)-b-poly(vinyl chloride)-b-poly(methyl acrylate) by the Cu(0)/tris(2-dimethylaminoethyl)amine-catalyzed living radical polymerization and block copolymerization of methyl acrylate initiated with 1,1-chloroiodoethane and α,ω-Di(iodo)poly(vinyl chloride) in dimethyl sulfoxide. *J. Polym. Sci., Part A: Polym. Chem.* **2005,** 43, (9), 1948-1954.

68. Percec, V.; Guliashvili, T.; Popov, A. V.; Ramirez-Castillo, E., Catalytic effect of dimethyl sulfoxide in the Cu(0)/tris(2-dimethylaminoethyl)amine-catalyzed living radical polymerization of methyl methacrylate at 0-90° initiated with CH3CHClI as a model compound for α,ω-Di(iodo)poly(vinyl chloride) chain ends. *J. Polym. Sci., Part A: Polym. Chem.* **2005,** 43, (9), 1935-1947.

69. Popov, A. V.; Hinojosa-Falcon, L. A., Private communication.

70. Percec, V.; Popov, A. V.; Ramirez-Castillo, E.; Coelho, J. F. J.; Hinojosa-Falcon, L. A., Non-transition metal-catalyzed living radical polymerization of vinyl chloride initiated with iodoform in water at 25°C. *J. Polym. Sci., Part A: Polym. Chem.* **2004,** 42, (24), 6267-6282.

71. Percec, V.; Popov, A. V.; Ramirez-Castillo, E., Single-electron-transfer/degenerative-chain-transfer mediated living radical polymerization of vinyl chloride catalyzed by thiourea dioxide/octyl viologen in water/tetrahydrofuran at 25 °C. *J. Polym. Sci., Part A: Polym. Chem.* **2004,** 43, (2), 287-295.

72. Percec, V.; Popov, A. V.; Ramirez-Castillo, E.; Coelho, J. F. J., Single electron transfer-degenerative chain transfer mediated living radical polymerization (SET-DTLRP) of vinyl chloride initiated with methylene iodide and catalyzed by sodium dithionite. *J. Polym. Sci., Part A: Polym. Chem.* **2005,** 43, (4), 773-778.

73. Percec, V.; Ramirez-Castillo, E.; Popov, A. V.; Hinojosa-Falcon, L. A.; Guliashvili, T., Ultrafast single-electron-transfer/degenerative-chain-transfer mediated living radical polymerization of acrylates initiated with iodoform in water at room temperature and catalyzed by sodium dithionite. *J. Polym. Sci., Part A: Polym. Chem.* **2005,** 43, (10), 2178-2184.

74. Percec, V.; Popov, A. V.; Ramirez-Castillo, E.; Hinojosa-Falcon, L. A., Synthesis of poly(vinyl chloride)-b-poly(2-ethylhexyl acrylate)-b-poly(vinyl chloride) by the competitive single-electron-transfer/degenerative-chain-transfer mediated living radical polymerization of vinyl chloride initiated from α,ω-di(iodo)poly(2-ethylhexyl acrylate) and catalyzed with sodium dithionite in water. *J. Polym. Sci., Part A: Polym. Chem.* **2005,** 43, (11), 2276-2280.

75. Coelho, J. F. J.; Silva, A. M. F. P.; Popov, A. V.; Percec, V.; Abreu, M. V.; Goncalves, P. M. O. F.; Gil, M. H., Single electron transfer-degenerative chain transfer living radical polymerization of N-butyl acrylate catalyzed by Na2S2O4 in water media. *J. Polym. Sci., Part A: Polym. Chem.* **2006,** 44, (9), 2809-2825.

76. Jiang, X.; Fleischmann, S.; Nguyen, N. H.; Rosen, B. M.; Percec, V., Cooperative and Synergistic Solvent Effects in SET-LRP of MA. *J. Polym. Sci., Part A: Polym. Chem.* **2009,** 47, (21), 5591-5605.

77. Samanta, S. R.; Anastasaki, A.; Waldron, C.; Haddleton, D. M.; Percec, V., SET-LRP of hydrophobic and hydrophilic acrylates in tetrafluoropropanol. *Polym. Chem.* **2013,** 4, (22), 5555-5562.

78. Zhang, Q.; Wilson, P.; Li, Z.; McHale, R.; Godfrey, J.; Anastasaki, A.; Waldron, C.; Haddleton, D. M., Aqueous Copper-Mediated Living Polymerization: Exploiting Rapid Disproportionation of CuBr with Me_6TREN. *J. Am. Chem. Soc.* **2013,** 135, (19), 7355-7363.

79. Matyjaszewski, K., Radical nature of Cu-catalyzed controlled radical polymerizations (atom transfer radical polymerization). *Macromolecules* **1998,** 31, (15), 4710-4717.

80. Matyjaszewski, K.; Tsarevsky, N. V.; Braunecker, W. A.; Dong, H.; Huang, J.; Jakubowski, W.; Kwak, Y.; Nicolay, R.; Tang, W.; Yoon, J. A., Role of Cu-0 in controlled/"living" radical polymerization. *Macromolecules* **2007,** 40, 7795-7806.

81. Konkolewicz, D.; Wang, Y.; Krys, P.; Zhong, M.; Isse, A. A.; Gennaro, A.; Matyjaszewski, K., SARA ATRP or SET-LRP. End of controversy? *Polym. Chem.* **2014,** 5, (15), 4396-4417.

82. Rosen, B. M.; Jiang, X.; Wilson, C. J.; Nguyen, N. H.; Monteiro, M. J.; Percec, V., The Disproportionation of Cu(I)X Mediated by Ligand and Solvent into Cu(0) and Cu(II)X-2 and Its Implications for SET-LRP. *J. Polym. Sci., Part A: Polym. Chem.* **2009,** 47, (21), 5606-5628.

83. Konkolewicz, D.; Wang, Y.; Zhong, M.; Krys, P.; Isse, A. A.; Gennaro, A.; Matyjaszewski, K., Reversible-Deactivation Radical Polymerization in the Presence of Metallic Copper. A Critical Assessment of the SARA ATRP and SET-LRP Mechanisms. *Macromolecules* **2013,** 46, (22), 8749-8772.

84. Levere, M. E.; Nguyen, N. H.; Leng, X.; Percec, V., Visualization of the crucial step in SET-LRP. *Polym. Chem.* **2013,** 4, (5), 1635-1647.

85. Nguyen, N. H.; Levere, M. E.; Kulis, J.; Monteiro, M. J.; Percec, V., Analysis of the Cu(0)-Catalyzed Polymerization of Methyl Acrylate in Disproportionating and Nondisproportionating Solvents. *Macromolecules* **2012,** 45, (11), 4606-4622.

86. Nguyen, N. H.; Sun, H.-J.; Levere, M. E.; Fleischmann, S.; Percec, V., Where is Cu(0) generated by disproportionation during SET-LRP? *Polym. Chem.* **2013,** 4, (5), 1328-1332.

87. Peng, C.-H.; Zhong, M.; Wang, Y.; Kwak, Y.; Zhang, Y.; Zhu, W.; Tonge, M.; Buback, J.; Park, S.; Krys, P.; Konkolewicz, D.; Gennaro, A.; Matyjaszewski, K.,

Reversible-Deactivation Radical Polymerization in the Presence of Metallic Copper. Activation of Alkyl Halides by Cu0. *Macromolecules* **2013,** 46, (10), 3803-3815.

88. Wang, Y.; Zhong, M.; Zhu, W.; Peng, C.-H.; Zhang, Y.; Konkolewicz, D.; Bortolamei, N.; Isse, A. A.; Gennaro, A.; Matyjaszewski, K., Reversible-Deactivation Radical Polymerization in the Presence of Metallic Copper. Comproportionation–Disproportionation Equilibria and Kinetics. *Macromolecules* **2013,** 46, (10), 3793-3802.

89. Zhang, Y.; Wang, Y.; Peng, C.-h.; Zhong, M.; Zhu, W.; Konkolewicz, D.; Matyjaszewski, K., Copper-Mediated CRP of Methyl Acrylate in the Presence of Metallic Copper: Effect of Ligand Structure on Reaction Kinetics. *Macromolecules* **2011,** 45, (1), 78-86.

90. Zhong, M.; Wang, Y.; Krys, P.; Konkolewicz, D.; Matyjaszewski, K., Reversible-Deactivation Radical Polymerization in the Presence of Metallic Copper. Kinetic Simulation. *Macromolecules* **2013,** 46, (10), 3816-3827.

91. Kolb, H. C.; Finn, M. G.; Sharpless, K. B., Click Chemistry: Diverse Chemical Function from a Few Good Reactions. *Angew. Chem. Int. Ed.* **2001,** 40, (11), 2004-2021.

92. Davis, K. A.; Matyjaszewski, K., Statistical, Gradient, Block, and Graft Copolymers by Controlled/Living Radical Polymerizations. In *Statistical, Gradient, Block and Graft Copolymers by Controlled/Living Radical Polymerizations*, Springer Berlin / Heidelberg: 2002; Vol. 159, pp 1-13.

93. Uhrig, D.; Mays, J., Synthesis of well-defined multigraft copolymers. *Polym. Chem.* **2011,** 2, (1), 69-76.

94. Tasdelen, M. A.; Kahveci, M. U.; Yagci, Y., Telechelic polymers by living and controlled/living polymerization methods. *Prog. Polym. Sci.* **2011,** 36, (4), 455-567.

95. Gao, H. F.; Matyjaszewski, K., Synthesis of functional polymers with controlled architecture by CRP of monomers in the presence of cross-linkers: From stars to gels. *Prog. Polym. Sci.* **2009,** 34, (4), 317-350.

96. Siegwart, D. J.; Oh, J. K.; Matyjaszewski, K., ATRP in the design of functional materials for biomedical applications. *Prog. Polym. Sci.* **2012,** 37, (1), 18-37.

97. Gregory, A.; Stenzel, M. H., The use of reversible addition fragmentation chain transfer polymerization for drug delivery systems. *Expert Opin. Drug Deliv.* **2011,** 8, (2), 237-269.

98. Xu, F. J.; Yang, W. T., Polymer vectors via controlled/living radical polymerization for gene delivery. *Prog. Polym. Sci.* **2011,** 36, (9), 1099-1131.

99. Qi, Y.; Chilkoti, A., Growing polymers from peptides and proteins: a biomedical perspective. *Polym. Chem.* **2014,** 5, (2), 266-276.

100. Dhal, P.; Holmes-Farley, S.; Huval, C.; Jozefiak, T., Polymers as Drugs. In *Polymer Therapeutics I*, Satchi-Fainaro, R.; Duncan, R., Eds. Springer Berlin / Heidelberg: 2006; Vol. 192, pp 9-58.

101. Duncan, R., The dawning era of polymer therapeutics. *Nat. Rev. Drug Discov.* **2003,** 2, (5), 347-360.

102. Liu, S.; Maheshwari, R.; Kiick, K. L., Polymer-Based Therapeutics. *Macromolecules* **2009,** 42, (1), 3-13.

103. Dhal, P. K.; Huval, C. C.; Holmes-Farley, S. R., Functional Polymers as Human Therapeutic Agents. *Ind. Eng. Chem. Res.* **2005,** 44, (23), 8593-8604.

104. Dhal, P. K.; Polomoscanik, S. C.; Avila, L. Z.; Holmes-Farley, S. R.; Miller, R. J., Functional polymers as therapeutic agents: Concept to market place. *Adv. Drug Delivery Rev.* **2009,** 61, (13), 1121-1130.

105. Dhal, P. K.; Huval, C. C.; Holmes-Farley, S. R., Biologically active polymeric sequestrants: Design, synthesis, and therapeutic applications. *Pure Appl. Chem.* **2007,** 79, (9), 1521-1530.

106. Barker, R. H.; Dagher, R.; Davidson, D. M.; Marquis, J. K., Review article: tolevamer, a novel toxin-binding polymer: overview of preclinical pharmacology and physicochemical properties. *Aliment. Pharmacol. Ther.* **2006,** 24, (11-12), 1525-1534.

107. Excellence, S. N. I. H. C., Lipid modification. Cardiovascular risk assessment and the modification of blood lipids for the primary and secondary prevention of cardiovascular disease. Rockville MD: Agency for Healthcare Research and Quality (AHRQ): 2008; p 11.

108. Reiner, Ž.; Catapano, A. L.; De Backer, G.; Graham, I.; Taskinen, M.-R.; Wiklund, O.; Agewall, S.; Alegria, E.; Chapman, M. J.; Durrington, P.; Erdine, S.; Halcox, J.; Hobbs, R.; Kjekshus, J.; Filardi, P. P.; Riccardi, G.; Storey, R. F.; Wood, D., ESC/EAS Guidelines for the management of dyslipidaemias. *Eur. Heart J.* **2011,** 32, (14), 1769-1818.

109. Hou, R.; Goldberg, A. C., Lowering Low-Density Lipoprotein Cholesterol: Statins, Ezetimibe, Bile Acid Sequestrants, and Combinations: Comparative Efficacy and Safety. *Clin. Endocrinol. Metab.* **2009,** 38, (1), 79-97.

110. Staels, B.; Fonseca, V. A., Bile Acids and Metabolic Regulation. *Diabetes Care* **2009,** 32, (suppl 2), S237-S245.

111. Einarsson, K.; Ericsson, S.; Ewerth, S.; Reihnér, E.; Rudling, M.; Ståhlberg, D.; Angelin, B., Bile acid sequestrants: Mechanisms of action on bile acid and cholesterol metabolism. *Eur. J. Clin. Pharmacol.* **1991,** 40, (1), S53-S58.

112. Staels, B.; Handelsman, Y.; Fonseca, V., Bile Acid Sequestrants for Lipid and Glucose Control. *Curr. Diabetes Rep.* **2010,** 10, (1), 70-77.

113. Lee, J. K.; Kim, S. Y.; Kim, S. U.; Kim, J. H., Synthesis of cationic polysaccharide derivatives and their hypocholesterolaemic capacity. *Biotechnol. Appl. Biochem.* **2002,** 35, 181-189.

114. Zarras, P.; Vogl, O., Polycationic salts as bile acid sequestering agents. *Prog. Polym. Sci.* **1999,** 24, (4), 485-516.

115. Swaan, P. W.; Szoka, F. C.; Øie, S., Use of the intestinal and hepatic bile acid transporters for drug delivery. *Adv. Drug Delivery Rev.* **1996,** 20, (1), 59-82.

116. Insull, W., Clinical utility of bile acid sequestrants in the treatment of dyslipidemia: A scientific review. *South. Med. J.* **2006,** 99, (3), 257-273.

117. Mandeville, W. H.; Goldberg, D. I., The sequestration of bile acids, a non-absorbed method for cholesterol reduction. A review. In *Curr. Pharm. Des.*, Sliskovic, D. R., Ed. Bentham science publishers: Hilversum, 1997; Vol. 3, pp 15-26.

118. Huval, C. C.; Holmes-Farley, S. R.; Mandeville, W. H.; Sacchiero, R.; Dhal, P. K., Syntheses of hydrophobically modified cationic hydrogels by copolymerization of alkyl substituted diallylamine monomers and their use as bile acid sequestrants. *Eur. Polym. J.* **2004,** 40, (4), 693-701.

119. Gore, M. A.; Kulkarni, M. G. K. Bile acid sequestrants and process for preparation therefor. US Patent 0122375, 2007.

120. Mandeville, W. H.; Holmes-Farley, S. R. Process for removing bile salts from a patient and alkylated compositions therefor. WO 95/34585, 1995.

121. Holmes-Farley, S. R.; Mandeville, W. H.; Burke, S. K.; Goldberg, D. I. Method for treating hypercholesterolemia with polyallylamine polymers. US Patent 6,423,754, 2002.

122. Holmes-Farley, S. R.; Dhal, P. K.; Petersen, J. S. Poly-(diallylamine)-based bile acid sequestrants. US Patent 7,125,547, 2006.

123. Research, F. C. f. D. E. a. FDA approved drug products. http://www.accessdata.fda.gov/scripts/cder/drugsatfda/ (11-01-2011).

124. Asami, T.; Uchiyama, M., Treatment of children with familial hypercholesterolemia with Colestilan, a newly developed bile acid-binding resin. *Atherosclerosis* **2002,** 164, (2), 381-382.

125. *Sweetman SC, editor, Martindale: the complete drug reference* 37th ed.; The Pharmaceutical Press: London, 2011.

126. Nichifor, M.; Zhu, X. X.; Baille, W.; Cristea, D.; Carpov, A., Bile acid sequestrants based on cationic dextran hydrogel microspheres. 2. Influence of the length of alkyl substituents at the amino groups of the sorbents on the sorption of bile salts. *J. Pharm. Sci.* **2001,** 90, (6), 681-689.

127. Primack, W. A.; Gartner, L. M.; McGurk, H. E.; Spitzer, A., Hyperchloremia and hypernatremia associated with Cholestyramine therapy. *Pediatr. Res.* **1977,** 11, (4), 520.

128. Harrold, M., Antihyperlipoproteinemics and inhibitors of cholesterol biosynthesis. In *Foye's principles of medicinal chemistry*, 6th ed.; Lemke, T. L.; Williams, D. A., Eds. Lippincott Williams & Wilkins: Philadelphia, 2007; pp 797-819.

129. Benson, G. M.; Haynes, C.; Blanchard, S.; Ellis, D., *In vitro* studies to investigate the reasons for the low potency of Cholestyramine and Colestipol. *J. Pharm. Sci.* **1993,** 82, (1), 80-86.

130. Pollex, R. L.; Joy, T. R.; Hegele, R. A., Emerging antidyslipidemic drugs. *Expert Opin. Emerg. Dr.* **2008,** 13, (2), 363-381.

131. Yoshiteru Honda; Nakano, M., Studies on adsorption characteristics of Bile Acids and methotrexate to a new type of anion-exchange resin, Colestimide. *Chem. Pharm. Bull.* **2000,** 48, (7), 978-981.

132. Alberto, C.; Eberhard, W.; Michel, F., Colesevelam hydrochloride: usefulness of a specifically engineered bile acid sequestrant for lowering LDL-cholesterol. *Eur. J. Cardiovasc. Prev. Rehabil.* **2009,** 16, (1), 1-9.

133. Davidson, M. H.; Dillon, M. A.; Gordon, B.; Jones, P.; Samuels, J.; Weiss, S.; Isaacsohn, J.; Toth, P.; Burke, S. K., Colesevelam Hydrochloride (Cholestagel): A New, Potent Bile Acid Sequestrant Associated With a Low Incidence of Gastrointestinal Side Effects. *Arch. Intern. Med.* **1999,** 159, (16), 1893-1900.

134. Steinmetz, K., Colesevelam hydrochloride. *Am. J. Health Syst. Pharm.* **2002,** 59, (10), 932-939.

135. Matsuzaki, Y., Colestimide: The efficacy of a novel anion-exchange resin in cholestatic disorders. *J. Gastroenterol. Hepatol.* **2002,** 17, (11), 1133-1135.

136. Wu, G. M.; Brown, G. R.; StPierre, L. E., Polymeric sorbents for bile acids .5. Polyacrylamide resins with ammonium-containing pendants. *Langmuir* **1996,** 12, (2), 466-471.

137. Huval, C. C.; Holmes-Farley, S. R.; Mandeville, W. H.; Petersen, J. S.; Sacchiero, R. J.; Maloney, C.; Dhal, P. K., Ammonium and Guanidinium Functionalized Hydrogels as Bile Acid Sequestrants: Synthesis, Characterization, and Biological Properties. *J. Macromol. Sci., Part A: Pure Appl. Chem.* **2004,** 41, (3), 231 - 244.

138. Cameron, N. S.; Eisenberg, A.; Brown, G. R., Amphiphilic block copolymers as bile acid sorbents: 2. Polystyrene-b-poly(N,N,N-trimethylammoniumethylene acrylamide chloride): Self-assembly and application to serum cholesterol reduction. *Biomacromolecules* **2002,** 3, (1), 124-132.

139. Nichifor, M.; Zhu, X. X.; Cristea, D.; Carpov, A., Interaction of hydrophobically modified cationic dextran hydrogels with biological surfactants. *J. Phys. Chem. B* **2001,** 105, (12), 2314-2321.

140. Anderson, J. W.; Baird, P.; Davis Jr, R. H.; Ferreri, S.; Knudtson, M.; Koraym, A.; Waters, V.; Williams, C. L., Health benefits of dietary fiber. *Nutr. Rev.* **2009,** 67, (4), 188-205.

141. Brownlee, I. A., The physiological roles of dietary fibre. *Food Hydrocolloids* **2011,** 25, (2), 238-250.

142. Chau, C. F.; Huang, Y. L.; Lin, C. Y., Investigation of the cholesterol-lowering action of insoluble fibre derived from the peel of Citrus sinensis L. cv. Liucheng. *Food Chem.* **2004,** 87, (3), 361-366.

143. Eastwood, M. A.; Hamilton, D., Studies on the adsorption of bile salts to non-absorbed components of diet. *BBA-Lipid Lipid Met.* **1968,** 152, (1), 165-173.

144. Elhardallou, S., The bile acids binding of the fibre-rich fractions of three starchy legumes. *Plant Foods Hum. Nutr.* **1992,** 42, (3), 207-218.

145. Hoagland, P. D., Binding of dietary anions to vegetable fiber. *J. Agric. Food Chem.* **1989,** 37, (5), 1343-1347.

146. Kritchesvsky, D., In vitro binding properties of dietary fibre. *Eur. J. Clin. Nutr.* **1995,** 49, 113-115.

147. Buhman, K. K.; Furumoto, E. J.; Donkin, S. S.; Story, J. A., Dietary Psyllium Increases Fecal Bile Acid Excretion, Total Steroid Excretion and Bile Acid Biosynthesis in Rats. *J. Nutr.* **1998,** 128, (7), 1199-1203.

148. Garcia Diez, F.; Garcia Mediavilla, V.; Bayon, J., Pectin feeding influences fecal bile acid excretion, hepatic bile acid and cholesterol synthesis and serum cholesterol in rats *J. Nutr.* **1996,** 126, (7), 1766-1771.

149. Kritchevsky, D.; Tepper, S. A., Influence of a fiber mixture on serum and liver lipids and on fecal fat excretion in rats. *Nutr. Res.* **2005,** 25, (5), 485-489.

150. Jenkins, D. J.; Kendall, C. W.; Vuksan, V., Viscous fibers, health claims, and strategies to reduce cardiovascular disease risk1. *Am. J. Clin. Nutr.* **2000,** 71, (2), 401-402.

151. Kendall, C. W. C.; Esfahani, A.; Jenkins, D. J. A., The link between dietary fibre and human health. *Food Hydrocolloids* **2010,** 24, (1), 42-48.

152. Brown, L.; Rosner, B.; Willett, W. W.; Sacks, F. M., Cholesterol-lowering effects of dietary fiber: a meta-analysis. *Am. J. Clin. Nutr.* **1999,** 69, (1), 30-42.

153. Rosendaal, G. M. V.; Shaffer, E. A.; Edwards, A. L.; Brant, R., Effect of time of administration on cholesterol-lowering by psyllium: a randomized cross-over study in

normocholesterolemic or slightly hypercholesterolemic subjects. *Nutrition Journal* **2004,** 3, (17).

154. Camire, M. E.; Dougherty, M. P., Raisin Dietary Fiber Composition and in Vitro Bile Acid Binding. *J. Agric. Food Chem.* **2002,** 51, (3), 834-837.

155. Kahlon, T. S.; Smith, G. E., In vitro binding of bile acids by bananas, peaches, pineapple, grapes, pears, apricots and nectarines. *Food Chem.* **2007,** 101, (3), 1046-1051.

156. Kahlon, T. S.; Woodruff, C. L., In vitro binding of bile acids by soy protein, pinto beans, black beans and wheat gluten. *Food Chem.* **2002,** 79, (4), 425-429.

157. Kongo-Dia-Moukala, J. U.; Zhang, H.; Irakoze, P. C., In Vitro Binding Capacity of Bile Acids by Defatted Corn Protein Hydrolysate. *Int. J. Mol. Sci.* **2011,** 12, 1066-1080.

158. Dongowski, G., Interactions between dietary fibre-rich preparations and glycoconjugated bile acids in vitro. *Food Chem.* **2007,** 104, (1), 390-397.

159. Cornfine, C.; Hasenkopf, K.; Eisner, P.; Schweiggert, U., Influence of chemical and physical modification on the bile acid binding capacity of dietary fibre from lupins (Lupinus angustifolius L.). *Food Chem.* **2010,** 122, (3), 638-644.

160. Kahlon, T. S.; Chiu, M.-C. M.; Chapman, M. H., Steam cooking significantly improves in vitro bile acid binding of beets, eggplant, asparagus, carrots, green beans, and cauliflower. *Nutr. Res.* **2007,** 27, (12), 750-755.

161. Kahlon, T. S.; Chiu, M.-C. M.; Chapman, M. H., Steam cooking significantly improves in vitro bile acid binding of collard greens, kale, mustard greens, broccoli, green bell pepper, and cabbage. *Nutr. Res.* **2008,** 28, (6), 351-357.

162. Zacheri, C.; Eisner, P.; Engel, K. H., In vitro model to correlate viscosity and bile acid-binding capacity of digested water-soluble and insoluble dietary fibres. *Food Chem.* **2011,** 126, 423-428.

163. Cohn, J. S.; Kamili, A.; Wat, E.; Chung, R. W. S.; Tandy, S., Reduction in intestinal cholesterol absorption by various food components: Mechanisms and implications. *Atherosclerosis Supp.* **2010,** 11, (1), 45-48.

164. Férézou, J.; Riottot, M.; Sérougne, C.; Cohen-Solal, C.; Catala, I.; Alquier, C.; Parquet, M.; Juste, C.; Lafont, H.; Mathé, D.; Corring, T.; Lutton, C., Hypocholesterolemic action of beta-cyclodextrin and its effects on cholesterol metabolism in pigs fed a cholesterol-enriched diet. *J. Lipid Res.* **1997,** 38, (1), 86-100.

165. Riottot, M.; Olivier, P.; Huet, A.; Caboche, J. J.; Parquet, M.; Khallou, J.; Lutton, C., Hypolipidemic effects of β-cyclodextrin in the hamster and in the genetically hypercholesterolemic rico rat. *Lipids* **1993,** 28, 181-188.

166. Trautwein, E. A.; Forgbert, K.; Rieckhoff, D.; Erbersdobler, H. F., Impact of beta-cyclodextrin and resistant starch on bile acid metabolism and fecal steroid excretion in regard to their hypolipidemic action in hamsters. *Biochim. Biophys. Acta, Mol. Cell Biol. Lipids* **1999,** 1437, (1), 1-12.

167. Baille, W. E.; Huang, W. Q.; Nichifor, M.; Zhu, X. X., Functionalized beta-cyclodextrin polymers for the sorption of bile salts. *J. Macromol. Sci., Part A: Pure Appl. Chem.* **2000,** 37, (7), 677-690.

168. Nichifor, M.; Cristea, D.; Carpov, A., Sodium cholate sorption on cationic dextran hydrogel microspheres. 1. Influence of the chemical structure of functional groups. *Int. J. Biol. Macromol.* **2000,** 28, (1), 15-21.

169. Nichifor, M.; Cristea, D.; Mocanu, G.; Carpov, A., Aminated polysaccharides as bile acid sorbents: in vitro study. *J. Biomater. Sci., Polym. Ed.* **1998,** 9, (6), 519-534.

170. Gallaher, C. M.; Munion, J.; Hesslink, R.; Wise, J.; Gallaher, D. D., Cholesterol Reduction by Glucomannan and Chitosan Is Mediated by Changes in Cholesterol Absorption and Bile Acid and Fat Excretion in Rats. *J. Nutr.* **2000,** 130, (11), 2753-2759.

171. Hirano, S.; Itakura, C.; Seino, H.; Akiyama, Y.; Nonaka, I.; Kanbara, N.; Kawakami, T., Chitosan as an ingredient for domestic animal feeds. *J. Agric. Food Chem.* **1990,** 38, (5), 1214-1217.

172. Sugano, M.; Watanabe, S.; Kishi, A.; Izume, M.; Ohtakara, A., Hypocholesterolemic action of chitosans with different viscosity in rats. *Lipids* **1988,** 23, 187-191.

173. Trautwein, E. A.; Jürgensen, U.; Erbersdobler, H. F., Cholesterol-lowering and gallstone-preventing action of chitosans with different degrees of deacetylation in hamsters fed cholesterol-rich diets. *Nutr. Res.* **1997,** 17, (6), 1053-1065.

174. Zhou, K.; Xia, W.; Zhang, C.; Yu, L., In vitro binding of bile acids and triglycerides by selected chitosan preparations and their physico-chemical properties. *LWT-Food Sci. Technol.* **2006,** 39, (10), 1087-1092.

175. Ikeda, I.; Sugano, M.; Yoshida, K.; Sasaki, E.; Iwamoto, Y.; Hatano, K., Effects of chitosan hydrolyzates on lipid absorption and on serum and liver lipid concentration in rats. *J. Agric. Food Chem.* **1993,** 41, (3), 431-435.

176. Lee, J. K.; Kim, S. U.; Kim, J. H., Modification of chitosan to improve its hypocholesterolemic capacity. *Biosci. Biotechnol. Biochem* **1999,** 63, (5), 833-839.

177. Kim, C. H.; Chun, H. J., A synthesis of O-diethylaminoethyl chitosan and its binding ability of cholate and deoxycholate anion in vitro. *Polym. Bull.* **1999,** 42, (1), 25-32.

178. Murata, Y.; Kodoma, Y.; Hirai, D.; Kofugi, K.; Kawashima, S., Properties of an Oral Preparation Containing a Chitosan Salt. *Molecules* **2009,** 14, 755-762.

179. Murata, Y.; Nagaki, K.; Kofuji, K.; Sanae, F.; Kontani, H.; Kawashima, S., Adsorption of bile acid by chitosan salts prepared with cinnamic acid and analogue compounds. *J. Biomater Sci. Polymer Ed.* **2006,** 17, 781-789.

180. Huval, C. C.; Bailey, M. J.; Braunlin, W. H.; Holmes-Farley, S. R.; Mandeville, W. H.; Petersen, J. S.; Polomoscanik, S. C.; Sacchiro, R. J.; Chen, X.; Dhal, P. K., Novel cholesterol lowering polymeric drugs obtained by molecular imprinting. *Macromolecules* **2001,** 34, (6), 1548-1550.

181. Zhang, L. H.; Janout, V.; Renner, J. L.; Uragami, M.; Regen, S. L., Enhancing the "stickiness" of bile acids to cross-linked polymers: A bioconjugate approach to the design of bile acid sequestrants. *Bioconjugate Chem.* **2000,** 11, (3), 397-400.

182. Figuly, G. D.; Royce, S. D.; Khasat, N. P.; Schock, L. E.; Wu, S. L. D.; Davidson, F.; Campbell, G. C.; Keating, M. Y.; Chen, H. W.; Shimshick, E. J.; Fischer, R. T.; Grimminger, L. C.; Thomas, B. E.; Smith, L. H.; Gillies, P. J., Preparation and characterization of novel poly(alkylamine)-based hydrogels designed for use as bile acid sequestrants. *Macromolecules* **1997,** 30, (20), 6174-6184.

183. Zhu, X. X.; Nichifor, M., Polymeric materials containing bile acids. *Acc. Chem. Res.* **2002,** 35, (7), 539-546.

184. Cameron, N. S.; Eisenberg, A.; Brown, G. R., Amphiphilic block copolymers as bile acid sorbents: 1. Synthesis of polystyrene-b-poly(N,N,N-trimethylammoniumethylene acrylamide chloride). *Biomacromolecules* **2002,** 3, (1), 116-123.

185. Huval, C. C.; Bailey, M. J.; Holmes-Farley, S. R.; Mandeville, W. H.; Miller-Gilmore, K.; Sacchiero, R. J.; Dhal, P. K., Amine functionalized polyethers as bile acid sequestrants: Synthesis and biological evaluation. *J. Macromol. Sci., Part A: Pure Appl. Chem.* **2001,** 38, (12), 1559-1574.

186. Huval, C. C.; Chen, X.; Holmes-Farley, S. R.; Mandeville, W. H.; Polomoscanik, S. C.; Sacchiero, R. J.; Dhal, P. K., Molecularly imprinted bile acid sequestrants: Synthesis and biological studies. *Mat. Res. Soc. Sym. Proc.* **2004,** 787, 85-90.

187. Wang, Y.; Zhang, J.; Zhu, X. X.; Yu, A., Specific binding of cholic acid by cross-linked polymers prepared by the hybrid imprinting method. *Polymer* **2007,** 48, (19), 5565-5571.

188. Yanez, F.; Chianella, I.; Piletsky, S. A.; Concheiro, A.; Alvarez-Lorenzo, C., Computational modeling and molecular imprinting for the development of acrylic polymers with high affinity for bile salts. *Anal. Chim. Acta* **2010,** 659, (1-2), 178-185.

189. Bergmann, N. M.; Peppas, N. A., Molecularly imprinted polymers with specific recognition for macromolecules and proteins. *Prog. Polym. Sci.* **2008,** 33, (3), 271-288.

190. Hillberg, A. L.; Tabrizian, M., Biomolecule imprinting: Developments in mimicking dynamic natural recognition systems. *Irbm* **2008,** 29, (2-3), 89-104.

191. Byrne, M. E.; Salian, V., Molecular imprinting within hydrogels II: Progress and analysis of the field. *Int. J. Pharm.* **2008,** 364, (2), 188-212.

192. Komiyama, M.; Takeuchi, T.; Mukawa, T.; Asanuma, H., Molecular imprinting: from fundamentals to applications. Co, W.-V. V. G., Ed. Wiley-VCH Verlag GmbH & Co: Weinheim, 2003.

193. Wang, N. X.; von Recum, H. A., Affinity-Based Drug Delivery. *Macromol. Biosci.* **2011,** 11, (3), 321-332.

Chapter 2

Copper-mediated RDRP in polar solvents: insights into some relevant mechanistic aspects

---

*The contents of this chapter are published in: Guliashvili T., **Mendonça P. V.**, Serra A. C., Popov A. V., Coelho J. F. J., "Copper-Mediated Controlled/"Living" Radical Polymerization in Polar Solvents: Insights into Some Relevant Mechanistic Aspects", Chemistry – A European Journal, 2012, 18, (15), 4607-4612.*

2.1. Abstract

The field of transition-metal-mediated reversible deactivation radical polymerization (RDRP) has become the subject of intense discussion regarding the mechanism of this widely-used and versatile process. Most mechanistic analyses (atom transfer radical polymerization (ATRP) *vs.* single electron transfer-living radical polymerization (SET-LRP)) have been based on model experiments, which cannot correctly mimic the true reaction conditions. In this work it is presented, for the first time, a determination of the [CuBr]/[L] (L: nitrogen-based chelating ligand) ratio and the extent of CuBr/L disproportionation during the RDRP of methyl acrylate (MA) in dimethyl sulfoxide (DMSO) with Cu(0) wire as a transition-metal catalyst source. The results revealed that Cu(0) acts as a supplemental activator and reducing agent of $CuBr_2$/L to CuBr/L. More importantly, the CuBr/L species seem to be responsible for the activation of alkyl halides in SET-LRP.

2.2. Introduction

In 1995, the groups of Matyjaszewski[1] and Sawamoto[2] independently discovered the RDRP of vinyl monomers mediated by transition-metal catalysts. Since then, this method has become the most versatile technique for the controlled synthesis of complex macromolecular architectures with predetermined molecular weight, narrow molecular weight distribution and useful chain-end functionality.[3-5] In the original publication[1] the authors coined the name for this new polymerization methodology as ATRP since it resembled the well-known atom transfer radical addition (ATRA) reaction.[6-11] Mechanistically, ATRP is based on the transition metal complex mediated fast equilibrium between dormant species (initiator and/or macroinitiator, P-X, X: halide or pseudohalide) and active species (radical and/or macroradical, $P^{\bullet}$). Homolytic cleavage of the C-X bond of the dormant species (P-X) is catalyzed by the lower oxidation state transition metal complex (activator - $M_t^nX_m$/L). The generated macroradical ($P^{\bullet}$) reacts with the higher oxidation state transition metal complex (deactivator - $M_t^{n+1}X_{m+1}$/L) forming dormant species and regenerating the activator (Scheme 2.1). In ATRP the radical-radical termination (recombination and/or disproportionation) and radical chain

transfer reactions are significantly suppressed due to the so-called persistent radical effect.[12] To ensure the "controlled/living" characteristics (control over molecular weight, dispersity ($Đ$), chain-end functionality, and so on) of ATRP, the equilibrium shown in Scheme 2.1 the must be shifted towards dormant species ($k_a << k_d$).

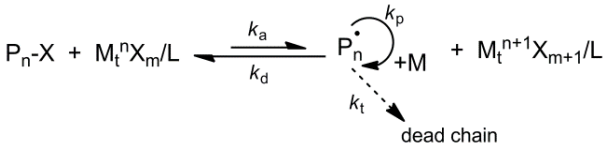

Scheme 2.1. General mechanism of ATRP (X = Cl, Br, I, SCN; L = N, P, Cp based ligands; M_t = Cu, Ru, Fe, Os, Ni, etc.; n = 0, 1, 2, etc.; m = 0, 1, 2, etc).

Among various transition metal catalysts, the copper-based complexes are the most widely used in ATRP[3-5, 13] as well as in related advanced developments such as activators regenerated by electron transfer (ARGET) ATRP,[14-16] initiators for continuous activator regeneration (ICAR) ATRP,[17] supplemental activator and reducing agent (SARA) ATRP[18, 19] and the so-called SET-LRP.[20-22] In the above-mentioned subclasses[14-22] the total amount of Cu catalyst present in the polymerization mixture is significantly diminished to ppm levels. Nevertheless, SET-LRP is also of particular interest because it offers very mild reaction conditions such as low temperatures, trace amount of catalyst (ppm) and the use of copper (powder or wire form) as the initial catalyst. These particular reaction conditions enable the synthesis of very high molar mass polymers using activated and non-activated monomers.[20] The SET-LRP was originally proposed to proceed via different mechanism than the classical ATRP.[20] In the classical ATRP, both the activation and the deactivation steps are based on the inner sphere (bonded) electron transfer (ISET) processe between R-X (dormant species) and transition metal catalyst in the lower oxidation state ($M_t^nX_m$/L activator). It is generally assumed that during the activation step of ATRP a complex between dormant species (R-X) and transition metal centre ($M_t^nX_m$/L) is formed via the halogen atom bridge (dormant species act as a "ligand" for transition metal complex). The ISET from transition metal complex to the dormant species and homolytic cleavage of C-X (X = Cl, Br) bond occurs in a concerted manner. By contrast, in the seminal SET-LRP paper from Percec's group[20] the authors proposed that the activation of dormant species (R-X) occurs exclusively by "nascent" Cu(0) species via outer sphere (non-bonded) electron transfer process (OSET). In addition, it

was postulated that the activation of dormant species under SET-LRP conditions involves the formation of radical-anion intermediates from an alkyl halide initiator and its stepwise decomposition via "heterolytic" cleavage of C-X bond. In SET-LRP it was also proposed that *in situ* generated complex CuX/L disproportionates "spontaneously" into Cu(0) and CuX_2/L species (regeneration of the activator and generation of the deactivator respectively, Scheme 2.2), thus assuming that the SET-LRP process is not based on the persistent radical effect (which means accumulation of an excess of deactivator species through the bimolecular termination of propagating radicals). The different mechanistic proposal for SET-LRP initiated an intense debate in the field of transition-metal-mediated RDRP.[23, 24] Understanding the real mechanism of SET-LRP is very important for further development of more powerful catalysts as well as to achieve successful RDRP of other monomer families.

In 2007, Matyjaszewski's research group reported extensive experimental studies[24] about the role of Cu(0) during SET-LRP and concluded that the mentioned process is based on the ARGET ATRP mechanism, where the main role of Cu(0) is the reduction of $CuBr_2$/L deactivator into Cu(I)Br/L activator (L: Me_6TREN: tris[2-(dimethylamino)ethyl]amine). Later, after the recognition of the activation of alkyl halides by Cu(0), the authors termed the method as SARA ATRP[19] (Scheme 2.2). In the same work,[24] it was also emphasized that the initial activator in SET-LRP must be Cu(0) species since in the absence of externally added $CuBr_2$/L there is no other mechanism available to activate initiator and produce CuBr/L catalyst. Based on the principle of microscopic reversibility it was postulated that in the solvents that favor disproportionation ($K_{disp} >> 1$, Scheme 2.3), the CuBr/L species must be more powerful activator than Cu(0) species. However in the real system, the preferable activation of dormant species with either CuBr/L or with Cu(0) depends, not only on the absolute rate constants (k_a^{CuBr} and $k_a^{Cu(0)}$), but also on the relative concentrations of the above species present during SET-LRP. In other words, without knowing the degree of disproportionation of CuBr/L species it is impossible to determine the relative concentrations of CuBr/L *vs.* Cu(0) under real SET-LRP conditions, and hence to identify the real activator. Although the K_{disp} values obtained in DMSO were also reported in the same work,[24] it is of little help to estimate the extent of disproportionation of CuBr/L during the SET-LRP unless the [L]/[CuBr] value is known.

No experimental data about the extent of disproportionation of CuBr/L is currently available for real SET-LRP conditions.

Although the degree of CuBr/L disproportionation and identification of the real catalyst during SET-LRP is still under debate, the heterogeneous reduction of alkyl halides at an inert electrode was recently reported.[23] This comprehensive theoretical and experimental work on the mechanism of C-Br bond reductive cleavage in alkyl halide (activated) initiators relevant to SET-LRP demonstrated that no "heterolytic" decomposition occurred for the studied alkyl halides under OSET conditions. It was also shown that there is no radical-anion intermediate formation possible during the activation step under the OSET mechanism, and that the reductive cleavage of alkyl bromides occurs in a concerted manner with a significant activation barrier. This is in sharp contrast with the mechanism described in earlier computational work about the activation of dormant species with Cu(0) catalyst via OSET pathway (formation and decomposition of intermediate radical anions from dormant species).[25, 26]

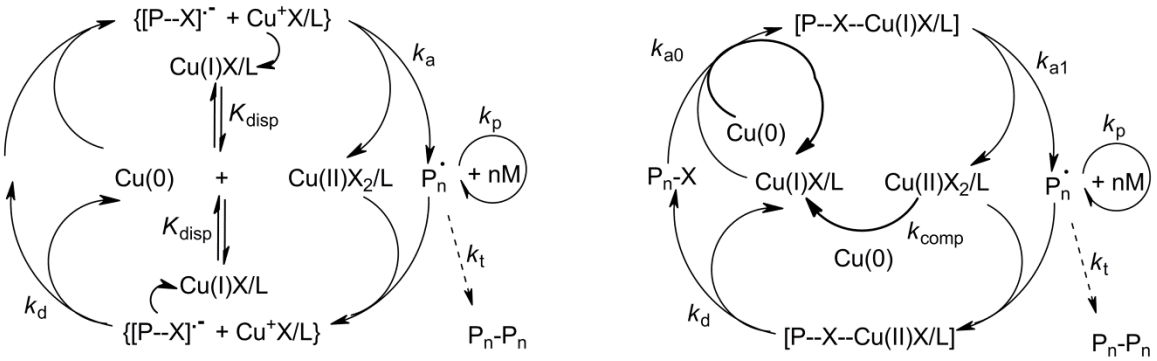

Scheme 2.2. Detailed mechanism of copper-catalyzed SET-LRP and SARA ATRP (in SARA ATRP various zerovalent transition metals can be used in place of Cu (0), such as Fe (0), etc., while SET-LRP is only postulated to occur exclusively with Cu(0)).

The role of Cu(0) during the SET-LRP of vinyl monomers in polar solvents and the extent of disproportionation of the *in situ* formed CuBr/L species are two main points of debate about the mechanism of this hypothetical process (Scheme 2.2).[23, 24] Most of the studies devoted to the clarification of the SET-LRP mechanism are based on model experiments, which in some important cases are not able to correctly mimic the true SET-

LRP conditions.[20, 23, 24, 27] Most importantly, the degree of disproportionation of CuX/L, which is the key requirement for SET-LRP mechanism, was only measured in pure solvents and/or solvent mixtures in a wide range of ligand concentrations. The degree of disproportionation of CuX/L depends on the nature of X, solvent and ligand, as well as on their concentrations relative to Cu(0).

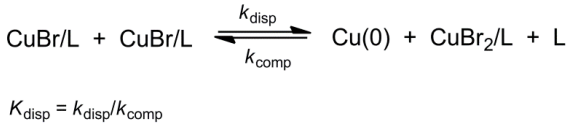

Scheme 2.3. Disproportionation of CuBr/L into Cu(0) and $CuBr_2$/L in DMSO; L: Me_6TREN or other chelating N ligands.

Even when the solvent and ligand combination favors disproportionation, the ligand concentration determined the degree of disproportionation. Percec and co-workers reported[27] that when [Me_6TREN]/[CuBr] value is greater than 1, the disproportionation diminishes exponentially and, for example, when [Me_6TREN]/[CuBr] $\geq \approx 2$, the disproportionation of CuBr/L is almost suppressed (less than ca. 15 %) in DMSO and other polar solvents. Thus, it is essential to know the [L]/[CuBr] ratio during the real SET-LRP conditions to estimate the degree of CuBr disproportionation and to identify the real catalyst.

The aim of this work was to measure the [Me_6TREN]/[CuBr] ratio and use this value to estimate the extent of Cu(I)Br/L disproportionation under the real SET-LRP conditions. For this purpose, a series of kinetic experiments of SET-LRP of MA in DMSO using Cu(0) wire (which is the most popular source of copper used for SET-LRP) as the catalyst were conducted and the consumption of Cu(0) was monitored.

2.3. Experimental

2.3.1. Materials

MA (Acros, 99% stabilized) was passed over a sand/alumina column before use in order to remove the radical inhibitor. CuBr (Fluka, > 98%), $CuBr_2$ (Acros, 99+% extra pure, anhydrous), deuterated chloroform ($CDCl_3$) (Euriso-top, +1%TMS), DMSO (Acros,

99.8+% extra pure), ethyl α-bromoisobutyrate (EBiB) (Sigma-Aldrich, 98%) and polystyrene (PS) standards (Polymer Laboratories) were used as received.

Zerovalent copper wire (Carlo Ebra; ≥ 99.9%, d = 0.1 cm) was washed with nitric acid and subsequently rinsed acetone and dried under a stream of nitrogen before use.

Tetrahydrofuran (THF) (Panreac, HPLC grade) was filtered under reduced pressure before use.

Me_6TREN was synthesized according procedures described in the literature.[28, 29]

2.3.2. Techniques

400 MHz ^{1}H NMR spectra of reaction mixture samples were recorded on a Bruker Avance III 400 MHz spectrometer, with a 5-mm TIX triple resonance detection probe, in $CDCl_3$ with tetramethylsilane (TMS) as an internal standard. Conversion of monomers was determined by integration of monomer and polymer peaks using MestRenova software version: 6.0.2-5475.

The chromatography parameters of the samples were determined using high performance size exclusion chromatography HPSEC; Viscotek (Viscotek TDAmax) with a differential viscometer (DV); right-angle laser-light scattering (RALLS, Viscotek); low-angle laser-light scattering (LALLS, Viscotek) and refractive index (RI). The column set consisted of a PL 10 μm guard column (50x7.5mm^2) followed by one MIXED-E PL column (3 μm) and two MIXED-C PL columns (5 μm). HPLC dual piston pump was set with the flow rate of 1 mL/min. The eluent (THF) was previously filtered through a 0.2 μm filter. The system was also equipped with an on-line degasser. The tests were done at 30 °C using an Elder CH-150 heater. Before the injection (100 μL), the samples were filtered through a polytetrafluoroethylene (PTFE) membrane with 0.2 mm pore. The system was calibrated with narrow PS standards. The *dn/dc* was determined as 0.063 for PMA. Molecular weights (M_n^{SEC}) and $Đ$ values of the synthesized polymers were determined by multidetectors calibration using the OmniSEC software version: 4.6.1.354.

The ultraviolet-visible (UV-Vis) studies were performed with a Jasco V-530 spectrophotometer. The analyses were carried in the 200 – 1100 nm range at room temperature.

2.3.3. Procedures

Typical procedure for the Cu wire/$[CuBr_2]_0$/$[Me_6TREN]_0$ = Cu wire/0.05/1 catalyzed RDRP of MA (DP = 222)

MA (3.1 mL; 34.8 mmol) was purified in a sand/alumina column just before reaction. Copper wire (d = 0.1 cm; l = 5 cm) was weighted, wrapped around a magnetic stirrer bar and charged to a Schlenk reactor. A mixture of $CuBr_2$ (1.8 mg, 0.008 mmol), Me_6TREN (36.1 mg, 0.157 mmol) and DMSO (1.6 mL) (previously bubbled with nitrogen for about 5 minutes) was placed in the reactor along with the monomer and EBiB (30.6 mg, 0.157 mmol). The reactor was sealed, frozen in liquid nitrogen and the mixture was deoxygenated with four freeze-vacuum-thaw cycles and purged with nitrogen. The Schlenk reactor was placed in a water bath at 25 °C with stirring (700 rpm). Different reaction mixture samples were collected during the polymerization by using an airtight syringe and purging the side arm of the Schlenk reactor with nitrogen. The samples were analyzed by ^{1}H NMR spectroscopy in order to determine the monomer conversion and theoretical molecular weight and by SEC, to determine molecular weight and $Đ$ of the polymers. The reactions were done for different amounts of Me_6TREN. By the end of the reaction, the copper wire was washed with acetone, dried and weighted, to determine the consumed amount.

UV-Vis spectroscopic study of Cu(I) stabilization

The catalyst(s) were placed in a quartz UV-Vis cuvette and purged with nitrogen. The DMSO and Me_6TREN were mixed in a vial and bubbled with nitrogen, for about 15 minutes, to remove oxygen. This solution was then added to the UV-Vis cuvette, which was sealed under nitrogen. After shaking, to dissolve all the catalyst(s), the cuvette was placed in the spectrometer for spectra acquisition. The absorbance was measured in different times, in the 200-1100 nm range, at room temperature.

2.4. Results and discussion

The kinetic plots of Cu(0)-catalyzed RDRP of MA in DMSO are shown in Figure 2.1. Note that in experiments in which only Cu(0) wire was used (no additional $CuBr_2$ or CuBr were added during the reaction), the polymerization showed some induction period (red and black symbols in Figure 2.1 (a)), which was also observed by other groups practicing SET-LRP.[30]

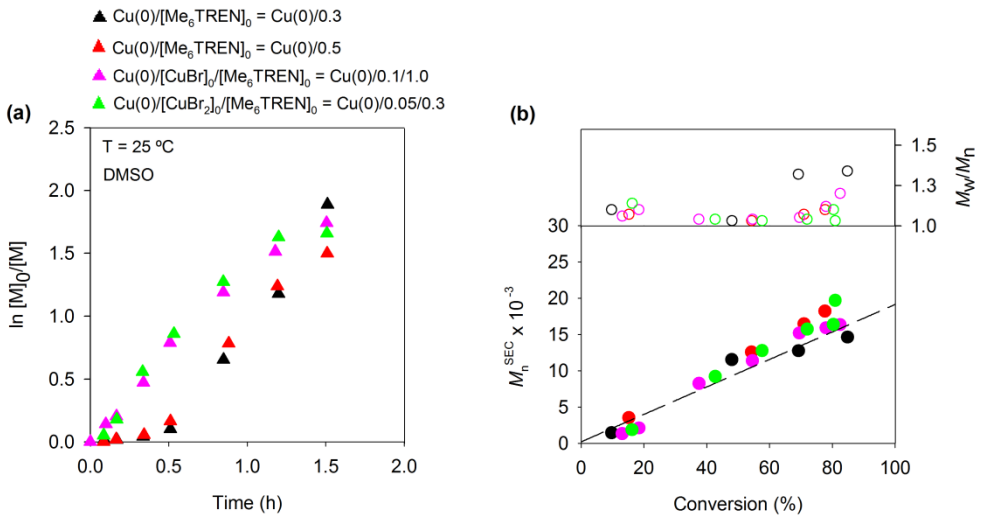

Figure 2.1. (a) Kinetic plots of conversion and $\ln[M]_0/[M]$ *vs.* time and (b) plot of number-average molecular weights (M_n^{SEC}) and *Đ* (M_w/M_n) *vs.* monomer conversion for the Cu(0)-catalyzed RDRP of MA in DMSO at 25 °C, using different metal catalyst/ligand ratios. Reaction conditions: $[MA]_0/[DMSO]$ = 2/1 (v/v); $[MA]_0/[EBiB]_0$ = 222.

This observation was explained by some oxidation of the copper surface (contamination with CuO), which slowed down the initial activation.[31] No induction period was found when mixtures of CuBr and Cu(0) or $CuBr_2$ and Cu(0) wire were used (pink and green symbols in Figure 2.1 (a)), which may also indicate that CuBr is a much stronger activator than Cu(0) or CuO.

The primary parameter evaluated during the kinetic experiments was the consumption of Cu(0) wire during the polymerization. Table 2.1 presents the data of the consumption of copper from the Cu(0) wire surface during the Cu(0)-catalyzed RDRP of MA in DMSO with different molar ratios of CuBr, $CuBr_2$ and ligand (Me_6TREN). The amount of copper consumed increased with monomer conversion, whereas the ratio $[Me_6TREN]/[Cu_{consumed}]$ decreased with monomer conversion (Figure 2.2). Under excess

ligand concentrations, the amount of copper consumed (Table 2.1) should be equal to the sum of [CuBr/Me_6TREN] and [$CuBr_2$/Me_6TREN].

Table 2.1. Consumption of copper from the Cu(0) wire surface during the Cu(0) wire-catalyzed RDRP of MA in DMSO, at 25 °C during 1.5 h.

Entry	$[M]_0/[I]_0/[Cu(0)\ wire]_0/[CuBr]_0/[CuBr_2]_0/[L]_0$ [a]	Conv. (%)	$[Cu_{consumed}]/[I]_0$ [b]	$[L]/[Cu_{total}]$ [c]
1	222/1/wire/0/0/0.3	77	0.17	≈ 1.8
2	222/1/wire/0/0/0.5	84	0.21	≈ 2.4
3	222/1/wire/0/0/1.0	74	0.25	≈ 4.0
4	222/1/wire/0/0.05/0.3	81	0.09	≈ 2.7
5	222/1/wire/0/0.05/0.5	74	0.16	≈ 2.8
6	222/1/wire/0/0.05/1.0	82	0.15	≈ 6.3
7	222/1/wire/0.05/0/1.0	81	0.15	≈ 5.0
8	222/1/wire/0.1/0/1.0	82	0.09	≈ 5.2
9	222/0/wire/0/0/0.5	0	–[d]	–

[a] M: MA; I: EBiB; Cu(0) wire: d = 0.1 cm and l = 5 cm; L: Me_6TREN

[b] [Cu consumed] = ((Cu wire wt. before reaction) - (Cu wire wt. after reaction))/63.55

[c] [Cu total] = [Cu consumed] + [CuBr externally added] + [$CuBr_2$ externally added]

[d] [Cu consumed] = 0 (control blank experiment)

It is very important to notice that, in all experiments, the molar ratio of copper consumed was significantly lower than both initiator and ligand concentrations. In addition, it should be emphasized that regardless the ratios [CuBr]/[Me_6TREN] and [$CuBr_2$]/[Me_6TREN] in the reaction mixture, the [Me_6TREN]/[CuBr] ratio must be always higher than [Me_6TREN]/[Cu consumed]. This observation directly indicates that under SET-LRP conditions the equilibrium shown in the Scheme 2.2 is always shifted towards the CuBr/L species. The stabilization of CuBr/L under excess ligand concentration was also supported by a model experiment shown in Figure 2.3 (quantitative comproportionation of $CuBr_2$/Me_6TREN deactivator complex with Cu(0) species under excess ligand concentration in DMSO).

One might assume that in SET-LRP the Cu(0) species (copper wire and trace amount of nascent Cu(0) species formed by limited disproportionation) is a more active catalyst than CuBr/Me_6TREN. However, it has been experimentally determined that in copper-

mediated radical polymerizations, the soluble CuBr/Me_6TREN is a much stronger activator than heterogeneous Cu(0)/Me_6TREN.

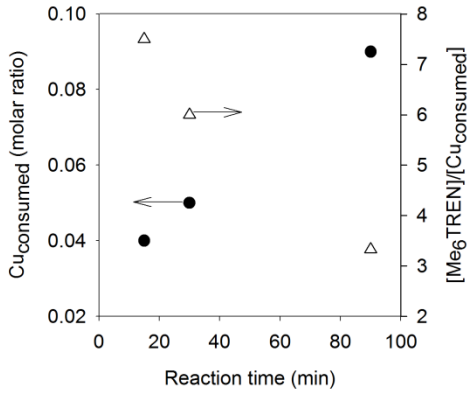

Figure 2.2. Consumption of copper during the Cu(0)-catalyzed RDRP of MA in DMSO at 25 °C. The molar ratio of copper consumed is relative to the initial amount of EBiB. Reaction conditions: $[MA]_0/[EBiB]_0/[Cu(0)\ wire]_0/[CuBr_2]_0/[Me_6TREN]_0$ = 222/1/Cu(0) wire/0.05/0.3; $[MA]_0/[DMSO]$ = 2/1 (v/v); Cu wire: *d* = 0.1 cm and *l* = 5 cm (entry 4 in Table 2.1).

The k_a of EBiB is approximately 1100 $M^{-1}\cdot s^{-1}$ (measured at ambient temperature in acetonitrile (CH_3CN) with CuBr/Me_6TREN activator),[32] whereas the k_a of the same initiator under SET-LRP conditions was reported to be approximately 4.3 $M^{-1}\cdot s^{-1}$ (measured at ambient temperature in DMSO with Cu(0)/Me_6TREN).[33] It appears that in SET-LRP the CuBr/Me_6TREN catalyst is the preferable activator by both thermodynamic ([CuBr/Me_6TREN] >> $[Cu(0)_{nascent}]$) and kinetic (k_a(CuBr/Me_6TREN) >> k_a(Cu(0)/Me_6TREN)) factors. The possibility that Cu(0) acts as a supplemental activator, however, cannot be completely excluded, although this reaction would be very slow because of the low concentration of Cu(0) nascent species, the low value of k_a(Cu(0)/Me_6TREN),[33] and the high barrier for activation of alkyl halide initiators under the proposed OSET conditions.[23] The main role of the Cu(0) species seems to be the reduction of $CuBr_2$/Me_6TREN (comproportionation reaction), which is produced at a high rate due to the high reactivity of CuBr/Me_6TREN with the (macro)initiator. Note that if MA polymerization is conducted with CuBr/Me_6TREN in the absence of Cu(0), the reaction stops due to rapid accumulation of $CuBr_2$/Me_6TREN. Addition of Cu(0), however, allows the reaction to proceed towards higher monomer conversion due to the reduction of $CuBr_2$/Me_6TREN with Cu(0).

Finally, it has been clearly demonstrated that the SET-LRP of MA in DMSO is, in fact, based on the SARA ATRP mechanism. The structure of the CuBr/Me_6TREN complex (mononuclear, binuclear, cationic, neutral, and so forth) is also strongly dependent on the value of [L]/[CuBr].[33] It can be assumed that, because the [Me_6TREN]/[CuBr] is 2.0-6.0, the most probable activator would be a cationic complex $Cu(I)^{(+)}$/Me_6TREN–$Br^{(-)}$.[34] However, the determination of the exact structure of the CuBr/Me_6TREN activator under Cu(0)-catalyzed RDRP conditions requires more complex experimental studies as outlined in the recent work by Gennaro *et al*.[34]

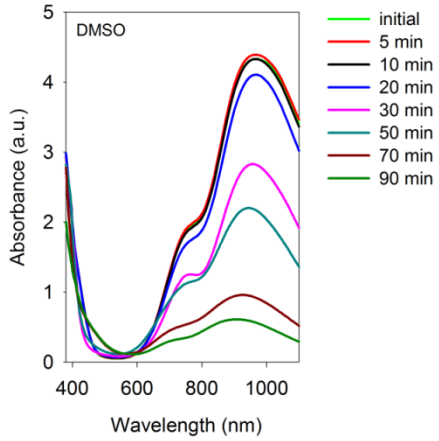

Figure 2.3. Comproportionation of $CuBr_2$/Me_6TREN with Cu(0) in DMSO in the presence of ligand excess, $[Cu\ wire]_0/[CuBr_2]_0/[Me_6TREN]_0$ = Cu wire/0.05/0.3 (conditions mimicking the experiment shown in Table 2.1 entry 4).

2.5. Conclusions

On the basis of kinetic experiments, it was demonstrated that the most probable activator under the SET-LRP conditions is the CuBr/Me_6TREN catalyst. The role of Cu(0) is to act as a supplemental activator of dormant species and also as a reducing agent (reduction of accumulated $CuBr_2$/Me_6TREN species into CuBr/Me_6TREN). More experimental studies are needed to identify the structure of the CuBr/Me_6TREN activator since it is known to be strongly dependent on the ligand concentration.[34] Of course, the present work is not the final word on the mechanism of the SET-LRP process; however, it provides additional insights into the details of this process. Determination of full reaction mechanism for the SET-LRP process will, without doubt, lead to the development of more powerful catalytic systems for metal-mediated RDRP.

2.6. References

1. Wang, J.-S.; Matyjaszewski, K., Controlled/"living" radical polymerization. Atom transfer radical polymerization in the presence of transition-metal complexes. *J. Am. Chem. Soc.* **1995,** 117, (20), 5614-5615.

2. Kato, M.; Kamigaito, M.; Sawamoto, M.; Higashimura, T., Polymerization of Methyl Methacrylate with the Carbon Tetrachloride/Dichlorotris-(triphenylphosphine)ruthenium(II)/Methylaluminum Bis(2,6-di-tert-butylphenoxide) Initiating System: Possibility of Living Radical Polymerization. *Macromolecules* **1995,** 28, (5), 1721-1723.

3. Kamigaito, M.; Ando, T.; Sawamoto, M., Metal-Catalyzed Living Radical Polymerization. *Chem. Rev.* **2001,** 101, (12), 3689-3746.

4. Matyjaszewski, K.; Xia, J., Atom Transfer Radical Polymerization. *Chem. Rev.* **2001,** 101, (9), 2921-2990.

5. Tsarevsky, N. V.; Matyjaszewski, K., "Green" Atom Transfer Radical Polymerization: From Process Design to Preparation of Well-Defined Environmentally Friendly Polymeric Materials. *Chem. Rev.* **2007,** 107, (6), 2270-2299.

6. Kharasch, M. S.; Jensen, E. V.; Urry, W. H., Addition of carbon tetrachloride and chloroform to olefins. *Science* **1945,** 102, 128.

7. Eckenhoff, W. T.; Pintauer, T., Copper Catalyzed Atom Transfer Radical Addition (ATRA) and Cyclization (ATRC) Reactions in the Presence of Reducing Agents. *Cat. Rev. - Sci. Eng.* **2010,** 52, (1), 1-59.

8. Minisci, F., Free-radical additions to olefins in the presence of redox systems. *Acc. Chem. Res.* **1975,** 8, (5), 165-171.

9. Pintauer, T., Catalyst Regeneration in Transition-Metal-Mediated Atom-Transfer Radical Addition (ATRA) and Cyclization (ATRC) Reactions. *Eur. J. Inorg. Chem.* **2010,** 2010, (17), 2449-2460.

10. Pintauer, T.; Matyjaszewski, K., Atom transfer radical addition and polymerization reactions catalyzed by ppm amounts of copper complexes. *Chem. Soc. Rev.* **2008,** 37, (6), 1087-1097.

11. Severin, K., Ruthenium catalysts for the Kharasch reaction. *Curr. Org. Chem.* **2006,** 10, (2), 217-224.

12. Fischer, H., The Persistent Radical Effect: A Principle for Selective Radical Reactions and Living Radical Polymerizations. *Chem. Rev.* **2001,** 101, (12), 3581-3610.

13. Matyjaszewski, K.; Tsarevsky, N. V., Nanostructured functional materials prepared by atom transfer radical polymerization. *Nat Chem* **2009,** 1, (4), 276-288.

14. de Vries, A.; Klumperman, B.; de Wet-Roos, D.; Sanderson, R. D., The Effect of Reducing Monosaccharides on the Atom Transfer Radical Polymerization of Butyl Methacrylate. *Macromol. Chem. Phys.* **2001,** 202, (9), 1645-1648.

15. Jakubowski, W.; Matyjaszewski, K., Activators Regenerated by Electron Transfer for Atom-Transfer Radical Polymerization of (Meth)acrylates and Related Block Copolymers. *Angew. Chem., Int. Ed.* **2006,** 45, (27), 4482-4486.

16. Jakubowski, W.; Min, K.; Matyjaszewski, K., Activators Regenerated by Electron Transfer for Atom Transfer Radical Polymerization of Styrene. *Macromolecules* **2005,** 39, (1), 39-45.

17. Matyjaszewski, K.; Jakubowski, W.; Min, K.; Tang, W.; Huang, J.; Braunecker, W. A.; Tsarevsky, N. V., Diminishing catalyst concentration in atom transfer radical polymerization with reducing agents. *Proc. Natl. Acad. Sci. U. S. A.* **2006,** 103, (42), 15309-15314.

18. Mendonça, P. V.; Serra, A. C.; Coelho, J. F. J.; Popov, A. V.; Guliashvili, T., Ambient temperature rapid ATRP of methyl acrylate, methyl methacrylate and styrene in polar solvents with mixed transition metal catalyst system. *Eur. Polym. J.* **2011,** 47, (7), 1460-1466.

19. Zhang, Y.; Wang, Y.; Matyjaszewski, K., ATRP of Methyl Acrylate with Metallic Zinc, Magnesium, and Iron as Reducing Agents and Supplemental Activators. *Macromolecules* **2011,** 44, (4), 683-685.

20. Percec, V.; Guliashvili, T.; Ladislaw, J. S.; Wistrand, A.; Stjerndahl, A.; Sienkowska, M. J.; Monteiro, M. J.; Sahoo, S., Ultrafast Synthesis of Ultrahigh Molar Mass Polymers by Metal-Catalyzed Living Radical Polymerization of Acrylates, Methacrylates, and Vinyl Chloride Mediated by SET at 25 °C. *J. Am. Chem. Soc.* **2006,** 128, (43), 14156-14165.

21. Percec, V.; Guliashvili, T.; Popov, A. V., Ultrafast synthesis of poly(methyl acrylate) and poly(methyl acrylate)-b-poly(vinyl chloride)-b-poly(methyl acrylate) by the Cu(0)/tris(2-dimethylaminoethyl)amine-catalyzed living radical polymerization and block copolymerization of methyl acrylate initiated with 1,1-chloroiodoethane and α,ω-Di(iodo)poly(vinyl chloride) in dimethyl sulfoxide. *J. Polym. Sci., Part A: Polym. Chem.* **2005,** 43, (9), 1948-1954.

22. Rosen, B. M.; Percec, V., Single-Electron Transfer and Single-Electron Transfer Degenerative Chain Transfer Living Radical Polymerization. *Chem. Rev.* **2009,** 109, (11), 5069-5119.

23. Isse, A. A.; Gennaro, A.; Lin, C. Y.; Hodgson, J. L.; Coote, M. L.; Guliashvili, T., Mechanism of Carbon−Halogen Bond Reductive Cleavage in Activated Alkyl Halide Initiators Relevant to Living Radical Polymerization: Theoretical and Experimental Study. *J. Am. Chem. Soc.* **2011,** 133, (16), 6254-6264.

24. Matyjaszewski, K.; Tsarevsky, N. V.; Braunecker, W. A.; Dong, H.; Huang, J.; Jakubowski, W.; Kwak, Y.; Nicolay, R.; Tang, W.; Yoon, J. A., Role of Cu0 in Controlled/"Living" Radical Polymerization. *Macromolecules* **2007,** 40, (22), 7795-7806.

25. Guliashvili, T.; Percec, V., A comparative computational study of the homolytic and heterolytic bond dissociation energies involved in the activation step of ATRP and SET-LRP of vinyl monomers. *J. Polym. Sci., Part A: Polym. Chem.* **2007,** 45, (9), 1607-1618.

26. Rosen, B. M.; Percec, V., Implications of monomer and initiator structure on the dissociative electron-transfer step of SET-LRP. *J. Polym. Sci., Part A: Polym. Chem.* **2008,** 46, (16), 5663-5697.

27. Rosen, B. M.; Jiang, X.; Wilson, C. J.; Nguyen, N. H.; Monteiro, M. J.; Percec, V., The disproportionation of Cu(I)X mediated by ligand and solvent into Cu(0) and Cu(II)X2 and its implications for SET-LRP. *J. Polym. Sci., Part A: Polym. Chem.* **2009,** 47, (21), 5606-5628.

28. Ciampoli.M; Nardi, N., 5-Coordinated high-spin complexes of bivalent cobalt nickel and copper with tris(2-dimethylaminoethyl)amine. *Inorg. Chem.* **1966,** 5, (1), 41-&.

29. Queffelec, J.; Gaynor, S. G.; Matyjaszewski, K., Optimization of atom transfer radical polymerization using Cu(I)/tris(2-(dimethylamino)ethyl)amine as a catalyst. *Macromolecules* **2000,** 33, (23), 8629-8639.

30. Levere, M. E.; Willoughby, I.; O'Donohue, S.; de Cuendias, A.; Grice, A. J.; Fidge, C.; Becer, C. R.; Haddleton, D. M., Assessment of SET-LRP in DMSO using online monitoring and Rapid GPC. *Polym. Chem.* **2010,** 1, (7), 1086-1094.

31. Nguyen, N. H.; Percec, V., Dramatic acceleration of SET-LRP of methyl acrylate during catalysis with activated Cu(0) wire. *J. Polym. Sci., Part A: Polym. Chem.* **2010,** 48, (22), 5109-5119.

32. Pintauer, T.; Braunecker, W.; Collange, E.; Poli, R.; Matyjaszewski, K., Determination of Rate Constants for the Activation Step in Atom Transfer Radical Polymerization Using the Stopped-Flow Technique. *Macromolecules* **2004,** 37, (8), 2679-2682.

33. Monteiro, M. J.; Guliashvili, T.; Percec, V., Kinetic simulation of single electron transfer–living radical polymerization of methyl acrylate at 25 °C. *J. Polym. Sci., Part A: Polym. Chem.* **2007,** 45, (10), 1835-1847.

34. Bortolamei, N.; Isse, A. A.; Di Marco, V. B.; Gennaro, A.; Matyjaszewski, K., Thermodynamic Properties of Copper Complexes Used as Catalysts in Atom Transfer Radical Polymerization. *Macromolecules* **2010,** 43, (22), 9257-9267.

Chapter 3

Accelerated ambient temperature SARA ATRP of methyl acrylate in alcohol/water solutions with mixed transition metal catalyst system

---

*Part of the contents of this chapter is published in: Carlos M. R. Abreu, **Patrícia V. Mendonça**, Arménio C. Serra, Jorge F. J. Coelho, Anatoliy V. Popov, and Tamaz Guliashvili, "Accelerated ambient temperature ATRP of methyl acrylate in alcohol–water solutions with a mixed transition-metal catalyst system", Macromolecular Chemistry and Physics, 2012, 213, (16), 1677–1687.*

3.1. Abstract

The current trend in developing the next generation of reversible deactivation radical polymerization (RDRP) methods and, in particular the atom transfer radical polymerization (ATRP) systems, involves reduction, elimination and/or replacement of toxic and highly expensive catalysts and solvents by environmentally friendly ones. Here, it is reported the accelerated ambient temperature supplemental activator and reducing agent (SARA) ATRP of methyl acrylate (MA) catalyzed by Fe(0)/$CuBr_2$/Me_6TREN (Me_6TREN: tris[2-(dimethylamino)ethyl]amine) in inexpensive and more environmentally friendly alcohols (methanol, ethanol and 1-propanol) and their mixtures with water, using a low concentration of soluble copper (50 ppm). The linear kinetic plots suggested a controlled polymerization. In addition, the dispersity (*Đ*) of the obtained poly(methylacrylate) (PMA) was very low throughout the polymerization (*Đ* ≈ 1.1). Well-defined functional star-shaped PMA samples have also been prepared. A relatively low molecular weight PMA with active Br-chain-ends (functionality ≈ 100%) was successfully used as a macroinitiator in a reinitiation experiment affording high molecular weight PMA with very low *Đ*. The data presented opens up the possibility of using fast SARA ATRP catalyzed by a mixed transition metal catalyst system in solvents that are inexpensive, ecofriendly and have low boiling point.

3.2. Introduction

The last decade has witnessed a remarkable development on the RDRP field.[1] This method allows the synthesis of tailor made polymers with controlled features (e.g., well-defined compositions, architectures, low molecular weight distribution and chain-end functionalities) by using the radical mechanism, which affords polymerization of a wide range of monomer classes and it is tolerant to many different types of solvents and additives. Transition metal-mediated RDRP[2] (also known as atom transfer radical polymerization or simply ATRP) is one of the most used methods to prepare a wide range of polymers with specified characteristics. The mechanism of ATRP is based on the metal complex mediated fast equilibrium between dormant (initiator and/or macroinitiator, P-X, where X = halide or pseudohalide) and active species (radical and/or macroradical, $P^{\bullet}$).

The dissociation of the C-X bond of dormant species (P-X) is catalyzed by a lower oxidation state transition metal complex (for example, the activator can be Cu(I)X/L), and the resulting macroradical ($P^{\bullet}$) reacts with a higher oxidation state transition metal complex (deactivator - $Cu(II)X_2/L$) producing a halogen-terminated macroinitiator and regenerating the low oxidation state catalyst (Scheme 3.1).

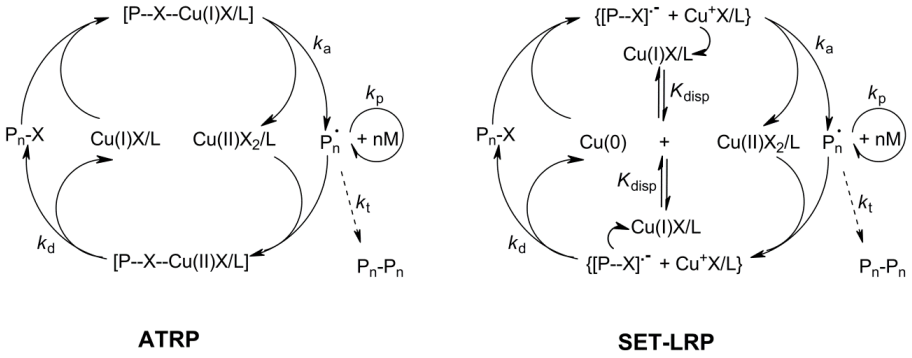

Scheme 3.1. Detailed mechanism of the copper-catalyzed ATRP and single electron transfer living radical polymerization (SET-LRP).

Several transition metal complexes can be used in ATRP, such as Cu, Ru, Fe, Ni, Os based ones,[2-4] in combination with different types of ligands, such as amines, phosphines, etc. The copper based catalyst, namely copper chloride or bromide in conjunction with nitrogen-based ligands, are the mostly used catalysts in ATRP. However, most of the transition metal catalysts used (including the copper-based ones) are relatively expensive and toxic. Furthermore, the removal of the catalyst from the polymer involves expensive time-cost technologies. Several different techniques based on ATRP have been developed to reduce the catalyst concentration to ppm levels, such as activators regenerated by electron transfer (ARGET) ATRP,[5] initiator for continuous activator regeneration (ICAR) ATRP,[6] supplemental activator and reducing agent (SARA) ATRP,[3, 7] and the so-called SET-LRP.[8-10] These methods only require ppm amounts of catalyst for fast preparation of polymers at different temperatures (including ambient temperature). Both SET-LRP and SARA ATRP are the recent development of the next generation methods for the synthesis of high molar mass polymers under very mild reaction conditions using inexpensive zero valent transition metals or mixed transition metal catalysts. During recent several years there has been an intense debate between protagonists of ATRP and SET-LRP (Scheme 3.1) in view to understand which species (Cu(I) *vs*. Cu(0)) is responsible for the activation

of the dormant species and the role of Cu(I) disproportionation. Several studies based on model experiments[11-13] and modeling calculations[14] argued a possible role of Cu(0) in SET-LRP of vinyl monomers in polar solvents and the extent of disproportionation of Cu(I)Br/L species formed *in situ* during the polymerization. In the recent publications from our research team,[3, 15] based on the extent of CuBr/L disproportionation in real polymerization conditions of MA in dimethylsulfoxide (DMSO) with Cu(0) wire, it was found that CuBr/L is the most probable activator.

A further development of ATRP methods involves the reduction or even elimination of toxic copper-based complexes used as catalysts. Despite the fact that the concentrations of copper required to control the polymerization are currently very small, iron-based systems can be very attractive for replacing and/or reducing the amount of copper-based catalysts. Iron is less expensive and the least toxic among the transition metals used in ATRP. In 1997, different research groups reported iron-based ATRP systems,[16, 17] followed by other reports involving different catalytic systems in bulk or in the presence of non-polar solvents.[18, 19] Recently, our research group and Matyjaszewski's research group reported the use of mixed transition metal catalyst using zero valent metals Fe(0),[3] Zn(0),[7] Mg(0)[7] - as initial activators together with very small amounts of $CuBr_2$/Me_6TREN or $CuBr_2$/PMDETA[7] as deactivator complexes for the SARA ATRP of MA, methyl methacrylate (MMA) and styrene (Sty) at room temperature. Although, the reported polymerizations were both extremely controlled and fast in DMSO, the use of this specific solvent can hamper future industrial implementation of this technology due to its very high boiling point and price. In addition, the use of more environmental friendly and less expensive solvents (or solvent mixtures) is a critical aspect that should be taken into consideration for a future large scale production. The use of alcohols and alcohol/water mixtures as solvents was already reported by different research groups.[20-23] Percec and co-authors have also used alcohol and alcohol/water mixtures for the controlled SET-LRP of MA monomer at 25 °C using Cu(0)/Me_6TREN as an initial catalyst.[24-26] The authors claimed to have used a maximum alcohol/water ratio of 90/10 (v/v) due to precipitation of PMA in the reaction medium.

In this work, the successful ambient temperature SARA ATRP of MA in alcohols and alcohol/water mixtures using Fe(0)/$CuBr_2$/Me_6TREN mixed transition metal catalyst is

reported. The solvent mixture with higher amount of water content (up to 30 vol%) still provided an excellent media for the successful synthesis of well-defined PMA under very mild reaction conditions. In addition, the initial concentration of soluble copper ($CuBr_2$) was reduced 10 times in comparison to the first system reported.[3]

3.3. Experimental

3.3.1. Materials

MA (Acros, 99% stabilized), was passed through a sand/alumina column before use in order to remove the radical inhibitor. Acetonitrile (MeCN) (Acros, 99,99%), CuBr (Fluka, >98%), $CuBr_2$ (Acros, 99+% extra pure, anhydrous), deuterated chloroform ($CDCl_3$) (Euriso-top, +1% TMS), DMSO (Acros, 99.8+% extra pure), ethyl α-bromoisobutyrate (EBiB) (Sigma-Aldrich, 98%), hexane (Fisher Chemical, 95%), PS standards (Polymer Laboratories), ethanol (Panreac, 99.5%), sodium azide (Panreac, 99%), 1-propanol (Sigma-Aldrich, 99.5%), methanol (Sigma-Aldrich, >99%), iron powder (Fe(0) (Acros, 99%, ~70 mesh), 2-(4-hydroxyphenylazo)benzoic acid (HABA) (Sigma–Aldrich, 99.5%) and 2,5-dihydroxybenzoic acid (DHB) (Sigma–Aldrich, >99%) were used as received.

Purified water (Milli-Q®, Millipore, resistivity >18 MΩ.cm) was obtained by reverse osmosis.

Tetrahydrofuran (THF) (Panreac, HPLC grade) was filtered under reduced pressure before use.

Dipentaerythritol hexakis(2-bromoisobutyrate) (6f-BiB),[27] pentaerythritol tetrakis(2-bromoisobutyrate) (4f-BiB)[27] and Me_6TREN[28] were synthesized according the procedures described in the literature.

3.3.2. Techniques

The chromatographic parameters of the samples were determined using high performance size exclusion chromatography HPSEC; Viscotek (Viscotek TDAmax) with a differential viscometer (DV); right-angle laser-light scattering (RALLS, Viscotek); low-angle laser-

light scattering (LALLS, Viscotek) and refractive index (RI) detectors. The column set consisted of a PL 10 mm guard column (50 × 7.5 mm^2) followed by one Viscotek T200 column (6 μm), one MIXED-E PLgel column (3 μm) and one MIXED-C PLgel column (5 μm). HPLC dual piston pump was set with a flow rate of 1 mL/min. The eluent (THF) was previously filtered through a 0.2 μm filter. The system was also equipped with an on-line degasser. The tests were done at 30 °C using an Elder CH-150 heater. Before the injection (100 μL), the samples were filtered through a polytetrafluoroethylene (PTFE) membrane with 0.2 μm pore. The system was calibrated with narrow PS standards. The *dn/dc* was determined as 0.063 for PMA. Molecular weight (M_n^{SEC}) and $Đ$ of the synthesized polymers were determined by multidetectors calibration using the OmniSEC software version: 4.6.1.354.

400 MHz ^1H NMR spectra of reaction mixture samples were recorded on a Bruker Avance III 400 MHz spectrometer, with a 5-mm TIX triple resonance detection probe, in $CDCl_3$ with tetramethylsilane (TMS) as an internal standard. Conversions of the monomer were determined by integration of monomer and polymer peaks using MestRenova software version: 6.0.2-5475.

For the MALDI-TOF-MS analysis, the PMA samples were dissolved in THF at a concentration of 10 mg/mL. DHB and HABA (0.05 M in THF) were used as matrix. The dried-droplet sample preparation technique was used to obtain 1:1 ratio (sample/matrix); an aliquot of 1 μL of each sample was directly spotted on the MTP AnchorChip TM 600/384 TF MALDI target, Bruker Daltonik (Bremen Germany) and, before the sample dry, 1 μL of matrix solution in THF was added and allowed to dry at room temperature, to allow matrix crystallization. External mass calibration was performed with a peptide calibration standard (PSCII) for the range 700-3000 (9 mass calibration points), 0.5 μL of the calibration solution and matrix previously mixed in an Eppendorf tube (1:2, v/v) were applied directly on the target and allowed to dry at room temperature. Mass spectra were recorded using an Autoflex III smartbeam1 MALDI-TOF-MS mass spectrometer Bruker Daltonik (Bremen, Germany) operating in the linear and reflection positive ion mode. Ions were formed upon irradiation by a smartbeam laser using a frequency of 200 Hz. Each mass spectrum was produced by averaging 2500 laser shots collected across the whole sample spot surface by screening in the range m/z 500-10000. The laser irradiance

was set to 35-40 % (relative scale 0-100) arbitrary units according to the corresponding threshold required for the applied matrix systems.

Fourier transform infrared attenuated total reflection (FTIR-ATR) spectroscopy was performed using a Jasco, model 4000 UK spectrometer. The samples were analyzed with 64 scans and 4 cm^{-1} resolution, between 500 and 3500 cm^{-1}.

3.3.3. Procedures

Typical procedure for the $[Fe(0)]_0/[CuBr_2]_0/[Me_6TREN]_0$ = 1/0.1/1.1 catalyzed SARA ATRP of MA (DP = 222) in ethanol/water (90/10) (v/v) mixture

The monomer (MA) was purified in a sand/alumina column just before reaction. A mixture of Fe(0) powder (17.5 mg, 0.314 mmol), $CuBr_2$ (7.0 mg, 0.031 mmol), Me_6TREN (79.5 mg, 0.345 mmol), ethanol (2.8 mL) and Milli Q water (0.3 mL) (both solvents previously bubbled with nitrogen for about 15 minutes) was placed in a Schlenk tube reactor. A mixture of MA (6.3 mL, 69.7 mmol) and EBiB (61.2 mg, 0.314 mmol) was added to the reactor that was sealed and frozen in liquid nitrogen. The Schlenk tube reactor containing the reaction mixture was deoxygenated with four freeze-vacuum-thaw cycles and purged with nitrogen. The Schlenk tube reactor was placed in a water bath at 30 °C with stirring (700 rpm). Different reaction mixture samples were collected during the polymerization by using an airtight syringe and purging the side arm of the Schlenk tube reactor with nitrogen. The samples were analyzed by ^1H NMR spectroscopy in order to determine the monomer conversion and by SEC, to determine molecular weight and $Đ$ of the PMA.

Chain extension experiment: polymerization from a Br-terminated PMA macroinitiator

A Br-terminated PMA obtained with a typical $Fe(0)/CuBr_2/Me_6TREN$-catalyzed SARA ATRP reaction was precipitated in hexane. The polymer was then dissolved in THF and filtered through a sand/alumina column, to remove trace catalyst, and precipitated again in hexane. The polymer was dried under vacuum until constant weight. The MA (9.2 mL, 102 mmol) was purified in a sand/alumina column just before reaction and then added to

the Br-terminated PMA macroinitiator (0.528 g, 1.02 mmol, M_n^{SEC} = 5 800; $Đ$ = 1.07) in the Schlenk tube reactor. Ethanol/water (90/10) (v/v) mixture (5.0 mL previously bubbled with nitrogen for about 15 min) was added to the mixture (monomer/macroinitiator) in order to dissolve all the macroinitiator. A mixture of ethanol/water (4.2 mL previously bubbled with nitrogen for about 15 min), Fe(0) (5.7 mg, 1.0 mmol), $CuBr_2$ (2.3 mg, 0.1 mmol) and Me_6TREN (25.9 mg, 1.1 mmol) was added to the reactor. The Schlenk tube was deoxygenated with four freeze-pump thaw cycles and purged with nitrogen. The Schlenk tube reactor was placed in a water bath at 30 °C with stirring (700 rpm). The reaction was stopped after 14 h and the mixture was analyzed by SEC.

Azide functionalization of Br-terminated star PMA

A Br-terminated 4-arm star-shaped PMA (1.80 g, 0.29 mmol, M_n^{SEC} = 6.2 x 10^3; $Đ$ = 1.04) prepared by SARA ATRP was dissolved in DMSO (15 mL) and the solution was transferred into a Schlenk tube reactor. Sodium azide (0.75 g, 11.6 mmol) and ascorbic acid (10.2 mg, 0.58 mmol) were added to the reactor. The Schlenk tube was deoxygenated with four freeze-pump-thaw cycles, purged with nitrogen and placed in an oil bath at 80 °C with stirring (700 rpm) overnight. The polymer was precipitated in methanol, vacuum dried and analyzed by FTIR in order to confirm the presence of the azide functionality.

3.4. Results and discussion

3.4.1. Influence of the different alcohols and alcohol/water mixtures

Our research team[3] and Matyjaszewski's group[7] have reported the use of the Fe(0)/$CuBr_2$/Me_6TREN catalytic system for the polymerization of MA, MMA and Sty in DMSO at ambient temperature. Aiming to enhance the possibilities of an industrial application of this catalytic system, the substitution of DMSO as a solvent was envisaged and the reaction was carried out in different alcohols (Table 3.1, entries 1-3). The results show that regardless the alcohol used as the solvent, the control over the polymers molecular weight was perfect since the M_n^{SEC} was similar to the M_n^{th} and the $Đ$ was below 1.1 (Table 3.1, entries 1-3). Taking into account that the reaction time and conditions used

were the same for the different alcohols tested, 1-propanol seemed to provide faster reactions, since higher monomer conversion was achieved (74%), from all the alcohols tested.

Table 3.1. Molecular weight and *Đ* of the PMA obtained by Fe(0)/$CuBr_2$/Me_6TREN = 1/0.1/1.1 catalyzed SARA ATRP at 30 °C during 16 h, using $[MA]_0$/[solvent] = 2/1 (v/v).

Entry	Solvent	Conv. (%)	M_n^{th} x 10^{-3}	M_n^{SEC} x 10^{-3}	*Đ*
1	Ethanol	41	8.0	7.9	1.04
2	1-Propanol	74	14.0	14.2	1.02
3	Methanol	27	5.1	5.0	1.02
4	Ethanol/H_2O[a]	93	17.9	17.8	1.04
5	Methanol/H_2O[a]	98	18.9	20.8	1.08

[a] Alcohol/water = 95/5 (v/v)

The effect of the presence of water in the reaction solvent was evaluated by carrying out experiments with ethanol or methanol/water mixture, using 5% of water (v/v) (Table 3.1, entries 4-5). The use of the alcohol/water mixtures as solvent resulted in PMA with low dispersity (*Đ* < 1.1). This indicates that it is possible to conduct the controlled synthesis of hydrophobic PMA in the presence of a small amount of water added to the polymerization mixture. Figure 3.1 shows representative SEC traces of PMA samples prepared by SARA ATRP in different alcohols or alcohol/water mixtures, confirming the polymers narrow molecular weight distributions.

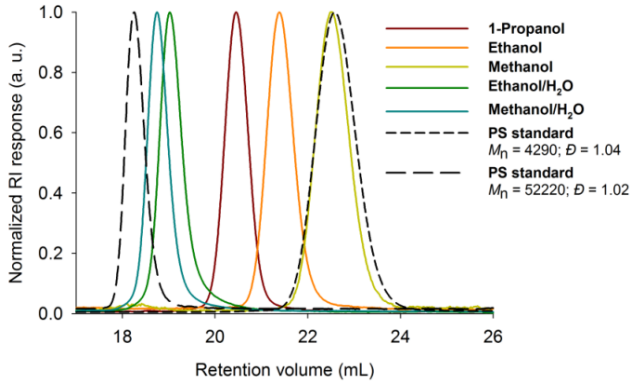

Figure 3.1. SEC traces of Br-terminated PMA obtained by Fe(0)/$CuBr_2$/Me_6TREN = 1/0.1/1.1-catalyzed SARA ATRP at 30 °C during 16 h, using $[MA]_0$/[solvent] = 2/1 (v/v), in different alcohols or alcohol/water mixtures. SEC traces of narrow PS standards (dashed lines) are presented for comparison purposes.

In order to find the optimal conditions, the polymerization of MA was studied in mixtures of alcohols (ethanol, 1-propanol or methanol) and water (10% of water content). The kinetic plots are shown in Figure 3.2.

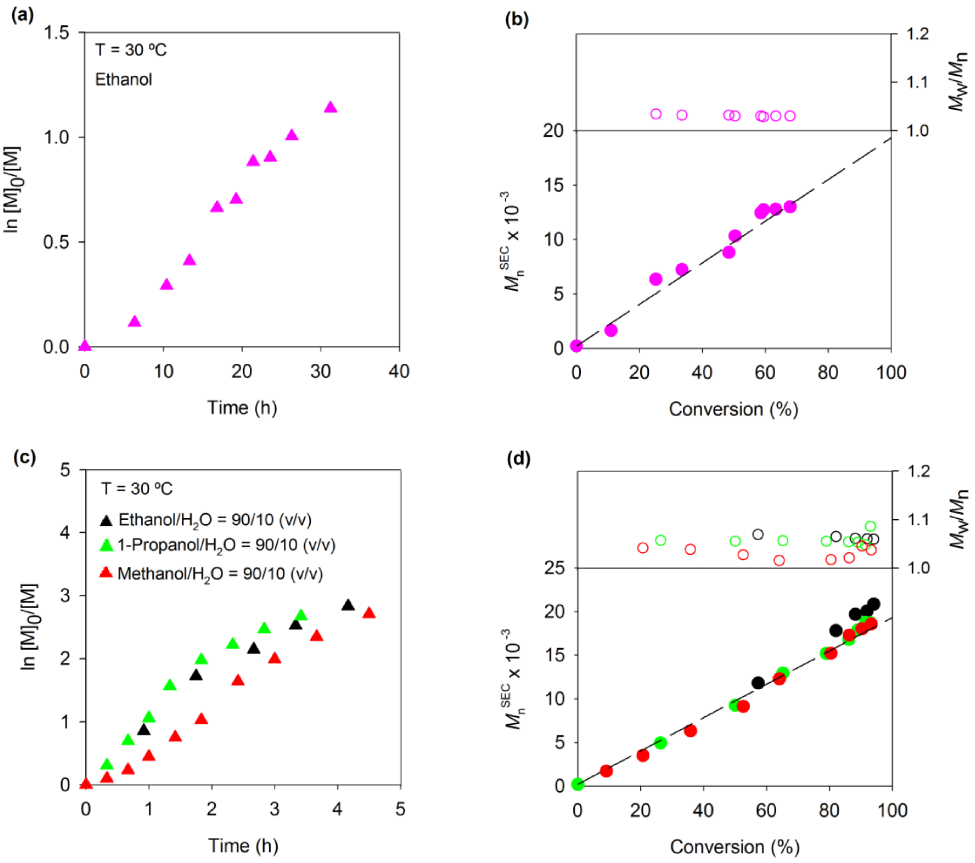

Figure 3.2. (a and c) Kinetic plots of conversion and ln[M]$_0$/[M] *vs.* time and (b and d) plot of number-average molecular weights (M_n^{SEC}) and *Đ* (M_w/M_n) *vs.* monomer conversion for the Fe(0)/CuBr$_2$/Me$_6$TREN-catalyzed SARA ATRP of MA in ethanol (a and b) and different alcohol/water mixtures (c and d) at 30 °C. Reaction conditions: [MA]$_0$/[EBiB]$_0$/[Fe(0)]$_0$/[CuBr$_2$]$_0$/[Me$_6$TREN]$_0$ = 222/1/1/0.1/1.1; [MA]$_0$/[solvent] = 2/1 (v/v); EBiB: ethyl α-bromoisobutyrate.

Ethanol was used in a control polymerization of PMA (Figure 3.2 (a) and (b)). With the addition of 10% of water to this solvent, the apparent constant rate of polymerization increased 20 times (Table 3.2 entries 2 and 4). The same effect on the reaction rate has been reported by Nguyen *et al.* for the controlled polymerization of MA using Cu(0)/Me$_6$TREN as the catalytic complex and methyl 2-bromopropionate as the initiator, at 25 °C.[26] However, in that case, the k_p^{app} increased only around 1.5 times from pure ethanol to ethanol/water = 90/10 (v/v). Besides a noticeable increase of the reaction rate,

the maximum conversion obtained in the case of an ethanol/water mixture was higher than that obtained using pure ethanol. Concerning the 1-propanol/water and methanol/water mixtures (green and red symbols, respectively, in Figure 3.2 (c)) , the results showed the same trend, with maximum monomer conversion achieving near 100% and with the apparent rate constant of polymerization of the same order as for the ethanol/water mixture. It is worth mentioning that the PMA was completely soluble in the reaction medium throughout the polymerization. This observation is in contrast with some results reported in the literature,[24] which suggested a poor control over the SET-LRP of MA, using metal catalysts in 1-propanol, due to the precipitation of polymer during the reaction. For the three alcohol/water mixtures studied, the rate of reaction was of first order relative to monomer conversion (Figure 3.2 (c)) and the molecular weights determined by SEC were in good agreement with the theoretical ones, indicating an excellent control during the polymerization (Figure 3.2 (d)). The kinetic data suggests that the alcohol structure does not have a significant impact on the reaction features of the Fe(0)/$CuBr_2$/Me_6TREN-catalyzed SARA ATRP of MA. Moreover, it is worth to emphasize that this system provided a high level of control over the PMA dispersity, regardless the solvent used, from the very beginning of the reaction to the highest conversion obtained. Table 3.2 presents the kinetic data obtained for the different solvents studied.

Table 3.2. Kinetic data for the SARA ATRP of MA at 30 °C. Reaction conditions: $[MA]_0/[solvent]$ = 2/1 (v/v); $[MA]_0/[EBiB]_0/[Fe(0)]_0/[CuBr_2]_0/[Me_6TREN]_0$ = 222/1/1/0.1/1.1.

Entry	Solvent	k_p^{app} (h^{-1})	$Đ^c$
1	DMSO[a]	0.247	1.04
2	Ethanol	0.037	1.03
3	Ethanol/water (95/5)[b]	0.272	1.03
4	Ethanol/water (90/10)[b]	0.764	1.06
5	1-Propanol/water (90/10)[b]	0.889	1.05
6	Methanol/water (90/10) [b]	0.619	1.04

[a] Values previously determined and reported elsewhere[3]

[b] %vol

[c] Correspondent to the last kinetic sample

The reaction rate was slower when pure ethanol was used as solvent in comparison with DMSO (Table 3.2, entries 1-2). However, the addition of either 5% or 10% of water to ethanol was responsible for a remarkable enhancement of the reaction rate, while the polymer dispersity values remained very low (Table 3.2, entries 3-4). The same trend was observed for the polymerizations conducted in 1-propanol/water or methanol/water mixtures. The dramatic acceleration of the polymerization with added water cannot be explained by the enhancement of the disproportionation of CuBr/L species formed during the deactivation step (as previously pointed out by the discoverers of SET-LRP).[9-11] The $[Me_6TREN]/[Cu_{total}]$ ratio is about 10 and under ligand excess conditions CuBr/L disproportionation is excluded.[15, 29] Most probably, the presence of water in the solvent mixture can cause a decrease in the activation barrier during the activation/deactivation steps and may also affect the k_p of MA (propagation rate constant may increase in more polar media). A more precise mechanistic explanation requires both additional kinetic experiments and theoretical work. The results reported here are extremely relevant from the industrial standpoint, since it is clearly shown the possibility of using alcohol/water mixtures instead of DMSO as solvents for the SARA ATRP. Ethanol was selected as the solvent of choice to continue the study, taking into account the favorable kinetic parameters presented in Table 3.2, the fact of being the most benign and inexpensive alcohol and also it can be easily removed from the reaction mixture at an industrial scale.

3.4.2. Influence of the water content

In order to find the optimal ratio of ethanol/water to afford the fastest polymerization possible while maintaining the "living" features of the reaction, different ratios ethanol/water were investigated (Figure 3.3). The water content in the reaction solvent mixture was increased, starting from 5 % (v/v), until a water amount that did not allow a polymerization with "controlled/living" features. Up to 35% (v/v) of water in the solvent mixture, the polymerization proceeded with first order kinetic relative to monomer conversion and the rate of polymerization increased with the increase of the water content (Figure 3.3). The upper limit of water content that could be used in the SARA ATRP of MA was found to be around 35%, with a k_p^{app} of 1.618 h^{-1}. Using a higher content of water (50 %), there was a delay of ≈1 h and a decrease of the reaction rate (Figure 3.3 (a)). In addition, due to the reduced solubility of the produced PMA in the solvent

mixture, the polymer precipitated during the reaction, which resulted in a poor control over the polymerization (Figure 3.3 (f)).

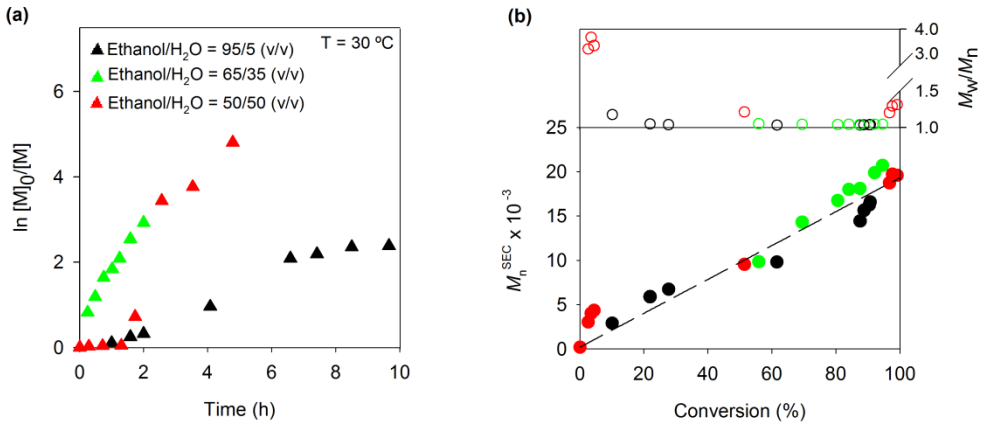

Figure 3.3 (a) Kinetic plots of conversion an $\ln[M]_0/[M]$ *vs.* time and (b) plot of number-average molecular weights (M_n^{SEC}) and *Đ* (M_w/M_n) *vs.* monomer conversion for the Fe(0)/$CuBr_2$/Me_6TREN-catalyzed SARA ATRP of MA in ethanol/water mixtures with different contents of water, at 30 ° C. Reaction conditions: $[MA]_0/[EBiB]_0/[Fe(0)]_0/[CuBr_2]_0/[Me_6TREN]_0$ = 222/1/1/0.1/1.1; $[MA]_0/[solvent]$ = 2/1 (v/v).

On this matter, preliminary experiments using different ethanol/water ratios to dissolve a PMA sample (M_n^{SEC} = 19.0 x 10^3) have shown that 35% of water was the maximum content that could be used to avoid polymer precipitation. Figure 3.4 shows the variation of k_p^{app} with the water content using an ethanol/water mixture as the solvent for the Fe(0)/$CuBr_2$/Me_6TREN-catalyzed SARA ATRP of MA at 30 °C.

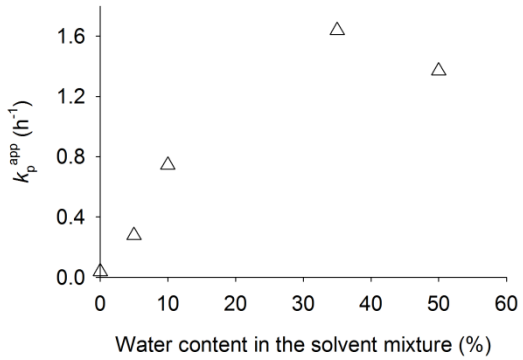

Figure 3.4. Influence of the water content on the k_p^{app} of the Fe(0)/$CuBr_2$/Me_6TREN-catalyzed SARA ATRP of MA in ethanol/water mixtures at 30 °C. Reaction conditions: $[MA]_0/[EBiB]_0$ = 222; $[solvent]/[monomer]_0$ = 1/2 (v/v).

The results presented in Figure 3.4 suggest that there is a maximum amount of water that can be used, which for the system described in this work is around 35% for a targeted degree of polymerization (DP) of 222. Apparently, this value is closely related to the solubility of the polymer in the solvent mixture. Therefore, it could vary for other acrylates using the same experimental conditions.

For comparative purposes, DMSO/water and MeCN/water mixtures were also examined as solvents for the SARA ATRP of MA with the reported catalyst system. The kinetic plots are shown in Figure 3.5. The polymerization rate increased (Figure 3.5 (a)) in comparison with the pure DMSO (Table 3.1, entry 1) with the addition of water, while the control during the polymerization was still excellent (Figure 3.5 (b)). The kinetic data obtained for the MeCN/water mixture, using the same experiment conditions, showed very similar values.

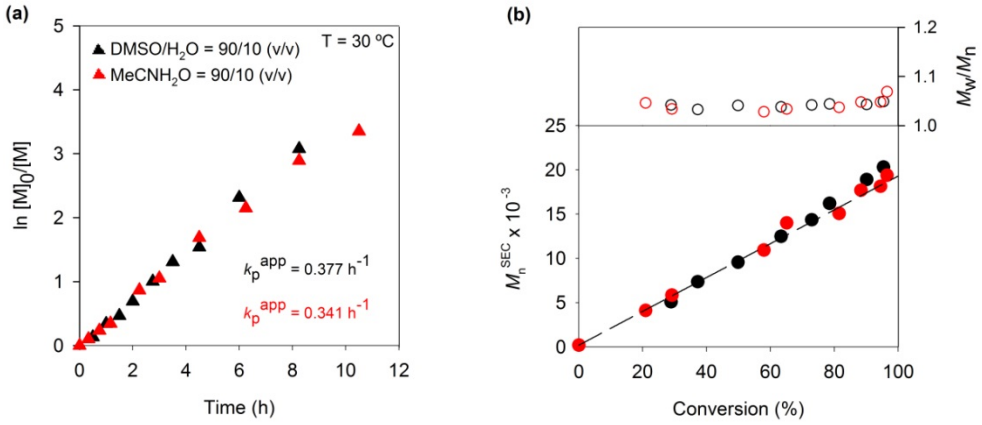

Figure 3.5. (a) Kinetic plots of conversion and ln[M]$_0$/[M] *vs.* time and (b) plot of number-average molecular weights (M_n^{SEC}) and *Đ* (M_w/M_n) *vs.* monomer conversion for the Fe(0)/CuBr$_2$/Me$_6$TREN-catalyzed SARA ATRP of MA in DMSO/H$_2$O = 90/10 (v/v) (black symbols) and in MeCN/H$_2$O = 90/10 (v/v) (red symbols). Reaction conditions: [MA]$_0$/[EBiB]$_0$/[Fe(0)]$_0$/[CuBr$_2$]$_0$/[Me$_6$TREN]$_0$ = 222/1/1/0.1/1.1; [MA]$_0$/[solvent] = 2/1 (v/v).

3.4.3. Influence of the reaction temperature

The ratio ethanol/water = 90/10 (v/v) was selected to investigate the influence of the reaction temperature on the polymerization kinetics. Three different temperatures, ranging from 30 °C to 50 °C, were studied (Figure 3.6).

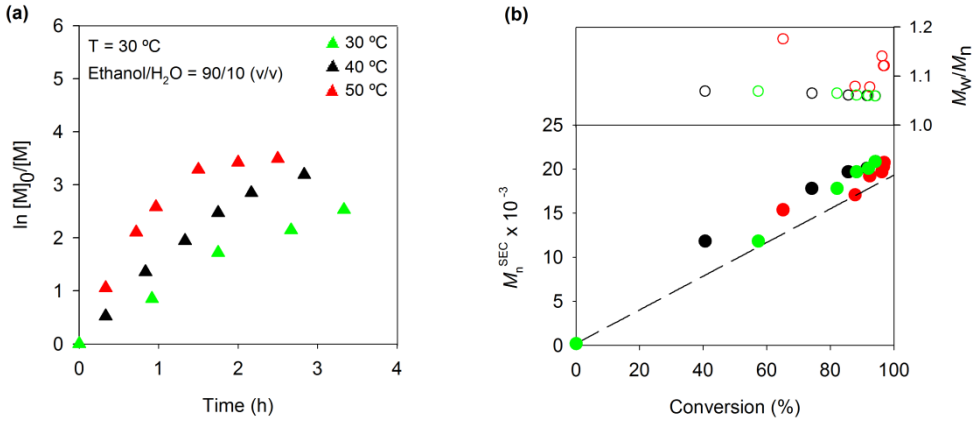

Figure 3.6. (a) Kinetic plots of conversion and $\ln[M]_0/[M]$ *vs.* time and (b) plot of number-average molecular weights (M_n^{SEC}) and *Đ* (M_w/M_n) *vs.* monomer conversion for the Fe(0)/$CuBr_2$/Me_6TREN-catalyzed SARA ATRP of MA in ethanol/water = 90/10 (v/v) at different temperatures. Reaction conditions: $[MA]_0/[EBiB]_0/[Fe(0)]_0/[CuBr_2]_0/[Me_6TREN]_0$ = 222/1/1/0.1/1.1; $[MA]_0/[solvent]$ = 2/1 (v/v).

The kinetic plots presented in Figure 3.6 show that the polymerization maintained its "living" features at 40 °C or 50 °C. As expected, the rate of polymerization increased with the increase of the reaction temperature (Figure 3.6 (a)), while the maximum monomer conversion obtained was similar for the range of temperatures investigated. The increase of the temperature seemed to have no negative effect on the control over the molecular weight, as the dispersity values were in the same range (Figure 3.6 (b)).

3.4.4. Influence of the soluble copper concentration

The metal catalyst used to mediate the polymerizations can difficult the purification process and ultimately, contaminate the final product. Therefore, it is important to decrease the concentration of soluble metal catalyst as much as possible, while maintaining a good control over the polymers dispersity. The first report on the Fe(0)/$CuBr_2$/Me_6TREN-catalyzed SARA ATRP of MA employed a minimum of 450

ppm of $CuBr_2$ for a well-controlled polymerization.[3] In this work, the concentration of $CuBr_2$ was investigated from 250 ppm to 10 ppm (determined as the initial molar ratio of $CuBr_2$ to the monomer) in the SARA ATRP of MA (Table 3.3).

Table 3.3. Molecular weight and *Đ* of the PMA obtained by SARA ATRP, using different concentrations of $CuBr_2$, in ethanol/water = 80/20 (v/v) at 30 °C. Conditions: $[MA]_0/[EBiB]_0/[Fe(0)]_0/[CuBr_2]_0/[Me_6TREN]_0$ = 100/1/1/0.1/1.1; $[MA]_0$/[solvent] = 2/1 (v/v).

Entry	$[CuBr_2]_0$ (ppm)	Time (h)	Conv. (%)	M_n^{th} x 10^{-3}	M_n^{SEC} x 10^{-3}	*Đ*
1	250	3	92	8.1	8.1	1.08
2	100	4	94	8.3	8.0	1.10
3	50	4	82	7.2	8.8	1.09
4	10	6.5	75	6.9	2.1	1.72

Regardless the concentration of copper used, high monomer conversion was achieved in all the polymerizations. The lowest concentration of copper studied (10 ppm) proved to be not adequate for the successfully mediation of the SARA ATRP equilibrium, leading to poor control over the PMA molecular weight (*Đ* > 1.50). Nevertheless, it is remarkable the excellent control achieved (*Đ* = 1.09) when a residual amount of 50 ppm of soluble copper was used in the beginning of the polymerization.

3.4.5. Study of different degrees of polymerization

The target molecular weight is a very important parameter to be considered for any catalytic system due to possible solubility issues for high molecular weight segments. Figure 3.7 presents the kinetic data obtained for the SARA ATRP of MA, with different targeted DP values (50, 500 and 1000), using ethanol/water = 90/10 (v/v) as the solvent mixture. As expected, the reaction rate decreased with the increase of the monomer/initiator ratio (DP) due to the lower number of radicals. It is remarkable to notice that even for DP = 1000, the *Đ* value remained very low throughout the reaction and high monomer conversion was achieved at ambient temperature.

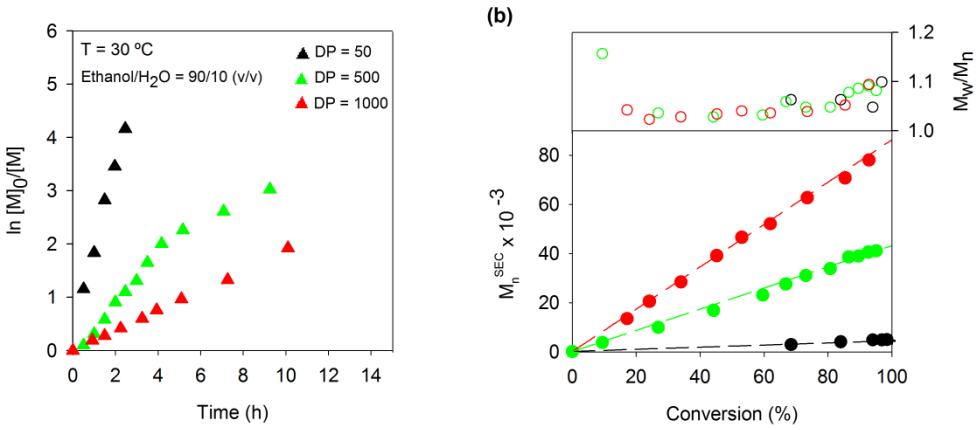

Figure 3.7 (a) Kinetic plots of conversion and $\ln[M]_0/[M]$ *vs.* time and (b) plot of number-average molecular weights (M_n^{SEC}) and *Đ* (M_w/M_n) *vs.* monomer conversion for the Fe(0)/$CuBr_2$/Me_6TREN-catalyzed SARA ATRP of MA in ethanol/water = 90/10 (v/v) for different targeted DP values. Reaction conditions: $[MA]_0/[EBiB]_0/[Fe(0)]_0/[CuBr_2]_0/[Me_6TREN]_0$ = DP/1/0.1/1.1; $[MA]_0/[solvent]$ = 2/1 (v/v).

3.4.6. Functional star-shaped PMA by SARA ATRP

The utility of the SARA ATRP method reported was extended to the preparation of branched PMA, namely star-shaped. Figure 3.8 shows the kinetic results for the SARA ATRP of MA initiated by a tetrafunctional initiator (4f-BiB).

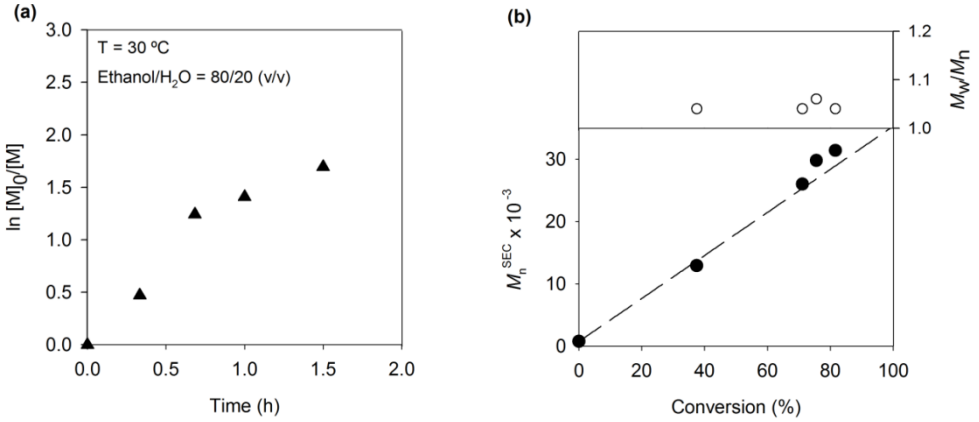

Figure 3.8 (a) Kinetic plot of conversion and $\ln[M]_0/[M]$ *vs.* time and (b) plot of number-average molecular weights (M_n^{SEC}) and *Đ* (M_w/M_n) *vs.* monomer conversion for the Fe(0)/$CuBr_2$/Me_6TREN-catalyzed SARA ATRP of MA in ethanol/water = 80/20 (v/v) for the preparation of 4-arm star-shaped PMA. Reaction conditions: $[MA]_0/[4f\text{-}BiB]_0/[Fe(0)]_0/[CuBr_2]_0/[Me_6TREN]_0$ = 400/1/0.1/1.1; $[MA]_0/[solvent]$ = 2/1 (v/v).

The polymerization was of first-order in respect to monomer conversion, as the one obtained for the linear PMA, with monomer reaching high conversion in 1.5 h (Figure 3.8 (a)). The polymers dispersity (Figure 3.8 (b)) remained very low throughout the polymerization ($Đ < 1.1$), suggesting that the SARA ATRP method reported is a robust method for the preparation of PMA stars. To confirm this hypothesis, different star-shaped PMA samples were prepared, varying both the DP value and number of arms of the star (Table 3.4). In the range of the DP values studied, well-controlled 4- and 6-arm star-shaped PMA structures were obtained, as judged by the low dispersity values ($Đ \leq 1.1$).

Due to their architecture, star-shaped polymers are very interesting materials showing unique properties. For instances, for high molecular weight values, a star polymer presents lower viscosity than a linear polymer of similar composition. As the star polymers synthesized by SARA ATRP present active-chain ends, it is possible to reinitiate them with further monomer supply, to prepare tailor-made star block copolymers. In addition, it is possible to modify the Br-chain-ends in order to introduce desired reactive functionalities. As a proof-of-concept, the star-shaped PMA prepared by SARA ATRP was subjected to azidation in the presence of sodium azide.

Table 3.4. Molecular weight and *Đ* of the star-shaped PMA obtained by SARA ATRP, using tetra' (4f-EBiB) or hexafunctional (6f-BiB) initiators, in ethanol/water = 80/20 (v/v) at 30 °C. Conditions: $[MA]_0/[\text{star initator}]_0/[Fe(0)]_0/[CuBr_2]_0/[Me_6TREN]_0$ = DP/1/1/$[CuBr_2]_0$/1.1; $[MA]_0/[\text{solvent}]$ = 2/1 (v/v).

Entry	Number of arms	DP	Time (h)	Conv. (%)	M_n^{th} x 10^{-3}	M_n^{th} x 10^{-3}	*Đ*
1	4	200	3	98	17.7	24.7	1.13
2	4	400	2.5	85	30.2	30.6	1.06
3	6	300	3	74	19.9	28.0	1.06
4	6	600	4	75	40.2	45.0	1.06

The success of the modification was confirmed by the appearance of the characteristic FTIR peak of the azide group at 2100 cm^{-1}. Additional proof was obtained by ^1H NMR spectroscopy, with the loss of the Br-chain-end signal (data not shown). Azide-terminated

polymers can be used for the preparation of complex polymeric structures, since they can easily react with alkyne moieties by "click" chemistry.[30]

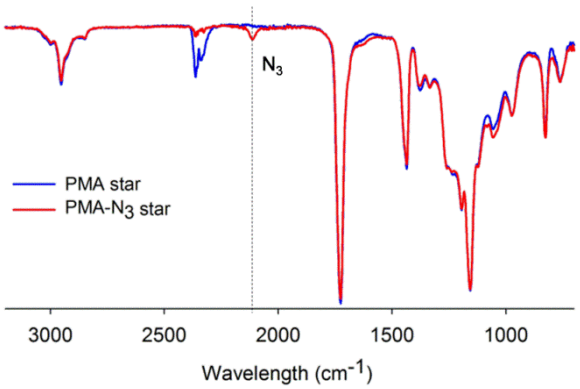

Figure 3.9. FTIR spectra of azide-terminated 4-arm star PMA (red line) and Br-terminated 4-arm star PMA (blue line).

3.4.7. NMR and MALDI-TOF analyses

The structure of the PMA obtained using the Fe(0)/$CuBr_2$/Me_6TREN catalytic system in ethanol/water = 90/10 (v/v) was studied by ^{1}H NMR (Figure 3.10) and MALDI-TOF-MS (Figure 3.11).

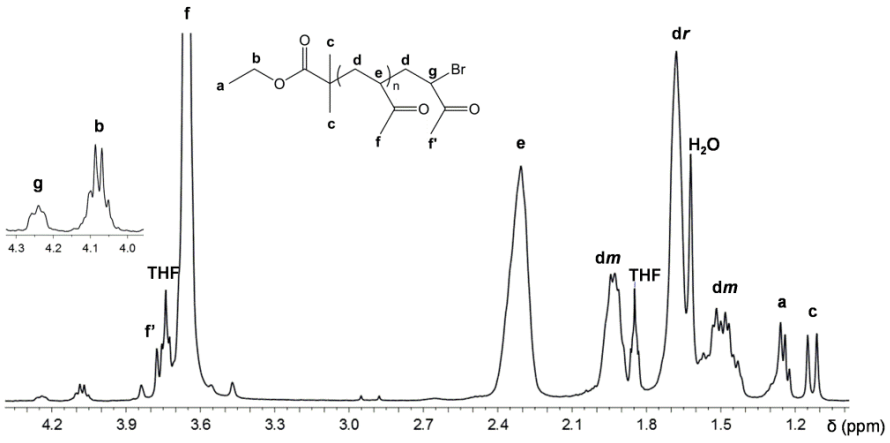

Figure 3.10. ^{1}H NMR spectrum of PMA–Br obtained at high conversion (M_n^{SEC} = 5.8 x 10^3; $Đ$ = 1.07; M_n^{NMR} = 5.5 x 10^3; active chain-end functionality = 99%); solvent $CDCl_3$.

A typical proton NMR spectrum of a PMA–Br is shown in Figure 3.10. The assignment of the proton resonances was done according to the references: (**e, g, f, f'**),[3, 8, 31] (**a, b, c**),[3, 32] (**d*r*, d*m***).[3, 33-36] The signal of the initiator methyl **a** is overlapped with the signal of

paraffin grease trace at 1.26 ppm[3, 37] and the signal of protons **d*r*** is partially overlapped with the signal of water trace of the $CDCl_3$ at 1.6 ppm.[3, 37] There are also traces of THF (resonances at 1.85 and 3.76 ppm),[37] which was used for the PMA purification. The percentage of the chain-end functionality was calculated as follows: % functionality = [I(g)/(I(c)/6)] x 100%; where I(**g**) is the integral of the PMA bromine chain-end $–CH_2$-C$\mathbf{H}_g$Br(CO_2Me) at 4.25 ppm and I(**c**) is the integral of the initiator fragment –CH(C$\mathbf{H}_{c3}$)$_2CO_2$Et at 1.1 ppm.[3] The PMA NMR molecular weight was calculated using the equation: $M_n^{NMR} = \{[I(\mathbf{e})/(I(\mathbf{c})/6)] + 1\} \times MW_{MA} + MW_{EBiB}$, where I(**e**) is the integral of the PMA main chain C-H proton $–CH_2$-C$\mathbf{H}_e$(CO_2Me)- at 2.3 ppm, I(**c**) is the integral of the initiator fragment –CH(C$\mathbf{H}_{c3}$)$_2CO_2$Et at 1.1 ppm, MW_{MA} is the molecular weight of the monomer and MW_{EBiB} is the molecular weight of the initiator. The ^{1}H NMR spectrum of the PMA (Figure 3.10) prepared by SARA ATRP in ethanol/water mixture using the Fe(0)/$CuBr_2$/Me_6TREN catalytic system matches the spectrum of PMA prepared using the same catalytic system in DMSO.[3]

In MALDI-TOF-MS experiments, two types of matrices, DHB and HABA were tested, but only the former gave a clearly resolved spectrum (Figure 3.11).

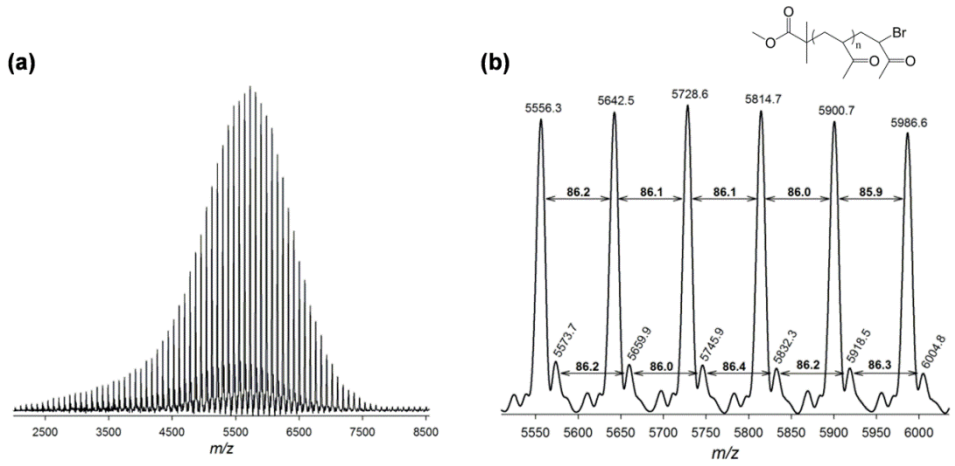

Figure 3.11. MALDI-TOF-MS (a) in the linear mode (using DHB as the matrix) of PMA-Br (M_n^{SEC} = 5.8 x 10^3, *Đ* = 1.07) prepared by SARA ATRP; (b) Enlargement of the MALDI-TOF-MS from *m/z* = 5550 to 6000 of PMA–Br.

The MALDI-TOF-MS of PMA-Br ranging from 2000 to 8500 is shown in Figure 3.11 (a). Enlargement of the 5550-6000 range is shown in Figure 3.11 (b). Importantly, two series of main peaks are separated by an interval corresponding to the monomer (MA)

repeating unit (86.1 mass units). The highest main series is attributed to a polymer chain $[R\text{-}(MA)_n\text{-}Br + Na]^+$ where R-Br is the initiator EBiB (5556.3 = 195.1 + 62 x 86.1 + 23, where 195.1, 86.1 and 23 correspond to the molecular weight of EBiB, MA and Na^+ respectively). The weaker peaks are attributed to the same polymer chain but with K^+ $[R\text{-}(MA)_n\text{-}Br + K]^+$ (5573.7 = 195.1 + 62 x 86.1 + 39.1, where 39.1 corresponds to the molecular weight of K^+). Therefore, the obtained PMA-Br has a well-defined structure (i.e., without any detectable structural defects). The presence of possible structural defects would cause a deviation of the *m*/*z* values distribution. The series of less intensive peaks (Figure 3.11 (b)) could not be ascribed to any chain-end structures expected. The presence of these peaks is probably due to the occurrence of polymer chain fragmentation during the ionization in the MALDI-TOF-MS analysis, as reported by other authors.[38-43]

3.4.8. Chain extension experiment

The "living" nature of the PMA-Br was confirmed by carrying out a chain extension experiment. A PMA-Br sample prepared by SARA ATRP in ethanol/water mixture was precipitated in hexane, isolated, dried and used as a macroinitiator. Figure 3.12 shows the complete shift of the low molecular weight PMA (M_n^{SEC} = 5.8 x 10^3; $Đ$ = 1.07) SEC trace towards a very high molecular weight (M_n^{SEC} = 102.6 x 10^3; $Đ$ = 1.13), confirming the "living" character of the polymer, as well as its high chain-end functionality.

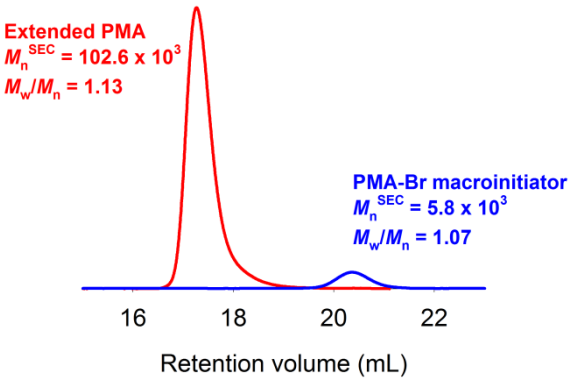

Figure 3.12. SEC traces of the PMA samples before (blue line) and after (red line) the chain extension experiment.

3.5. Conclusions

In resume, this work reports the ultrafast ambient temperature SARA ATRP of MA catalyzed by Fe(0)/$CuBr_2$/Me_6TREN in a mixture of inexpensive and environmental friendly solvents that can replace the "traditional" use of DMSO, using 50 ppm of soluble copper. In addition, the method proved to be useful for the preparation of star-shaped PMA with different number of arms. The "living" character of the PMA was proved by ^{1}H NMR, MALDI-TOF-MS and by the success of a chain extension experiment. The results presented here open a real possibility of scale-up the SARA ATRP method to large scale productions using an affordable technology.

3.6. References

1. Tasdelen, M. A.; Kahveci, M. U.; Yagci, Y., Telechelic polymers by living and controlled/living polymerization methods. *Prog. Polym. Sci.* **2011,** 36, (4), 455-567.

2. Ouchi, M.; Terashima, T.; Sawamoto, M., Transition Metal-Catalyzed Living Radical Polymerization: Toward Perfection in Catalysis and Precision Polymer Synthesis. *Chem. Rev.* **2009,** 109, (11), 4963-5050.

3. Mendonça, P. V.; Serra, A. C.; Coelho, J. F. J.; Popov, A. V.; Guliashvili, T., Ambient temperature rapid ATRP of methyl acrylate, methyl methacrylate and styrene in polar solvents with mixed transition metal catalyst system. *Eur. Polym. J.* **2011,** 47, (7), 1460-1466.

4. Pintauer, T.; Matyjaszewski, K., Structural aspects of copper catalyzed atom transfer radical polymerization. *Coord. Chem. Rev.* **2005,** 249, (11–12), 1155-1184.

5. Jakubowski, W.; Matyjaszewski, K., Activators Regenerated by Electron Transfer for Atom-Transfer Radical Polymerization of (Meth)acrylates and Related Block Copolymers. *Angew. Chem., Int. Ed.* **2006,** 45, (27), 4482-4486.

6. Matyjaszewski, K.; Jakubowski, W.; Min, K.; Tang, W.; Huang, J.; Braunecker, W. A.; Tsarevsky, N. V., Diminishing catalyst concentration in atom transfer radical

polymerization with reducing agents. *Proc. Natl. Acad. Sci. U.S.A.* **2006,** 103, (42), 15309-15314.

7. Zhang, Y.; Wang, Y.; Matyjaszewski, K., ATRP of Methyl Acrylate with Metallic Zinc, Magnesium, and Iron as Reducing Agents and Supplemental Activators. *Macromolecules* **2011,** 44, (4), 683-685.

8. Percec, V.; Guliashvili, T.; Ladislaw, J. S.; Wistrand, A.; Stjerndahl, A.; Sienkowska, M. J.; Monteiro, M. J.; Sahoo, S., Ultrafast Synthesis of Ultrahigh Molar Mass Polymers by Metal-Catalyzed Living Radical Polymerization of Acrylates, Methacrylates, and Vinyl Chloride Mediated by SET at 25 °C. *J. Am. Chem. Soc.* **2006,** 128, (43), 14156-14165.

9. Percec, V.; Guliashvili, T.; Popov, A. V., Ultrafast synthesis of poly(methyl acrylate) and poly(methyl acrylate)-b-poly(vinyl chloride)-b-poly(methyl acrylate) by the Cu(0)/tris(2-dimethylaminoethyl)amine-catalyzed living radical polymerization and block copolymerization of methyl acrylate initiated with 1,1-chloroiodoethane and α,ω-Di(iodo)poly(vinyl chloride) in dimethyl sulfoxide. *J. Polym. Sci., Part A: Polym. Chem.* **2005,** 43, (9), 1948-1954.

10. Rosen, B. M.; Percec, V., Single-Electron Transfer and Single-Electron Transfer Degenerative Chain Transfer Living Radical Polymerization. *Chem. Rev.* **2009,** 109, (11), 5069-5119.

11. Guliashvili, T.; Percec, V., A comparative computational study of the homolytic and heterolytic bond dissociation energies involved in the activation step of ATRP and SET-LRP of vinyl monomers. *J. Polym. Sci., Part A: Polym. Chem.* **2007,** 45, (9), 1607-1618.

12. Matyjaszewski, K.; Tsarevsky, N. V.; Braunecker, W. A.; Dong, H.; Huang, J.; Jakubowski, W.; Kwak, Y.; Nicolay, R.; Tang, W.; Yoon, J. A., Role of Cu0 in Controlled/"Living" Radical Polymerization. *Macromolecules* **2007,** 40, (22), 7795-7806.

13. Rosen, B. M.; Percec, V., Implications of monomer and initiator structure on the dissociative electron-transfer step of SET-LRP. *J. Polym. Sci., Part A: Polym. Chem.* **2008,** 46, (16), 5663-5697.

14. Isse, A. A.; Gennaro, A.; Lin, C. Y.; Hodgson, J. L.; Coote, M. L.; Guliashvili, T., Mechanism of Carbon−Halogen Bond Reductive Cleavage in Activated Alkyl Halide Initiators Relevant to Living Radical Polymerization: Theoretical and Experimental Study. *J. Am. Chem. Soc.* **2011,** 133, (16), 6254-6264.

15. Guliashvili, T.; Mendonca, P. V.; Serra, A. C.; Popov, A. V.; Coelho, J. F. J., Copper-Mediated Controlled/"Living" Radical Polymerization in Polar Solvents: Insights into Some Relevant Mechanistic Aspects. *Chem.Eur. J.* **2012,** 18, (15), 4607.

16. Ando, T.; Kamigaito, M.; Sawamoto, M., Iron(II) Chloride Complex for Living Radical Polymerization of Methyl Methacrylate1. *Macromolecules* **1997,** 30, (16), 4507-4510.

17. Matyjaszewski, K.; Wei, M.; Xia, J.; McDermott, N. E., Controlled/"Living" Radical Polymerization of Styrene and Methyl Methacrylate Catalyzed by Iron Complexes1. *Macromolecules* **1997,** 30, (26), 8161-8164.

18. Kotani, Y.; Kamigaito, M.; Sawamoto, M., FeCp(CO)2I: A Phosphine-Free Half-Metallocene-Type Iron(II) Catalyst for Living Radical Polymerization of Styrene1. *Macromolecules* **1999,** 32, (20), 6877-6880.

19. Matyjaszewski, K.; Coca, S.; Gaynor, S. G.; Wei, M.; Woodworth, B. E., Zerovalent Metals in Controlled/"Living" Radical Polymerization. *Macromolecules* **1997,** 30, (23), 7348-7350.

20. Bontempo, D.; Heredia, K. L.; Fish, B. A.; Maynard, H. D., Cysteine-Reactive Polymers Synthesized by Atom Transfer Radical Polymerization for Conjugation to Proteins. *J. Am. Chem. Soc.* **2004,** 126, (47), 15372-15373.

21. Kimani, S. M.; Moratti, S. C., Ambient-temperature copper-catalyzed atom transfer radical polymerization of methacrylates in ethylene glycol solvents. *J. Polym. Sci., Part A: Polym. Chem.* **2005,** 43, (8), 1588-1598.

22. Lobb, E. J.; Ma, I.; Billingham, N. C.; Armes, S. P.; Lewis, A. L., Facile Synthesis of Well-Defined, Biocompatible Phosphorylcholine-Based Methacrylate Copolymers via Atom Transfer Radical Polymerization at 20 °C. *J. Am. Chem. Soc.* **2001,** 123, (32), 7913-7914.

23. McDonald, S.; Rannard, S. P., Room Temperature Waterborne ATRP of n-Butyl Methacrylate in Homogeneous Alcoholic Media. *Macromolecules* **2001,** 34, (25), 8600-8602.

24. Lligadas, G.; Percec, V., Ultrafast SET-LRP of methyl acrylate at 25 degrees C in alcohols. *J. Polym. Sci., Part A: Polym. Chem.* **2008,** 46, (8), 2745-2754.

25. Nguyen, N. H.; Percec, V., Disproportionating versus nondisproportionating solvent effect in the SET-LRP of methyl acrylate during catalysis with nonactivated and activated cu(0) wire. *J. Polym. Sci., Part A: Polym. Chem.* **2011,** 49, (19), 4227-4240.

26. Nguyen, N. H.; Rosen, B. M.; Jiang, X.; Fleischmann, S.; Percec, V., New efficient reaction media for SET-LRP produced from binary mixtures of organic solvents and H2O. *J. Polym. Sci., Part A: Polym. Chem.* **2009,** 47, (21), 5577-5590.

27. Matyjaszewski, K.; Miller, P. J.; Pyun, J.; Kickelbick, G.; Diamanti, S., Synthesis and Characterization of Star Polymers with Varying Arm Number, Length, and Composition from Organic and Hybrid Inorganic/Organic Multifunctional Initiators. *Macromolecules* **1999,** 32, (20), 6526-6535.

28. Ciampolini, M.; Nardi, N., Five-Coordinated High-Spin Complexes of Bivalent Cobalt, Nickel, andCopper with Tris(2-dimethylaminoethyl)amine. *Inorg. Chem.* **1966,** 5, (1), 41-44.

29. Rosen, B. M.; Jiang, X.; Wilson, C. J.; Nguyen, N. H.; Monteiro, M. J.; Percec, V., The disproportionation of Cu(I)X mediated by ligand and solvent into Cu(0) and Cu(II)X2 and its implications for SET-LRP. *J. Polym. Sci., Part A: Polym. Chem.* **2009,** 47, (21), 5606-5628.

30. Kolb, H. C.; Finn, M. G.; Sharpless, K. B., Click Chemistry: Diverse Chemical Function from a Few Good Reactions. *Angew. Chem., Int. Ed.* **2001,** 40, (11), 2004-2021.

31. Lligadas, G.; Ladislaw, J. S.; Guliashvili, T.; Percec, V., Functionally terminated poly(methyl acrylate) by SET-LRP initiated with $CHBr_3$ and CHI_3. *J. Polym. Sci., Part A: Polym. Chem.* **2008,** 46, (1), 278-288.

32. Hasneen, A.; Kim, S. J.; Paik, H.-j., Synthesis and characterization of low molecular weight poly(methyl acrylate)-b-polystyrene by a combination of ATRP and click coupling method. *Macromol. Res.* **2007,** 15, (6), 541-546.

33. Coelho, J. F. J.; Carvalho, E. Y.; Marques, D. S.; Popov, A. V.; Goncalves, P. M.; Gil, M. H., Synthesis of poly(lauryl acrylate) by single-electron transfer/degenerative chain transfer living radical polymerization catalyzed by Na2S2O4 in water. *Macromol. Chem. Phys.* **2007,** 208, (11), 1218-1227.

34. Coelho, J. F. J.; Carvalho, E. Y.; Marques, D. S.; Popov, A. V.; Percec, V.; Goncalves, P. M. F. O.; Gil, M. H., Synthesis of poly(ethyl acrylate) by single electron transfer-degenerative chain transfer living radical polymerization in water catalyzed by Na2S2O4. *J. Polym. Sci., Part A: Polym. Chem.* **2007,** 46, (2), 421-432.

35. Coelho, J. F. J.; Gois, J.; Fonseca, A. C.; Carvalho, R. A.; Popov, A. V.; Percec, V.; Gil, M. H., Synthesis of poly(2-methoxyethyl acrylate) by single electron transfer-Degenerative transfer living radical polymerization catalyzed by Na2S2O4 in water. *J. Polym. Sci., Part A: Polym. Chem.* **2009,** 47, (17), 4454-4463.

36. Tabuchi, M.; Kawauchi, T.; Kitayama, T.; Hatada, K., Living polymerization of primary alkyl acrylates with t-butyllithium/bulky aluminum Lewis acids. *Polymer* **2002,** 43, (25), 7185-7190.

37. Gottlieb, H. E.; Kotlyar, V.; Nudelman, A., NMR Chemical Shifts of Common Laboratory Solvents as Trace Impurities. *J. Org. Chem.* **1997,** 62, (21), 7512-7515.

38. Abreu, C. M. R.; Mendonca, P. V.; Serra, A. C.; Coelho, J. F. J.; Popov, A. V.; Gryn'ova, G.; Coote, M. L.; Guliashvili, T., Reversible Addition-Fragmentation Chain Transfer Polymerization of Vinyl Chloride. *Macromolecules* **2012,** 45, (5), 2200-2208.

39. Beyou, E.; Chaumont, P.; Chauvin, F.; Devaux, C.; Zydowicz, N., Study of the Reaction between Nitroxide-Terminated Polymers and Thiuram Disulfides. Toward a Method of Functionalization of Polymers Prepared by Nitroxide Mediated Free "Living" Radical Polymerization. *Macromolecules* **1998,** 31, (20), 6828-6835.

40. Coca, S.; Jasieczek, C. B.; Beers, K. L.; Matyjaszewski, K., Polymerization of acrylates by atom transfer radical polymerization. Homopolymerization of 2-hydroxyethyl acrylate. *J. Polym. Sci., Part A: Polym. Chem.* **1998,** 36, 1417-1424.

41. Pound, G.; Aguesse, F.; McLeary, J. B.; Lange, R. F. M.; Klumperman, B., Xanthate-Mediated Copolymerization of Vinyl Monomers for Amphiphilic and Double-Hydrophilic Block Copolymers with Poly(ethylene glycol). *Macromolecules* **2007,** 40, (25), 8861-8871.

42. Schilli, C.; Lanzendoerfer, M. G.; Mueller, A. H. E., Benzyl and cumyl dithiocarbamates as chain transfer agents in the RAFT polymerization of N-isopropylacrylamide. In situ FT-NIR and MALDI-TOF MS investigation. *Macromolecules* **2002,** 35, (18), 6819-6827.

43. Yan, Y.; Zhang, W.; Qiu, Y.; Zhang, Z.; Zhu, J.; Cheng, Z.; Zhang, W.; Zhu, X., Universal xanthate-mediated controlled free radical polymerizations of the "less activated" vinyl monomers. *J. Polym. Sci., Part A: Polym. Chem.* **2010,** 48, (22), 5206-5214.

Chapter 4

Facile synthesis of well-defined telechelic alkyne-terminated polystyrene in polar media using SARA ATRP with mixed Fe/Cu transition metal catalyst

---

*The contents of this chapter are published in: Nuno Rocha, **Patrícia V. Mendonça**, Joana P. Mendes, Pedro N. Simões, Anatoliy V. Popov, Tamaz Guliashvili, Arménio C. Serra, and Jorge F. J. Coelho, "Facile synthesis of well-defined telechelic alkyne-terminated polystyrene in polar media using ATRP with mixed Fe/Cu transition metal catalyst", Macromolecular Chemistry and Physics, 2013, 214, 76−84.*

4.1. Abstract

This work reports for the first time the synthesis of polystyrene (PS) by supplemental activator and reducing agent atom transfer radical polymerization (SARA ATRP) using Fe(0)/$CuBr_2$/L (L = Me_6TREN: tris[2-(dimethylamino)ethyl]amine or PMDETA: *N*,*N*′,*N*″,*N*‴-pentamethyldiethylenetriamine) catalytic system in dimethylformamide (DMF) under mild reaction conditions. The effect of the reaction temperature, ligand nature, initiator structure and monomer/solvent ratio on the polymerization kinetics in DMF was evaluated. The results suggested that under the reported reaction conditions, the catalytic system is suitable to afford PS with high molecular weight, low dispersity (*Đ*) and well-controlled structure for different types of initiators. DMF plays an important role in the polymerization kinetics since it allows achieving faster polymerizations compared to the data available in the scarce reports found in the literature. The "living" character of the polymer chains was assessed by reinitiation experiment. The usefulness of the catalytic system was demonstrated by carrying out a "click" reaction using the copper(I)-catalyzed Huisgen 1,3-dipolar cycloaddition between the synthesized alkyne-terminated PS and an azide-terminated PS (previously prepared by azidation of Br-terminated PS). The method reported here can be very useful in macromolecular engineering to afford PS-based materials with controlled structure.

4.2. Introduction

The growing demand for polymers with well-defined structure and functionalities increased the interest in reversible deactivation radical polymerization (RDRP) methods. Due to their radical nature, these approaches present several key advantages over the classic ionic living polymerization, such as: mild reaction conditions, high tolerance to different functional monomer families and the possibility of carrying out the polymerization in aqueous medium. Among the most common RDRP methods, atom transfer radical polymerization (ATRP)[1] has received enormous attention from both academic and industrial circles. The mechanism of ATRP is based on the metal complex mediated fast equilibrium between dormant (initiator and/or macroinitiator, P–X, where X: halide or pseudohalide) and active species (radical and/or macroradical, $P^{\bullet}$). The

dissociation of the C–X bond of dormant species (P–X) is catalyzed by a lower oxidation state transition metal complex (for example CuX/L), and the resulting macroradical (P$^{\bullet}$) reacts with a higher oxidation state transition metal complex (deactivator - CuX_2/L)[2, 3] producing a halogen chain-terminated macroinitiator and regenerating the lower oxidation state metal catalyst. This mechanism has been successfully applied to the polymerization of a vast range of monomers with different functionalities, including acrylates,[3] methacrylates,[3, 4] acrylamides,[5] acrylonitrile,[6] and non-activated monomers (e.g., vinyl chloride[7] and vinyl acetate[8]). Aiming to reduce the catalyst concentration to ppm levels, different variations of the classical ATRP have been proposed, namely, activators regenerated by electron transfer (ARGET) ATRP,[9] initiator for continuous activator regeneration (ICAR) ATRP,[10] supplemental activator and reducing agent (SARA) ATRP[3, 11] and the so-called sigle electron transfer living radical polymerization (SET-LRP).[12] Other important development in this area dealt with the substitution of Cu-based catalysts with less expensive and non-toxic transition metal complexes, using Fe(0)-based systems. In this regard, and at the same time, our research group and Matyjaszewski's research group reported the use of a mixed transition metal catalytic system using zero valent metals Fe(0),[3] Zn(0),[11] Mg(0)[11] - as initial activators together with very small amounts of $CuBr_2$/Me_6TREN[3] or $CuBr_2$/PMDETA[11] as deactivator complexes for the SARA ATRP of methyl acrylate (MA)[3] methyl methacrylate (MMA)[3, 11] and styrene (Sty)[3, 11] at room temperature. This is a very attractive system due to both lower toxicity and lower cost of iron when compared with other transition metal complexes currently used in ATRP. Moreover, the very low concentration of copper complexes used along with heterogeneous iron is of great industrial significance. For Sty, the poorly reported results with this catalytic system presented very limited monomer conversion, despite the low molar mass dispersity (*Đ*) obtained. Also, the low propagation rate constant of Sty compared to acrylates,[13] thermal self-initiation of Sty[14] and the occurrence of irreversible termination reactions[15] are known to limit the PS molecular weight that can be achieved using RDRP methods.[13] Deviations from the ideal "living" behavior in the ATRP polymerization of Sty, such as the loss of the bromine functionality for high monomer conversions, are also well-described in the literature.[16] It has been reported that the use of ARGET methods with low concentration of copper/ligand complex could reduce the loss of the bromine functionality in Sty polymerization, due to the reduction of side reactions

between growing radicals and the copper catalyst.[17] PS with molecular weight up to 1,000,000 and reasonably low dispersity could be obtained by accelerating radical propagation and suppressing radical termination, due to the use of high pressure (6 kbar) during polymerization.[18] For Sty polymerizations carried out with zerovalent metals, such as Cu(0), it has been observed that the addition of a small amount $CuBr_2$, leads to an improvement of the control over the polymer chain growth, while having a high retention of the active chain-ends.[19]

Recently, the polymerization of Sty using Fe(0) and $CuBr_2$ has been carried out in ambient conditions with different solvents, but the difficulty to obtain high monomer conversions and polymers with low dispersity, at the same time, was still evident.[20] This research aimed to use the previously developed mixed transition metal catalyst system based on Fe(0)/$CuBr_2$/Me_6TREN[3] for the SARA ATRP of Sty, in order to achieve high monomer conversions, at a reasonable rate of polymerization, while maintaining a good control over both polymers dispersity and chain-end functionality. Additionally, the developed method has shown to be effective for the preparation of PS with chain-end functionalities that are suitable for "click" reactions.[21, 22] These synthetic approaches are very attractive due to the low occurrence of side reactions and almost quantitative yields. In this work, the SARA ATRP of Sty using Fe(0)/$CuBr_2$/L as the catalytic system in DMF, under mild reaction conditions, was studied. The influence of critical parameters such as: reaction temperature, ligand structure, initiator structure and monomer/solvent ratio on the polymerization kinetics was evaluated.

4.3. Experimental

4.1.1. Materials

Sty (Sigma-Aldrich, +99%) was passed over a sand/alumina column before use in order to remove the radical inhibitor. Ascorbic acid (Fluka), copper (I) bromide (CuBr) (Fluka, + 98%), copper (II) bromide ($CuBr_2$) (Acros, + 99% extra pure, anhydrous), deuterated chloroform ($CDCl_3$) (Euriso-top, +1% TMS), DMF (Sigma-Aldrich, +99.8%), ethyl α-bromoisobutyrate (EBiB) (Aldrich, 98%), formaldehyde solution 37% (Sigma-Aldrich), formic acid (Acros, 88%), PS standards (Polymer Laboratories), iron powder (Fe(0))

(Acros, 99%, ~70 mesh), PMDETA (Aldrich, 99%), propargyl alcohol (PgOH) (Aldrich, 99%), sodium azide (Aldrich, 99%), sodium hydroxide (Panreac pellets, 98%), sodium sulfate (anhydrous), tris(2-aminoethyl)amine (Aldrich, 96%) and α-bromoisobutyryl bromide (BBiB) (Aldrich, 98%) were used as received.

Dichloromethane (DCM) (Sigma-Aldrich, + 99.9%) and triethylamine (TEA) (Sigma-Aldrich, + 99%) were dried over CaH_2 and distilled prior to use.

Tetrahydrofuran (THF) (Panreac, HPLC grade) was filtered under reduced pressure before use.

Propargyl α-bromoisobutyrate (PgBiB)[23] and Me_6TREN[24] were synthesized as reported in the literature.

4.1.2. Techniques

The chromatographic parameters of the samples were determined using high performance size exclusion chromatography HPSEC; Viscotek (Viscotek TDAmax) with a differential viscometer (DV); right-angle laser-light scattering (RALLS, Viscotek); low-angle laser-light scattering (LALLS, Viscotek) and refractive index (RI) detectors. The column set consisted of a PL 10 mm guard column (50 × 7.5 mm^2) followed by one Viscotek T200 column (6 μm), one MIXED-E PLgel column (3 μm) and one MIXED-C PLgel column (5 μm). HPLC dual piston pump was set with a flow rate of 1 mL/min. The eluent (THF) was previously filtered through a 0.2 μm filter. The system was also equipped with an on-line degasser. The tests were done at 30 °C using an Elder CH-150 heater. Before the injection (100 μL), the samples were filtered through a polytetrafluoroethylene (PTFE) membrane with 0.2 μm pore. The system was calibrated with narrow PS standards. The *dn/dc* was determined as 0.185 for PS. The number-average molecular weight (M_n^{SEC}) and *Đ* of the synthesized polymers were determined by multidetectors calibration using the OmniSEC software version: 4.6.1.354.

400 MHz ^{1}H NMR spectra of reaction mixture samples were recorded on a Bruker Avance III 400 MHz spectrometer, with a 5-mm TIX triple resonance detection probe, in $CDCl_3$ with tetramethylsilane (TMS) as an internal standard. Conversion of monomers

was determined by integration of monomer and polymer peaks using MestRenova software version: 6.0.2-5475.

Fourier transform infrared attenuated total reflection (FTIR-ATR) spectroscopy was performed using a Jasco, model 4000 UK spectrometer. The samples were analyzed with 64 scans and 4 cm^{-1} resolution, between 500 and 3500 cm^{-1}.

4.1.3. Procedures

Typical procedure for the $[Fe(0)]_0/[CuBr_2]_0/[Me_6TREN]_0$ = 1/0.1/1.1 catalyzed SARA ATRP of Sty (DP = 125)

The monomer (Sty) was purified in a sand/alumina column just before the reaction. A mixture of Fe(0) powder (11.7 mg, 0.209 mmol), $CuBr_2$ (4.7 mg, 0.021 mmol), Me_6TREN (53.0 mg, 0.230 mmol) and DMF (1.5 mL) (previously bubbled with nitrogen for about 15 minutes) was placed in a Schlenk tube reactor. A mixture of Sty (3.0 mL, 26.1 mmol) and EBiB (40.9 mg, 0.209 mmol) was added to the reactor that was sealed and frozen in liquid nitrogen. The Schlenk tube reactor containing the reaction mixture was deoxygenated with four freeze-vacuum-thaw cycles and purged with nitrogen. The Schlenk tube reactor was placed in an oil bath at 70 °C with stirring (700 rpm). Different reaction mixture samples were collected during the polymerization by using an airtight syringe and purging the side arm of the Schlenk tube reactor with nitrogen. The samples were analyzed by ^1H NMR spectroscopy in order to determine the monomer conversion and by SEC, to determine the molecular weight and $Đ$ of the polymers.

Chain extension of Br-terminated PS

A Br-terminated PS obtained with a typical Fe(0)/$CuBr_2$/Me_6TREN catalyzed SARA ATRP reaction was precipitated in methanol. The polymer was then dissolved in THF and filtered through a sand/alumina column and precipitated again in methanol. The polymer was dried until constant weight and used as the macroinitiator. The monomer (Sty) (1.5 mL, 13.1 mmol) was purified in a sand/alumina column just before the reaction and then added to the Br-terminated PS macroinitiator (419 mg, 0.035 mmol, M_n^{SEC} = 4.0 x 10^3; $Đ$ = 1.06) in a Schlenk tube reactor. A mixture of DMF (0.8 mL previously bubbled with

nitrogen for about 15 minutes), Fe(0) powder (5.8 mg, 0.105 mmol), $CuBr_2$ (2.3 mg, 0.010 mmol) and Me_6TREN (26.5 mg, 0.115 mmol) was added to the reactor. The Schlenk tube was deoxygenated with four freeze-pump-thaw cycles and purged with nitrogen. The Schlenk tube reactor was placed in the oil bath at 70 °C with stirring (700 rpm) for 24 h.

Azide-functionalization of Br-terminated PS

A Br-terminated PS (300 mg, 0.018 mmol, M_n^{SEC} = 16.4 x 10^3; $Đ$ = 1.05) prepared by SARA ATRP was dissolved in DMF (5 mL) and the solution was transferred into a Schlenk tube reactor. Sodium azide (13.0 mg, 0.20 mmol) and ascorbic acid (1.80 mg, 0.01 mmol) were added to the reactor. The Schlenk tube was deoxygenated with four freeze-pump-thaw cycles, purged with nitrogen and placed into the oil bath at 80 °C with stirring (700 rpm) for 22 h. The polymer was precipitated in methanol, vacuum dried and analyzed by ^{1}H NMR and FTIR in order to confirm the loss of the bromine chain-end and the appearance of the azide-functionality.

"Click" reaction between alkyne–PS and PS–N_3

Both PS–N_3 (200 mg, 0.012 mmol, M_n^{SEC} = 16.4 x 10^3; $Đ$ = 1.05) and a PS–alkyne (200 mg, 0.012 mmol, M_n^{SEC} = 17.5 x 10^3; $Đ$ = 1.20) synthesized by SARA ATRP, were dissolved in DMF (2 mL), previously bubbled with nitrogen for about 15 min. CuBr (3.50 mg, 0.024 mmol) and PMDETA (4.20 mg, 0.024 mmol) were added to the solution. The mixture was charged into a Schelnk tube reactor, deoxygenated with four freeze-pump-thaw cycles and purged with nitrogen. The reactor was placed in an oil bath at 70 °C with stirring (700 rpm) for 66 h. The polymer was precipitated in methanol and analyzed by SEC and ^{1}H NMR in order to confirm the success of the "click" reaction.

4.4. Results and discussion

Fe(0)-mediated SARA ATRP of Sty using $CuBr_2$/Me_6TREN as a deactivator complex at 30 °C was recently reported by our research group, allowing to achieve a good polymerization control, however the monomer conversion was found to be relatively low.[3] In fact, it is known from the literature that either in bulk or in solvent media, the ATRP of Sty is usually carried out at higher temperatures (90-110 °C)[16, 17, 19, 25] in order to afford large propagation rates, to minimize vitrification at high monomer conversions and, sometimes, to improve the solubility of the catalysts.[1] In this work, the effect of the reaction temperature on the polymerization features, using DMF as the reaction solvent, has been studied for the first time. The reaction temperature is a particularly relevant parameter, knowing the very low monomer conversions obtained for Sty polymerization at room temperature.[3, 20] DMF was selected because of the high solubility of PS in this solvent. In addition, DMF has shown a rate-enhancing effect for the polymerization of *tert*-butyl acrylate (*t*BA) initiated by 4-oxo-2,2,6,6-tetramethylpiperidinooxy (TEMPO)-capped PS macroinitiator, which was ascribed to the increase of the activation rate constant k_a–*t*BA and the decrease of the recombination rate constant k_{rec}–*t*BA.[26] Figure 4.1 presents the kinetic data obtained for the SARA ATRP of Sty at 70 °C and 90 °C.

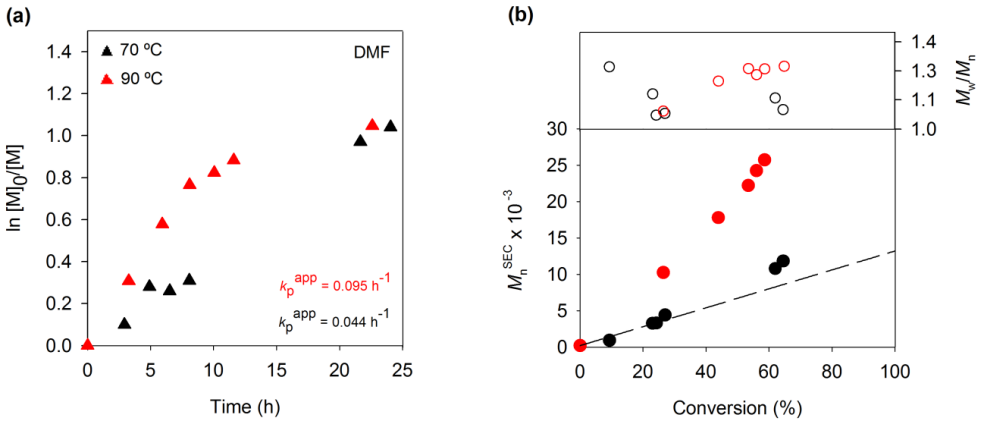

Figure 4.1. (a) Kinetic plots of conversion and ln[M]$_0$/[M] *vs.* time and (b) plot of number-average molecular weights (M_n^{SEC}) and *Đ* (M_w/M_n) *vs.* monomer conversion for the Fe(0)/$CuBr_2$/Me_6TREN-catalyzed SARA ATRP of Sty in DMF at 70 °C (black symbols) and 90 °C (red symbols). Reaction conditions: [Sty]$_0$/[DMF] = 2/1 (v/v); [Sty]$_0$/[EBiB]$_0$/[Fe(0)]$_0$/[$CuBr_2$]$_0$/[Me_6TREN]$_0$= 125/1/1/0.1/1.1 (molar); EBiB: ethyl α-bromoisobutyrate.

The direct comparison of the kinetic data obtained at these two temperatures (70 °C and 90 °C) showed that an increase in the polymerization temperature could increase very significantly the Sty conversion rate. However, in spite of the higher polymerization rate, the maximum conversion achieved is still limited to about 60%, with the disadvantage of causing broader molecular weight distribution than when using 70 °C as the polymerization temperature. In fact, very high temperatures are known to lead to side reactions, such as the loss of bromine chain-end functionality or even Sty thermal self-initiation.[1] However, when this polymerization is carried out at room temperature, the polymerization becomes too slow. Recently, another research group[20] has reproduced our previous results using a mixture of metal catalysts[3] and confirmed the low Sty polymerization rate at ambient temperature conditions.

Figure 4.1 (b) also highlights the fact the apparent initiator efficiency at 90 °C was much lower than that at 70 °C. However, significant deviations seemed to occur at high monomer conversions, and, thus, an increase in the M_n^{SEC} values seemed to be more related to non-ideal "living" behavior than to real initiator efficiency. This conclusion is supported by a greater increase in the dispersity ($Đ$) values when the apparent efficiency is lower. The selection of 70 °C as the polymerization temperature seemed to be an optimal balance between the rate of polymerization and the dispersity of the final polymer. In fact, the kinetic data presented in Figure 4.1 show a linear dependence of the M_n^{SEC} *vs* monomer conversion and $\ln[M]_0/[M]$ *vs*. polymerization time, which indicates a controlled polymerization. Moreover, the molar mass dispersity remained narrow throughout the polymerization. However, from the two polymerization kinetics shown in Figure 4.1 (b), it can be observed that an increase in the M_n^{SEC} values above the M_n^{th} seems to be correlated with an increase in the dispersity values, supporting the idea that this behavior is related to deviations from the ideal "living" character of the ATRP of Sty. Recently, a contribution was published that relates the Fe/Cu ratio, in a zero-valent bimetallic catalyzed SET-LRP system, with the initiator efficiency.[20] According to such work, lower Fe(0)/Cu(II) ratios decreased the efficiency of the initiators. Thus, M_n^{SEC} *vs* monomer conversion kinetic curves using the mixed Fe(0)/Cu(II) catalytic system are expected to be affected by the equilibrium of these species and different oxidation states during the course of the reaction. The results presented in this work suggest that, for high Sty monomer conversions, the presence of Fe species at high-oxidation states leads to a

poorer control over the chain growth, causing a dramatic decrease in the apparent initiator efficiency. Figure 4.2 shows smooth, unimodal, and symmetric SEC traces for the PS sample taken after 24 h (conv. = 40.5%). SEC traces (RI signal) of PS samples taken at different times of reaction showed a smooth shift of the entire molecular weight distribution towards high molecular weight values with increasing reaction time (conversion). However, a tailing in the SEC curve can be observed, becoming more predominant for higher Sty conversions. This visible tailing effect of low molecular weight fractions[19] has been reported[8] for the ATRP of Sty, and typically results showed a loss of active chain-end functionality. This loss has been ascribed to the occurrence of β-H elimination reactions induced by the Cu(II) deactivator.[16, 17] Using the ARGET ATRP method, Matyjaszewski's research group has diminished the occurrence of this type of side reaction in bulk polymerization of Sty.[19]

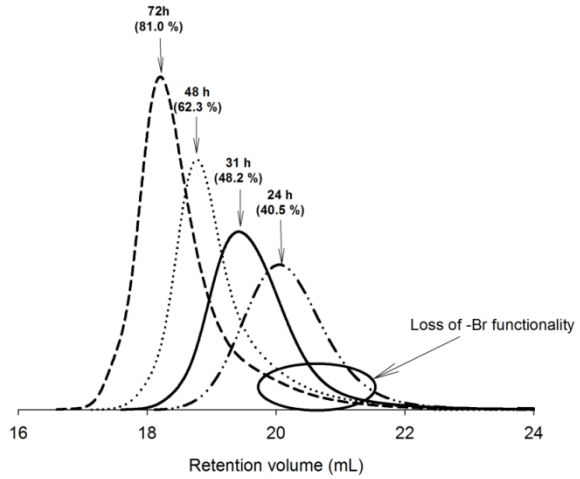

Figure 4.2. SEC traces (RI signal) of PS samples taken at different times of reaction (different monomer conversions). Conditions: $[Sty]_0/[EBiB]_0/[Fe(0)]_0/[CuBr_2]_0/[Me_6TREN]_0$ =125/1/1/0.1/1.1 (molar); $[Sty]_0/[DMF]$ = 2/1 (v/v); T = 70 °C.

To evaluate the effect of the DMF content on the SARA ATRP of Sty, different Sty/DMF ratios were investigated. The kinetic data (Figure 4.3) showed that slower polymerization occurred for bulk conditions. This result is somehow unexpected since in this case the concentration of monomer is higher, which could provide a faster reaction. The results suggest that DMF plays an important role in the polymerization, probably due to the decrease of the viscosity during the reaction and its influence in the k_a and k_d parameters during the SARA ATRP. Although the polymerization proceeded at a similar rate for

Sty/DMF ratios of 2/1 and 1/1, a significant increase in the molecular weight was observed for high monomer conversions of the more diluted polymerization mixture. This behavior suggests that bimolecular coupling may be more significant at these conditions, explaining the higher dispersity values that were obtained for high conversions and the lower apparent initiator efficiency. Conversely, in the polymerization that was carried out in bulk, the molecular weight for higher Sty conversions was below the theoretical line, suggesting that chain transfer to monomer may have played an important role during the polymerization. This effect can be attributed to the very high monomer concentration.

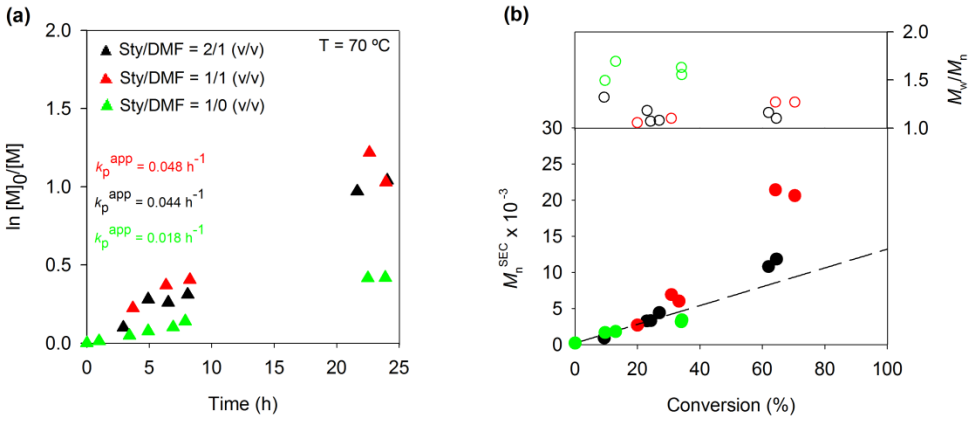

Figure 4.3. (a) Kinetic plots of conversion and ln[M]$_0$/[M] *vs.* time and (b) plot of number-average molecular weights (M_n^{SEC}) and *Đ* (M_w/M_n) *vs.* monomer conversion for the Fe(0)/CuBr$_2$/Me$_6$TREN-catalyzed SARA ATRP of Sty at 70 °C in: bulk (green symbols); [Sty]$_0$/[DMF] = 1/1 (v/v) (red symbols) or [Sty]$_0$/[DMF] = 2/1 (v/v) (black symbols). Reaction conditions: [Sty]$_0$/[EBiB]$_0$/[Fe(0)]$_0$/[CuBr$_2$]$_0$/[Me$_6$TREN]$_0$= 125/1/1/0.1/1.1 (molar).

In recent years, the preparation of well-defined polymeric structures that can be further functionalized through "click" reactions has attracted significant attention.[27] This strategy has been used to prepare PS-based block copolymers with complex molecular architectures and low dispersity.[21, 28, 29] It is, therefore, of great interest to prove that the newly developed mixed transition metal catalytic system is suitable to prepare functionalized PS structures to participate in further "click" reactions. On this matter, the inclusion of both azide and alkyne functionalities for subsequent Cu(I)-catalyzed azide-alkyne cycloaddition, which is the most commonly used "click" reaction,[30] is of particular interest. Figure 4.4 presents the kinetic data obtained for the SARA ATRP of Sty catalyzed by Fe(0)/CuBr$_2$/(Me$_6$TREN or PMDETA) and initiated by an alkyne-terminated initiator (PgBiB). Me$_6$TREN is generally considered one of the most frequently used and

powerful ligands for ATRP[1] and it has also already been successfully used for the ARGET ATRP of Sty.[17, 25] The other ligand studied (PDMETA) is also very attractive due to its wide commercial availability and low price. It has been used in the ATRP of Sty with acceptable values of monomer conversion (conv. ≈ 80%) and low polymer dispersity ($Đ \approx 1.2$).[19] Comparing with the kinetics of Sty polymerization when EBiB was used as the initiator (Figure 4.1 and Figure 4.3), the results showed that the rates of polymerization are close to each other. However, when PMDETA was used as the ligand, the rate of polymerization was significantly lower, but allowed achieving PS with very low dispersity. The polymers prepared from PgBiB initiator, with Me_6TREN as the ligand, showed a slight increase in their dispersity values when compared with those that were initiated by EBiB (Figure 4.1 and Figure 4.3). As shown in previously presented kinetics, the increase in the dispersity values was accompanied by a significant decrease in the apparent initiator efficiency.

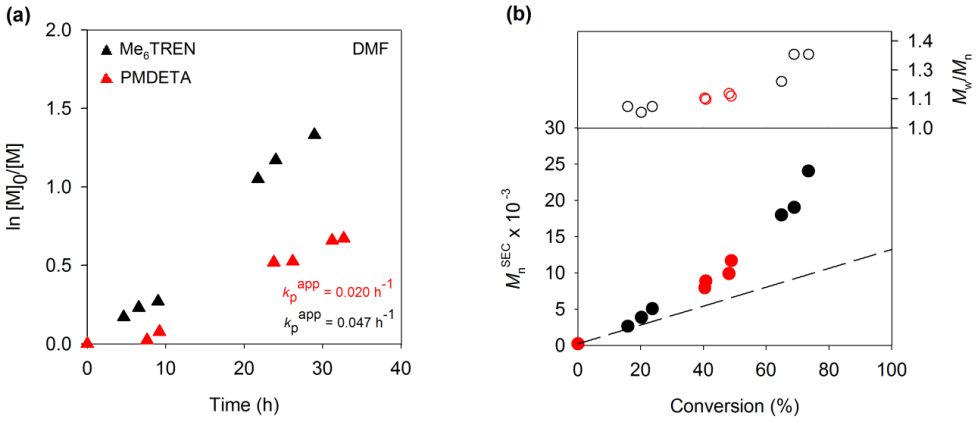

Figure 4.4. (a) Kinetic plots of conversion and ln$[M]_0/[M]$ *vs.* time and (b) plot of numberaverage molecular weights (M_n^{SEC}) and $Đ$ (M_w/M_n) *vs.* monomer conversion for the Fe(0)/$CuBr_2$/ligand-catalyzed SARA ATRP of Sty in DMF at 70 °C, using Me_6TREN (black symbols) or PMDETA (red symbols) as the ligand. Reaction conditions: $[Sty]_0/[DMF]$ = 2/1 (v/v); $[Sty]_0/[PgBiB]_0/[Fe(0)]_0/[CuBr_2]_0/[ligand]_0$= 125/1/1/0.1/1.1 (molar).

The presence of the chain-end functionality was evaluated by ^{1}H NMR spectroscopy (Figure 4.5) and there was no evidence of termination by β-H elimination reactions.[16] The absence of these elimination reactions has also been previously reported for ARGET systems.[17] Based on the ratio between the integrals of the aromatic protons peaks at 6.00-7.50 ppm (a, 5H) and that of the methylene protons from the initiator fragment at 4.20-3.70 ppm (c, 2H), the number-average molecular weight of the telechelic alkyne-

terminated PS could be estimated as M_n^{NMR} = 13.1 x 10^3. Direct comparison with the value that was obtained from the SEC analysis (M_n^{SEC} = 11.4 x 10^3) suggests that chain transfer to monomer is expected to be not very significant. In fact, chain transfer to monomer was even lower than that occurring in the recently reported Fe(0)-mediated Sty ATRP at ambient temperature,[20] in spite of the greater polymerization temperature that was used. The bromine chain-end functionality percentage could be estimated as approximately 79%, from the ratio between the integrals of the peaks of the hydrogen that is adjacent to bromine at 4.40-4.70 ppm (d, 1H) and that of the methylene protons from the initiator fragment at 4.20-3.80 ppm. On the basis of the previously proposed functionality loss mechanisms,[16] and due to the negligible elimination and low chain transfer to monomer reactions, bimolecular coupling is, thus, expected to have a considerable contribution to the loss of the bromine chain-ends.

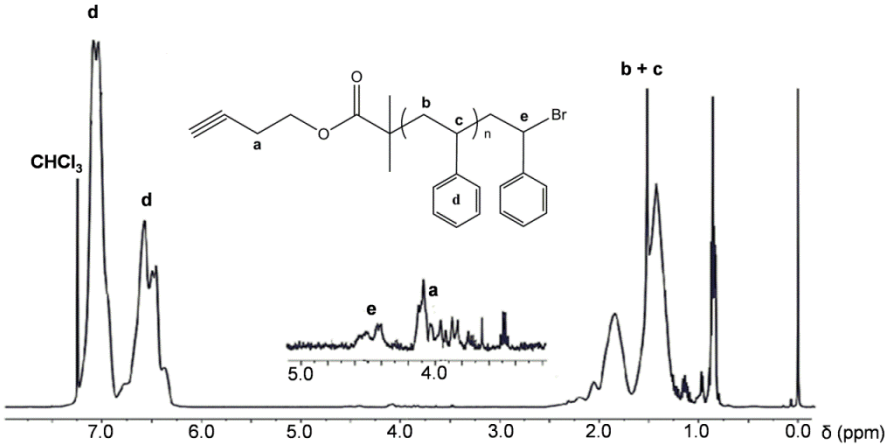

Figure 4.5. ^{1}H NMR spectrum of the PS (M_n^{SEC} = 11.4 x 10^3; $Đ$ = 1.07) obtained by Sty initiation with PgBiB at 70 °C in DMF. Conditions: $[Sty]_0/[DMF]$ = 2/1 (v/v); $[Sty]_0/[PgBiB]_0/[Fe(0)]_0/[CuBr_2]_0/[Me_6TREN]_0$ = 125/1/1/0.1/1.1 (molar); solvent $CDCl_3$.

The possibility of including polymer chain-ends (derived from functional initiators) that are able to react through "click" chemistry is an important tool for designing block copolymers with narrow molecular weight distributions and different architectures. In addition, the active chain-end (e.g., bromine), derived from the "living" character of the polymers, can be used for reinitiation or further functionalization with other end-groups using nucleophilic substitution reactions.

The "living" character of the Br-terminated PS prepared with the catalytic system presented in this paper was evaluated by performing a successful chain extension experiment, using the same catalytic system described ($Fe(0)/CuBr_2/Me_6TREN$ in DMF at 70 °C). Figure 4.6 shows the complete movement of the SEC trace towards higher molecular weight values (lower retention volume). The significant shift in the SEC trace is a clear indication of the retention of high degree of chain-end functionality of the PS obtained by SARA ATRP at low conversion (conv. = 12%). The narrow molecular weight distribution ($Đ \approx 1.10$) and the high degree of bromine chain-end functionality that can be obtained with this catalytic system can, thus, be a key tool for preparing controlled PS-based block copolymer structures. Moreover, the bromine chain-end can be easily converted into an azide chain-end, which can participate in "click" chemistry reactions with alkyne-terminated polymers to afford block copolymers with low dispersity.[31]

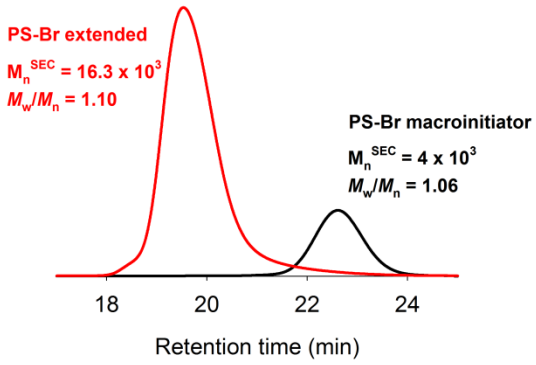

Figure 4.6. Displacement of the SEC trace of a Br-terminated PS obtained at 12% of monomer conversion by SARA ATRP (black line) towards high molecular weight values after a chain extension experiment (red line). Conditions: $[Sty]_0/[DMF]$ = 2/1 (v/v); $[Sty]_0/[PS\text{-}Br]_0/[Fe(0)]_0/[CuBr_2]_0/[Me_6TREN]_0$ = 300/1/1/0.1/1.1 (molar); T = 70 °C.

The azidation of the Br-terminated PS, prepared with EBIB initiator, was carried out using NaN_3 to afford azide-terminated PS. This product was purified, isolated and then reacted with an alkyne-terminated PS (prepared with PgBiB initiator) to demonstrate the viability of these homopolymers to be coupled by a "click" reaction. Figure 4.7 presents the SEC traces of both functionalized homopolymers and "click" product obtained. After the "click" reaction, the RI trace moved significantly from the homopolymers retention volumes towards a lower one, which is indicative of the formation of PS with higher molecular weight. The existence of a shoulder in the alkyne-PS molecular weight distribution can be attributed to the previously discussed termination side reactions, which

increased its dispersity. Since the two starting PS homopolymers (both alkyne and azide-end functionalized) were previously purified, no Sty monomer was present in the "click" reaction pot and, therefore, the significant increase in the PS molecular weight can only be attributed to the "click" reaction. However, based on the RI signal area (Figure 4.7), the "click" efficiency was estimated to be 73%. One should note that, since both starting materials presented narrow molecular weight distributions, an unimodal distribution would be expected.[32] Therefore, the presence of a lower molecular weight fraction can only be attributed to non-reacted polymer segments and not to "clicked" products. According to the number of moles of the reactants, an excess of 3.4% of PS-N_3 was present and, therefore, non-"clicked" products may be ascribed to non-functionalized PS-N_3 (approximately 20%). The high "click" efficiency is also indicative of the successful modification of a PS sample with relatively high molecular weight ($M_n^{SEC} \approx 16 \times 10^3$). It should be noted that such strategies reported in the literature typically involve PS with much lower molecular weight.[21, 29]

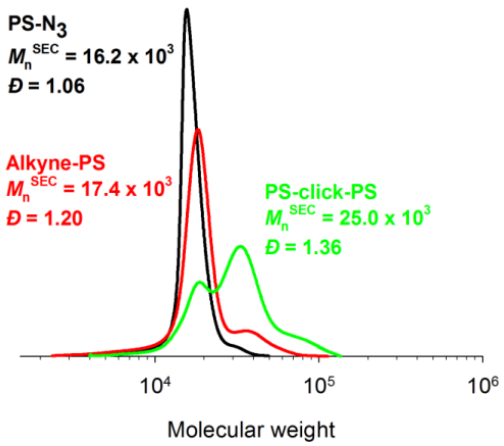

Figure 4.7. SEC traces of the alkyne- and azide-end-functionalized PS homopolymers (red and black lines, respectively) obtained by SARA ATRP and the PS obtained after the "click" reaction (green line).

Figure 4.8 presents the ^{1}H NMR spectrum of the "click" reaction product. It can be observed that, in addition to the methine proton adjacent to the bromine active chain-end that was kept from the alkyne-functionalized PS (signal j at δ = 4.9-5.0 ppm), it is also present the terminal methine proton from the azide-end functionalized PS, which becomes adjacent (signal g at δ = 5.1-5.2 ppm) to the triazol ring formed in the "click" reaction. The azidation of the bromine chain-ends provides the possibility of preparing α-alkyne-ω-

azido terminated PS with relatively low molecular weight, which can be used to afford PS materials with high molecular weight and narrow molecular weight distributions by "click" chemistry. On this matter, it should be mentioned that for high monomer/initiator ratio the *Đ* tends to increase due to the occurrence of a side reaction between the propagating PS radical and the Cu(II)/ligand complex used.[18]

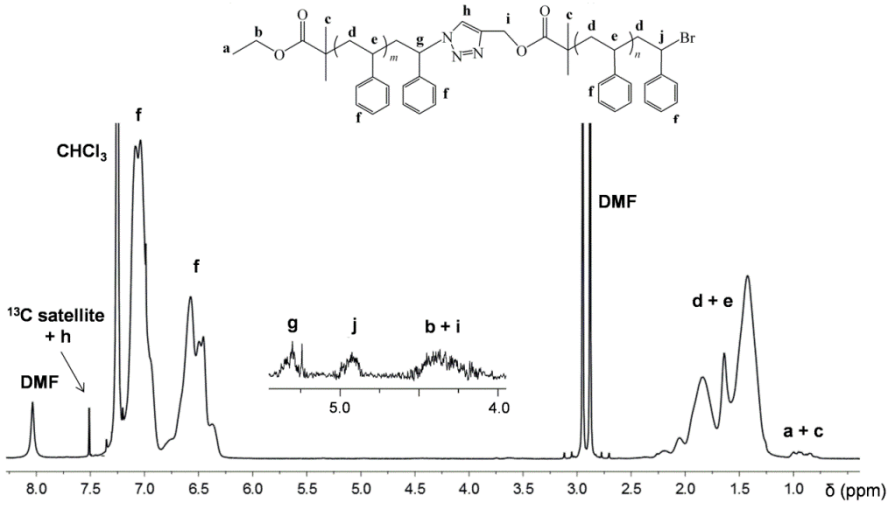

Figure 4.8. ^{1}H NMR spectrum of the PS obtained by the "click" reaction between the alkyne-PS and the PS-N_3 homopolymers. Solvent: $CDCl_3$.

4.5. Conclusions

A successful strategy to use an environmentally attractive Fe(0)/$CuBr_2$/Me_6TREN catalytic system for the SARA ATRP of Sty, affording PS with narrow molecular weight distribution was presented. This catalytic system allowed obtaining Sty conversions similar those reported for other ATRP systems, but at a polymerization rate that was significantly higher than other Fe(0)-mediated Sty ATRP systems. It was further observed that the use of Me_6TREN as the ligand increased the apparent rate constant of polymerization, while maintaining a good control over the PS chain growth, when compared with PMDETA. Narrow polymer molar mass distributions could be obtained at different polymerization conditions. However, deviation from the "living" behavior could be observed only for high monomer conversions, accompanied by a decrease in the apparent initiator efficiency. Moreover, the catalytic system reported was also used to

prepare telechelic PS that could be used in "click" reactions, to afford well-defined PS-based block copolymers.

4.6. References

1. Matyjaszewski, K.; Xia, J. H., Atom transfer radical polymerization. *Chem. Rev.* **2001,** 101, (9), 2921-2990.

2. Guliashvili, T.; Mendonça, P. V.; Serra, A. C.; Popov, A. V.; Coelho, J. F. J., Copper-Mediated Controlled/"Living" Radical Polymerization in Polar Solvents: Insights into Some Relevant Mechanistic Aspects. *Chem. –Eur. J.* **2012,** 18, (15), 4607-4612.

3. Mendonça, P. V.; Serra, A. C.; Coelho, J. F. J.; Popov, A. V.; Guliashvili, T., Ambient temperature rapid ATRP of methyl acrylate, methyl methacrylate and styrene in polar solvents with mixed transition metal catalyst system. *Eur. Polym. J.* **2011,** 47, (7), 1460-1466.

4. Percec, V.; Guliashvili, T.; Popov, A. V.; Ramirez-Castillo, E.; Coelho, J. F. J.; Hinojosa-Falcon, L. A., Accelerated synthesis of poly(methyl methacrylate)-b-poly(vinyl chloride)-b-poly(methyl methacrylate) block copolymers by the CuCl/tris(2-dimethylaminoethyl)amine-catalyzed living radical block copolymerization of methyl methacrylate initiated with α,ω-di(iodo)poly(vinyl chloride) in dimethyl sulfoxide at 90 °C. *J. Polym. Sci., Part A: Polym. Chem.* **2005,** 43, (8), 1649-1659.

5. Masci, G.; Giacomelli, L.; Crescenzi, V., Atom Transfer Radical Polymerization of N-Isopropylacrylamide. *Macromol. Rapid Commun.* **2004,** 25, (4), 559-564.

6. Matyjaszewski, K.; Mu Jo, S.; Paik, H.-j.; Gaynor, S. G., Synthesis of Well-Defined Polyacrylonitrile by Atom Transfer Radical Polymerization. *Macromolecules* **1997,** 30, (20), 6398-6400.

7. Percec, V.; Popov, A. V.; Ramirez-Castillo, E.; Monteiro, M.; Barboiu, B.; Weichold, O.; Asandei, A. D.; Mitchell, C. M., Aqueous Room Temperature Metal-Catalyzed Living Radical Polymerization of Vinyl Chloride. *J. Am. Chem. Soc.* **2002,** 124, (18), 4940-4941.

8. Tang, H.; Radosz, M.; Shen, Y., Atom transfer radical polymerization and copolymerization of vinyl acetate catalyzed by copper halide/terpyridine. *AlChE J.* **2009,** 55, (3), 737-746.

9. Jakubowski, W.; Matyjaszewski, K., Activators regenerated by electron transfer for atom-transfer radical polymerization of (meth)acrylates and related block copolymers. *Angew. Chem. Int. Ed.* **2006,** 45, (27), 4482-4486.

10. Matyjaszewski, K.; Jakubowski, W.; Min, K.; Tang, W.; Huang, J.; Braunecker, W. A.; Tsarevsky, N. V., Diminishing catalyst concentration in atom transfer radical polymerization with reducing agents. *Proc Natl Acad Sci* **2006,** 103, (42), 15309-15314.

11. Zhang, Y. Z.; Wang, Y.; Matyjaszewski, K., ATRP of Methyl Acrylate with Metallic Zinc, Magnesium, and Iron as Reducing Agents and Supplemental Activators. *Macromolecules* **2011,** 44, (4), 683-685.

12. Percec, V.; Guliashvili, T.; Popov, A. V., Ultrafast synthesis of poly(methyl acrylate) and poly(methyl acrylate)-b-poly(vinyl chloride)-b-poly(methyl acrylate) by the Cu(0)/tris(2-dimethylaminoethyl)amine-catalyzed living radical polymerization and block copolymerization of methyl acrylate initiated with 1,1-chloroiodoethane and α,ω-Di(iodo)poly(vinyl chloride) in dimethyl sulfoxide. *J. Polym. Sci., Part A: Polym. Chem.* **2005,** 43, (9), 1948-1954.

13. Beuermann, S.; Buback, M., Rate coefficients of free-radical polymerization deduced from pulsed laser experiments. *Prog. Polym. Sci.* **2002,** 27, (2), 191-254.

14. Mayo, F. R., The dimerization of styrene. *J. Am. Chem. Soc.* **1968,** 90, (5), 1289-1295.

15. Moad, G.; Solomon, D. H., *The Chemistry of Radical Polymerization*. Elsevier: 2006.

16. Lutz, J. F.; Matyjaszewski, K., Nuclear magnetic resonance monitoring of chain-end functionality in the atom transfer radical polymerization of styrene. *J. Polym. Sci., Part A: Polym. Chem.* **2005,** 43, (4), 897-910.

17. Jakubowski, W.; Kirci-Denizli, B.; Gil, R. R.; Matyjaszewski, K., Polystyrene with improved chain-end functionality and higher molecular weight by ARGET ATRP. *Macromol. Chem. Phys.* **2008,** 209, (1), 32-39.

18. Mueller, L.; Jakubowski, W.; Matyjaszewski, K.; Pietrasik, J.; Kwiatkowski, P.; Chaladaj, W.; Jurczak, J., Synthesis of high molecular weight polystyrene using AGET ATRP under high pressure. *Eur. Polym. J.* **2011,** 47, (4), 730-734.

19. Tom, J.; Hornby, B.; West, A.; Harrisson, S.; Perrier, S., Copper(0)-mediated living radical polymerization of styrene. *Polym. Chem.* **2010,** 1, (4), 420-422.

20. Zhou, L. L.; Zhang, Z. B.; Cheng, Z. P.; Zhou, N. C.; Zhu, J.; Zhang, W.; Zhu, X. L., Fe(0) Powder/CuBr2-Mediated "Living"/Controlled Radical Polymerization of Methyl Methacrylate and Styrene at Ambient Temperature. *Macromol. Chem. Phys.* **2012,** 213, (4), 439-446.

21. Tsarevsky, N. V.; Sumerlin, B. S.; Matyjaszewski, K., Step-growth "click" coupling of telechelic polymers prepared by atom transfer radical polymerization. *Macromolecules* **2005,** 38, (9), 3558-3561.

22. Munoz-Bonilla, A.; van Herk, A. M.; Heuts, J. P. A., Preparation of Hairy Particles and Antifouling Films Using Brush-Type Amphiphilic Block Copolymer Surfactants in Emulsion Polymerization. *Macromolecules* **2010,** 43, (6), 2721-2731.

23. Reinicke, S. R. S.; Schmalz, H., Combination of living anionic polymerization and ATRP via "click" chemistry as a versatile route to multiple responsive triblock terpolymers and corresponding hydrogels. *Colloid Polym. Sci.* **2011,** 289, (5-6), 497-512.

24. Ciampolini, M.; Nardi, N., Five-Coordinated High-Spin Complexes of Bivalent Cobalt, Nickel, andCopper with Tris(2-dimethylaminoethyl)amine. *Inorg. Chem.* **1966,** 5, (1), 41-44.

25. Jakubowski, W.; Min, K.; Matyjaszewski, K., Activators regenerated by electron transfer for atom transfer radical polymerization of styrene. *Macromolecules* **2006,** 39, (1), 39-45.

26. Kuo, K.-H.; Chiu, W.-Y.; Cheng, K.-C., Influence of DMF on the polymerization of tert-butyl acrylate initiated by 4-oxo-TEMPO-capped polystyrene macroinitiator. *Polym. Int.* **2008,** 57, (5), 730-737.

27. Mansfeld, U.; Pietsch, C.; Hoogenboom, R.; Becer, C. R.; Schubert, U. S., Clickable initiators, monomers and polymers in controlled radical polymerizations - a prospective combination in polymer science. *Polym. Chem.* **2010,** 1, (10), 1560-1598.

28. Lonsdale, D. E.; Monteiro, M. J., Synthesis and Self-Assembly of Amphiphilic Macrocyclic Block Copolymer Topologies. *J. Polym. Sci., Part A: Polym. Chem.* **2011,** 49, (21), 4603-4612.

29. Degirmenci, M.; Alter, S.; Genli, N., Synthesis and Characterization of Well-Defined Mid-Chain Functional Macrophotoinitiators of Polystyrene by Combination of ATRP and "Click" Chemistry. *Macromol. Chem. Phys.* **2011,** 212, (15), 1575-1581.

30. Golas, P. L.; Matyjaszewski, K., Marrying click chemistry with polymerization: expanding the scope of polymeric materials. *Chem. Soc. Rev.* **2010,** 39, (4), 1338-1354.

31. Fournier, D.; Hoogenboom, R.; Schubert, U. S., Clicking polymers: a straightforward approach to novel macromolecular architectures. *Chem. Soc. Rev.* **2007,** 36, (8), 1369-1380.

32. Barner-Kowollik, C., On the Quantitative Click Conjugation of Molecular Weight Distributions: What Can Theoretically Be Expected? *Macromol. Rapid Commun.* **2009,** 30, (19), 1625-1631.

Chapter 5

Synthesis of cationic poly((3-acrylamidopropyl) trimethylammonium chloride) by SARA ATRP in ecofriendly solvent mixtures

---

Part of the contents of this chapter is published in: ***Patrícia V. Mendonça****, Dominik Konkolewicz, Saadyah E. Averick, Arménio C. Serra, Anatoliy V. Popov, Tamaz Guliashvili, Krzysztof Matyjaszewski and Jorge F. J. Coelho, "Synthesis of cationic poly((3-acrylamidopropyl) trimethylammonium chloride) by SARA ATRP in ecofriendly solvent mixtures", Polymer Chemistry, 2014, 5, 5829-5836.*

5.1. Abstract

Supplemental activator and reducing agent atom transfer radical polymerization (SARA ATRP) of the cationic monomer (3-acrylamidopropyl)trimethylammonium chloride (AMPTMA) was successfully performed for the first time. The polymerizations were performed in water or ethanol/water mixtures at room temperature in the presence of Cu(0), using relatively low concentrations of soluble copper catalyst and an excess of ligand (Me_6TREN: tris(2-(dimethylamino)ethyl)amine)). The reaction conditions were optimized to give the best control over the polymerization under environmentally friendly conditions. The polymerization data showed good control over the molecular weights with narrow molecular weight distributions for the entire reaction time. The preservation of the chain-end functionality was confirmed by self-chain extension and the synthesis of hydrophilic block copolymers containing AMPTMA and oligo(ethylene oxide) methyl ether acrylate (OEOA) or *N*-isopropylacrylamide (NIPAAm). The SARA ATRP was also extended to the synthesis of alkyne-terminated poly-AMPTMA (PAMPTMA), which was subsequently functionalized, using copper(I) catalyzed azide-alkyne cycloaddition (CuAAC), with an azido-functionalized coumarin derivative.

5.2. Introduction

Reversible deactivation radical polymerization (RDRP) techniques are powerful tools for the synthesis of well-defined functional polymeric materials with complex structures. RDRP methods provide control over the polymers molecular weight and architecture, with low molecular weight dispersity (*Đ*) and high chain-end functionality.[1] Atom transfer radical polymerization (ATRP) is one of the most versatile RDRP techniques, as it can be applied to a wide range of monomers under mild conditions.[2-4] In ATRP, control over the molecular weight is gained through a dynamic equilibrium between radicals ($P_n^{\bullet}$) and alkyl halide dormant species. ATRP uses transition metal complexes in a low oxidation state to activate the alkyl halide, giving a radical and the metal complex in a higher oxidation state.[5] The radical typically adds several monomer units before reacting with the higher oxidation state complex to return to the dormant alkyl halide species. Copper-based complexes with nitrogen-based ligands are the most often used in ATRP.[6, 7]

Typically, high concentrations of the metal catalyst, often greater than 1000 parts per million (ppm), are required to perform normal ATRP reactions, which complicates the purification of the polymer. This issue is critically important for biomedical applications and also from the environmental standpoint. That is why new ATRP techniques[8-11] have been developed to reduce the amount of metal catalyst used in the polymerizations to less than 1000 ppm, as well as to avoid/reduce the use of organic solvents. One such method is the SARA ATRP, which uses zero-valent transition metals[11-15] or inorganic sulfites[16, 17] as both reducing agents and supplemental activators. When Cu(0) is used in the reaction, it slowly regenerates CuX species as a reducing agent, and it slowly generates radicals and CuX by a supplemental activation (Scheme 5.1).[5]

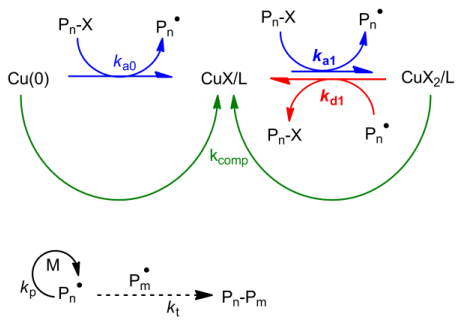

Scheme 5.1. General mechanism of the SARA ATRP mediated by Cu(0) and CuX_2.

Apart from the low amount of catalyst used in SARA ATRP, this method is also very useful for the preparation of biomaterials, since the polymerization can be conducted using environmentally friendly solvents/solvent mixtures at room temperature. Recently, SARA ATRP of acrylates and methacrylates was successfully performed in ethanol/water mixtures using sodium dithionite as a supplemental activator and reducing agent.[12] In addition, well-controlled polymers of OEOA were synthesized by SARA ATRP in water, using a combination of Cu(0) and $CuBr_2$/Me_6TREN with an excess of both Me_6TREN and bromide salts.[18]

Cationic polymers have found extended biomedical applications due to their unique physicochemical properties. These polymers have been extensively studied for gene delivery, tissue engineering and antifouling surfaces.[19, 20] To maximize their therapeutic efficacy, well-defined polymers with precise architecture have been synthesized, mainly by RDRP methods or a combination of RDRP and "click" chemistry strategies.[21-23] Due to the anticipated demand for these products, it is important to develop ecofriendly ATRP

systems for cationic monomers. The cationic monomer AMPTMA has been investigated for various applications. AMPTMA has been included in temperature-responsive copolymers[24-26] with potential to be used as drug delivery systems[27] and as a microcarrier for cell proliferation[28] or in gene delivery.[29, 30] The existing protocols for the ATRP of AMPTMA require more than 10 000 ppm of CuCl or $CuCl_2$ coordinated with Me_6TREN, in DMF/water mixtures (DMF: dimethylformamide), using ethyl 2-chloropropionate (ECP) as the initiator.[24-30] To perform these reactions under more ecofriendly conditions, lower catalyst loadings and less toxic solvents are desired.

Here, reaction conditions for the synthesis of well-defined poly((3-acrylamidopropyl)trimethylammonium chloride) (PAMPTMA) by SARA ATRP in water or ethanol/water mixtures at room temperature (25 °C), using Cu(0) wire in combination with a small amount of $CuCl_2$ (Scheme 5.2) were developed. Importantly, the amount of soluble copper used in the reaction was at least ten times lower than the one reported for the ATRP of AMPTMA.[24-30] In addition, DMF was replaced by ethanol (EtOH), which is a much less toxic solvent. The SARA ATRP method reported herein was also extended to the preparation of PAMPTMA-based block copolymers as well as alkyne-terminated PAMPTMA, which was used for the synthesis of a fluorescent dye chain-end via the CuAAC.

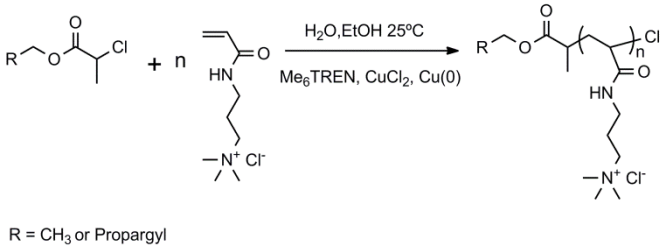

Scheme 5.2. Synthesis of PAMPTMA by SARA ATRP.

5.3. Experimental

5.3.1. Materials

Acetone (Fisher Scientific), AMPTMA (solution 75 wt. % in H_2O, Aldrich), alumina (basic, Fisher Scientific), anhydrous magnesium sulfate (99%, Aldrich), 2-chloropropionyl chloride (97%, Aldrich), copper (II) chloride (97%, Aldrich), copper (II) sulfate pentahydrate (≥ 98 %, Aldrich), deuterated chloroform ($CDCl_3$, 99.8 % Cambridge Isotope Laboratories), deuterated methanol (CD_3OD, 99.8%, Euroisotop), deuterium oxide (99.9%, Cambridge Isotope Laboratories), dichloromethane (DCM, HPLC grade, Fisher Scientific), DMF (Aldrich), EtOH (Fisher Scientific), ECP (97%, Aldrich), glacial acetic acid (Fisher Chemical), hydrochloric acid (Fisher Scientific), 2-hydroxyethyl α-bromoisobutyrate (HBiB, 95%, Aldrich), methanol (Fisher Scientific), propargyl alcohol (PgOH, 99%, Aldrich), sodium ascorbate (crystalline, ≥ 98%, Aldrich), sodium chloride (Fisher Scientific), triethylamine (TEA, ≥ 99%, Sigma Aldrich), tris(2-aminoethyl)amine (TREN, 96%, Aldrich) and water (HPLC grade, Fisher Scientific) were used as received.

CuCl (97%, Aldrich) was washed with glacial acetic acid, followed by 1% aqueous HCl solution. Finally, it was washed with acetone and dried under nitrogen, to give a white powder.

Metallic copper (Cu(0), d = 1 mm, Alfa Aesar) was washed with HCl in methanol and subsequently rinsed with methanol and dried under a stream of nitrogen following the literature procedures.[31]

NIPAAm was recrystallized from hexane.

OEOA (99%, average molecular weight 480, Aldrich) was passed over a column filled with basic alumina to remove inhibitor prior to use.

Me_6TREN,[32] tris(pyridin-2-ylmethyl)amine (TPMA)[32] and 3-azido-7-diethylaminocoumarin[33] were synthesized as reported in the literature.

5.3.2. Techniques

Monomer conversion was measured using ^{1}H NMR spectroscopy in D_2O using a Bruker Avance 500 MHz spectrometer at 27 °C, with spectra analyzed using MestRenova software version: 6.0.2-5475. The coumarin-functionalized PAMPTMA was analyzed by ^{1}H NMR spectroscopy in CD_3OD, using Bruker Avance III 400 MHz spectrometer, with a 5 mm TIX triple resonance detection probe.

Polymers number-average molecular weights (M_n^{SEC}) and dispersity ($Đ$) were determined by using a size exclusion chromatography (SEC) Water 2695 Series with a data processor (Empower Pro), equipped with three columns (Waters Ultrahydrogel Linier, 500 and 250), using 100 mM sodium phosphate buffer with 0.2 vol % trifluoroacetic acid (pH = 2) as an eluent at a flow rate 1.0 mL/min, with detection by a refractive index (RI) detector. Before the injection (100 μL), the samples were filtered through a hydrophilic polyethersulfon membrane with 0.2 μm pore. The system was calibrated with six narrow poly(ethylene glycol) standards and the molecular weights were determined by conventional calibration.

5.3.3. Procedures

Synthesis of propargyl 2-chloropropionate (PgCP)

A mixture of PgOH (2.0 mL, 34 mmol), TEA (5.7 mL, 41 mmol) and dry DCM (15 mL) was added to a two-neck round flask, equipped with a magnetic stirrer bar. The solution was cooled to 0 °C and purged with nitrogen. A mixture of 2-chloropropionyl chloride (4 mL, 41 mmol) and dry DCM (10 mL) was added dropwise to the flask under nitrogen. The mixture was allowed to react at 0 °C for 2 h and then at room temperature overnight. The reaction mixture was filtered, washed with aqueous sodium chloride (100 mL, 3 times), water (100 mL, 2 times) and dried over anhydrous magnesium sulfate. The DCM was removed under reduced pressure and the crude product was purified by distillation under reduced pressure (2.1 g; 41.7%). The purity of the compound was confirmed by ^{1}H NMR spectroscopy.

Typical procedure for the SARA ATRP of AMPTMA

A series of aqueous SARA ATRP reactions were carried out with systematically varied conditions to determine optimal conditions for the SARA ATRP of AMPTMA. Generally, the SARA ATRP of AMPTMA followed this procedure: AMPTMA (2.0 mL, 7.26 mmol), a solution of $CuCl_2$ (2.9 mg, 22 μmol) and Me_6TREN (10 mg, 44 μmol) in water (2.4 mL) and a solution of ECP (9.9 mg, 73 μmol) in EtOH (2.0 mL) were added to a 10 mL Schlenk flask equipped with a magnetic stirrer bar. Next, Cu(0) wire (l = 10 cm; d = 1 mm) was added to the Schlenk flask, which was sealed with a glass stopper, deoxygenated with three freeze-vacuum-thaw cycles and purged with nitrogen. The reaction was allowed to proceed with stirring (700 rpm) at room temperature (25 °C). Different reaction mixture samples were collected during the polymerization. The samples were analyzed by ^{1}H NMR spectroscopy in order to determine the monomer conversion, and by aqueous SEC to determine the molecular weights and dispersity of the polymers. The final reaction mixture was dialyzed (cut-off 3500 Da) against deionized water and the polymer was obtained after freeze drying.

Typical "one-pot" chain extension of PAMPTMA-Cl

AMPTMA (0.5 mL, 1.8 mmol), a solution of $CuCl_2$ (2.4 mg, 18 μmol) and Me_6TREN (8.4 mg, 36 μmol) in water (0.5 mL) and a solution of ECP (5.0 mg, 36 μmol) in EtOH (0.6 mL) were added to a 10 mL Schlenk flask equipped with a magnetic stirrer bar. Next, Cu(0) wire (l = 5 cm; d = 1 mm) was added to the Schlenk flask, which was sealed with a glass stopper, deoxygenated with three freeze-vacuum-thaw cycles and purged with nitrogen. The reaction was allowed to proceed with stirring (700 rpm) at room temperature. When the monomer conversion reached more than 90%, a degassed mixture of AMPTMA (1 mL, 5.4 mmol), water (740 μL) and EtOH (740 μL) were added to the Schlenk flask under nitrogen. In the case of the PAMPTMA-Cl chain extension with NIPAAm, the Schlenk flask was placed in a water bath at 4 °C after the addition of the second monomer (NIPAAm), to avoid polymer precipitation during polymerization. The monomer conversion was determined by ^{1}H NMR spectroscopy and the molecular weights and dispersities were determined by aqueous SEC.

Typical block copolymerization of AMPTMA and OEOA

AMPTMA (0.5 mL, 1.8 mmol), a solution of $CuCl_2$ (4.9 mg, 36 μmol) and Me_6TREN (16.7 mg, 73 μmol) in water (0.5 mL) and a solution of ECP (9.9 mg, 73 μmol) in EtOH (0.6 mL) were added to a 25 mL Schlenk flask equipped with a magnetic stirrer bar. Next, Cu(0) wire (l = 5 cm; d = 1 mm) was added to the Schlenk flask, which was sealed with a glass stopper, deoxygenated with three freeze-vacuum-thaw cycles and purged with nitrogen. The reaction was allowed to proceed with stirring (700 rpm) at room temperature. When the monomer conversion reached more than 90%, a degassed mixture of OEOA (1.6 mL, 3.6 mmol), previously passed over a basic alumina column, water (3.9 mL) and EtOH (3.9 mL) were added to the Schlenk flask under nitrogen. The monomer conversion was determined by ^{1}H NMR spectroscopy and the molecular weights and dispersities were determined by aqueous SEC.

"Click" reaction between alkyne-terminated PAMPTMA and (3-azido-7-diethylaminocoumarin)

An alkyne-terminated PAMPTMA sample (M_n^{SEC} = 5000; $Đ$ = 1.17) was purified through dialysis (cut-off 3500 Da) against water and the polymer was obtained after freeze drying. A solution of (3-azido-7-diethylaminocoumarin) (3.1 mg; 12 μmol), alkyne-terminated PAMPTMA (50 mg; 10 μmol) and $CuSO_4.5H_2O$ (1.2 mg; 5 μmol) in water (100 μL) and EtOH (500 μL) was placed in a round-bottom flask equipped with a magnetic stirrer bar, which was sealed with a rubber septum. The mixture was bubbled with nitrogen for 20 min to remove the oxygen. Finally, a degassed stock solution of sodium ascorbate in water (125 mM; 100 μL) was injected into the flask under nitrogen atmosphere. The reaction was allowed to proceed with stirring (700 rpm) at room temperature for 72 h. The product was purified through dialysis (cut-off 3500 Da) against water, followed by dialysis against EtOH. The organic solvent was evaporated under reduced pressure and the functionalized polymer was analyzed by ^{1}H NMR spectroscopy. The fluorescence confirmed by irradiation at 366 nm.

5.4. Results and discussion

The ATRP system described in the literature for the polymerization of AMPTMA, employed more than 10 000 ppm of CuCl (or CuCl/$CuCl_2$) coordinated with Me_6TREN in a DMF/H_2O = 50/50 (v/v) mixture.[25, 29] It is known that CuX/Me_6TREN complexes (X – halide) undergo rapid disproportionation in the presence of water, producing soluble CuX_2/Me_6TREN and Cu(0) particles.[34] The Cu(I) disproportionation could occur even during the preparation of the reaction system, prior to the polymerization.[34] However, recent investigations on the polymerization of water soluble monomers, catalyzed by Cu(0)/$CuBr_2$/Me_6TREN, in aqueous medium, revealed that the polymerization is governed by the SARA ATRP mechanism.[5, 18] This is because the very high activity of Cu(I) towards the activation of alkyl halides ensures that Cu(I) is the major activator.[5, 18] Furthermore, due to the high activity of Cu(I) in activating alkyl halides, its concentration is at so low levels that disproportionation occurs at a very low rate and can be neglected during the polymerization.[18] In this case, Cu(0) acts as a supplemental activator and a reducing agent, to slowly regenerate Cu(I) and radicals. In this system, the majority of the alkyl halide activation events and deactivations of growing radicals are ruled by the ATRP equilibrium.[31, 35] To the best of our knowledge, detailed kinetic studies on the ATRP of AMPTMA[29] have never been discussed in the literature.

The initial experiments employed Cu(0) wire in combination with $CuCl_2$ as a catalyst in the polymerization of AMPTMA. These experiments were designed to confirm that the SARA ATRP mechanism governs the process, and that similar results to the ones in the literature could be obtained using Cu(0) wire rather than relying on predisproportionation of Cu(I) species.[29] The initial reactions were performed in a DMF/H_2O = 50/50 (v/v) mixture at room temperature, targeting degree of polymerization (DP) of 100 and using ECP as the initiator. After 1.5 h of polymerization, the monomer conversion was approximately 90% and the control achieved over the PAMPTMA molecular weight was similar for both polymerization methods, with $Đ \approx 1.2$ (Figure 5.1).

The SARA ATRP method, using Cu(0) and Cu(II)X_2, is attractive, since lower copper catalyst concentration can be used than in normal ATRP systems. In addition, because it starts with the oxidatively stable Cu(II)X_2 deactivator species, the polymerization is

tolerant to a limited amount of oxygen, especially if oxygen is removed prior to the polymerization.[11-14, 36] Therefore, a series of variables associated with the SARA ATRP were investigated in this work, to allow the synthesis of well-defined PAMPTMA under environmentally friendly reaction conditions.

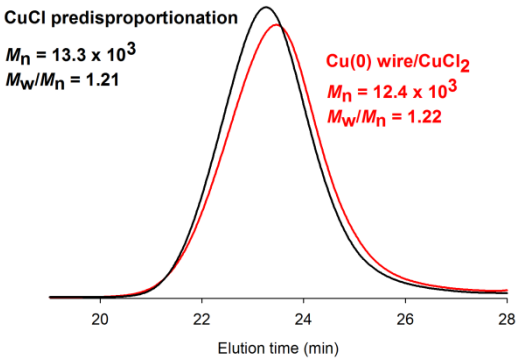

Figure 5.1. SEC traces of the polymers obtained by the use of predisproportionation of CuCl: $[AMPTMA]_0/[ECP]_0/[CuCl]_0/[Me_6TREN]_0$ = 100/1/1/1; DMF/H_2O = 50/50 (v/v); $V_{solvent}$ = 2 mL; (black line) and Cu(0) wire/$CuCl_2$: $[AMPTMA]_0/[ECP]_0/[CuCl_2]_0/[Me_6TREN]_0$/Cu(0) wire = 100/1/0.5/1.0/Cu (0) wire; DMF/H_2O = 50/50 (v/v); Cu(0) wire: *l* = 5 cm; *d* = 1 mm; $V_{solvent}$ = 2 mL (red line) of AMPTMA during 1.5 h at room temperature.

5.4.1. Effect of the water content in the solvent mixture

It is commonly accepted that water is the best solvent from the environmental point-of-view and it is also attractive for industrial applications due to its low toxicity. The use of polar organic solvents or their mixtures with water is sometimes inevitable due to solubility issues of monomers, polymers and catalysts. Ideally, only environmentally benign solvents should be used. In this work, DMF was replaced by EtOH, since EtOH solubilizes both the monomer and the polymer and EtOH is less toxic than DMF. The effect of the content of water in the alcohol/water reaction mixture was varied from 50% to 70%, on the SARA ATRP of AMPTMA. In all cases, the monomer conversion reached 90% in less than 1 h and the kinetics were of first-order with respect to monomer conversion (Figure 5.2 (a)). Changing the ratio of H_2O to EtOH had minimal influence on the control over the molecular weights (Figure 5.2 (b)), since the experimental number average molecular weights were in good agreement with the predicted values and the dispersity values were low ($Đ \approx$ 1.3) throughout the reaction. The next step involved the polymerization in aqueous system (green symbols in Figure 5.2), using the water soluble

2-bromoisobutyrate (HBiB) as the initiator. It is known that aqueous ATRP systems present some challenges that can contribute to poor level of control, mainly due to the high activity of Cu(I) species as well as the dissociation of the halide anion from the X-Cu(II) deactivator complex, which gives a free halide anion and a Cu(II) complex that cannot deactivate radicals.[37] These challenges can be overcome by slowly regenerating Cu(I) species through the addition of an excess of halide salt to promote the formation of the X-Cu(II) deactivator complex.[18, 38-40] Since the AMPTMA monomer inherently contains a chloride anion, well-controlled polymerization in aqueous medium was achieved, without adding any external halide salt, as shown in Figure 5.2 (b) (green symbols) by the narrow molecular weight distributions. After the induction period the reaction was very fast, reaching 95% conversion in 30 min.

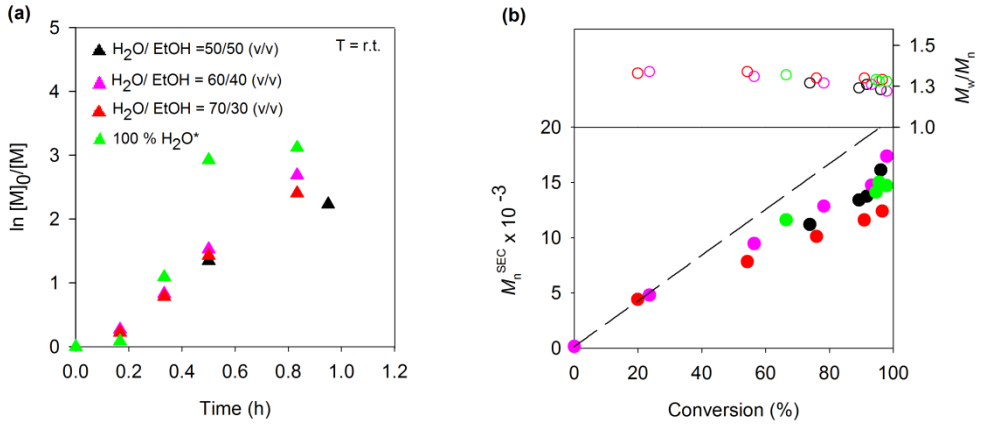

Figure 5.2. (a) Kinetic plots of ln$[M]_0/[M]$ *vs.* time and (b) plot of number–average molecular weights (M_n^{SEC}) and *Đ* (M_w/M_n) *vs.* monomer conversion (the dashed line represents theoretical molecular weight at a given conversion) for the SARA ATRP of AMPTMA initiated by ECP or HBiB* (green symbols), for different water contents in the EtOH/H_2O (v/v) solvent mixture. Conditions: $[AMPTMA]_0/[ECP$ or $EBiB^*]_0/[CuCl_2]_0/[Me_6TREN]_0$/Cu(0) wire = 100/1/0.5/1.0/Cu(0) wire; $[AMPTMA]_0$ = 1.45 M; Cu(0) wire: *l* = 10 cm; *d* = 1 mm; $V_{solvent}$ = 5 mL.

Control experiments using different concentrations of NaCl were performed and showed no effect on the polymerization control. The use of the heterogeneous Cu(0) wire as a reducing agent for the (re)generation of Cu(I)X species in aqueous medium is an attractive feature of the SARA ATRP method reported here.

5.4.2. Effect of the ligand nature and concentration

The next parameters investigated were the structure and concentration of the ligand used in the polymerization. The performance of TPMA was compared to Me_6TREN, since TPMA forms very stable Cu(I) complexes, which prevents disproportionation, although Me_6TREN complexes are more active.[41] The results showed that TPMA could also mediate the SARA ATRP of AMPTMA providing good control over the molecular weight (Figure A.1 (b) in Appendix A). However, the polymerization was considerably slower than with Me_6TREN and the maximum monomer conversion was limited to 35% (Figure A.1 (b) in Appendix A). The decrease of the polymerization rate when TPMA complexes are used in the presence of high concentration of salt has been previously reported for other ATRP systems.[39, 40] Therefore, Me_6TREN was used for all subsequent experiments aiming to achieve high monomer conversion, while ensuring the synthesis of well-defined polymers.

In this work, three different copper to ligand ratios (1/1.2, 1/2 and 1/4) were studied (Figure 5.3).

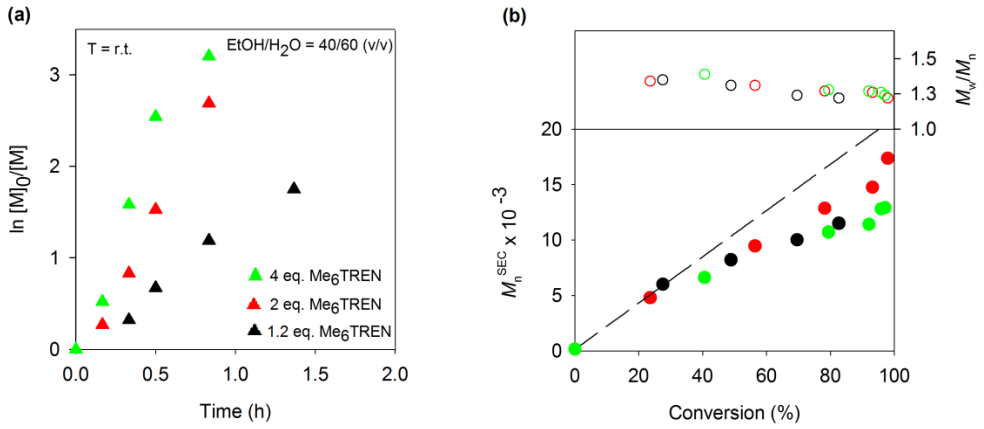

Figure 5.3. (a) Kinetic plots of $\ln[M]_0/[M]$ *vs.* time and (b) plot of number–average molecular weights (M_n^{SEC}) and *Đ* (M_w/M_n) *vs.* monomer conversion (the dashed line represents theoretical molecular weight at a given conversion) for the SARA ATRP of AMPTMA initiated by ECP, for different amounts of ligand. Conditions: $[AMPTMA]_0$ = 1.45 M; $[AMPTMA]_0/[ECP]_0$ = 100; $[CuCl_2]_0$ = 5000 ppm; Cu(0) wire: *l* = 10 cm; *d* = 1 mm; $V_{solvent}$ = 5 mL.

The ligand concentration is an important parameter to consider in SARA ATRP reactions. It should be high enough to coordinate with the all soluble copper in the reaction mixture, to ensure good control over the polymers molecular weight. Since the concentration of

soluble copper increases during the reaction, the ligand is often used in a large excess compared to the initial amount of soluble copper. However, the ligand could lead to undesired side reactions and could also affect both the "livingness" of the polymers and control over the reaction.[42-44] As shown in Figure 5.3, the rate of polymerization increased with the Me_6TREN concentration, while the control over the polymers structure was similar in all cases. Using the copper to ligand ratio of 1/2 (red symbols in Figure 5.3) it was possible to reach a fast reaction and high monomer conversion, obtaining polymers with low dispersity. Increasing the ligand concentration above that value led to a slight enhancement in the polymerization rate with negligible improvement in the control over the molecular architecture. Therefore, for this particular system, two-fold excess of Me_6TREN to $CuCl_2$ (molar) seems to be the optimum ratio.

5.4.3. Effect of the soluble copper concentration

In developing "green" ATRP systems it is important to consider the total amount of soluble copper present in the reaction medium, since copper complexes are mildly toxic and often require additional processes to remove them. In this work, the $CuCl_2$ concentration was decreased from 5000 ppm to 1000 ppm (determined as the initial molar ratio of $CuCl_2$ to the monomer) (Figure 5.4).

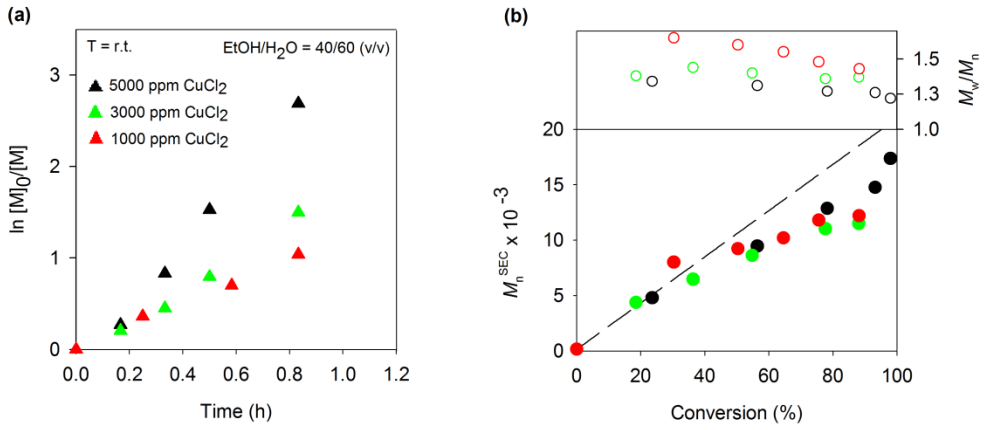

Figure 5.4. (a) Kinetic plots of $\ln[M]_0/[M]$ *vs.* time and (b) plot of number-average molecular weights (M_n^{SEC}) and *Đ* (M_w/M_n) *vs.* monomer conversion for the SARA ATRP of AMPTMA initiated by ECP, for different amounts of initial soluble copper. Conditions:* $[AMPTMA]_0$ = 1.45 M; $[AMPTMA]_0/[ECP]_0$ = 100; $[Me_6TREN]_0/[CuCl_2]_0$ = 2/1; Cu(0) wire: l = 10 cm; d = 1 mm; $V_{solvent}$ = 5 mL.

The results show that the rate of polymerization as well as the control over the polymers molecular weight decreased with the decrease in the initial concentration of $CuCl_2$. Despite the decrease in rate and control over the polymerization, Figure 5.4 shows that even the use of 1000 ppm of $CuCl_2$ provided a reasonable rate of polymerization, reaching 65% of monomer conversion after an hour, and relatively well-controlled polymers with $Đ \approx 1.4$ at a high conversion. Therefore a tradeoff exists between the rate and control over the polymerization and total amount of soluble copper species in the polymerization. For certain applications polymers with narrow molecular weight distributions are necessary, and in these cases higher catalyst loadings may be required. For other applications tolerating broader molecular weight distributions, lower catalyst loadings can be used.

5.4.4. Effect of the Cu(0) wire length

Typically, the Cu(0) wire surface influences the rate of activation of alkyl halides by Cu(0) as well as the rate of copper comproportionation, leading to faster polymerizations with higher Cu(0) surface area.[18, 34, 45, 46] In this section, the Cu(0) wire length was decreased from 10 cm to 2.5 cm in the SARA ATRP of AMPTMA (Cu(0): d = 1 mm). Table 5.1 summarizes the rate of polymerization as well as the polymers molecular weights obtained after 30 min of reaction.

Table 5.1. SARA ATRP of AMPTMA initiated by ECP, for different lengths of Cu(0) wire. Conditions: $[AMPTMA]_0/[ECP]_0/[CuCl_2]_0/[Me_6TREN]_0$/Cu(0) wire = 100/1/0.3/0.6/Cu (0) wire; EtOH/H_2O = 40/60 (v/v); T = 25 °C.; $[AMPTMA]_0$ = 1.45 M; $V_{solvent}$ = 5 mL, t_{rx} = 30 min.

Entry	Cu(0) length[1] (cm)	Cu (0) SA[2] (cm^2)	m $_{Cu(0)}$/SA (g/cm^2)	k_p^{app} (h^{-1})	Conv. (%)	M_n^{SEC} x 10^{-3}	$Đ$
1	10	3.14	0.703	1.578	55	8.6	1.40
2	2.5	0.78	0.176	1.308	49	8.2	1.37

[1] Cu(0) wire: d = 1 mm; [2] SA: surface area

The rate of polymerization was higher when 10 cm of Cu(0) wire was used (Table 5.1, entry 1), reaching 55% of monomer conversion in 30 min. Interestingly, when the copper surface area was decreased 4 times (Table 5.1, entry 2), the reaction still maintained a high rate of polymerization, reaching 49% of monomer conversion in 30 min. These

results suggest that, in this system, it is possible to use a relatively small surface area of copper wire without compromising the rate of polymerization. Further, the control of the reaction was similar in both polymerizations, with final dispersities around 1.4. Kinetic plots of the polymerizations are shown in the Appendix A (Figure A.2).

5.4.5. Chain "livingness" and preparation of block copolymers

The "livingness" of the PAMPTMA chains was evaluated by a "one-pot" chain extension experiment with the same monomer. The first block (targeted DP of 50) was synthesized by SARA ATRP in EtOH/H_2O = 50/50 (v/v) mixture at ambient temperature. After the monomer reached high conversion (> 90%), a degassed solution of AMTPMA in EtOH/H_2O = 50/50 (v/v) was injected into the reaction mixture. Figure 5.5 (a) shows a clear shift on the SEC trace towards high molecular weight (lower retention volume), upon the formation of the extended polymer. However, a low molecular weight tailing was noticeable and was attributed to some terminated chains formed during the first polymerization. Nevertheless, the control over the molecular weight was good, as the extended polymer presented narrow molecular weight distribution ($Đ$ = 1.27).

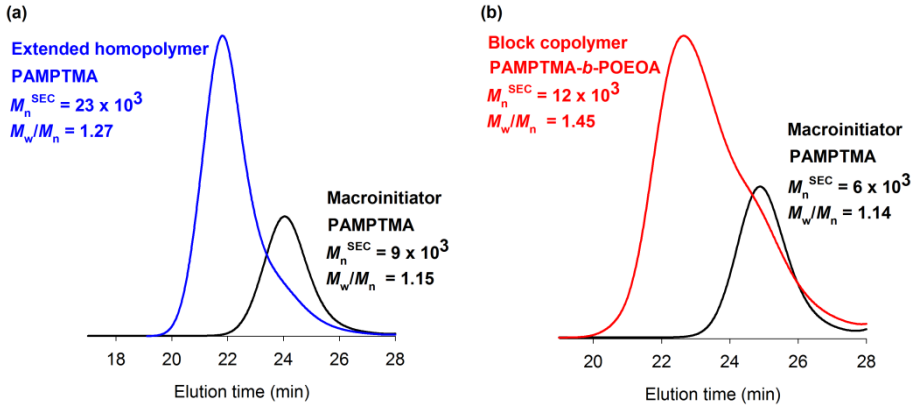

Figure 5.5. SEC traces of PAMPTMA before and after: (a) self-chain extension: first block - $[AMPTMA]_0/[ECP]_0/[CuCl_2]_0/[Me_6TREN]_0$ = 50/1/0.5/1.0; conversion = 92%; second block - $[AMPTMA]_0$ = 1.45 M; $[AMPTMA]_0/[ECP]_0$ = 150; conversion = 94%; (b) extension with $OEOA_{480}$: first block - $[AMPTMA]_0/[ECP]_0/[CuCl_2]_0/[Me_6TREN]_0$ = 25/1/0.5/1.0; conversion = 97%; second block - $[OEOA]_0$ = 0.4 M; $[OEOA]_0/[ECP]_0$ = 50; conversion = 91%. Both chain extensions were done by "one-pot" SARA ATRP, in EtOH/H_2O = 50/50 (v/v) at 25 °C; Cu(0) wire: l = 5 cm; d = 1 mm; $[AMPTMA]_0$ (first block) = 1.45 M; $V_{solvent}$ (first block) = 1.25 mL.

The SARA ATRP system was also extended to the preparation of hydrophilic block copolymers containing two distinct monomers (Table 5.2). In this case the first block was PAMPTMA, and the second block contained either poly(oligo(ethylene oxide) acrylate) (POEOA) or the temperature-responsive poly(*N*-isopropylacrylamide) (PNIPAAm). These block copolymers can find application in the biomedical field. The method proved to be suitable for the preparation of water-soluble PAMPTMA-*b*-POEOA block copolymer with a relatively low dispersity of 1.45, as shown in Figure 5.5 (b). Regarding the PAMPTMA-*b*-PNIPAAm block copolymer, it was not possible to determine its molecular weight parameters due to the inadequate elution in the SEC columns. Some authors have also described the impossibility of analyzing PAMPTMA-*b*-PNIPAAm block copolymers by SEC in several eluents, such as 0.1 M $NaNO_3$:acetonitrile 80:20 (v/v), 0.2 M $NaNO_3$, 0.5 M Na_2SO_4, water or DMF.[29, 30] Samples of both block copolymers were purified by dialysis against (cut-off 3500 Da) water and their structures were confirmed by ^{1}H NMR spectroscopy (Figure A.3 and Figure A.4 in Appendix A).

Table 5.2. PAMPTMA-based block copolymers prepared by "one-pot" SARA ATRP, initiated by ECP at 25 °C. Conditions: $[CuCl_2]_0/[Me_6TREN]_0$/Cu(0) wire = 0.5/1.0/Cu (0) wire (*l* = 5 cm; *d* = 1 mm); EtOH/H_2O = 50/50 (v/v); $[AMPTMA]_0$ = 1.45 M; $[NIPAAm]_0$ = 2 M; $[OEOA_{480}]_0$ = 0.4 M.

	1st block[a]		2nd block			
Targeted copolymer	M_n^{SEC} x 10^{-3}	*Đ*	**Time (h)**	**Conv. (%)**	M_n^{SEC} x 10^{-3}	*Đ*
$PAMPTMA_{50}$-*b*-$PAMPTMA_{150}$	9.1	1.15	2	94	23	1.27
$PAMPTMA_{50}$-*b*-$PNIPAAm_{150}$[b]	9.1	1.15	16	41	[c]	[c]
$PAMPTMA_{25}$-*b*-$(POEOA_{480})_{50}$	6.0	1.14	10	91	12	1.45

[a] Conversion higher than 90%

[b] The second block (NIPAAm) was polymerized at 4 °C

[c] It was not possible to determine

5.4.6. Preparation of alkyne-functionalized PAMPTMA by SARA ATRP

To further explore the potential of the SARA ATRP, the catalytic system developed was used for the preparation of alkyne-functionalized PAMPTMA, using the alkyne bearing initiator propargyl 2-chloropropionate (PgCP) (Figure 5.6). The alkyne functionality allows the polymer to be coupled with a wide library of azide-containing molecules by

"click" chemistry, which could be employed in the design of well-defined copolymers with different architectures or containing different functional groups. The concentration of PgCP was varied to prepare alkyne-functionalized PAMPTMA with several chain lengths. As expected, the rate of polymerization decreased with the increase of the targeted DP (Figure 5.6 (a)), since the supplemental activation reaction rate, which is often rate determining,[47] is dependent on the initiator concentration. The polymerizations showed first-order kinetics (Figure 5.6 (a)) and good control over the PAMPTMA molecular weight, with low dispersity values throughout the polymerizations (Figure 5.6 (b)). These results suggest that the SARA ATRP is a robust method to prepare well-defined end-functional polymers.

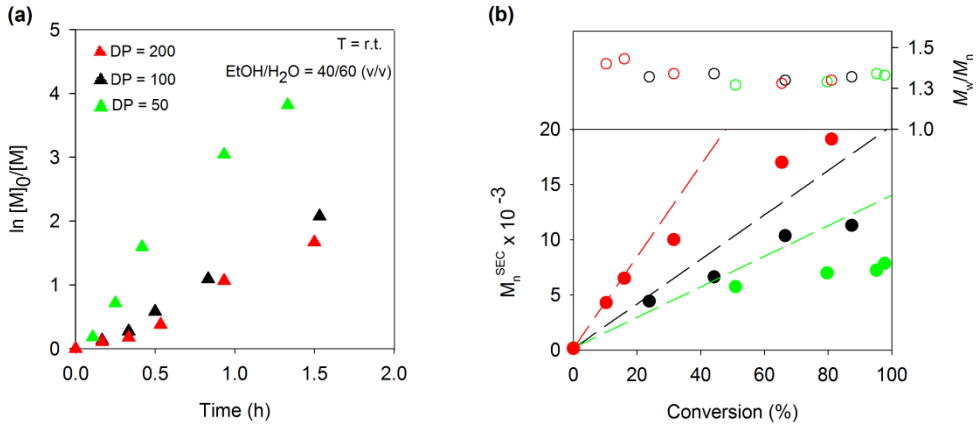

Figure 5.6. (a) Kinetic plots of $\ln[M]_0/[M]$ *vs.* time and (b) plot of number–average molecular weights (M_n^{SEC}) and *Đ* (M_w/M_n) *vs.* monomer conversion (the dashed lines represent theoretical molecular weight at a given conversion) for the SARA ATRP of AMPTMA initiated by alkyne-terminated initiator (PgCP), for different DP values. Conditions: $[AMPTMA]_0/[ECP]_0/[CuCl_2]_0/[Me_6TREN]_0$/Cu(0) wire = DP/1/0.5/1.0/Cu (0) wire; $[AMPTMA]_0$ = 1.45 M; Cu(0) wire: *l* = 10 cm; *d* = 1 mm; $V_{solvent}$ = 5 mL.

The molecular structure of the alkyne-terminated PAMPTMA prepared by SARA ATRP was characterized by ^{1}HNMR spectroscopy (Figure 5.7). The characteristic signals of the polymer assigned agree with those reported in the literature.[29, 30] Additionally, the presence of the active chain-end at 4.14 ppm (h) (1H, –CHCl) and the presence of the alkyne moiety at 2.73 ppm (a) (1H, HC≡C–) were identified.

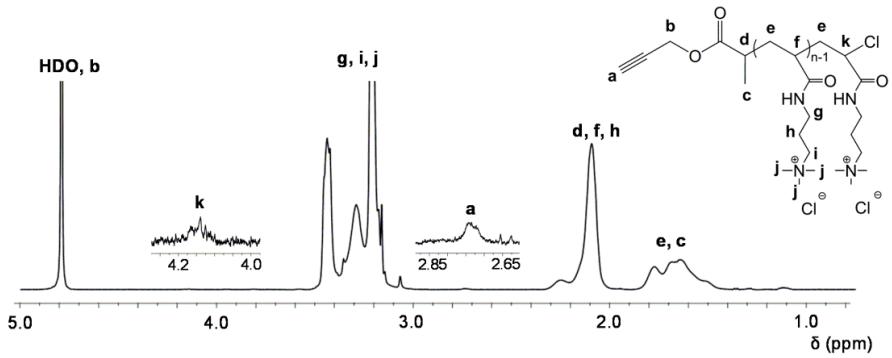

Figure 5.7. 500 MHz ^{1}H NMR spectrum, in D_2O, of purified alkyne-terminated PAMPTMA (M_n^{SEC} = 9600; $Đ$ = 1.17) obtained by SARA ATRP. Reaction conditions: $[AMPTMA]_0/[ECP]_0/[Me_6TREN]_0/[CuCl_2]_0$ = 50/1/0.5/1.0; $[AMPTMA]_0$ = 1.45 M; Cu(0) wire: l = 10 cm; d = 1 mm; $V_{solvent}$ = 5 mL; EtOH/H_2O = 40/60 (v/v).

To confirm that these polymers can participate in "click" reactions, an alkyne-terminated PAMPTMA sample was coupled with an azide-terminated non-fluorescent coumarin derivative (3-azido-7-diethylaminocoumarin), through CuAAC. Coumarin was chosen since it is often used in the biomedical field.[48] Moreover, upon the formation of the triazole ring, the 3-azido-7-diethylaminocoumarin becomes fluorescent (Figure A.5 in Appendix A), which makes the material a potential candidate for imaging applications.[33] The success of the "click" reaction was confirmed by the appearance of the triazole ring proton signal (e) at 8.59 ppm[49] in the ^{1}H NMR spectrum of the purified product (Figure 5.8).

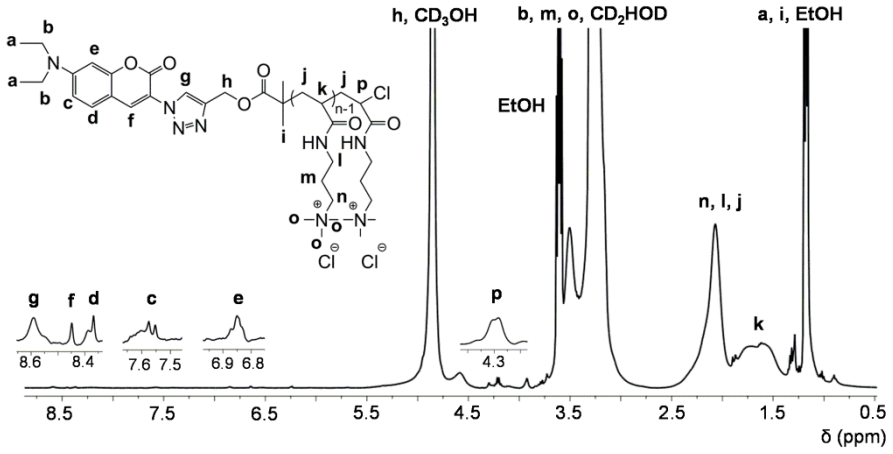

Figure 5.8. 400 MHz ^{1}H NMR spectrum, in CD_3OD, of purified coumarin-functionalized PAMPTMA obtained by a "click" reaction.

5.5. Conclusions

Well-controlled polymers of AMPTMA were synthesized under environmentally friendly conditions using SARA ATRP. The conditions for the polymerization of AMPTMA were optimized for various targets such as low catalyst concentrations or narrow molecular weight distributions. Remarkably, the reaction could be performed in aqueous medium, using a relatively low amount of soluble $CuCl_2$ (1000 ppm) with 2-fold excess of Me_6TREN ligand, at ambient temperature. In addition to narrow molecular weight distributions, the polymers had a high degree of "livingness" as confirmed by both self-blocking chain extension and by the preparation of well-defined PAMPTMA-*b*-POEOA and PAMPTMA-*b*-PNIPAAm block copolymers. Finally, a reactive moiety was introduced onto the initiator giving PAMPTMA with an alkyne end-group. This alkyne group was subsequently reacted with an azido-functionalized coumarin derivative using "click" chemistry giving a fluorescent PAMPTMA molecule.

5.6. References

1. Braunecker, W. A.; Matyjaszewski, K., Controlled/living radical polymerization: Features, developments, and perspectives. *Prog. Polym. Sci.* **2007,** 32, (1), 93-146.

2. Kamigaito, M.; Ando, T.; Sawamoto, M., Metal-Catalyzed Living Radical Polymerization. *Chem. Rev.* **2001,** 101, (12), 3689-3746.

3. Matyjaszewski, K.; Tsarevsky, N. V., Nanostructured functional materials prepared by atom transfer radical polymerization. *Nat. Chem.* **2009,** 1, (4), 276-288.

4. Matyjaszewski, K.; Xia, J., Atom Transfer Radical Polymerization. *Chem. Rev.* **2001,** 101, (9), 2921-2990.

5. Guliashvili, T.; Mendonça, P. V.; Serra, A. C.; Popov, A. V.; Coelho, J. F. J., Copper-Mediated Controlled/"Living" Radical Polymerization in Polar Solvents: Insights into Some Relevant Mechanistic Aspects. *Chem. Eur. J.* **2012,** 18, (15), 4607-4612.

6. di Lena, F.; Matyjaszewski, K., Transition metal catalysts for controlled radical polymerization. *Prog. Polym. Sci.* **2010,** 35, (8), 959-1021.

7. Matyjaszewski, K., Atom Transfer Radical Polymerization (ATRP): Current Status and Future Perspectives. *Macromolecules* **2012,** 45, (10), 4015-4039.

8. Jakubowski, W.; Matyjaszewski, K., Activators Regenerated by Electron Transfer for Atom-Transfer Radical Polymerization of (Meth)acrylates and Related Block Copolymers. *Angew. Chem., Int. Ed.* **2006,** 45, (27), 4482-4486.

9. Magenau, A. J. D.; Strandwitz, N. C.; Gennaro, A.; Matyjaszewski, K., Electrochemically Mediated Atom Transfer Radical Polymerization. *Science* **2011,** 332, (6025), 81-84.

10. Matyjaszewski, K.; Jakubowski, W.; Min, K.; Tang, W.; Huang, J.; Braunecker, W. A.; Tsarevsky, N. V., Diminishing catalyst concentration in atom transfer radical polymerization with reducing agents. *Proc. Natl. Acad. Sci. U.* **2006,** 103, (42), 15309-15314.

11. Zhang, Y.; Wang, Y.; Matyjaszewski, K., ATRP of Methyl Acrylate with Metallic Zinc, Magnesium, and Iron as Reducing Agents and Supplemental Activators. *Macromolecules* **2011,** 44, (4), 683-685.

12. Abreu, C. M. R.; Mendonca, P. V.; Serra, A. C.; Coelho, J. F. J.; Popov, A. V.; Guliashvili, T., Accelerated Ambient-Temperature ATRP of Methyl Acrylate in Alcohol-Water Solutions with a Mixed Transition-Metal Catalyst System. *Macromol. Chem. Phys.* **2012,** 213, (16), 1677-1687.

13. Cordeiro, R. A.; Rocha, N.; Mendes, J. P.; Matyjaszewski, K.; Guliashvili, T.; Serra, A. C.; Coelho, J. F. J., Synthesis of well-defined poly(2-(dimethylamino)ethyl methacrylate) under mild conditions and its co-polymers with cholesterol and PEG using Fe(0)/Cu(II) based SARA ATRP. *Polym. Chem.* **2013,** 4, (10), 3088-3097.

14. Mendonca, P. V.; Serra, A. C.; Coelho, J. F. J.; Popov, A. V.; Guliashvili, T., Ambient temperature rapid ATRP of methyl acrylate, methyl methacrylate and styrene in polar solvents with mixed transition metal catalyst system. *Eur. Polym. J.* **2011,** 47, (7), 1460-1466.

15. Rocha, N.; Mendonca, P. V.; Mendes, J. P.; Simoes, P. N.; Popov, A. V.; Guliashvili, T.; Serra, A. C.; Coelho, J. F. J., Facile Synthesis of Well-Defined Telechelic Alkyne-Terminated Polystyrene in Polar Media Using ATRP With Mixed Fe/Cu Transition Metal Catalyst. *Macromol. Chem. Phys.* **2013,** 214, (1), 76-84.

16. Abreu, C. M. R.; Mendonca, P. V.; Serra, A. C.; Popov, A. V.; Matyjaszewski, K.; Guliashvili, T.; Coelho, J. F. J., Inorganic Sulfites: Efficient Reducing Agents and Supplemental Activators for Atom Transfer Radical Polymerization. *ACS Macro Lett.* **2012,** 1, (11), 1308-1311.

17. Abreu, C. M. R.; Serra, A. C.; Popov, A. V.; Matyjaszewski, K.; Guliashvili, T.; Coelho, J. F. J., Ambient temperature rapid SARA ATRP of acrylates and methacrylates in alcohol-water solutions mediated by a mixed sulfite/Cu(ii)Br2 catalytic system. *Polym. Chem.* **2013,** 4, (23), 5629-5636.

18. Konkolewicz, D.; Krys, P.; Góis, J. R.; Mendonça, P. V.; Zhong, M.; Wang, Y.; Gennaro, A.; Isse, A. A.; Fantin, M.; Matyjaszewski, K., Aqueous RDRP in the Presence of Cu0: The Exceptional Activity of CuI Confirms the SARA ATRP Mechanism. *Macromolecules* **2014,** 47, (2), 560–570.

19. Lee, S. B.; Koepsel, R. R.; Morley, S. W.; Matyjaszewski, K.; Sun, Y.; Russell, A. J., Permanent, Nonleaching Antibacterial Surfaces. 1. Synthesis by Atom Transfer Radical Polymerization. *Biomacromolecules* **2004,** 5, (3), 877-882.

20. Samal, S. K.; Dash, M.; Van Vlierberghe, S.; Kaplan, D. L.; Chiellini, E.; van Blitterswijk, C.; Moroni, L.; Dubruel, P., Cationic polymers and their therapeutic potential. *Chem. Soc. Rev.* **2012,** 41, (21), 7147-7194.

21. Fu, R.; Fu, G.-D., Polymeric nanomaterials from combined click chemistry and controlled radical polymerization. *Polym. Chem.* **2011,** 2, (3), 465-475.

22. Golas, P. L.; Matyjaszewski, K., Click chemistry and ATRP: A beneficial union for the preparation of functional materials. *QSAR Comb. Sci.* **2007,** 26, (11-12), 1116-1134.

23. Ladmiral, V.; Mantovani, G.; Clarkson, G. J.; Cauet, S.; Irwin, J. L.; Haddleton, D. M., Synthesis of neoglycopolymers by a combination of "click chemistry" and living radical polymerization. *J. Am. Chem. Soc.* **2006,** 128, (14), 4823-4830.

24. Bayati, S.; Zhu, K.; Trinh, L. T. T.; Kjoniksen, A.-L.; Nystrom, B., Effects of Temperature and Salt Addition on the Association Behavior of Charged Amphiphilic Diblock Copolymers in Aqueous Solution. *J. Phys. Chem. B* **2012,** 116, (36), 11386-11395.

25. Dedinaite, A.; Thormann, E.; Olanya, G.; Claesson, P. M.; Nystrom, B.; Kjoniksen, A.-L.; Zhu, K., Friction in aqueous media tuned by temperature-responsive polymer layers. *Soft Matter* **2010,** 6, (11), 2489-2498.

26. Shovsky, A.; Knohl, S.; Dedinaite, A.; Zhu, K.; Kjoniksen, A.-L.; Nystrom, B.; Linse, P.; Claesson, P. M., Cationic Poly(N-isopropylacrylamide) Block Copolymer Adsorption Investigated by Dual Polarization Interferometry and Lattice Mean-Field Theory. *Langmuir* **2012,** 28, (39), 14028-14038.

27. Oddo, L.; Masci, G.; Di Meo, C.; Capitani, D.; Mannina, L.; Lamanna, R.; De Santis, S.; Alhaique, F.; Coviello, T.; Matricardi, P., Novel thermosensitive calcium alginate microspheres: Physico-chemical characterization and delivery properties. *Acta Biomater.* **2010,** 6, (9), 3657-3664.

28. Tamura, A.; Nishi, M.; Kobayashi, J.; Nagase, K.; Yajima, H.; Yamato, M.; Okano, T., Simultaneous Enhancement of Cell Proliferation and Thermally Induced Harvest Efficiency Based on Temperature-Responsive Cationic Copolymer-Grafted Microcarriers. *Biomacromolecules* **2012,** 13, (6), 1765-1773.

29. Patrizi, M. L.; Diociaiuti, M.; Capitani, D.; Masci, G., Synthesis and association properties of thermoresponsive and permanently cationic charged block copolymers. *Polymer* **2009,** 50, (2), 467-474.

30. Utsel, S.; Malmstrom, E. E.; Carlmark, A.; Wagberg, L., Thermoresponsive nanocomposites from multilayers of nanofibrillated cellulose and specially designed N-isopropylacrylamide based polymers. *Soft Matter* **2010,** 6, (2), 342-352.

31. Zhang, Y.; Wang, Y.; Peng, C.-h.; Zhong, M.; Zhu, W.; Konkolewicz, D.; Matyjaszewski, K., Copper-Mediated CRP of Methyl Acrylate in the Presence of Metallic Copper: Effect of Ligand Structure on Reaction Kinetics. *Macromolecules* **2011,** 45, (1), 78-86.

32. Britovsek, G. J. P.; England, J.; White, A. J. P., Non-heme Iron(II) Complexes Containing Tripodal Tetradentate Nitrogen Ligands and Their Application in Alkane Oxidation Catalysis. *Inorg. Chem.* **2005,** 44, (22), 8125-8134.

33. Sivakumar, K.; Xie, F.; Cash, B. M.; Long, S.; Barnhill, H. N.; Wang, Q., A Fluorogenic 1,3-Dipolar Cycloaddition Reaction of 3-Azidocoumarins and Acetylenes†. *Org. Lett.* **2004,** 6, (24), 4603-4606.

34. Zhang, Q.; Wilson, P.; Li, Z.; McHale, R.; Godfrey, J.; Anastasaki, A.; Waldron, C.; Haddleton, D. M., Aqueous Copper-Mediated Living Polymerization: Exploiting Rapid Disproportionation of CuBr with Me6TREN. *J. Am. Chem. Soc.* **2013,** 135, (19), 7355-7363.

35. Konkolewicz, D.; Wang, Y.; Zhong, M.; Krys, P.; Isse, A. A.; Gennaro, A.; Matyjaszewski, K., Reversible-Deactivation Radical Polymerization in the Presence of Metallic Copper. A Critical Assessment of the SARA ATRP and SET-LRP Mechanisms. *Macromolecules* **2013,** 46, (22), 8749-8772.

36. Matyjaszewski, K.; Coca, S.; Gaynor, S. G.; Wei, M.; Woodworth, B. E., Zerovalent Metals in Controlled/"Living" Radical Polymerization. *Macromolecules* **1997,** 30, (23), 7348-7350.

37. Tsarevsky, N. V.; Pintauer, T.; Matyjaszewski, K., Deactivation Efficiency and Degree of Control over Polymerization in ATRP in Protic Solvents. *Macromolecules* **2004,** 37, (26), 9768-9778.

38. Averick, S.; Simakova, A.; Park, S.; Konkolewicz, D.; Magenau, A. J. D.; Mehl, R. A.; Matyjaszewski, K., ATRP under Biologically Relevant Conditions: Grafting from a Protein. *ACS Macro Lett.* **2011,** 1, (1), 6-10.

39. Konkolewicz, D.; Magenau, A. J. D.; Averick, S. E.; Simakova, A.; He, H.; Matyjaszewski, K., ICAR ATRP with ppm Cu Catalyst in Water. *Macromolecules* **2012,** 45, (11), 4461-4468.

40. Simakova, A.; Averick, S. E.; Konkolewicz, D.; Matyjaszewski, K., Aqueous ARGET ATRP. *Macromolecules* **2012,** 45, (16), 6371-6379.

41. Tsarevsky, N. V.; Braunecker, W. A.; Matyjaszewski, K., Electron transfer reactions relevant to atom transfer radical polymerization. *J. Organomet. Chem.* **2007,** 692, (15), 3212-3222.

42. Anastasaki, A.; Waldron, C.; Wilson, P.; McHale, R.; Haddleton, D. M., The importance of ligand reactions in Cu(0)-mediated living radical polymerisation of acrylates. *Polym. Chem.* **2013,** 4, (9), 2672-2675.

43. Pintauer, T.; Matyjaszewski, K., Atom transfer radical addition and polymerization reactions catalyzed by ppm amounts of copper complexes. *Chem. Soc. Rev.* **2008,** 37, (6), 1087-1097.

44. Wang, Y.; Zhong, M.; Zhu, W.; Peng, C.-H.; Zhang, Y.; Konkolewicz, D.; Bortolamei, N.; Isse, A. A.; Gennaro, A.; Matyjaszewski, K., Reversible-Deactivation Radical Polymerization in the Presence of Metallic Copper. Comproportionation-Disproportionation Equilibria and Kinetics. *Macromolecules* **2013,** 46, (10), 3793-3802.

45. Chan, N.; Cunningham, M. F.; Hutchinson, R. A., Continuous controlled radical polymerization of methyl acrylate with copper wire in a CSTR. *Polym. Chem.* **2012,** 3, (2), 486-497.

46. Harrisson, S.; Couvreur, P.; Nicolas, J., Comproportionation versus Disproportionation in the Initiation Step of Cu(0)-Mediated Living Radical Polymerization. *Macromolecules* **2012,** 45, (18), 7388-7396.

47. Zhong, M.; Wang, Y.; Krys, P.; Konkolewicz, D.; Matyjaszewski, K., Reversible-Deactivation Radical Polymerization in the Presence of Metallic Copper. Kinetic Simulation. *Macromolecules* **2013,** 46, (10), 3816-3827.

48. Trenor, S. R.; Shultz, A. R.; Love, B. J.; Long, T. E., Coumarins in Polymers: From Light Harvesting to Photo-Cross-Linkable Tissue Scaffolds. *Chem. Rev.* **2004,** 104, (6), 3059-3078.

49. Martwiset, S.; Yavuzcetin, O.; Thorn, M.; Versek, C.; Tuominen, M.; Coughlin, E. B., Proton conducting polymers containing 1H-1,2,3-triazole moieties. *J. Polym. Sci., Part A: Polym. Chem.* **2009,** 47, (1), 188-196.

Chapter 6

Straightforward ARGET ATRP for the synthesis of primary amine polymethacrylate with improved chain-end functionality under mild reaction conditions

---

The contents of this chapter are published in: ***Patrícia V. Mendonça****, Saadyah E. Averick, Dominik Konkolewicz, Arménio C. Serra, Anatoliy V. Popov, Tamaz Guliashvili, Krzysztof Matyjaszewski and Jorge F. J. Coelho, "Straightforward ARGET ATRP for the Synthesis of Primary Amine Polymethacrylate with Improved Chain-End Functionality under Mild Reaction Conditions", Macromolecules, 2014, 47 (14), 4615–4621.*

6.1. Abstract

Activators regenerated by electron transfer atom transfer radical polymerization (ARGET ATRP) of 2-aminoethyl methacrylate hydrochloride (AMA) was successfully performed for the first time. The polymerizations were conducted at 35 °C in isopropanol (IPA)/water mixtures or pure water, using $CuBr_2$/TPMA (TPMA: tris(2-pyridylmethyl)-amine) as a metal catalyst complex with slow feeding of ascorbic acid (AscA) to allow regeneration of the activator species. The reactions showed first-order kinetics with monomer conversion, high monomer conversion (> 90%) and controlled polymers ($Đ \approx$ 1.3) were obtained using optimized conditions. For the first time, as a result of the poly(2-aminoethyl methacrylate hydrochloride)'s (PAMA) high chain-end functionality, it was possible to extend the polymer and synthesize a well-defined block copolymer (PAMA-*b*-POEOMA) (OEOMA: oligo(ethylene oxide) methyl ether methacrylate) by ATRP techniques, using AMA as the first block. PAMA based nanogels, with potential biomedical applications, were prepared by ARGET ATRP in inverse miniemulsion.

6.2. Introduction

Atom transfer radical polymerization (ATRP) is a popular reversible deactivation radical polymerization (RDRP) technique, which allows the preparation of polymers with controlled molecular weight, low molar mass dispersity ($Đ$), complex architectures and high chain-end functionality.[1, 2] The control of the polymerization is achieved by reversible cycles of activation/deactivation of alkyl halide polymer chains. A transition metal/ligand catalytic complex in a lower oxidation state is responsible for the activation of the dormant alkyl halide chains, to generate the corresponding alkyl radical and the catalytic complex in a higher oxidation state. The radical can then propagate by adding a limited number of monomer units before being deactivated by the higher oxidation state catalytic complex to form a dormant alkyl chain.[2-4] Polymers prepared by ATRP have active chain-ends which can be used for chain extension or functionalization, allowing the preparation of copolymers, supramolecular architectures and bioconjugates.[2, 5-7]

ATRP techniques have been used for the controlled polymerization of a wide range of monomers, including functional monomers, such as (meth)acrylates,[3, 8-11]

(meth)acrylamides,[12] styrene[13, 14] and 4-vinyl pyridine.[15, 16] However, there are still important challenges associated with the ATRP of functional monomers bearing primary amine groups or free acidic groups. Primary amine groups can participate in side reactions with the growing polymer halide chain-ends, resulting in dead chains.[17, 18] Further, a competitive complex formation between the amino groups in the monomer/polymer and the metal catalyst can occur.[19] Finally, the acidic character of some monomers can contribute to catalyst poisoning and loss of activity, resulting in uncontrolled reactions. 2- AMA is a synthetically useful monomer due its amine reactive handle (Scheme 6.1) which can be used in several postpolymerization reactions, such as Michael addition or ring-opening of epoxy groups, to afford functional materials for different applications. AMA is a challenging monomer to polymerize by ATRP due to the amino functionality and its acidic character, both interfering with catalyst stability. Moreover, it is well-known that both AMA and PAMA are not chemically stable under basic conditions (pH > 9) and undergo rapid rearrangement to give 2-hydroxyethyl methacrylamide and poly(2-hydroxyethyl methacrylamide), respectively.[20, 21] PAMA homopolymers and copolymers have been successfully used in the preparation of drug/gene delivery carriers[22-29] and we expect that the development of ARGET ATRP conditions for this monomer could lead to a wide-spread utilization of PAMA in new applications. The ARGET ATRP could be advantageous over the normal ATRP technique, for instances considering biomedical applications, since it allows the use of lower amount of metal catalyst to achieve control over the polymerization. In this variation, reducing agents such as AscA are used to (re)generate, *in situ*, Cu(I) activator species from oxidatively stable Cu(II) complexes.[30] In addition, ARGET ATRP was already successfully implemented in aqueous medium.[31]

The first controlled ATRP synthesis of PAMA was reported by Leroux´s research group who employed CuBr/PMDETA (PMDETA: pentamethyldiethylenetriamine) as a catalytic system in tetrahydrofuran (THF) at 65 °C.[26] *t*-Boc-protected AMA was used in order to avoid side reactions with the amino groups.[26, 28] The Armes group reported the direct polymerization of AMA in its hydrochloride salt form by normal ATRP in isopropanol (IPA)/water mixtures at 50 °C, using CuBr/bpy (bpy: 2,2′-bipyridyl) as a catalyst.[20, 21] This strategy presented a significant improvement since it allowed the direct polymerization of AMA, avoiding troublesome protection/deprotection procedures.

However, a critical issue related with the lack of chain-end functionality of the PAMA-Br synthesized by normal ATRP remained to be addressed. Therefore, the preparation of well-defined block copolymers, using AMA as the monomer of the first block, was not possible.[32] Controlled polymerization of AMA has been also achieved by reversible addition-fragmentation chain transfer (RAFT) to produce both well-defined homopolymers and copolymers.[20, 33-35] In opposition to ATRP, the Armes group was able to prepare primary amine-based block copolymers, with reasonable dispersity ($Đ \approx 1.4$), by RAFT with AMA as the first building block.[20] However, the RAFT polymerization required the use of organic solvents (DMSO/1,4-dioxane mixture) at a relatively high temperature (70 °C). Therefore, considering the utility of primary amines in the preparation of functional polymers, the development of new ATRP systems which allow the controlled synthesis of these polymers with high chain-end functionality under aqueous conditions is desirable.

Herein, the controlled synthesis of PAMA was accomplished using ARGET ATRP in IPA/water mixtures or aqueous medium, near room temperature (35 °C), using slow feeding of AscA for the regeneration of the activator (Scheme 6.1). In addition, AMA was successfully copolymerized with water-soluble OEOMA monomer. To the best of our knowledge, this was the first time that PAMA-Br, synthesized by ATRP techniques, was used as the first block of a well-defined block copolymer. Finally, the application of the ARGET ATRP system was expanded to the preparation of PAMA-based nanogels, which could be used as nanomaterials for biomedical applications.

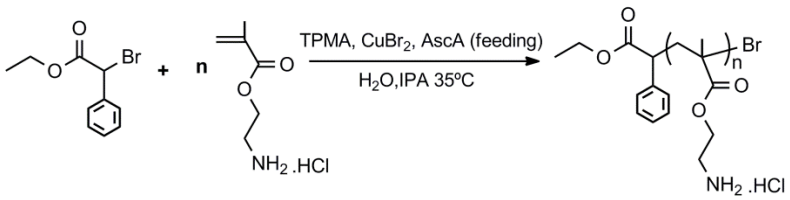

Scheme 6.1. Polymerization of AMA in its hydrochloride salt form by ARGET ATRP.

6.3. Experimental

6.3.1. Materials

Acetone (Fisher Scientific), AMA (≥ 95%, Polysciences), AscA (Sigma-Aldrich), bpy (≥ 99%, Sigma Aldrich), copper(II) bromide (99.999%, Aldrich), deuterium oxide (99.9%, Cambridge Isotope Laboratories), ethyl α-bromoisobutyrate (EBiB, 98%, Sigma Aldrich), ethyl α-bromophenyl acetate (EBPA, Alfa Aesar), glacial acetic acid (Fisher Chemical), hydrochloric acid (Fisher Scientific), 2-hydroxyethyl 2-bromoisobutyrate (HBiB, 95%, Aldrich), isopropanol (Fisher Scientific), sodium bromide (≥ 99%, Sigma Aldrich), Span-80 (Sigma-Aldrich) and water (HPLC grade, Fisher Scientific) were used as received.

Inhibitor was removed from $OEOMA_{300}$ (average molecular weight ≈ 300, Aldrich) and $OEOMA_{475}$ (99%, average molecular weight 475, Aldrich) by passing through a basic alumina column prior to use.[36]

Poly(ethylene oxide) monomethyl ether 2-bromoisobutyrate ester (PEO_{2k}iBBr, M_n = 2000) and poly(ethylene oxide) dimethacrylate (PEO_{4k}DM, M_n = 4000) were prepared as previously described in the literature.[37]

CuCl (97%, Aldrich) was washed with glacial acetic acid, followed by 1 % aqueous HCl solution. Finally, it was washed with acetone and dried under nitrogen, to give a white powder.

TPMA was synthesized as reported in the literature.[38, 39]

6.3.2. Techniques

A syringe pump (KDS Scientific, Legato 101) was used for the continuous feeding of the reducing agent at the rate of 1 μL/min.

Monomer conversion was measured using ^{1}H NMR spectroscopy in D_2O using a Bruker Avance 500 MHz spectrometer at 27 °C.

Polymers number-average molecular weights (M_n^{SEC}) and dispersity ($Đ$) were determined by using a size exclusion chromatography (SEC) Water 2695 Series with a data processor (Empower Pro), equipped with three columns (Waters Ultrahydrogel Linier, 500 and 250), using 100 mM sodium phosphate buffer with 0.2 vol % trifluoroacetic acid (pH = 2) as an eluent at a flow rate 1.0 mL/min, with detection by a refractive index (RI) detector. Before the injection (100 μL), the samples were filtered through a hydrophilic polyethersulfone (PES) membrane with 0.2 μm pore. The system was calibrated with six narrow poly(ethylene glycol) standards and the molecular weights were determined by conventional calibration.

Particle size of the nanogels was measured using a Zetasizer Nano from Malvern Instruments.

6.3.3. Procedures

Typical procedure for the ARGET ATRP of AMA

AMA (0.6 g, 3 mmol), $CuBr_2$ (3.8 mg, 17 μmol), TPMA (20 mg, 69 μmol) and EBPA (8.4 mg, 84 μmol) were dissolved in water (1.2 mL)/IPA (0.52 mL). The mixture was added to a 10 mL Schlenk flask, equipped with a magnetic stirrer bar, and purged with nitrogen for 30 min. The flask was placed in an oil bath at 35 °C and a deoxygenated ascorbic acid solution (10 mM) was continuously injected into the reaction medium using a syringe pump at the rate of 1 μL/min. Different reaction mixture samples were collected during the polymerization. The samples were analyzed by ^{1}H NMR spectroscopy in order to determine the monomer conversion, and by aqueous SEC to determine the molecular weights and dispersity of the polymers. The final reaction mixture was dialyzed (cut-off 3500 Da) against deionized water and the polymer was obtained after freeze drying.

Typical procedure for the normal ATRP of AMA

Normal ATRP of AMA was performed following a procedure reported elsewhere.[20] CuCl (13.2 mg, 014 mmol) was placed in a Schlenk flask, equipped with a magnetic stirrer bar, deoxygenated with three freeze-vacuum-thaw cycles and purged with nitrogen. AMA (0.7 g, 4.02 mmol), bpy (42 mg, 0.27mmol) and EBiB (26.1 mg, 0.14 mmol) were dissolved in water (400 μL)/IPA (1.61 mL) and purged with nitrogen for 30 min. The mixture was

added to the Schlenk flask, containing the CuCl, under nitrogen. The flask was placed in an oil bath at 50 °C and the reaction was allowed to proceed for 2.5 h. At the end, water was added to the flask in order to dissolve the precipitated polymer. A sample was collected and analyzed by both ^{1}H NMR spectroscopy and SEC to determine the monomer conversion and the molecular weight and dispersity of the polymer, respectively.

Typical "one-pot" chain extension of PAMA-Br with $OEOMA_{475}$

AMA (0.3 g, 1.72 mmol), $CuBr_2$ (6.4 mg, 29 μmol), TPMA (33 mg, 115 μmol) and EBPA (14 mg, 57 μmol) were dissolved in water (600 μL)/IPA (60 μL). The mixture was added to a 10 mL Schlenk flask, equipped with a magnetic stirrer bar, and purged with nitrogen for 30 min. The flask was placed in an oil bath at 35 °C and a deoxygenated ascorbic acid solution (10 mM) was continuously injected into the reaction medium using a syringe pump at the rate of 1 μL/min. When the monomer conversion reached more than 90%, a degassed mixture of $OEOMA_{475}$ (2 mL, 4.0 mmol), water (2.2 mL) and IPA (0.9 mL) were added to the Schlenk flask under nitrogen. The monomer conversion was determined by ^{1}H NMR spectroscopy and the molecular weights and dispersities were determined by aqueous SEC.

Typical procedure for the preparation of PAMA-based nanogels

Amine-nanogels were prepared through a water-in-oil inverse miniemulsion using ARGET ATRP. The inverse miniemulsion was composed of a water phase consisting of $CuBr_2$ (1.9 mg, 0.0085 mmol)/TPMA (2.9 mg, 0.01 mmol), PEO_{2k}iBBr (33.4 mg, 0.017 mmol, M_n = 2000), $OEOMA_{300}$ (1450 mg, 4.8 mmol, M_n = 300), AMA (88 mg, 0.53 mmol), PEO_{4k}DM (226 mg, 0.56 mmol) and 66 mg PEO-OH (as a stabilizer) dissolved in 1.4 mL of ultrapure water and emulsified with 20 g of a 0.05% (w/w) of Span-80 in cyclohexane using ultrasonication (3 minutes) to form stable droplets. After degassing, ascorbic acid 100 μL (100 mg/mL degassed) was injected to initiate the ARGET ATRP which was stopped after 24 hours at 30 °C. The nanogels were purified by precipitation into THF followed by dialysis (cut-off 50000 Da) into THF and then into water to remove unreacted reagents.

6.4. Results and discussion

6.4.1. ARGET ATRP of AMA

The first report on the normal ATRP of AMA in its hydrochloride salt form reported in the literature required high concentration of CuCl catalyst coordinated with bpy (see Table 6.1).[20] In order to overcome such issue, a new ARGET ATRP system was tested for the polymerization of the primary amine monomer. The polymerization was performed in IPA/water mixtures at 35 °C, using AscA as a reducing agent and $CuBr_2$/TPMA catalytic complex. Ligand selection was based on the stability of $CuBr_2$/TPMA in water,[31] even at low pH. In addition it was experimentally determined that TPMA complexes proved to better control the ARGET polymerization of AMA than bpy complexes (see Figure B.1 in Appendix B).

Table 6.1. Molecular weight parameters of PAMA obtained by both normal ATRP and ARGET ATRP.

Entry	Method	DP	Time (h)	Conv. (%)	M_n^{th} x 10^{-3}	M_n^{SEC} x 10^{-3}	$Đ$
1	Normal ATRP[a]	100	2.4	63	10.5	9.9	1.36
2	ARGET ATRP[b]	100	2.8	79	12.8	7.6	1.35
3	Normal ATRP[a]	30	2.3	91	4.8	6.3	1.33
4	ARGET ATRP[c]	30	4.5	93	4.8	4.4	1.30

[a] Reaction conditions: $[AMA]_0/[EBiB]_0/[CuCl]_0/[bpy]_0$ = DP/1/2; IPA/H_2O = 80/20 (v/v); T = 50 °C; $[AMA]_0$ = 2 M

[b] Reaction conditions: $[AMA]_0/[EBPA]_0/[CuBr_2]_0/[TPMA]_0$= DP/0.5/2; FR_{AscA} = 43 nmol/min; IPA/H_2O = 30/70 (v/v); T = 35 °C; $[AMA]_0$ = 2 M

[c] Same reaction conditions as those mentioned in entry 2, but with FR_{AscA} = 10 nmol/min

Initial attempts of the ARGET ATRP of AMA were done by adding the total amount of AscA (molar ratio of 0.3 in comparison to the initiator) at the beginning of the polymerization. However, a fast reduction of Cu(II) species was observed by the disappearance of the green color, characteristic of $CuBr_2$/TPMA complexes, after approximately 1 hour of reaction. This resulted in an uncontrolled polymerization ($Đ$ > 1.5) with limited monomer conversion of 60 %. Alternatively, ascorbic acid was fed to the reaction via a syringe pump, to regenerate the Cu(I) activator species in a slow and controlled manner. Using this strategy, it was possible to achieve high monomer conversion (> 90 %) and controlled polymerizations ($Đ$ ≈ 1.3). The level of control

obtained by the new ARGET ATRP was comparable to that of normal ATRP for different targeted degree of polymerization (DP) values (Table 6.1). In addition, ^{1}H NMR spectra of samples collected during the ARGET ATRP showed that there was no sign of the formation of methacrylamide derivatives resultant from the AMA/PAMA rearrangement (Figure 6.1), which is known to happen under basic conditions.[20, 21]

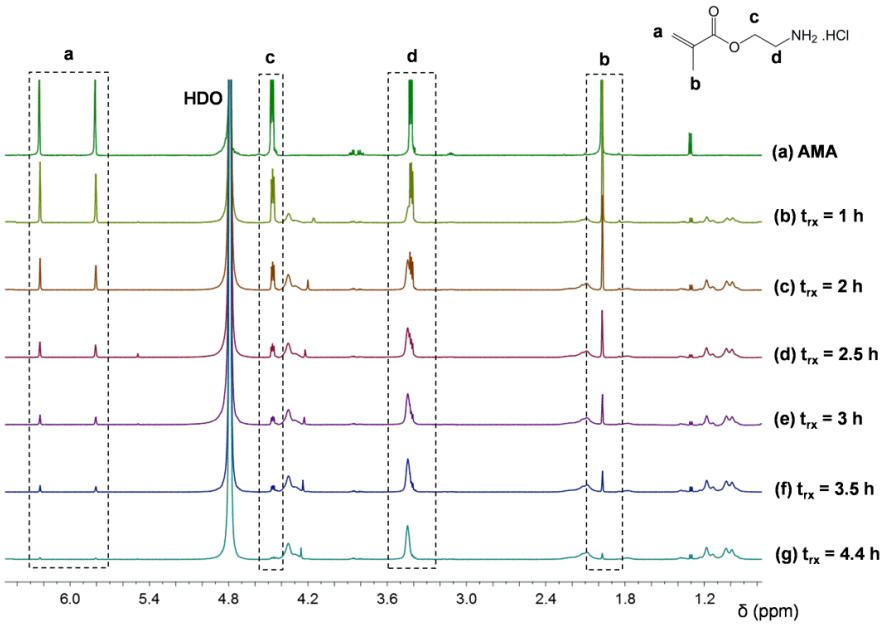

Figure 6.1. ^{1}H NMR spectra, in D_2O, of: (a) AMA monomer and (b) to (g) reaction mixture samples collected during the ARGET ATRP in water at 35 °C. Reaction conditions: $[AMA]_0/[EBPA]_0/[CuBr_2]_0/[TPMA]_0$ = 100/1/0.5/02.0; FR_{AscA} = 43 nmol/min; $[AMA]_0$ = 2 M.

The initial experiments (Table 6.1) indicated that the reaction conditions required optimization to achieve control over the ARGET ATRP of AMA. Therefore, a range of polymerization conditions were studied to understand their influence on AMA's polymerization.

6.4.2. Influence of the reaction temperature

The reports on the controlled polymerization of AMA, either in its *t*-Boc-protected or hydrochloride salt form, employ reaction temperatures of 50 °C[20, 21, 29, 32, 40] or higher.[25, 26] To understand the influence of the temperature on the ARGET ATRP of AMA, three different temperatures were studied to find a balance between the lowest polymerization temperature, while still retaining a good control over the PAMA molecular weight at a

reasonable polymerization rate. Table 6.2 shows that the polymerization rate was similar for 44 °C and 35 °C. However, at 25 °C the reaction was much slower and, after 5 hours, the mixture lost its green color indicating that the $CuBr_2$ was completely reduced. Therefore, based on a compromise between the rate of reaction and temperature, 35 °C was determined as the optimal value for this study.

Table 6.2. Kinetic parameters for the ARGET ATRP of AMA at different temperatures. Conditions: $[AMA]_0/[EBPA]_0/[CuBr_2]_0/[TPMA]_0$ = 100/1/0.3/1.2 with $[NaBr]_0$ = 30 mM; $[AMA]_0$ = 2 M; FR_{AscA} = 43 nmol/min in IPA/H_2O = 50/50 (v/v).

Entry	T (°C)	k_p^{app} (h^{-1})	Time (h)	Conv. (%)	M_n^{SEC} x 10^{-3}	$Đ$
1	44	0.563	3.3	89	9.1	1.40
2	35	0.545	3.3	77	6.6	1.45
3	25	0.229	4.5	42	5.7	1.41

In aqueous initiators for continuous activator regeneration (ICAR),[41] ARGET[31] or supplemental activator and reducing agent (SARA)[42] ATRP systems of neutral monomers, the addition of halide salts (e.g., NaCl and NaBr) enhanced the control over the polymerization. The halide salt helps to maintain the sufficiently high concentration of the deactivator complex, which can partially dissociate and loose activity in water during the polymerization. In the initial experiments (Table 6.1 and Figure 6.2) 30 mM of NaBr were added. However, the use of extra halide salt revealed no improvement in the control over the polymerization (Figure B.2 in Appendix B), since AMA monomer provides intrinsically enough halide anions (Cl^-). Therefore, in the remaining experiments no additional halide salts were added.

6.4.3. Influence of the copper concentration

Typically, ARGET ATRP systems use a lower concentration of catalyst compared to normal ATRP. However, for some challenging monomers (e.g., primary amines), higher catalyst loadings may be required to effectively control the polymerization. The influence of copper concentration on the control of the ARGET ATRP of AMA was evaluated from 10000 to 3000 ppm (Figure 6.2). The three amounts of deactivator complex studied afforded reactions with similar rates of polymerization (Figure 6.2 (a)). When the higher amount of $CuBr_2$ was used, the reaction was slightly faster, most probably due to a higher

rate of reduction and no induction period was observed. As expected, the increase of the deactivator concentration led to better control over the polymerization (Figure 6.2 (b)). However, there was a slight increase of the PAMA $Đ$ during the polymerization, especially for monomer conversions above ≈ 60%.

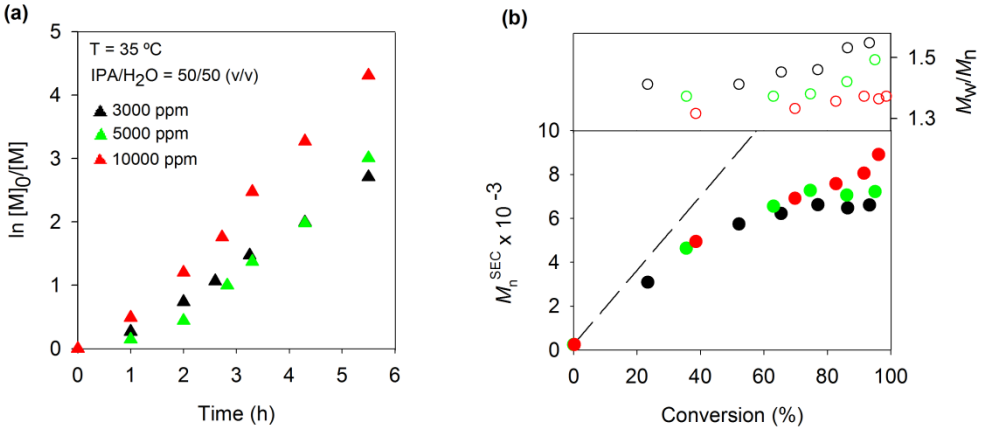

Figure 6.2. (a) Kinetic plots of conversion and $\ln[M]_0/[M]$ vs. time and (b) plot of number-average molecular weights (M_n^{SEC}) and $Đ$ (M_w/M_n) *vs.* monomer conversion for the ARGET ATRP of AMA in IPA/H_2O = 50/50 (v/v) at 35 °C, using different amounts of deactivator complex. Reaction conditions: $[AMA]_0/[EBPA]_0/[CuBr_2]_0/[TPMA]_0$ = 100/1/$[CuBr_2]_0/[TPMA]_0$; FR_{AscA} = 43 nmol/min; [NaBr] = 30 mM; $[AMA]_0$ = 2 M.

The deviation of the observed molecular weights from theoretical molecular weights (Figure 6.2 (b)) can be attributed to the use of conventional calibration using poly(ethylene glycol) standards, which have different hydrodynamic volumes than PAMA. Similar limitations have also been reported by other authors in the polymerization of AMA[20] and other hydrophilic monomers.[43-45] Therefore, to confirm the level of control obtained during the ARGET ATRP, a sample of PAMA obtained at 86% monomer conversion (targeted DP of 100) was isolated from the reaction mixture and the molecular weight of the polymer was determined by ^{1}H NMR (see details in Figure B.3 in Appendix B) as being M_n^{NMR} = 17 x 10^3. This value is much closer to the theoretical molecular weight (M_n^{th} = 15 x 10^3) than the one obtained by SEC, suggesting that the ARGET ATRP is a suitable method for the control polymerization of the primary amine monomer.

6.4.4. Influence of the solvent mixture composition

Prior reports have found that the use of 20% of water in the IPA/water solvent mixture for the normal ATRP of AMA lead to minimal polymer precipitation during the reaction.[20] However, in this work, the same conditions resulted in complete precipitation of the polymer during the reaction, even for a targeted DP as low as 30 (see Figure B.4 in Appendix B). To avoid the precipitation of PAMA during the ARGET ATRP several ratios of IPA to water were used to polymerize AMA (Figure 6.3).

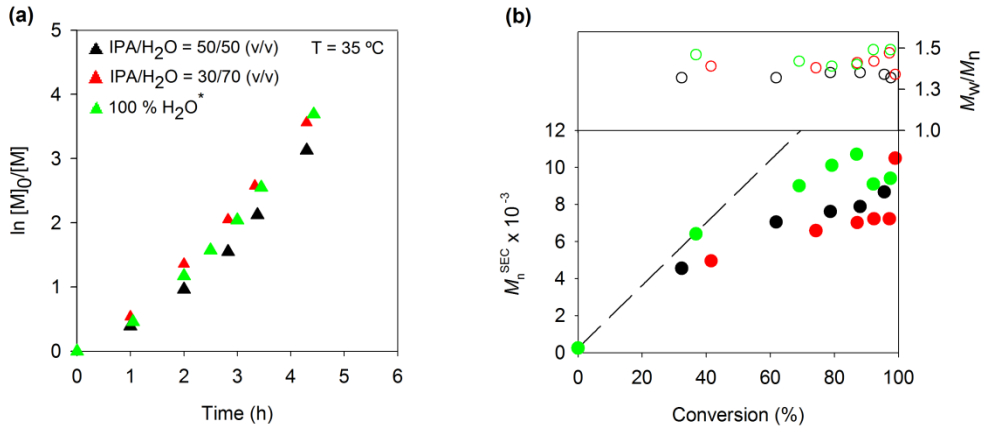

Figure 6.3. (a) Kinetic plots of conversion and ln[M]$_0$/[M] vs. time and (b) plot of number-average molecular weights (M_n^{SEC}) and $Đ$ (M_w/M_n) *vs.* monomer conversion for the ARGET ATRP of AMA at 35 °C, using different amounts water in the solvent mixture. Reaction conditions: [AMA]$_0$/[EBPA or HBiB*]$_0$/[CuBr$_2$]$_0$/[TPMA]$_0$ = 100/1/0.5/02.0; FR$_{AscA}$ = 43 nmol/min; [AMA]$_0$ = 2 M.

Polymerization of AMA in IPA/water = 50/50 (v/v) formed minor amounts of precipitate during the reaction, and decreasing the amount of IPA to 30% and 0% led to homogeneous and precipitate-free polymerizations (see Figure B.5 in Appendix B). Overall the results indicate that both control over the molecular weight distribution as well as the rate of polymerization are not influenced by increased water content in the reaction media.[46]

6.4.5. Influence of the ascorbic acid feeding rate

It has been reported that the feeding rate of the AscA (FR$_{AscA}$) influences both the polymerization rate and the control over the polymers molecular weight.[31] Usually, higher feeding rates provide faster reactions but poorer control. The FR$_{AscA}$ acid was studied

from 10 to 43 nmol/min in the ARGET ATRP of AMA (Figure 6.4). As expected, the lowest rate of polymerization was obtained for FR_{AscA} of 10 nmol/min (Figure 6.4 (a)), whereas 20 and 43 nmol/min gave higher polymerization rates. Despite the difference in polymerization rates, there was no significant improvement of the control over the PAMA molecular weight during the polymerization in the range of FR_{AscA} studied (Figure 6.4 (b)).

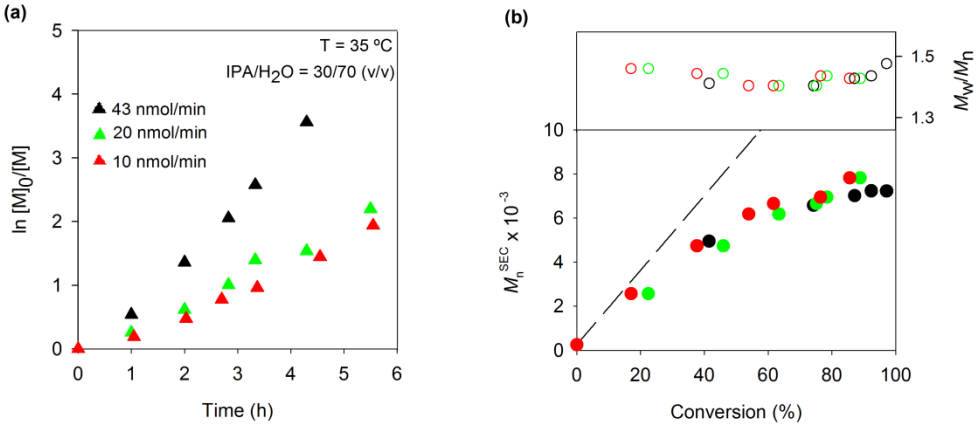

Figure 6.4. (a) Kinetic plots of conversion and $\ln[M]_0/[M]$ vs. time and (b) plot of number–average molecular weights (M_n^{SEC}) and $Đ$ (M_w/M_n) *vs.* monomer conversion for the ARGET ATRP of AMA in IPA/H_2O = 30/70 (v/v) at 35 °C, using different feeding rates of the ascorbic acid. Reaction conditions: $[AMA]_0/[EBPA]_0/[AscA]/[CuBr_2]_0/[TPMA]_0 = 100/1/FR_{AscA}/0.5/02.0$; $[AMA]_0 = 2$ M.

6.4.6. Evaluation of the PAMA "livingness"

A PAMA-Br macroinitiator obtained at high conversion (> 90%) by ARGET ATRP was extended with the water-soluble $OEOMA_{475}$ monomer. The complete shift of the SEC trace confirmed the formation of a well-defined block copolymer with $Đ$ = 1.25 (Figure 6.5). No tailing was observed in the block copolymer molecular weight distribution, which suggests that the PAMA-Br prepared by ARGET ATRP retains high chain-end functionality. These results present a significant improvement in the controlled synthesis of PAMA in comparison with the normal ATRP reported in the literature, which showed low chain-end functionality preventing the successful extension of the polymer.[32] For the first time, it was possible to prepare a well-defined PAMA-based block copolymer using AMA as the monomer of the first block. Similar increase on the chain-end functionality of polymers prepared by ARGET ATRP was previously reported for the polymerization

of styrene.[47] This result was attributed to the lower concentration of metal catalyst/ligand complex used in ARGET ATRP, in comparison with normal ATRP, which decreased the rate of catalyst-induced side reactions.[47, 48]

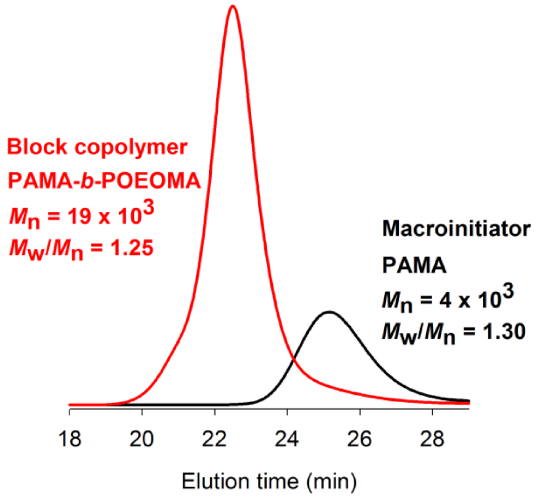

Figure 6.5. SEC traces of PAMA before and after the extension with $OEOMA_{475}$: macroinitiator obtained at 93% of monomer conversion (black line) and block copolymer at 90% of AMA conversion (red line); first block - $[AMA]_0/[EBPA]_0/[CuBr_2]_0/[TPMA]_0/[AscA]$ = 30/1/0.5/2.0/10 nmol/min; second block - $[OEOMA_{475}]_0$ = 1 M; $[OEOMA_{475}]_0/[EBPA]_0$ = 70. Chain-extension was done by "one-pot" ARGET ATRP in IPA/H_2O = 30/70 (v/v) at 35 °C; $[AMA]_0$ = 2M; $V_{solvent}$ (first block) = 860 µL.

The validation of this hypothesis on the ARGET ATRP of AMA requires further investigation. The chemical structure of the PAMA-*b*-POEOMA was confirmed by ^{1}H NMR spectroscopy (Figure 6.6).

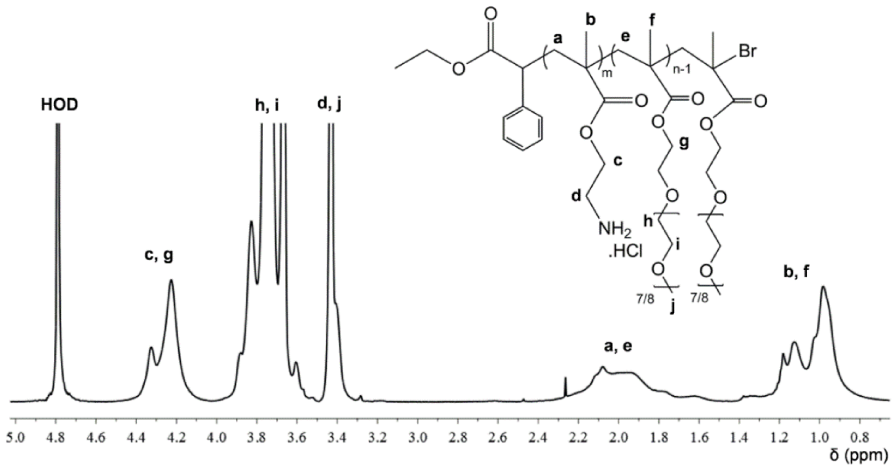

Figure 6.6. 400 MHz ^{1}H NMR spectrum, in D_2O, of the PAMA-*b*-POEOMA block copolymer obtained by "one-pot" ARGET ATRP.

6.4.7. Preparation of PAMA nanogels by ARGET ATRP

The potential of the ARGET ATRP was explored for the preparation of PAMA-based nanogels (see size distribution on Figure 6.7). Nanogels are a diverse class of nano-sized hydrogels prepared using inverse miniemulsion and have been used in many biomedical applications including as drug or gene delivery agents.[49-51]

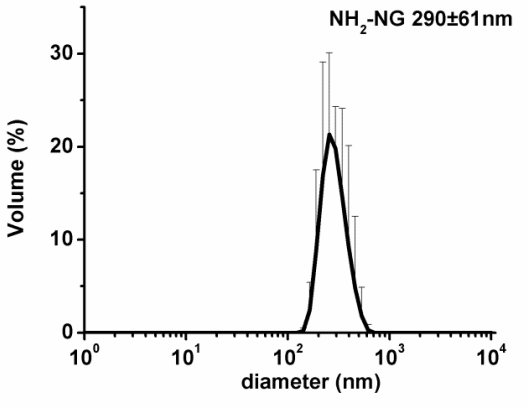

Figure 6.7. **Volume distribution of PAMA-based nanogels (NH_2-NG) prepared by ARGET ATRP in inverse miniemulsion measured using DLS. Samples were measured in 10 mM acetate buffer (pH = 4.5).**

To demonstrate the feasibility of preparing PAMA-based nanogels by ARGET ATRP, a stable and inverse miniemulsion was prepared by ultrassonication using an aqueous phase containing AMA and $OEOMA_{300}$ with an organic phase comprised of Span-80 in cyclohexane. The active catalyst was (re)generated by injection of AscA. After 24 hours the reaction was stopped, precipitated and purified using dialysis. The nanogels were characterized using dynamic light scattering in 10 mM acetate buffer (pH = 4.5) and their diameter was determined to be 290±61 nm (Figure 6.7). Due to the cationic nature of PAMA at low pH, we anticipate that these nanogels could be promising materials for gene delivery applications.

6.5. Conclusions

An ARGET ATRP system was developed for the preparation of well-defined PAMA in isopropanol/water mixtures or aqueous medium at 35 °C using $CuBr_2$/TPMA as the catalytic complex. AscA, which was used as the reducing agent for the regeneration of

Cu(I) activator species, had to be slowly feed into the reaction mixture to afford high monomer conversions (> 90%) and reasonable control ($Đ \approx 1.3$). For the first time, PAMA prepared by ATRP techniques retained high chain-end functionality, allowing the preparation of a well-defined block copolymer (PAMA-*b*-POEOMA). The ARGET ATRP was also used for the synthesis of PAMA-based nanogels, which can form interesting materials for biomedical applications.

6.6. References

1. Kamigaito, M.; Ando, T.; Sawamoto, M., Metal-Catalyzed Living Radical Polymerization. *Chem. Rev.* **2001,** 101, (12), 3689-3746.

2. Matyjaszewski, K.; Xia, J., Atom Transfer Radical Polymerization. *Chem. Rev.* **2001,** 101, (9), 2921-2990.

3. Wang, J.-S.; Matyjaszewski, K., Controlled/"living" radical polymerization. atom transfer radical polymerization in the presence of transition-metal complexes. *J. Am. Chem. Soc.* **1995,** 117, (20), 5614-5615.

4. Guliashvili, T.; Mendonça, P. V.; Serra, A. C.; Popov, A. V.; Coelho, J. F. J., Copper-Mediated Controlled/“Living” Radical Polymerization in Polar Solvents: Insights into Some Relevant Mechanistic Aspects. *Chem. Eur. J* **2012,** 18, (15), 4607-4612.

5. Matyjaszewski, K.; Tsarevsky, N. V., Nanostructured functional materials prepared by atom transfer radical polymerization. *Nat. Chem.* **2009,** 1, (4), 276-288.

6. Matyjaszewski, K.; Tsarevsky, N. V., Macromolecular Engineering by Atom Transfer Radical Polymerization. *J. Am. Chem. Soc.* **2014,** 136, (18), 6513-6533.

7. Matyjaszewski, K., Atom Transfer Radical Polymerization (ATRP): Current Status and Future Perspectives. *Macromolecules* **2012,** 45, (10), 4015-4039.

8. Mendonca, P. V.; Serra, A. C.; Coelho, J. F. J.; Popov, A. V.; Guliashvili, T., Ambient temperature rapid ATRP of methyl acrylate, methyl methacrylate and styrene in

polar solvents with mixed transition metal catalyst system. *Eur. Polym. J.* **2011,** 47, (7), 1460-1466.

9. Cordeiro, R. A.; Rocha, N.; Mendes, J. P.; Matyjaszewski, K.; Guliashvili, T.; Serra, A. C.; Coelho, J. F. J., Synthesis of well-defined poly(2-(dimethylamino)ethyl methacrylate) under mild conditions and its co-polymers with cholesterol and PEG using Fe(0)/Cu(ii) based SARA ATRP. *Polym. Chem.* **2013,** 4, (10), 3088-3097.

10. Gois, J. R.; Rocha, N.; Popov, A. V.; Guliashvili, T.; Matyjaszewski, K.; Serra, A. C.; Coelho, J. F. J., Synthesis of well-defined functionalized poly(2-(diisopropylamino)ethyl methacrylate) using ATRP with sodium dithionite as a SARA agent. *Polym. Chem.* **2014**.

11. Wang, J.-S.; Matyjaszewski, K., Controlled/"Living" Radical Polymerization. Halogen Atom Transfer Radical Polymerization Promoted by a Cu(I)/Cu(II) Redox Process. *Macromolecules* **1995,** 28, (23), 7901-7910.

12. Teodorescu, M.; Matyjaszewski, K., Controlled polymerization of (meth)acrylamides by atom transfer radical polymerization. *Macromol. Rapid Commun.* **2000,** 21, (4), 190-194.

13. Rocha, N.; Mendonça, P. V.; Mendes, J. P.; Simões, P. N.; Popov, A. V.; Guliashvili, T.; Serra, A. C.; Coelho, J. F. J., Facile Synthesis of Well-Defined Telechelic Alkyne-Terminated Polystyrene in Polar Media Using ATRP With Mixed Fe/Cu Transition Metal Catalyst. *Macrom. Chem. Phys.* **2013,** 214, (1), 76-84.

14. Qiu, J.; Matyjaszewski, K., Polymerization of Substituted Styrenes by Atom Transfer Radical Polymerization. *Macromolecules* **1997,** 30, (19), 5643-5648.

15. Rocha, N.; Mendes, J.; Duraes, L.; Maleki, H.; Portugal, A.; Geraldes, C. F. G. C.; Serra, A.; Coelho, J., Poly(ethylene glycol)-block-poly(4-vinyl pyridine) as a versatile block copolymer to prepare nanoaggregates of superparamagnetic iron oxide nanoparticles. *J. Mater. Chem. B* **2014,** 2, (11), 1565-1575.

16. Xia, J.; Zhang, X.; Matyjaszewski, K., Atom Transfer Radical Polymerization of 4-Vinylpyridine. *Macromolecules* **1999,** 32, (10), 3531-3533.

17. Coessens, V.; Matyjaszewski, K., Synthesis of polymers with amino end groups by atom transfer radical polymerization. *J. Macromol. Sci., Pure Appl. Chem.* **1999,** A36, (5-6), 811-826.

18. Coessens, V.; Pintauer, T.; Matyjaszewski, K., Functional polymers by atom transfer radical polymerization. *Prog. Polym. Sci.* **2001,** 26, (3), 337-377.

19. Tang, W.; Kwak, Y.; Braunecker, W.; Tsarevsky, N. V.; Coote, M. L.; Matyjaszewski, K., Understanding Atom Transfer Radical Polymerization: Effect of Ligand and Initiator Structures on the Equilibrium Constants. *J. Am. Chem. Soc.* **2008,** 130, (32), 10702-10713.

20. He, L. H.; Read, E. S.; Armes, S. P.; Adams, D. J., Direct synthesis of controlled-structure primary amine-based methacrylic polymers by living radical polymerization. *Macromolecules* **2007,** 40, (13), 4429-4438.

21. Thompson, K. L.; Read, E. S.; Armes, S. P., Chemical degradation of poly(2-aminoethyl methacrylate). *Polym. Degrad. Stab.* **2008,** 93, (8), 1460-1466.

22. Chang, Y.; Ahn, Y. S.; Hahn, H. T.; Chen, Y., Sub-micrometer Patterning of Proteins by Electric Lithography. *Langmuir* **2007,** 23, (8), 4112-4114.

23. Kim, M. R.; Jeong, J. H.; Park, T. G., Swelling Induced Detachment of Chondrocytes Using RGD-Modified Poly(N-isopropylacrylamide) Hydrogel Beads. *Biotechnol. Progr.* **2002,** 18, (3), 495-500.

24. Kuroda, K.; DeGrado, W. F., Amphiphilic Polymethacrylate Derivatives as Antimicrobial Agents. *J. Am. Chem. Soc.* **2005,** 127, (12), 4128-4129.

25. Ji, W.; Panus, D.; Palumbo, R. N.; Tang, R.; Wang, C., Poly(2-aminoethyl methacrylate) with Well-Defined Chain Length for DNA Vaccine Delivery to Dendritic Cells. *Biomacromolecules* **2011,** 12, (12), 4373-4385.

26. Dufresne, M. H.; Leroux, J. C., Study of the micellization behavior of different order amino block copolymers with heparin. *Pharm Res* **2004,** 21, (1), 160-9.

27. Cheng, Q.; Huang, Y.; Zheng, H.; Wei, T.; Zheng, S.; Huo, S.; Wang, X.; Du, Q.; Zhang, X.; Zhang, H.-Y.; Liang, X.-J.; Wang, C.; Tang, R.; Liang, Z., The effect of guanidinylation of PEGylated poly(2-aminoethyl methacrylate) on the systemic delivery of siRNA. *Biomaterials* **2013,** 34, (12), 3120-3131.

28. Tang, R.; Palumbo, R. N.; Nagarajan, L.; Krogstad, E.; Wang, C., Well-defined block copolymers for gene delivery to dendritic cells: Probing the effect of polycation chain-length. *J. Control. Release* **2010,** 142, (2), 229-237.

29. Ding, J.; Xiao, C.; He, C.; Li, M.; Li, D.; Zhuang, X.; Chen, X., Facile preparation of a cationic poly(amino acid) vesicle for potential drug and gene co-delivery. *Nanotechnology* **2011,** 22, (49).

30. Jakubowski, W.; Matyjaszewski, K., Activators Regenerated by Electron Transfer for Atom-Transfer Radical Polymerization of (Meth)acrylates and Related Block Copolymers. *Angew. Chem.* **2006,** 118, (27), 4594-4598.

31. Simakova, A.; Averick, S. E.; Konkolewicz, D.; Matyjaszewski, K., Aqueous ARGET ATRP. *Macromolecules* **2012,** 45, (16), 6371-6379.

32. Read, E. S.; Thompson, K. L.; Armes, S. P., Synthesis of well-defined primary amine-based homopolymers and block copolymers and their Michael addition reactions with acrylates and acrylamides. *Polym. Chem.* **2010,** 1, (2), 221-230.

33. Locock, K. E. S.; Michl, T. D.; Valentin, J. D. P.; Vasilev, K.; Hayball, J. D.; Qu, Y.; Traven, A.; Griesser, H. J.; Meagher, L.; Haeussler, M., Guanylated Polymethacrylates: A Class of Potent Antimicrobial Polymers with Low Hemolytic Activity. *Biomacromolecules* **2013,** 14, (11), 4021-4031.

34. Li, Y. T.; Armes, S. P., Synthesis of Model Primary Amine-Based Branched Copolymers by Pseudo-Living Radical Copolymerization and Post-polymerization Coupling of Homopolymers. *Macromolecules* **2009,** 42, (4), 939-945.

35. Wu, D.-Q.; Li, Z.-Y.; Li, C.; Fan, J.-J.; Lu, B.; Chang, C.; Cheng, S.-X.; Zhang, X.-Z.; Zhuo, R.-X., Porphyrin and Galactosyl Conjugated Micelles for Targeting Photodynamic Therapy. *Pharm Res* **2010,** 27, (1), 187-199.

36. Cho, H. Y.; Srinivasan, A.; Hong, J.; Hsu, E.; Liu, S.; Shrivats, A.; Kwak, D.; Bohaty, A. K.; Paik, H.-j.; Hollinger, J. O.; Matyjaszewski, K., Synthesis of Biocompatible PEG-Based Star Polymers with Cationic and Degradable Core for siRNA Delivery. *Biomacromolecules* **2011,** 12, (10), 3478-3486.

37. Bencherif, S. A.; Washburn, N. R.; Matyjaszewski, K., Synthesis by AGET ATRP of Degradable Nanogel Precursors for In Situ Formation of Nanostructured Hyaluronic Acid Hydrogel. *Biomacromolecules* **2009,** 10, (9), 2499-2507.

38. Britovsek, G. J. P.; England, J.; White, A. J. P., Non-heme Iron(II) Complexes Containing Tripodal Tetradentate Nitrogen Ligands and Their Application in Alkane Oxidation Catalysis. *Inorg. Chem.* **2005,** 44, (22), 8125-8134.

39. Xia, J.; Matyjaszewski, K., Controlled/"Living" Radical Polymerization. Atom Transfer Radical Polymerization Catalyzed by Copper(I) and Picolylamine Complexes. *Macromolecules* **1999,** 32, (8), 2434-2437.

40. Topham, P. D.; Sandon, N.; Read, E. S.; Madsen, J.; Ryan, A. J.; Armes, S. P., Facile Synthesis of Well-Defined Hydrophilic Methacrylic Macromonomers Using ATRP and Click Chemistry. *Macromolecules* **2008,** 41, (24), 9542-9547.

41. Konkolewicz, D.; Magenau, A. J. D.; Averick, S. E.; Simakova, A.; He, H.; Matyjaszewski, K., ICAR ATRP with ppm Cu Catalyst in Water. *Macromolecules* **2012,** 45, (11), 4461-4468.

42. Konkolewicz, D.; Krys, P.; Góis, J. R.; Mendonça, P. V.; Zhong, M.; Wang, Y.; Gennaro, A.; Isse, A. A.; Fantin, M.; Matyjaszewski, K., Aqueous RDRP in the Presence of Cu0: The Exceptional Activity of CuI Confirms the SARA ATRP Mechanism. *Macromolecules* **2014,** 47, (2), 560–570.

43. Convertine, A. J.; Lokitz, B. S.; Vasileva, Y.; Myrick, L. J.; Scales, C. W.; Lowe, A. B.; McCormick, C. L., Direct Synthesis of Thermally Responsive DMA/NIPAM Diblock and DMA/NIPAM/DMA Triblock Copolymers via Aqueous, Room Temperature RAFT Polymerization. *Macromolecules* **2006,** 39, (5), 1724-1730.

44. Favier, A.; Charreyre, M.-T.; Chaumont, P.; Pichot, C., Study of the RAFT Polymerization of a Water-Soluble Bisubstituted Acrylamide Derivative. 1. Influence of the Dithioester Structure. *Macromolecules* **2002,** 35, (22), 8271-8280.

45. Locock, K. E. S.; Meagher, L.; Haeussler, M., Oligomeric Cationic Polymethacrylates: A Comparison of Methods for Determining Molecular Weight. *Anal. Chem.* **2014,** 86, (4), 2131-2137.

46. Tsarevsky, N. V.; Pintauer, T.; Matyjaszewski, K., Deactivation Efficiency and Degree of Control over Polymerization in ATRP in Protic Solvents. *Macromolecules* **2004,** 37, (26), 9768-9778.

47. Jakubowski, W.; Kirci-Denizli, B.; Gil, R. R.; Matyjaszewski, K., Polystyrene with Improved Chain-End Functionality and Higher Molecular Weight by ARGET ATRP. *Macrom. Chem. Phys.* **2008,** 209, (1), 32-39.

48. Wang, Y.; Soerensen, N.; Zhong, M.; Schroeder, H.; Buback, M.; Matyjaszewski, K., Improving the "Livingness" of ATRP by Reducing Cu Catalyst Concentration. *Macromolecules* **2013,** 46, (3), 683-691.

49. Oh, J. K.; Drumright, R.; Siegwart, D. J.; Matyjaszewski, K., The development of microgels/nanogels for drug delivery applications. *Prog. Polym. Sci.* **2008,** 33, (4), 448-477.

50. Oh, J. K.; Siegwart, D. J.; Matyjaszewski, K., Synthesis and Biodegradation of Nanogels as Delivery Carriers for Carbohydrate Drugs. *Biomacromolecules* **2007,** 8, (11), 3326-3331.

51. Averick, S. E.; Paredes, E.; Irastorza, A.; Shrivats, A. R.; Srinivasan, A.; Siegwart, D. J.; Magenau, A. J.; Cho, H. Y.; Hsu, E.; Averick, A. A.; Kim, J.; Liu, S.; Hollinger, J. O.; Das, S. R.; Matyjaszewski, K., Preparation of Cationic Nanogels for Nucleic Acid Delivery. *Biomacromolecules* **2012,** 13, (11), 3445-3449.

Chapter 7

Efficient RAFT polymerization of *N*-(3-aminopropyl)methacrylamide hydrochloride using unprotected "clickable" chain transfer agents

---

The contents of this chapter are published in: ***Patrícia V. Mendonça****, Arménio C. Serra, Anatoliy V. Popov, Tamaz Guliashvili and Jorge F.J. Coelho, "Efficient RAFT polymerization of N-(3-aminopropyl)methacrylamide hydrochloride using unprotected "clickable" chain transfer agents", Reactive and Functional Polymers, 2014, 81, 1–7.*

7.1. Abstract

Reversible addition-fragmentation chain transfer (RAFT) of *N*-(3-aminopropyl)methacrylamide hydrochloride (APMA) using unprotected "clickable" chain transfer agents in water/dioxane mixtures is reported. The controlled character of the polymerization was confirmed by the linear increase of the polymers molecular weight with monomer conversion, narrow molecular weight distributions ($Đ \leq 1.1$) and chain extension experiments. Alkyne-terminated PAPMA was further functionalized, by "click" chemistry, with an azido-functionalized coumarin derivative. The method reported here can be very useful for the preparation of novel PAPMA-based materials for biomedical applications, using a strategy that does not require troublesome protection/deprotection steps.

7.2. Introduction

Reversible deactivation radical polymerization (RDRP)[1] has been studied for the past two decades, as a powerful tool for the preparation of complex polymer structures with well-defined molecular weight, molecular weight distribution, composition, architecture, topology and chain-end functionality. RAFT[2] is one of the most versatile RDRP techniques, due to its tolerance to different functionalities, range of monomers that can be polymerized and diversity of affordable polymer architectures.[3] Several polymers, such as poly(meth)acrylates,[4, 5] poly(meth)acrylamides[6-9] and polystyrene,[10, 11] have been successfully synthesized by RAFT polymerization and used in innumerous applications. Special attention is given to polymers with functionalized chain-ends, which can be used in further post-modification reactions[12-14] to produce very unique polymer structures.

One of the most popular post-polymerization reactions, involving polymers prepared by RDRP, is the Huisgen 1,3-dipolar cycloaddition between azide and acetylene chain-end functionalities, mostly catalyzed by copper(I) complexes.[15] This type of "click" chemistry reactions became very attractive due to its high yield, mild reaction conditions and absence of by-products.[16] The "click" strategies are particularly useful for the synthesis of well-defined block copolymers.[17] Using this technique, it is possible to combine homopolymers with very distinct natures, derived from monomers with different

reactivity, which eventually could not be copolymerized to afford block copolymers using the conventional polymerization methods. Also, it is possible to maintain the low dispersity (*Đ*) of the block copolymers, as the building blocks can be synthesized separately, by using suitable RDRP techniques, and further coupled by "click" reaction.[18] The combination of RDRP and "click" chemistry has been extensively reported in the literature,[19-23] as it allows the design of high performance materials with very unique structures and properties, which can be applied in relevant areas (e.g., biomedical field).[24-26]

Polymers with pendant primary amino groups, which can be used for post-polymerization modification reactions,[27-29] such as Michael addition reactions, are of prime importance for the development of new materials for biomedical applications. For instance, APMA has been used in the preparation of copolymers and crosslinked micelles for gene delivery[30, 31] and drug delivery.[32-34] The controlled synthesis of this polymer is usually performed by RAFT polymerization mediated by 4-cyano-4-(phenylcarbonothioylthio)pentanoic acid (CTP)[35] or by RAFT copolymerization with other (meth)acrylamide monomers[30-32, 36, 37] or with 2-(diisopropylamino)ethyl methacrylate.[33, 34] Post-polymerization modification of "controlled/living" poly(*N*-(3-aminopropyl)methacrylamide) (PAPMA) typically involves the reaction of the amino groups to either prepare shell crosslinked micelles[34] or to attach some molecules of interest (e.g., D-glucuronic acid sodium salt)[38] for the studied application. To the best of our knowledge, the chain-ends of "controlled/living" PAPMA have never been used in post-polymerization modification reactions.

Here it is reported the successful synthesis of PAPMA by RAFT polymerization mediated by non-protected acetylene or azide functionalized chain transfer agents (CTAs), to allow further modification of the PAPMA chain-ends. An alkyne-terminated PAPMA was coupled with a biocompatible coumarin derivative, via copper (I) catalyzed azide-alkyne cycloaddition, to prove the usefulness of the strategy. The main goal of this work was to develop suitable polymerization conditions and an easy procedure for the preparation of controlled chain-end functionalized PAPMA which can allow further modifications, expanding the range of the applications of this polymer.[39]

7.3. Experimental

7.3.1. Materials

Acetic acid glacial (Fisher Scientific, 99.79%), acetone (Fisher Scientific, HPLC grade), APMA (Polysciences, > 98%), deuterated chloroform ($CDCl_3$, Euriso-top, 99.5% D), 3-chloro-1-propanol (Aldrich, 98%), copper (II) sulfate pentahydrate (≥ 98%, Aldrich), CTP (Sigma Aldrich, > 97%), dichloromethane (DCM, Fisher Scientific, 99.99%), diethyl ether (Fisher Scientific, 99.85%), 4-dimethylaminopyridine (DMAP, Acros Organics, 99%), deuterium oxide (D_2O, Euroiso-top, 99.90% D), 1-ethyl-3-(3-dimethylaminopropyl)carbodiimide (EDC, Sigma Aldrich, ≥ 98.0%), ethanol (EtOH, absolute, Fisher Chemical), ethyl acetate (99.98 %, Fisher Scientific), hexane (Fisher Scientific, 99.05%), propargyl alcohol (PgOH, Aldrich, 99%), silica gel (Panreac, 63-200 μm), sodium ascorbate (crystalline, ≥ 98%, Aldrich) and sodium azide (Panreac, 99%) were used as obtained.

1,4-dioxane (Sigma Aldrich, 99+%) was passed through a basic alumina column before use, in order to remove any peroxides.

4,4′-Azobis(4-cyanovaleric acid) (ACVA) (Aldrich, 75%) was recrystallized from methanol before use.

Deionized water was obtained from a Milli-Q ®, Millipore reverse osmosis unit (resistivity = 18.0 MΩ).

3-azido-7-diethylaminocoumarin was synthesized as reported in the literature.[40]

7.3.2. Techniques

The polymers were analyzed by a size exclusion chromatography (SEC) system equipped with an online degasser, a refractive index (RI) detector and a set of columns: Shodex OHpak SB-G guard column, OHpak SB-804HQ and OHpak SB-804HQ columns. The polymers were eluted at a flow rate of 0.5 mL/min with 0.1 M Na_2SO_4 (aq)/1 wt % acetic acid/0.02 % NaN_3 at 40 °C. Before the injection (50 μL), the samples were filtered

through a polytetrafluoroethylene (PTFE) membrane with 0.45 μm pore. The system was calibrated with five narrow poly(ethylene glycol) (PEG) standards and the polymers molecular weights (M_n^{SEC}) and $Đ$ (M_w/M_n) were determined by conventional calibration using the Clarity software version 2.8.2.648.

400 MHz ^{1}H NMR spectra of reaction mixture samples were recorded on a Bruker Avance III 400 MHz spectrometer, with a 5-mm TIX triple resonance detection probe, in D_2O. Conversion of monomers was determined by integration of monomer and polymer ^{1}H NMR signals using MestRenova software version: 6.0.2-5475.

Fourier transform infrared attenuated total reflection (FTIR-ATR) spectroscopy was performed using a Jasco, model 4000 UK spectrometer. The samples were analyzed with 64 scans and 4 cm^{-1} resolution, between 500 and 3500 cm^{-1}.

7.3.3. Procedures

Synthesis of the alkyne-CTP

The synthesis of the alkyne-terminated chain transfer agent was adapted from a procedure described in the literature.[41] Briefly, a mixture of CTP (700 mg, 2.51 mmol), PgOH (170 mg, 3.01 mmol) and DCM (40 mL) was added to a round bottom flask equipped with a magnetic bar and a rubber stopper. The solution was cooled to 0 °C and purged with argon. A solution of EDC (720 mg, 3.76 mmol) and DMAP (50 mg, 0.38 mmol) in DCM (10 mL) was added to the flask under argon atmosphere. The mixture was allowed to react at 0 °C for 2 h and then at room temperature overnight. The reaction mixture was washed with water (100 mL, 3 times) and dried over anhydrous Na_2SO_4. The DCM was removed under reduced pressure and the crude product was purified by column chromatography (silicagel, CH_2Cl_2 and hexane/ethyl acetate = 4/1 (v/v)). The pure product (0.60 g, 75 %) was analyzed by ^{1}H NMR (400 MHz, $CDCl_3$), δ (TMS, ppm): 1.94 (s, 3H, (CN)C-CH_3); 2.49 (t, 1H, HC≡C); 2.5-2.8 (t(x2), 4H, -CH_2-CH_2); 4.72 (d, 2H, CH_2-O-C); 7.4-7.9 (t (x2), d, 5H, ArH).

Synthesis of the azido-CTP

The synthesis of the azide-terminated chain transfer agent was adapted from a procedure described in the literature.[41] Firstly, 3-chloro-1-propanol (3 g, 31.7 mmol) and NaN_3 (3.5

g, 54.0 mmol) were dissolved in a mixture of acetone (50 mL) and water (5 mL) and refluxed overnight. Acetone was removed under reduced pressure and 35 mL of water were added to the remaining solution. The product was extracted with diethyl ether (3 x 70 mL), the organic layer was dried over anhydrous Na_2SO_4 and the 3-azido-1-propanol was obtained as a colorless oil (1.6 g, 50%) after solvent removal under reduced pressure. The product was analyzed by FTIR: ν_{max}/cm^{-1} 3340, 2949, 2884, 2098, 1449, 1262, 1051, 955, 900. In a second step, a mixture of CTP (700 mg, 2.51 mmol), 3-azido-1-propanol (380 mg, 3.76 mmol) and DCM (40 mL) was added to a round flask equipped with a magnetic bar and a rubber stopper. The solution was cooled to 0 °C and purged with argon. A solution of EDC (720 mg, 3.76 mmol) and DMAP (50 mg, 0.38 mmol) in DCM (10 mL) was added to the flask under argon atmosphere. The mixture was allowed to react at 0 °C for 2 h and then at room temperature overnight. The reaction mixture was washed with water (100 mL, 3 times) and dried over anhydrous Na_2SO_4. The DCM was removed under reduced pressure and the crude product was purified by column chromatography (SiO_2, CH_2Cl_2 and hexane/ethyl acetate = 4/1 (v/v)). The pure product (0.61 g, 67%) was analyzed by ^{1}H NMR (400 MHz, $CDCl_3$), δ (TMS, ppm): 1.94 (s, 3H, -C(CN)CH_3); 2.04-2.18 (m, 2H, -CH_2-CH_2-N_3); 2.30-2.80 (m, 4H, (CN)C-CH_2-CH_2-C(=O)); 3.60 (t, 2H, CH_2-N_3); 4.28 (t, 2H, -CH_2-CH_2- CH_2-N_3); 7.40-7.90 (t (x2), d, 5H, ArH).

Typical procedure for the RAFT polymerization of APMA

APMA (0.5 g, 2.80 mmol) was dissolved in deionized water (1 mL), CTP (7.82 mg, 0.028 mmol) was dissolved in 1,4-dioxane (0.5 mL) and both solutions were inserted in a Schlenk tube reactor. AVCA (1.57 mg, 0.0056 mmol) was weighted and added to the reactor, which was subsequently sealed and frozen in liquid nitrogen. The Schlenk tube reactor containing the reaction mixture was deoxygenated with four freeze-vacuum-thaw cycles and purged with nitrogen. The Schlenk tube reactor was placed in an oil bath at 70 °C with stirring (700 rpm). Different reaction mixture samples were collected during the polymerization by using an airtight syringe and purging the side arm of the Schlenk reactor with nitrogen. The samples were analyzed by ^{1}H NMR spectroscopy in order to determine the monomer conversion and by aqueous SEC, to determine the molecular weights and dispersity of the polymers. The final reaction mixture was dialyzed (cut-off 3500 Da) against deionized water and the polymer was obtained after freeze drying. The

other RAFT polymerizations were conducted under the same procedure described, but using alkyne-CTP or azido-CTP as chain transfer agents.

Typical procedure for the chain extension of PAMA

A sample of alkyne-terminated PAPMA (M_n^{SEC} = 10.4 x 10^3; M_w/M_n = 1.19), obtained after dialysis and freeze drying, was used as a macro-CTA in a new RAFT polymerization. Briefly, the macro-CTA (43.7 mg, 0.0042 mmol) and APMA (300 mg, 1.70 mmol) were dissolved in a mixture of water (1.93 mL) and 1,4-dioxane (0.97 mL) inside a Schlenk tube reactor. Subsequently, AVCA (0.59 mg, 0.0021 mmol) was weighted and added to the reactor, which was immediately frozen in liquid nitrogen. The Schlenk tube reactor containing the reaction mixture was deoxygenated with four freeze-vacuum-thaw cycles, purged with nitrogen and placed in an oil bath at 70 °C with stirring (700 rpm). After 24 h of reaction, a sample was collected and analyzed by SEC in order to see the movement of the SEC trace towards higher molecular weight, in comparison to that of the macro-CTA.

"Click" reaction between alkyne-terminated PAPMA and (3-azido-7-diethylaminocoumarin)

An alkyne-terminated PAPMA sample (M_n^{SEC} = 8.7 x 10^3; $Đ$ = 1.08) was purified through dialysis (cut-off 3500 Da) against deionized water and the polymer was recovered after freeze drying. A solution of (3-azido-7-diethylaminocoumarin) (0.6 mg; 2.2 μmol) and alkyne-terminated PAPMA (15.6 mg; 1.79 μmol) in deionized water (100 μL)/EtOH (300 μL) mixture and a stock solution of $CuSO_4.5H_2O$ (28 mM; 100 μL) in deionized water were placed in a round-bottom flask equipped with a magnetic stirrer bar, which was sealed with a rubber septum. The mixture was bubbled with nitrogen for 20 min to remove oxygen. Finally, a degassed stock solution of sodium ascorbate in water (11 mM; 100 μL) was injected into the flask under nitrogen atmosphere. The reaction was allowed to proceed with stirring (700 rpm) at room temperature for 96 h. The product was purified through dialysis against water, followed by dialysis against ethanol and finally water again (cut-off 3500 Da) and recovered by freeze drying. The functionalized polymer was analyzed by ^{1}H NMR spectroscopy.

7.4. Results and discussion

7.4.1. RAFT homopolymerization of APMA

CTP with a phenyl Z group that strongly stabilizes the intermediate radical has already been used for the successful RAFT polymerization of a wide range of activated monomers, including both acrylamide and methacrylamide monomers.[8, 35, 42] To the best of our knowledge, there are only two reports that show kinetic data regarding the RAFT of APMA using CTP as a chain transfer agent.[35, 36] Other publications report the synthesis of responsive block copolymers including PAPMA segments, mainly with the purpose to be used on the biomedical field.[30-34, 36, 37] In this work, the RAFT system described in the literature for the successful polymerization of PAPMA[35, 36] was used as a starting point for the evaluation of the synthesized "clickable" CTAs chain transfer activity. Alkyne- and azido-CTP derivatives (Figure 7.1) were prepared by esterification with PgOH (with no protection of the alkyne termini) and 3-azido-1-propanol, respectively, following procedures reported elsewhere[41] (see Figure C.1 in Appendix C). The chemical structure and purity of the CTAs were confirmed by ^{1}H NMR spectroscopy (see Figure C.2 in Appendix C) to ensure that all RAFT polymerizations were performed using the same conditions and free of significant impurities, allowing the data comparison. The polymerizations were conducted at 70 °C using a solvent mixture of water/1,4-dioxane = 2/1 (v/v) and ACVA as the initiator, under nitrogen atmosphere. The pH of the reaction mixture was measured before the polymerization to ensure a value between 4 and 5, in order to avoid CTP hydrolysis and/or aminolysis.[43] It is worth to mention that no pH adjustment was necessary in the polymerizations. Monomer conversions were determined by ^{1}H NMR spectroscopy, comparing the integrals of the vinyl protons of the monomer at 5.80-5.35 ppm and the methylene protons of the PAPMA backbone at 1.25-0.70 ppm.

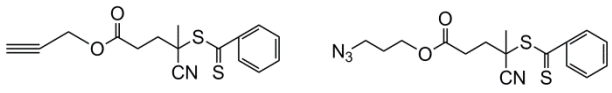

alkyne-CTP **azido-CTP**

Figure 7.1. Chemical structures of both alkyne-CTP and azido-CTP.

Initially, both alkyne-CTP and azido-CTP were tested in the RAFT polymerization of APMA for different targeted degree of polymerization (DP) values, using the same experimental conditions. The kinetic parameters presented in Table 7.1 show that both CTAs were able to mediate a successful RAFT polymerization of APMA for different chain lengths, as judged by the very low *Đ* values. Polymerization control decreased for shorter polymer chains, as expected, but still affording PAPMA with narrow molecular weight distribution (*Đ* ≈1.2).

Table 7.1. Kinetic parameters for the RAFT polymerization of APMA, using azido-CTP or alkyne-CTP, in water/1,4-dioxane = 2/1 (v/v) at 70 °C. Conditions: $[APMA]_0$ = 1.87 M; $[ACVA]_0$ = 0.5 (molar ratio in comparison to the CTA number of moles).

Entry	CTA	Targeted DP	Time (h)	Conv. (%)	M_n^{SEC} x 10^{-3}	*Đ*
≡$PAPMA_{25}$[a]	alkyne-CTP	25	5	82	10.4	1.19
≡$PAPMA_{50}$	alkyne-CTP	50	18	98	29.4	1.08
≡$PAPMA_{100}$	alkyne-CTP	100	4	95	25.1	1.07
N_3PAPMA_{25}	azido-CTP	25	4	94	16.2	1.21
N_3PAPMA_{100}	azido-CTP	100	4	50	19.1	1.11

[a] An ACVA molar ratio of 0.2 was used in this polymerization.

Kinetic studies were conducted in order to evaluate the usefulness of the synthesized CTAs on the control of the PAPMA molecular weight during the polymerization. Under the experimental conditions used in this work, the maximum monomer conversion achieved (red symbols in Figure 7.2) in the RAFT of APMA mediated by CTP was lower than that reported in the literature.[35] Taking this into consideration, the reaction was done three times and the same results were obtained in all cases. Nevertheless, the control over the polymer molecular weight was very good, as the *Đ* was always lower than 1.1, with the exception of the first kinetic point (Figure 7.2 (b)). In addition, the SEC traces (see Figure C.3 in Appendix C) of the different samples were unimodal and symmetric with no tailing, suggesting no termination reactions during the polymerization. In terms of monomer conversion evolution, the results were consistent with the literature, showing first-order kinetics with respect to monomer conversion (Figure 7.2 (a)).

It has been reported that the use of unprotected alkyne-terminated CTAs could interfere with the RAFT polymerization process.[41] The synthesized unprotected alkyne-CTP was

used to mediate the RAFT polymerization of APMA under the same conditions previously described for the CTP.

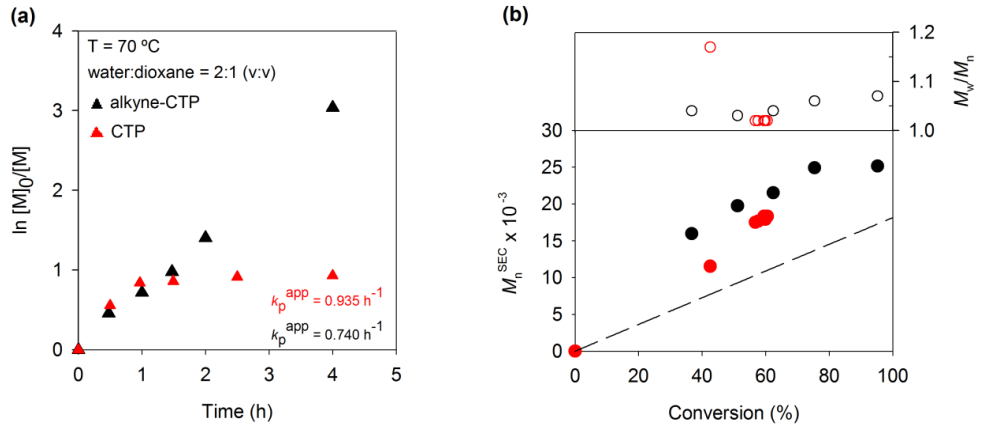

Figure 7.2. (a) Kinetic plots ln[M]$_0$/[M] *vs.* time and (b) plot of number-average molecular weights (M_n^{SEC}) and *Đ* (M_w/M_n) *vs.* monomer conversion (the dashed line represents theoretical molecular weight at a given conversion) for the RAFT of APMA at 70 °C in water/1,4-dioxane = 2/1 (v/v) mixture, using CTP (red symbols) and alkyne-CTP (black symbols) as a CTA. Reaction conditions: [APMA]$_0$/[CTA]$_0$/[ACVA]$_0$ = 100/1/0.5; [APMA]$_0$ = 1.87 M.

The kinetic results presented in Figure 7.2 (black symbols) show that the alkyne-CTP has a higher chain transfer activity than the CTP, as high monomer conversion (≈ 95%) was achieved after 4 h of reaction. This behavior can be attributed to the reported strong dependence between the nature of the CTAs R group and their efficiency, considering that both CTAs have the same Z group.[3] The polymers molecular weight was well controlled throughout the polymerization (*Đ* < 1.1) and the molecular weight distribution was characterized by unimodal SEC traces (see Figure C.4 in Appendix C). Despite the low *Đ* values, the experimental molecular weights of PAPMA determined by SEC were not in close agreement with the corresponding theoretical ones (Figure 7.2 (b)). The observed differences can be explained considering that the molecular weight values were determined by conventional calibration using PEG standards, which have a different hydrodynamic volume than PAPMA. These results are extremely promising, since it was shown that alkyne-terminated PAPMA could be prepared and directly used in further "click" reactions, without the need of protection-deprotection steps.

Alternatively to the use of the alkyne functionality, one can take advantage of azide-terminated polymers for "click" chemistry purposes. An experimental study reported by

Ladmiral and co-workers showed that azido-groups can undergo 1,3-cycloaddition with the double bond of some monomers, in the absence of catalyst, especially for long reaction times and high temperatures.[44] In the case of APMA RAFT polymerization, the results suggested that the occurrence of this type of side reactions can be neglected, as the *Đ* of the polymer decreased with the polymerization time (Figure 7.3 (b)). The low reactivity of acrylamides as well as the presence of the methylene group at the double bond of APMA, which causes steric hindrance, may prevent this type of side reactions.

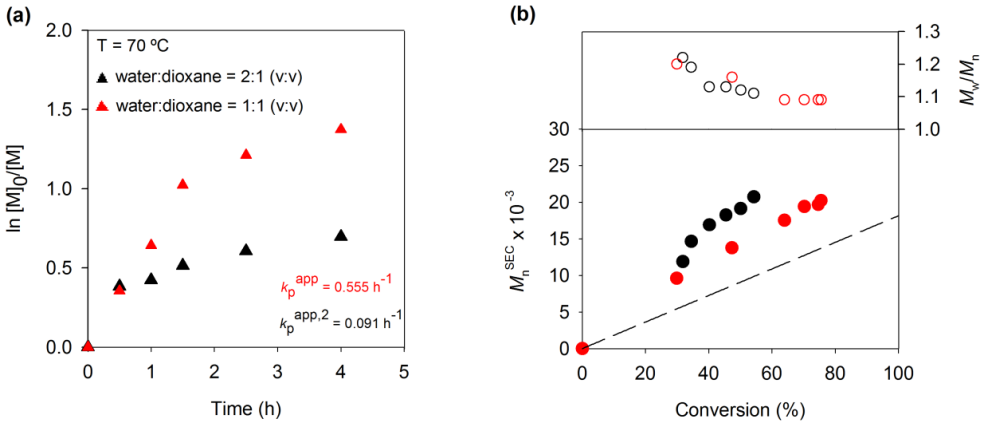

Figure 7.3. (a) Kinetic plots ln[M]$_0$/[M] *vs.* time and (b) plot of number-average molecular weights (M_n^{SEC}) and *Đ* (M_w/M_n) *vs.* monomer conversion (the dashed line represents theoretical molecular weight at a given conversion) for the RAFT of APMA at 70 °C in water/1,4-dioxane = 2/1 (v/v) (black symbols) and water/1,4-dioxane = 1/1 (v/v) (red symbols) mixtures. Reaction conditions: [APMA]$_0$/[azido-CTP]$_0$/[ACVA]$_0$ = 100/1/0.5; [APMA]$_0$ = 1.87 M.

In addition, it was possible to confirm the polymers functionality by identifying the –CH_2 protons near the N_3 group by ^{1}H NMR spectroscopy (Figure 7.5 (b)). Nevertheless, the kinetic results showed that the azido-CTP did not allow the level of control over PAPMA molecular weight as both CTP and alkyne-CTP did, for the same experimental conditions (black symbols in Figure 7.3). The *Đ* of the polymers was slightly higher, mostly due to the presence of tailing in the molecular weights distribution curves (Figure 7.4 (a)). This observation can be due to some radical termination reactions occurred in the beginning of the polymerization. By comparing the area of the low molecular weight shoulder with the total area of the SEC chromatogram, it was possible to estimate that after 30 min of polymerization there were ≈ 27% of dead polymer chains. The poor control exhibited by the azido-CTP could potentially be associated to the low solubility of this compound in the reaction solvent mixture, even at 70 °C. In comparison with both CTP and alkyne-

CTP, the azido-CTP R group has a longer aliphatic chain (Figure 7.1), which decreases its solubility in water. In order to confirm this hypothesis, the effect of the solvent mixture composition on the control of the RAFT polymerization of PAPMA, mediated by the azido-CTP, was also examined.

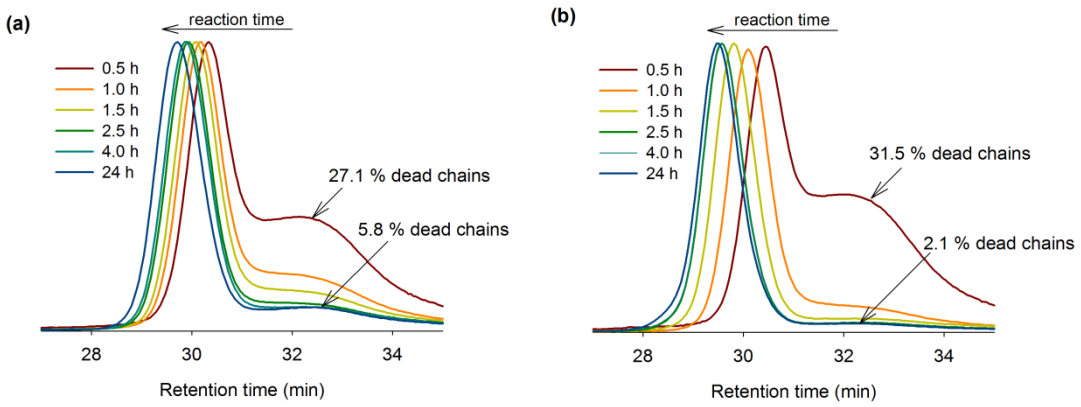

Figure 7.4. SEC chromatograms of PAPMA samples during the RAFT polymerization at 70 °C in (a) water/1,4-dioxane = 2/1 (v/v) mixture and (b) water/1,4-dioxane = 1/1 (v/v) mixture. Conditions: $[APMA]_0/[azido\text{-}CTP]_0/[ACVA]_0 = 100/1/0.5$; $[APMA]_0 = 1.87$ M.

The percentage of dioxane in the solvent mixture was increased up to 50% and the other experimental conditions were conserved. The results showed that significant improvements were achieved in terms of polymerization control, with 64% decrease in the PAPMA dead chains (Figure 7.4 (b)), as well a 39% increase in the maximum monomer conversion achieved (red symbols in Figure 7.3). In addition, better control was obtained as the $Đ$ of PAPMA was lower and the experimental molecular weights were closer to the theoretical ones (dashed line in Figure 7.3 (b)). These results corroborate the idea that the poorer control exhibited by the azido-CTP, in this particular RAFT system, was related with its solubility in the reaction solvent mixture. Some authors suggested that the marked chain transfer activity differences between "clickable" CTAs, derived from the same molecule, could be related to both the leaving ability and the reinitiating ability of each R group.[9] However, this work shows that it is also important to consider other reaction parameters, namely the type of solvent, and make small adjustments in order to improve the CTAs efficacy.

7.4.2. ^{1}H NMR analysis and chain extension reaction

The chemical structure of low molecular weight "clickable" polymers prepared by RAFT polymerization was confirmed by ^{1}H NMR spectroscopy. Figure 7.5 (a) presents the ^{1}H NMR spectrum of a purified alkyne-terminated PAPMA sample. The characteristic signals of the PAPMA structure shown at 3.23 ppm (f) (2H, -CH_2-C**H_2**-NH_2), 3.06 ppm (d) (2H, -NH-C**H_2**-CH_2-), 1.91 ppm (e) (2H, -CH_2-C**H_2**-NH_2), 1.76 ppm (b) (2H, C-CH_3-CN-C**H_2**-C-) and 1.25-0.70 ppm (c) (3H, -CC**H_3**S-), were in agreement with the data reported in the literature.[35, 36] It was also possible to identify the alkyne chain-end (a) (1H, C**H**≡C, 2.63 ppm)[45] from the alkyne-CTP, which confirms the retention of the functionality. The same analysis was done to the N_3-terminated PAPMA (Figure 7.5 (b)), which proved to have the methylene protons (i and g) associated to the azido-CTP R group (4H, N_3-C**H_2**-CH_2-C**H_2**-), while the signal of the methylene protons (h) (2H, N_3-CH_2-C**H_2**-CH_2-) was overlapped with the signals (m) and (j). It was not possible to determine both the percentage of functionality and the average-number molecular weight (M_n^{NMR}) of the PAPMA samples by ^{1}H NMR spectroscopy, since the protons of the aromatic ring (Z group) were partially overlapped with –NH protons of the polymers.

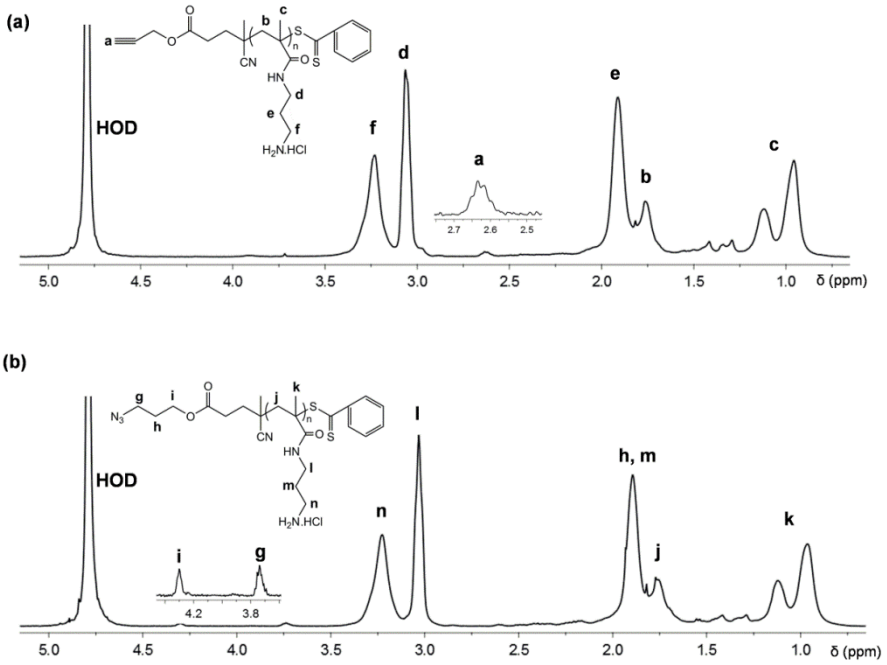

Figure 7.5. 400 MHz ^{1}H NMR spectra, in D_2O, of (a) alkyne-terminated PAPMA (M_n^{th} = 3.7 x 10^3; M_n^{SEC} = 10.4 x 10^3; $Đ$ = 1.19) and (b) azide-terminated PAPMA (M_n^{th} = 4.5 x 10^3; M_n^{SEC} = 16.3 x 10^3; $Đ$ = 1.21) obtained by RAFT polymerization.

One of the most effective ways to demonstrate the "livingness" of the polymers is by performing a chain extension reaction, in which the polymerization is reinitiated from a macro-CTA. A sample of alkyne-terminated PAPMA (M_n^{SEC} = 10.4 x 10^3; $Đ$ = 1.19), prepared by RAFT polymerization, was isolated by extensive dialysis (cut-off 3500 Da) against deionized water (pH ≈ 5). This polymer was then used as a macro-CTA in a self-blocking experiment with a targeted DP of 400. Figure 7.6 shows the clear shift of the molecular weight distribution curve of the macro-PAPMA towards higher molecular weight values, confirming the "living" character of the polymer. It is also important to note that the resultant extended PAPMA presented some low molecular weight tailing as well as higher $Đ$ than the macro-CTA. This result can be due to the occurrence of some radical termination reactions or due to partial macro-CTA hydrolysis during the purification process by dialysis, which may have decreased the macro-CTA efficiency, as reported by other authors for similar polymers.[42] The same experiment was done using an azide-terminated PAPMA sample and the results obtained were similar to those of the alkyne-terminated PAPMA chain extension (see Figure C.5 in Appendix C).

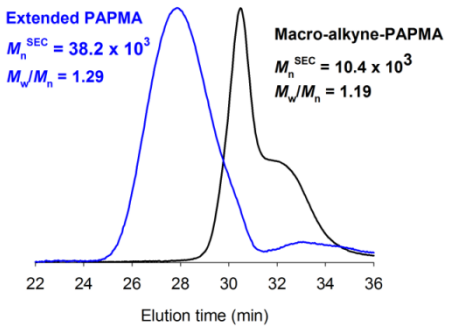

Figure 7.6. SEC traces of the macro-PAPMA (alkyne-terminated) and extended PAPMA obtained in a RAFT polymerization at 70 °C in water/1,4-dioxane = 2/1 (v/v).

7.4.3. Functionalization of alkyne-PAPMA by "click" chemistry

In order to prove the reactivity of the "click" moieties introduced in the PAPMA structure, an alkyne-terminated PAPMA sample was functionalized with a biocompatible azido-terminated coumarin derivative (3-azido-7-diethylaminocoumarin), via copper(I) catalyzed azide-alkyne cycloaddition. The success of the "click" reaction was confirmed by the appearance of the triazole ring proton signal (g) at 8.47 ppm[46] in the ^{1}H NMR spectrum of the functionalized polymer (Figure 7.7). Besides the functionalization

through "click" chemistry, PAPMA structure allows further modification through other strategies involving the reaction of the amino-groups, such as Michael addition reactions,[37] to expand the range of structures/applications of this polymer. Due to the biorelevance of coumarin[47] as well as the possibility of double functionalization of the alkyne-functionalized PAPMA, it is expected that the strategy reported here will allow the preparation of complex polymeric structures useful for biomedical applications.

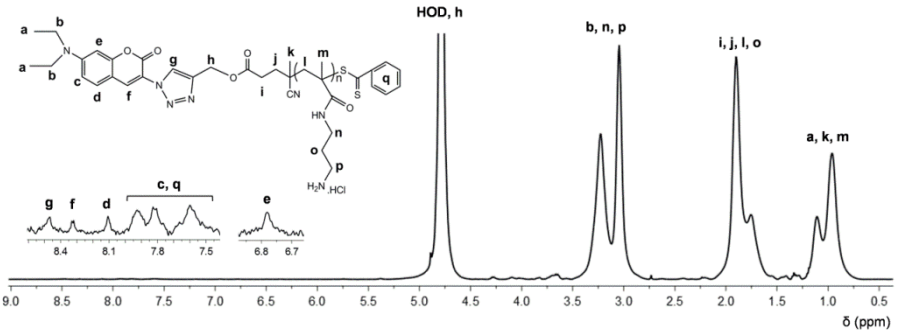

Figure 7.7. 400 MHz ^{1}H NMR spectrum, in D_2O, of purified coumarin-functionalized PAPMA obtained by a "click" reaction.

7.5. Conclusions

The synthesis of "clickable" PAPMA by RAFT polymerization, using azido-CTP or alkyne-CTP as chain transfer agents without any protection/deprotection steps is reported. Both "clickable" CTAs exhibited similar or higher chain transfer activity when compared to the commercial analogue CTP, under the experimental conditions used. The control over the PAPMA molecular weight was very good, as the polymers dispersity was lower than 1.1 during the polymerization. Chain extension experiments demonstrated the "livingness" of the synthesized PAPMA. The retention of the "clickable" chain-end functionality was confirmed by ^{1}H NMR spectroscopy. In addition, the alkyne-terminated PAPMA was functionalized with a biocompatible coumarin molecule by "click" chemistry, resulting in a material that could be applied in the biomedical field.

7.6. References

1. Braunecker, W. A.; Matyjaszewski, K., Controlled/living radical polymerization: Features, developments, and perspectives. *Prog. Polym. Sci.* **2007,** 32, (1), 93-146.

2. Moad, G., The emergence of RAFT polymerization. *Aust. J. Chem.* **2006,** 59, (10), 661-662.

3. Perrier, S.; Takolpuckdee, P., Macromolecular design via reversible addition–fragmentation chain transfer (RAFT)/xanthates (MADIX) polymerization. *J. Polym. Sci., Part A: Polym. Chem.* **2005,** 43, (22), 5347-5393.

4. Zhang, W.; D'Agosto, F.; Dugas, P.-Y.; Rieger, J.; Charleux, B., RAFT-mediated one-pot aqueous emulsion polymerization of methyl methacrylate in presence of poly(methacrylic acid-co-poly(ethylene oxide) methacrylate) trithiocarbonate macromolecular chain transfer agent. *Polymer* **2013,** 54, (8), 2011-2019.

5. Lin, C.; Zhan, H.; Liu, M.; Habibi, Y.; Fu, S.; Lucia, L. A., RAFT synthesis of cellulose-g-polymethylmethacrylate copolymer in an ionic liquid. *J. Appl. Polym. Sci.* **2013,** 127, (6), 4840-4849.

6. Thomas, D. B.; Sumerlin, B. S.; Lowe, A. B.; McCormick, C. L., Conditions for Facile, Controlled RAFT Polymerization of Acrylamide in Water†. *Macromolecules* **2003,** 36, (5), 1436-1439.

7. Convertine, A. J.; Ayres, N.; Scales, C. W.; Lowe, A. B.; McCormick, C. L., Facile, controlled, room-temperature RAFT polymerization of N-isopropylacrylamide. *Biomacromolecules* **2004,** 5, (4), 1177-1180.

8. Thomas, D. B.; Convertine, A. J.; Myrick, L. J.; Scales, C. W.; Smith, A. E.; Lowe, A. B.; Vasilieva, Y. A.; Ayres, N.; McCormick, C. L., Kinetics and molecular weight control of the polymerization of acrylamide via RAFT. *Macromolecules* **2004,** 37, (24), 8941-8950.

9. Liu, X.; Feng, X.; Chen, J.; Cao, Y., Synthesis of Block Copolymers Based on N-alkyl Substituted Acrylamide via Combination of Reversible Addition-Fragmentation

Transfer Polymerization and Click Chemistry. *J. Macrom. Sci. Part A:Pure and Appl. Chem.* **2012,** 50, (1), 65-71.

10. Huo, F.; Wang, X.; Zhang, Y.; Zhang, X.; Xu, J.; Zhang, W., RAFT Dispersion Polymerization of Styrene in Water/Alcohol: The Solvent Effect on Polymer Particle Growth during Polymer Chain Propagation. *Macromolecular Chemistry and Physics* **2013,** 214, (8), 902-911.

11. Xu, S.; Huang, J.; Xu, S.; Luo, Y., RAFT ab initio emulsion copolymerization of gamma-methyl-alpha-methylene-gamma-butyrolactone and styrene. *Polymer* **2013,** 54, (7), 1779-1785.

12. Moad, G.; Chong, Y. K.; Postma, A.; Rizzardo, E.; Thang, S. H., Advances in RAFT polymerization: the synthesis of polymers with defined end-groups. *Polymer* **2005,** 46, (19), 8458-8468.

13. Harvison, M. A.; Roth, P. J.; Davis, T. P.; Lowe, A. B., End Group Reactions of RAFT-Prepared (Co)Polymers. *Aust. J. Chem.* **2011,** 64, (8), 992-1006.

14. Roth, P. J.; Boyer, C.; Lowe, A. B.; Davis, T. P., RAFT Polymerization and Thiol Chemistry: A Complementary Pairing for Implementing Modern Macromolecular Design. *Macromol. Rapid Commun.* **2011,** 32, (15), 1123-1143.

15. Kolb, H. C.; Finn, M. G.; Sharpless, K. B., Click Chemistry: Diverse Chemical Function from a Few Good Reactions. *Angew. Chem. Int. Ed.* **2001,** 40, (11), 2004-2021.

16. Moses, J. E.; Moorhouse, A. D., The growing applications of click chemistry. *Chem. Soc. Rev.* **2007,** 36, (8), 1249-1262.

17. Gregory, A.; Stenzel, M. H., Complex polymer architectures via RAFT polymerization: From fundamental process to extending the scope using click chemistry and nature's building blocks. *Prog. Polym. Sci.* **2012,** 37, (1), 38-105.

18. Hasneen, A.; Han, H. S.; Paik, H.-J., Synthesis of linear tetrablock quaterpolymers via atom transfer radical polymerization and a click coupling approach. *React. Funct. Polym.* **2009,** 69, (9), 681-687.

19. Fournier, D.; Hoogenboom, R.; Schubert, U. S., Clicking polymers: a straightforward approach to novel macromolecular architectures. *Chem. Soc. Rev.* **2007,** 36, (8), 1369-1380.

20. Whittaker, M. R.; Urbani, C. N.; Monteiro, M. J., Synthesis of 3-miktoarm stars and 1st generation mikto dendritic copolymers by "living" radical polymerization and "click" chemistry. *J. Am. Chem. Soc.* **2006,** 128, (35), 11360-11361.

21. Ladmiral, V.; Mantovani, G.; Clarkson, G. J.; Cauet, S.; Irwin, J. L.; Haddleton, D. M., Synthesis of neoglycopolymers by a combination of "click chemistry" and living radical polymerization. *J. Am. Chem. Soc.* **2006,** 128, (14), 4823-4830.

22. Opsteen, J. A.; van Hest, J. C. M., Modular synthesis of block copolymers via cycloaddition of terminal azide and alkyne functionalized polymers. *Chem. Commun.* **2005**, (1), 57-59.

23. Golas, P. L.; Matyjaszewski, K., Marrying click chemistry with polymerization: expanding the scope of polymeric materials. *Chem. Soc. Rev.* **2010,** 39, (4), 1338-1354.

24. Yuan, W.; Zhang, J.; Zou, H.; Ren, J., Synthesis, Crystalline Morphologies, Self-Assembly, and Properties of H-Shaped Amphiphilic Dually Responsive Terpolymers. *J. Polym. Sci., Part A: Polym. Chem.* **2012,** 50, (13), 2541-2552.

25. Semsarilar, M.; Ladmiral, V.; Perrier, S., Highly Branched and Hyperbranched Glycopolymers via Reversible Addition-Fragmentation Chain Transfer Polymerization and Click Chemistry. *Macromolecules* **2010,** 43, (3), 1438-1443.

26. Yang, J.; Luo, K.; Pan, H.; Kopečková, P.; Kopeček, J., Synthesis of biodegradable multiblock copolymers by click coupling of RAFT-generated heterotelechelic polyHPMA conjugates. *React. Funct. Polym.* **2011,** 71, (3), 294-302.

27. Topham, P. D.; Sandon, N.; Read, E. S.; Madsen, J.; Ryan, A. J.; Armes, S. P., Facile Synthesis of Well-Defined Hydrophilic Methacrylic Macromonomers Using ATRP and Click Chemistry. *Macromolecules* **2008,** 41, (24), 9542-9547.

28. Li, Y. T.; Armes, S. P., Synthesis of Model Primary Amine-Based Branched Copolymers by Pseudo-Living Radical Copolymerization and Post-polymerization Coupling of Homopolymers. *Macromolecules* **2009,** 42, (4), 939-945.

29. Read, E. S.; Thompson, K. L.; Armes, S. P., Synthesis of well-defined primary amine-based homopolymers and block copolymers and their Michael addition reactions with acrylates and acrylamides. *Polym. Chem.* **2010,** 1, (2), 221-230.

30. York, A. W.; Huang, F.; McCormick, C. L., Rational Design of Targeted Cancer Therapeutics through the Multiconjugation of Folate and Cleavable siRNA to RAFT-Synthesized (HPMA-s-APMA) Copolymers. *Biomacromolecules* **2010,** 11, (2), 505-514.

31. York, A. W.; Zhang, Y.; Holley, A. C.; Guo, Y.; Huang, F.; McCormick, C. L., Facile Synthesis of Multivalent Folate-Block Copolymer Conjugates via Aqueous RAFT Polymerization: Targeted Delivery of siRNA and Subsequent Gene Suppression†. *Biomacromolecules* **2009,** 10, (4), 936-943.

32. Xu, X.; Flores, J. D.; McCormick, C. L., Reversible Imine Shell Cross-Linked Micelles from Aqueous RAFT-Synthesized Thermoresponsive Triblock Copolymers as Potential Nanocarriers for "pH-Triggered" Drug Release. *Macromolecules* **2011,** 44, (6), 1327-1334.

33. Xu, X.; Smith, A. E.; Kirkland, S. E.; McCormick, C. L., Aqueous RAFT Synthesis of pH-Responsive Triblock Copolymer mPEO-PAPMA-PDPAEMA and Formation of Shell Cross-Linked Micelles. *Macromolecules* **2008,** 41, (22), 8429-8435.

34. Xu, X.; Smith, A. E.; McCormick, C. L., Facile 'One-Pot' Preparation of Reversible, Disulfide-Containing Shell Cross-Linked Micelles from a RAFT-Synthesized, pH-Responsive Triblock Copolymer in Water at Room Temperature. *Aust. J. Chem.* **2009,** 62, (11), 1520-1527.

35. Deng, Z.; Bouchékif, H.; Babooram, K.; Housni, A.; Choytun, N.; Narain, R., Facile synthesis of controlled-structure primary amine-based methacrylamide polymers via the reversible addition-fragmentation chain transfer process. *J. Polym. Sci., Part A: Polym. Chem.* **2008,** 46, (15), 4984-4996.

36. Li, Y.; Lokitz, B. S.; McCormick, C. L., Thermally Responsive Vesicles and Their Structural "Locking" through Polyelectrolyte Complex Formation. *Angew. Chem.* **2006,** 118, (35), 5924-5927.

37. Gao, G.; Yu, K.; Kindrachuk, J.; Brooks, D. E.; Hancock, R. E. W.; Kizhakkedathu, J. N., Antibacterial Surfaces Based on Polymer Brushes: Investigation on the Influence of Brush Properties on Antimicrobial Peptide Immobilization and Antimicrobial Activity. *Biomacromolecules* **2011,** 12, (10), 3715-3727.

38. Alidedeoglu, A. H.; York, A. W.; Rosado, D. A.; McCormick, C. L.; Morgan, S. E., Bioconjugation of D-glucuronic acid sodium salt to well-defined primary amine-containing homopolymers and block copolymers. *J. Polym. Sci., Part A: Polym. Chem.* **2010,** 48, (14), 3052-3061.

39. Adzima, B. J.; Bowman, C. N., The emerging role of click reactions in chemical and biological engineering. *AlChE J.* **2012,** 58, (10), 2952-2965.

40. Sivakumar, K.; Xie, F.; Cash, B. M.; Long, S.; Barnhill, H. N.; Wang, Q., A Fluorogenic 1,3-Dipolar Cycloaddition Reaction of 3-Azidocoumarins and Acetylenes. *Org. Lett.* **2004,** 6, (24), 4603-4606.

41. Quemener, D.; Davis, T. P.; Barner-Kowollik, C.; Stenzel, M. H., RAFT and click chemistry: A versatile approach to well-defined block copolymers. *Chem. Commun.* **2006,** 0, (48), 5051-5053.

42. Vasilieva, Y. A.; Scales, C. W.; Thomas, D. B.; Ezell, R. G.; Lowe, A. B.; Ayres, N.; McCormick, C. L., Controlled/living polymerization of methacrylamide in aqueous media via the RAFT process. *J. Polym. Sci., Part A: Polym. Chem.* **2005,** 43, (14), 3141-3152.

43. Thomas, D. B.; Convertine, A. J.; Hester, R. D.; Lowe, A. B.; McCormick, C. L., Hydrolytic Susceptibility of Dithioester Chain Transfer Agents and Implications in Aqueous RAFT Polymerizations. *Macromolecules* **2004,** 37, (5), 1735-1741.

44. Ladmiral, V.; Legge, T. M.; Zhao, Y.; Perrier, S. b., "Click" Chemistry and Radical Polymerization: Potential Loss of Orthogonality. *Macromolecules* **2008,** 41, (18), 6728-6732.

45. Patel, V. K.; Vishwakarma, N. K.; Mishra, A. K.; Biswas, C. S.; Maiti, P.; Ray, B., Synthesis of alkyne-terminated xanthate RAFT agents and their uses for the controlled radical polymerization of *N*-vinylpyrrolidone and the synthesis of its block copolymer using click chemistry. *J. Appl. Polym. Sci.* **2013,** 127, (6), 4305-4317.

46. Lu, J.; Zhang, W.; Richards, S.-J.; Gibson, M. I.; Chen, G., Glycopolymer-coated gold nanorods synthesised by a one pot copper(0) catalyzed tandem RAFT/click reaction. *Polym. Chem.* **2014,** 5, (7), 2326-2332.

47. Trenor, S. R.; Shultz, A. R.; Love, B. J.; Long, T. E., Coumarins in Polymers: From Light Harvesting to Photo-Cross-Linkable Tissue Scaffolds. *Chem. Rev.* **2004,** 104, (6), 3059-3078.

Chapter 8

Synthesis of new bile acid sequestrants by supplemental activator and reducing agent atom transfer radical polymerization

8.1. Abstract

This work reports the synthesis of a new generation of tailor-made polymeric bile acid sequestrants (BAS) by supplemental activator and reducing agent atom transfer radical polymerization (SARA ATRP) using ecofriendly conditions. The new materials were based on amphiphilic poly(methyl acrylate)-*b*-poly((3-acrylamidopropyl)trimethylammonium chloride) (PMA-*b*-PAMPTMA) star block copolymers and PAMPTMA-based cationic hydrogels. The *in vitro* bile acids sequestration ability of the polymers was investigated in simulated intestinal fluid (SIF) using sodium cholate (NaCA) as the bile salt model molecule. Both polymeric structures investigated showed to have higher affinity towards NaCA micelles than unimers. The cationic hydrogels proved to be attractive BAS candidates, with binding parameters similar to those of the commercial BAS Colesevelam hydrochloride. Several polymer features, such as the length of the cationic arms, were investigated for the amphiphilic star block copolymers in order to understand the structure/performance relationship. It was found that the binding parameters can be tuned by targeting different compositions of the block copolymers and, typically, longer cationic arms led to enhanced binding capacity. Finally, both PMA and PAMPTMA polymeric segments showed no sign of degradation in solutions mimicking the gastrointestinal (GI) tract conditions.

8.2. Introduction

Polymeric BAS are polymers used as therapeutic agents for the treatment of hypercholesteremia.[1] These polymers can selectively bind and remove bile salts from the enterohepatic circulation, which will ultimately lead to the reduction of the plasma cholesterol level.[2] Unlike statins, which act directly on the cholesterol synthesis by inhibiting the HMG-CoA reductase, the BAS mechanism of action is restricted to the GI tract.[3, 4] Therefore, there are several advantages associated with the use of BAS over statins, such as the absence of complications in the liver by long-term administration and the fact that BAS can be safer for pregnant women or patients with hepatic dysfunction.[5] Currently, there are a few BAS available on the market, being Colesevelam hydrochloride (Welchol® or Cholestagel®) the most recent and effective one.[6] However, the therapeutic

efficacy of BAS is still rather low in comparison to statins. This output is mainly due to the low selectivity of BAS for trihydroxylic bile acids, as well as the fast dissociation of the BAS-bile acid complex in the presence of the active bile acids reuptake transporter system of the GI tract.[3] Therefore, high doses of BAS (16-24 g/day) are usually required to produce desirable therapeutic effects, which most of the times results in poor patient compliance.

There are several reports in the literature dedicated to the preparation of BAS.[7-13] Cationic hydrogels based on (meth)acrylates, vinyl polymers, allyl polymers, poly(meth)acrylamides and polyethers are the most common used polymeric structures. Also, polymers based on polystyrene backbones (as a hydrophobic segment), containing amine/ammonium pendant groups (as a cationic, hydrophilic segment) have been employed.[2, 3, 14] It is known that the binding process is mainly ruled by both electrostatic and hydrophobic interactions.[15] Therefore, an appropriate balance between the charged groups and the hydrophobic segments of the polymer is required in order to achieve high maximum binding capacity. In addition, the degree of crosslinking of the hydrogel (swelling characteristics) should be adjusted to allow the diffusion of bile acids through the polymer network. Despite the findings on the importance of controlling the BAS structure, these materials have been prepared mainly by conventional polymerization techniques, which hamper any fine control over the polymeric structures. To the best of our knowledge, there is only one work[11, 16] which describes the controlled synthesis of polystyrene-*b*-poly(*N*,*N*,*N*-trimethylammoniumethylene acrylamide chloride) block copolymers by anionic polymerization, as new BAS candidates. However, the reaction conditions employed were very strict (e.g., T = -78 °C) and it was necessary to perform post-polymerization reactions to obtain the cationic segment. Reversible deactivation radical polymerization (RDRP) techniques could be a very useful tool for the design of tailor-made BAS. By this mean, it could be also possible to deepen the understanding of the polymer structure-performance relationship.

The aim of this work was to prepare alternative structures to the commercial hydrogels, namely amphiphilic star block copolymers, using an ecofriendly SARA ATRP system. To the best of our knowledge, this is the first time that such polymer structures are studied as potential BAS. Controlled PAMPTMA-based cationic hydrogels were also synthesized by

SARA ATRP to assess the influence of the architecture on the performance of the materials. The binding capacity of the synthesized polymers was evaluated by *in vitro* equilibrium binding experiments with NaCA.

8.3. Experimental

8.3.1. Materials

Acetonitrile (high-performance liquid chromatography (HPLC) grade, Fisher Chemical), ((3-acrylamidopropyl)trimethylammonium chloride) (AMPTMA, solution 75 wt. % in H_2O, Aldrich), alumina (basic, Fisher Scientific), 1,4 butanediol diacrylate (BDDA, 99+%, Alfa Aesar), $CuBr_2$ (Acros, 99+% extra pure, anhydrous), $CuCl_2$ (99% Sigma Aldrich), NaCA (99% Acros Organics), deuterated chloroform ($CDCl_3$, 99.8% Cambridge Isotope Laboratories), deuterated ethanol (Ethanol-d_6, +99.90%, Cambridge Isotope Laboratories), deuterium oxide (99.9%, Cambridge Isotope Laboratories), dimethylformamide (DMF, Sigma-Aldrich, +99.8%), potassium dihydrogen phosphate (Merck), ethanol (99.5%, Panreac), ethyl 2-chloropropionate (ECP, 97%, Aldrich), hydrochloric acid (37%, Fisher Scientific), pancreatin from porcine pancreas (Sigma), pepsin (Sigma Aldrich), phosphoric acid (85 % Fisher Scientific), Potassium hydrogen phosphate (Merck), sodium chloride (99.5%, Acros Organics), tetrabutylammonium hydroxide 30-hydrate (≥ 99.0%, Sigma-Aldrich) and tetra(ethylene glycol) diacrylate (TEGDA, Sigma Aldrich) were used as received.

Colesevelam hydrochloride was kindly supplied by Bluepharma and it was used as received.

Dipentaerythritol hexakis(2-bromoisobutyrate) (6f-BiB),[17] pentaerythritol tetrakis(2-bromoisobutyrate) (4f-BiB)[17] and tris[2-(dimethylamino)ethyl]amine (Me_6TREN)[18] were synthesized according the procedures described in the literature.

Metallic copper (Cu(0), d = 1 mm, Sigma Aldrich) was washed with HCl in methanol and subsequently rinsed with methanol and dried under a stream of nitrogen following the literature procedure.[19]

Methyl acrylate (MA) (Acros, 99% stabilized), was passed through a sand/alumina column before use in order to remove the radical inhibitor.

Purified water (Milli-Q®, Millipore, resistivity >18 MΩ.cm) was obtained by reverse osmosis.

Simulated gastric fluid (SGF) was prepared by dissolving sodium chloride (100 mg) and pepsin (160 mg) in hydrochloric acid (350 µL) and the volume was adjusted to 50 mL with water to give a solution with pH = 1.2.

SIF was prepared by dissolving potassium hydrogen phosphate (203 mg), potassium dihydrogen phosphate (182 mg) and pancreatin (500 mg) in water (40 mL). The pH was adjusted with 0.2 N NaOH or 0.2 N HCl to 6.8 and the volume was completed to 50 mL with water.

8.3.2. Techniques

PAMPTMA samples were analyzed by a size exclusion chromatography (SEC) system equipped with an online degasser, a refractive index (RI) detector and a set of columns: Shodex OHpak SB-G guard column, OHpak SB-804HQ and OHpak SB-804HQ columns. The polymers were eluted at a flow rate of 0.5 mL/min with 0.1 M Na_2SO_4 (aq)/1 wt% acetic acid/0.02% NaN_3 at 40 °C. Before the injection (50 µL), the samples were filtered through a polytetrafluoroethylene (PTFE) membrane with 0.45 µm pore. The system was calibrated with five narrow poly(ethylene glycol) standards and the polymers molecular weights (M_n^{SEC}) and $Đ$ (M_w/M_n) were determined by conventional calibration using the Clarity software version 2.8.2.648.

PMA samples were analyzed by a high performance size exclusion chromatography HPSEC; Viscotek (Viscotek TDAmax) with a differential viscometer (DV), right-angle laser-light scattering (RALLS, Viscotek), low-angle laser-light scattering (LALLS, Viscotek) and RI detectors. The column set consisted of a PL 10 mm guard column (50 × 7.5 mm^2) followed by one Viscotek T200 column (6 µm), one MIXED-E PLgel column (3 µm) and one MIXED-C PLgel column (5 µm). HPLC dual piston pump was set with a flow rate of 1 mL/min. The eluent (THF) was previously filtered through a 0.2 µm filter.

The system was also equipped with an on-line degasser. The tests were done at 30 °C using an Elder CH-150 heater. Before the injection (100 µL), the samples were filtered through a PTFE membrane with 0.2 µm pore. The system was calibrated with narrow polystyrene standards. The dn/dc was determined as 0.063 for PMA. Molecular weight (M_n^{SEC}) and $Đ$ of the synthesized polymers were determined by Multidetectors calibration using OmniSEC software version: 4.6.1.354.

400 MHz ^{1}H NMR spectra of reaction mixture samples were recorded on a Bruker Avance III 400 MHz spectrometer, with a 5-mm TIX triple resonance detection probe, in D_2O or $CDCl_3$. Conversion of monomers was determined by integration of monomer and polymer NMR signals using MestRenova software version: 6.0.2-5475.

Fourier transform infrared attenuated total reflection (FTIR-ATR) spectroscopy was performed using a Jasco, model 4000 UK spectrometer. The samples were analyzed with 64 scans and 4 cm^{-1} resolution, between 500 and 3500 cm^{-1}.

The concentration of free NaCA remaining after the equilibrium binding experiments was determined by HPLC. The analyses were conducted at 25 °C using an Agilent Zorbax ODS, 5µm, 4.6 x 250 mm column, under isocratic elution. The mobile phase used was 20 mM tetrabutylammonium hydroxide 30-hydrate (pH adjusted to 7.5 with phosphoric acid)/acetonitrile = 55/45 (v/v), with a flow rate of 0.7 mL/min. The NaCA was detected by ultraviolet light at 210 nm. A NaCA standard calibration curve ($R^2 > 0.99$) was constructed for the quantification of the NaCA present in the injected sample. For the quantification of low concentrations (0.1–3 mM), a 200 µL injection loop was used. For concentrations above 3 mM, a 20 µL injection loop was used. To check the system stability, one NaCA standard solution was injected after every 10 sample injections.

Isothermal titration calorimetry (ITC) analyses were performed on a VP-ITC instrument from MicroCal (Northampton, MA) with a reaction cell volume of 1410.9 µL, containing an amphiphilic star block copolymer solution, at 37 °C. A 5 mM solution of NaCA was injected at a speed of 0.5 $\mu L.s^{-1}$, stirring speed was 459 rpm, and the reference power was 10 $\mu cal.s^{-1}$. As recommended by the manufacturer, a first injection of 4 µL was performed before the experiment was considered to start, to account for diffusion from/into the syringe during the equilibration period. The titration proceeded with

additions of 10 μL per injection. All solutions were previously degassed for 15 min under reduced pressure.

The content of nitrogen in the amphiphilic star block copolymers was determined by elemental analysis using a Fisons - EA-1108 CHNS-O Element Analyzer.

8.4. Procedures

Typical procedure for the preparation of amphiphilic star block copolymers by SARA ATRP

A series of amphiphilic star block copolymers were synthesized by SARA ATRP, varying the number of arms of the star and the degree of polymerization (DP) of both MA and AMPTMA monomers. Generally, the SARA ATRP followed this procedure: a solution of $CuBr_2$ (1.2 mg, 5.5 μmol) and Me_6TREN (6.4 mg, 27.6 μmol) in water (0.2 mL) and a solution of 4f-BiB (40.4 mg, 55.2 μmol) in ethanol (0.8 mL) and MA (2.0 mL, 22.1 mmol), were added to a 10 mL Schlenk tube equipped with a magnetic stirrer bar. Next, Cu(0) wire (l = 5 cm; d = 1 mm) was added to the Schlenk tube, which was sealed with a glass stopper, deoxygenated with three freeze-vacuum-thaw cycles and purged with nitrogen. The reaction was allowed to proceed with stirring (700 rpm) at 30 °C. When MA reached high conversion, one sample was collected and analyzed by ^{1}H NMR spectroscopy in order to determine the monomer conversion, and by SEC to determine the M_n^{SEC} and $Đ$ of the polymer. Then, the reaction mixture (Br–PMA macroinitiator) was transferred to a 25 mL Schlenk flask containing a degassed mixture of AMPTMA (3.8 mL, 13.8 mmol), $CuBr_2$ (12.3 mg, 55.2 μmol), Me_6TREN (7.6 mg, 33.1 μmol), Cu(0) wire (l = 10 cm; d = 1 mm), water (0.1 mL) and ethanol (5.2 mL), under nitrogen. The second monomer (AMPTMA) was allowed to react at 30 °C for 20 h. The product solution was purified through dialysis (cut-off 3500 Da) against ethanol and then water and the amphiphilic star block copolymer was recovered after freeze drying. The polymer was analyzed by elemental analysis in order to estimate the DP of the AMPTMA.

Typical procedure for the preparation of hydrogels by SARA ATRP

Several PAMPTMA-based hydrogels were synthesized by SARA ATRP, using two different crosslinkers (BDDA and TEGDA). Generally, the SARA ATRP followed this procedure: a solution of $CuCl_2$ (5.4 mg, 40.0 μmol) and Me_6TREN (21.5 mg, 80.6 μmol) in water (760 μL) and a solution of ECP (11.3 mg, 80.6 μmol) in ethanol (1.26 mL), AMPTMA (2.0 mL, 8.05 mmol) and TEGDA (244 mg, 0.8 mmol), were added to a 10 mL Schlenk tube equipped with a magnetic stirrer bar. DMF (30 μL) was added to the mixture to serve as the internal standard for the determination of the monomers conversion by ^{1}H NMR spectroscopy. Next, Cu(0) wire (l = 5 cm; d = 1 mm) was added to the Schlenk tube, which was sealed with a glass stopper, deoxygenated with three freeze-vacuum-thaw cycles and purged with nitrogen. The reaction was allowed to proceed with stirring at room temperature during 24 h. Finally, the reaction mixture was washed several times with ethanol and water and the hydrogel was recovered by freeze drying.

Swelling tests

The hydrogel samples were soaked in SIF (without pancreatin) for 24 h at 37 °C (100 rpm), and then centrifuged sufficiently to pellet the swollen polymer. The supernatant was discarded and the remaining water was gently removed using filter paper. The swelling capacity of the hydrogels was determined from Equation 8.1:

$$\text{Swelling capacity}(\%) = \frac{w_s - w_d}{w_d} \times 100 \qquad \textbf{(Equation 8.1)}$$

In the Equation 8.1, w_s is the weight of the swollen sample after immersion and w_d is the weight of the dry sample before immersion. The samples were analyzed in duplicate.

***In vitro* degradation studies**

The degradation of linear PAMPTMA and star-shaped PMA was evaluated in both SGF and SIF solutions. Briefly, 30 mg of purified polymer was immersed in 3 mL of each solution in 10 mL screw-cap glass tubes. The samples were incubated at 37 °C under continuous shaking at 100 rpm. After a predetermined incubation time (2 h for SGF and 3

h for SIF), the samples were analyzed by SEC and NMR to evaluate the extent of degradation. The experiments were done in triplicate.

Cholic acid sodium salt equilibrium binding experiments

The equilibrium binding studies were performed by varying the initial concentration of NaCA ($[NaCA]_0$) in the SIF (without pancreatin). For each polymer, eight incubation flasks containing a 10 mg sample were set up. Next, 2 mL of SIF were added to the flasks and the polymers were allowed to soak at room temperature overnight. In the following day, predetermined volumes of SIF and 40 mM stock solution of NaCA were added to the flasks to make the final volume of the solvent mixture 10 mL with target concentrations of 0.1, 0.3, 1, 3, 7, 10, 20 and 30 mM. A blank incubation tube containing just 10 mL of SIF (control) was also prepared for each polymer. The nine flasks were incubated at 37 °C (100 rpm) for 24 h and then filtered. The hydrogel samples were filtered with polyvinylidene fluoride (PVDF) syringe filters (0.45 μm), while the amphiphilic star block copolymers were filtered using Macrosep® Advance Centrifugal Devices With Supor® Membrane 10 kDa (Pall Corporation). The first 5 mL of filtrate were discarded and then an aliquot of 2.5 mL was collected for further analysis. The filtrates were analyzed by HPLC in order to determine the free concentration of NaCA. The amount of NaCA bonded to the polymers was calculated from the difference between the initial amount of NaCA introduced in the binding assays and the amount of free NaCA in the filtrates. The Hill equation (Equation 8.2) was used to fit the experimental data and to deterrmine the binding parameters for each polymer, using the SigmaPlot software.

$$q_e = \frac{q_{max} \times K^n \times C_e^n}{1 + K^n \times C_e^n} \qquad \textbf{(Equation 8.2)}$$

In the Equation 8.2, q_e is the ammount of NaCA bonded to the polymer in mg/g polymer, q_{max} is the apparent maximum amount of NaCA binded to the polymer (binding capacity) in mg/g polymer, K is the intrinsic binding constant (relative to the strength of binding) in $L \cdot mg^{-1}$, C_e is the free NaCA concentration in mg/L and n is the cooperative parameter (measure of the cooperativity of binding). For n = 1, the Equation 8.2 corresponds to the Langmuir isotherm (noncooperative binding).

8.5. Results and discussion

8.5.1. Polymer synthesis and characterization

The potential of the SARA ATRP method to produce unique and controlled polymeric structures was explored for the preparation of novel BAS candidates based on star-shaped amphiphilic block copolymers. These copolymers were designed to contain a PMA hydrophobic core, which could avoid the dissolution of the polymer in aqueous environment, and cationic PAMPTMA hydrophilic arms, that could be able to bind bile salts (Figure 8.1). In this case, the binding of bile acids through electrostatic interactions should not be affected by the changes in the pH value along the intestine environment, due to the presence of permanent positive charges in the polymeric hydrophilic segment. It is also expected that the star-shaped architecture could provide high surface area that could favor the binding process. In addition, it is known that star-shaped amphiphilic polymers can form very stable nanoassemblies in solution in a vast range of concentrations, in opposition to micelles formed by the self-assembly of linear amphiphilic block copolymers.[20]

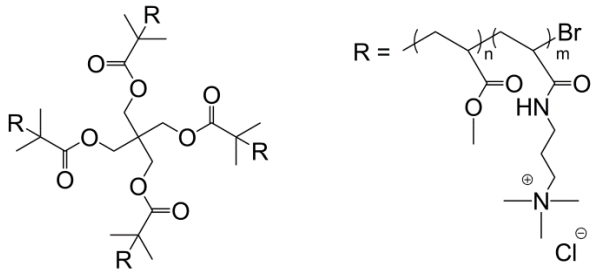

Figure 8.1. Generic structure of the amphiphilic star block copolymers (PMA-*b*-PAMPMTA) prepared by SARA ATRP.

Star-shaped polymeric architectures with controlled structure can only be prepared by advanced polymerization techniques, such as ATRP. Previous publications by our research group[21, 22] reported the development of ecofriendly SARA ATRP systems for the synthesis of both PMA and PAMPTMA in ethanol/water mixtures near room temperature. In this work, the SARA ATRP method developed was extended to the preparation of the new star-shaped PMA-*b*-PAMPTMA block copolymers by "one-pot" polymerization in ethanol/water = 80/20 (v/v). The direct copolymerization of MA and

AMPTMA is a notable achievement, considering the very different nature of these two monomers. However, due to solubility issues, it was not possible to find an appropriate solvent for the SEC analysis, in order to determine both block copolymers molecular weight and dispersity. Alternatively, the molecular weight of the block copolymers was estimated taking into account the molecular weight of the star-shaped PMA (first stage of the polymerization), which was determined by SEC in THF, and the content of nitrogen from the PAMPTMA block on the final block copolymer. Additionally, the success of the copolymerization was confirmed by the appearance of the characteristic adsorption bands of the PAMPMTA block in the FTIR spectrum of the copolymers (Figure 8.2): quaternary ammonium group at 1470 cm^{-1}; N–H stretching at 1540 cm^{-1} and C=O stretching at 1630 cm^{-1}.[23]

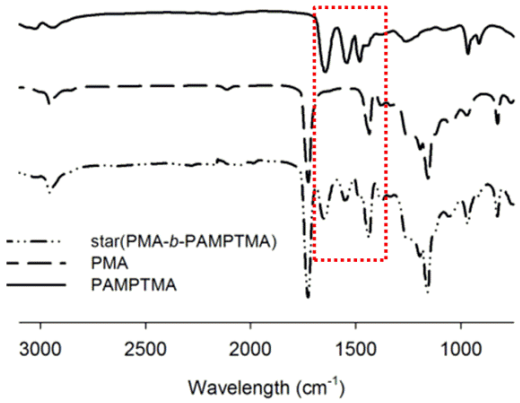

Figure 8.2. FTIR spectra of PMA, PAMPTMA and amphiphilic star block copolymer (PMA-*b*-PAMPTMA) samples prepared by SARA ATRP.

Block copolymers with different targeted properties, such as the number of arms, were prepared in order to evaluate the influence of the polymer structure/composition on the binding of bile acids. Table 8.1 summarizes the main features of the amphiphilic star block copolymers produced by SARA ATRP.

Table 8.1. Composition and molecular weight of the star-shaped PMA-*b*-PAMPTMA block copolymers synthesized by "one-pot" SARA ATRP in ethanol/water = 80/20 (v/v) at room temperature.

	1st block		2nd block	Block copolymer	
Sample code	**MA DP/arm[a]**	**$Đ$[b]**	**AMPTMA DP/arm[a]**	**Number of arms**	**M_n x 10^{-3}[c]**
4(PMA$_{95}$-*b*-PAMPTMA$_{50}$)	95	1.09	50	4	74.8
4(PMA$_{94}$-*b*-PAMPTMA$_{24}$)	94	1.13	24	4	52.9
4(PMA$_{94}$-*b*-PAMPTMA$_{16}$)	94	1.07	16	4	46.3
4(PMA$_{199}$-*b*-PAMPTMA$_{52}$)	199	1.08	52	4	112.2
6(PMA$_{98}$-*b*-PAMPTMA$_{52}$)	98	1.09	52	6	116.2
6(PMA$_{106}$-*b*-PAMPTMA$_{38}$)	106	1.09	38	6	103.0
6(PMA$_{104}$-*b*-PAMPTMA$_{18}$)	104	1.10	18	6	77.2

[a] $[monomer]_0/[initiator]_0$/number of arms

[b] Determined by SEC in THF at 30 °C

[c] The molecular weight of the second block (PAMPTMA) was estimated by elemental analysis

The SARA ATRP method was also employed for the preparation of PAMPTMA-based hydrogels (Figure 8.3), commonly polymeric architecture used as BAS. It is expected that hydrogels prepared by ATRP present more homogeneous structure that the ones obtained by conventional free radical polymerization techniques, due to the fast initiation and reversible deactivation reactions.[24-26]

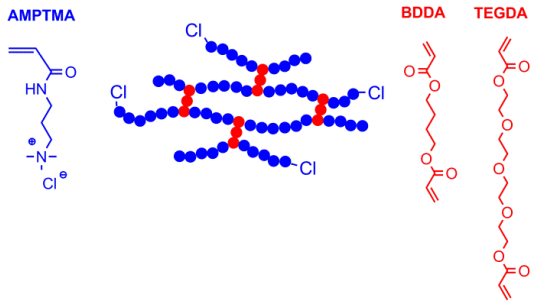

Figure 8.3. Generic structure of the cationic hydrogels prepared by SARA ATRP.

ECP was chosen to initiate the polymerization since it was previously demonstrated that this is an effective initiator for the SARA ATRP of AMPTMA in ethanol/water mixtures.[22] The monomer concentration was maintained in all the polymerizations ($[AMPTMA]_0$ = 2 M) and two different diacrylate crosslinkers with distinct hydrophilicities were tested (BDDA and TEGDA). Different targeted DP values of both

monomer and crosslinker were investigated and the main results are summarized in Table 8.2.

Table 8.2. Targeted DP and conversion achieved of both monomer (AMPTMA) and crosslinker in the preparation of cationic hydrogels by SARA ATRP. Reaction conditions: $[AMPTMA]_0$ = 2 M; $[ECP]_0/[CuCl_2]_0/[Me_6TREN]_0$ = 1/0.5/1.0; Cu(0) wire: *l* = 5 cm and *d* = 1 mm; ethanol/water = 50/50; T = 25 °C; t = 24 h.

Sample code	Crosslinker	AMPTMA DP[b]	Crosslinker DP[b]	AMPTMA conv. (%)	Crosslinker conv. (%)
AT 100/10	TEGDA	100	10	50	49
AT 50/10	TEGDA	50	10	[c]	[c]
AT 50/3[a]	TEGDA	50	3	[c]	[c]
AB 100/10	BDDA	100	10	35	35
AB 50/10	BDDA	50	10	61	42
AB 50/5	BDDA	50	5	61	63
AB 50/3[a]	BDDA	50	3	[c]	[c]

[a] No macroscopic gelation was observed

[b] $[AMPTMA \text{ or crosslinker}]_0/[ECP]_0$

[c] Data not available

It was reported that the concentration of monomer influences the gelation point and ultimately it could prevent the formation of a crosslinked polymeric structure, due to the occurrence of intramolecular cyclization under dilute conditions.[27] In this work, the AMPTMA concentration proved to be sufficient to allow macroscopic gelation (change from viscous liquid to elastic gel)[24] of the polymer, for $[crosslinker]_0/[ECP]_0$ = 5 or 10 (Table 8.2). For a targeted ratio $[crosslinker]_0/[ECP]_0$ = 3, the polymer remained soluble after the predetermined time of reaction (24 h) (AT 50/3 and AB 50/3 in Table 8.2). In this case, the system did not reach the gel point, probably due to a low conversion of the crosslinker achieved after 24 h (data not available). Macroscopic gelation should occur when, on an average basis, each primary chain contains at least one crosslink point, meaning that the ratio [reacted crosslinker]/[initiator] should be one, considering a high initiation efficiency (each molecule of initiator originates one primary polymer chain).[28]

Regarding the AMPTMA conversion, the value achieved was not high as it was expected from the results obtained in the reported AMPTMA homopolymerization by SARA ATRP (conv. > 90 % in less than 2 hours).[22] Similarly, both crosslinkers did not reach

very high conversion. This observation could mean that the reaction was not kept during enough time to allow full monomer conversion, considering the diffusion limitations experienced by monomers and catalytic complex in the polymer network after the gelation point.[25] A control SARA ATRP reaction was allowed to proceed during seven days and led to similar results (compared with a 24 h reaction) in terms of both monomer and crosslinker conversions. In order to prepared PAMPMTA-based hydrogels with targeted properties, such as crosslink density, further investigation of the gelation process is required. This includes kinetic studies and the determination of both the gelation points and the gel fractions for different hydrogels. Nevertheless, the results are reproducible and this works demonstrates the potential of the SARA ATRP as versatile tool for the preparation of cationic hydrogels.

8.5.2. Cholic acid sodium salt equilibrium binding by cationic hydrogels

Bile acids are amphiphilic molecules that are usually conjugated with the amino acids taurine or glycine in the human bile.[7] Under the small intestine conditions, these complexes are in their ionized form and for that reason they are also known as bile salts. In this work, NaCA was used as a model bile salt molecule for the preliminary equilibrium binding studies, due to its low price in comparison with bile acid conjugates. In addition, cholic acid based bile salts represent a large part (30-40 %) of the bile salts existing in the human bile.[29] Therefore, the results obtained wit NaCA are a good indicator of the binding capacity of the new BAS candidates. The PAMPTMA-based hydrogels prepared by SARA ATRP exhibited sigmoidal binding curves (Figure 8.4). These results suggest the existence of cooperative binding, meaning that the affinity of the hydrogel for the bile salts changes with the amount of bile salts already bonded. Therefore, the Hill equation was fitted to the data, with high R^2 values (Table 8.3). This type of binding process has been also observed for other polymeric hydrogels.[9, 10, 30] Nichifor and co-authors suggested that the cooperative binding of bile salts by cationic hydrogels could be interpreted as a two-step process.[9, 10] First, the binding is initiated by an electrostatic interaction between the hydrogel and the bile salt. The formation of the hydrogel–bile salt complex is characterized by the K_0 constant. In a second step, the hydrophobic interactions between both free and already bonded bile salt molecules

originate an increase of the rate of bile salts addition. This second step is described by the cooperative parameter (n).

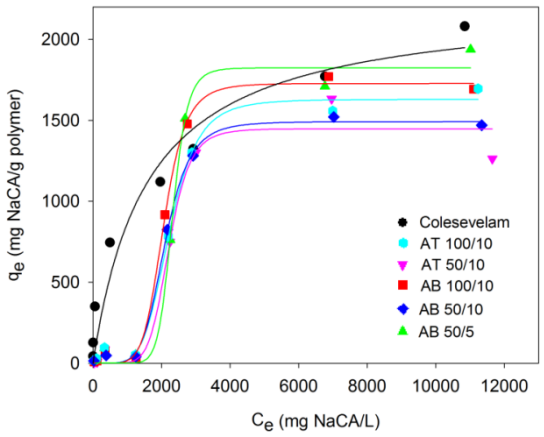

Figure 8.4. Isotherms for the binding of NaCA by the Colesevelam and the hydrogels prepared by SARA ATRP. Binding conditions: 50 mM phosphate buffer (pH 6.8) at 37 °C. The lines represent the fitting to Langmuir or Hill models for the Colesevelam and hydrogels, respectively.

Both the overall binding constant (K) and the cooperative parameter were determined directly from the Hill model fitted to the experimental data. The K_0 value (Table 8.3) was determined by the ratio between K and n, as reported in the literature.[9, 10] The equilibrium binding of NaCA by the Colesevelam (black symbols in Figure 8.4) followed a typical Langmuir isotherm (Hill equation with n = 1, meaning no cooperativity), as reported by other authors for the binding of conjugated bile salts.[31]

Table 8.3. Binding parameters of the cationic hydrogels prepared by SARA ATRP and the commercial BAS Colesevelam. The errors presented were obtained from the model fitting using the SigmaPlot software.

Sample code	R^2	K ($L.mg^{-1}$) x 10^4	n	K_0 ($L.mg^{-1}$) x 10^4	q_{max} $(mg/g)^a$ x 10^{-3}
Colesevelam	0.9771	6.0 ± 2.0	1.0	-	2.2 ± 0.24
AT 100/10	0.9949	4.0 ± 0.1	5.4 ± 0.9	0.7 ± 0.2	1.6 ± 0.04
AT 50/10	0.9868	5.0 ± 0.2	7.3 ± 4.3	0.7 ± 0.6	1.5 ± 0.10
AB 100/10	0.9988	5.0 ± 0.1	6.5 ± 0.8	0.8 ± 0.1	1.7 ± 0.03
AB 50/10	0.9983	5.0 ± 0.1	5.9 ± 0.6	0.8 ± 0.1	1.5 ± 0.02
AB 50/5	0.9962	4.0 ± 0.1	10.7 ± 2.3	0.4 ± 0.1	1.8 ± 0.06

[a] mg NaCA/g polymer.

Due to time constrains, it was not possible to replicate the equilibrium binding experiments for all the samples investigated. In order to validate the results obtained, one of the samples (AB 100/10) was analyzed in triplicate. The results (Figure D.1 in Appendix D) showed that despite the existing errors, which can be inherent to the HPLC analysis, there was an evident trend of the concentration values determined. Table 8.3 summarizes the binding parameters obtained for the cationic hydrogels prepared by SARA ATRP. The strength of binding of NaCA by the cationic hydrogels prepared was comparable to that of the commercial BAS Colesevelam, as judged by the similar K values. In addition, the cooperative parameter was higher than 1 for all the hydrogels, which indicates that the cooperative binding is positive. This parameter remained relatively constant, regardless the type of crosslinker used. The hydrogel samples prepared by SARA ATRP revealed to be promising candidates for BAS, as the maximum NaCA binding capacity (q_{max}) was close to that of Colesevelam, without optimization of the hydrogel composition. As previously mentioned, due to the limited monomer conversions achieved, some of the hydrogel samples prepared by SARA ATRP presented similar composition (different from the one targeted) which did not allow the investigation of the polymer composition/binding parameters relationship. Besides the hydrogels composition, their swelling capacity can also influence the binding parameters. It was reported that a more elastic polymer network could promote the cooperativity of the binding.[9] The swelling capacities of the hydrogels prepared by SARA ATRP were determined in duplicate and the results are summarized in Table 8.4.

Table 8.4. Composition, cooperative parameter and swelling capacity of the hydrogels prepared by SARA ATRP and Colesevelam.

Sample code	Crosslinker	AMPTMA DP[a]	Crosslinker DP[a]	n	Swelling capacity x 10^{-3} (%)
Colesevelam	-	-	-	1.0	0.64 ± 0.07
AT 100/10	TEGDA	50	4.9	5.4 ± 0.9	2.11 ± 0.47
AT 50/10	TEGDA	[b]	[b]	7.3 ± 4.3	1.77 ± 0.09
AB 100/10	BDDA	35	3.5	5.7 ± 1.1	1.96 ± 0.08
AB 50/10	BDDA	30	6.1	5.9 ± 0.6	2.00 ± 0.29
AB 50/5	BDDA	30	3.0	10.5 ± 2.5	2.42 ± 0.33

[a] Determined by ^{1}H NMR spectroscopy

[b] Data not available.

The Colesevelam and the purified hydrogel samples prepared by SARA ATRP were obtained as fine powders, which were impossible to handle after swelling a great amount of water. Due to this limitation, the determination of the swelling capacity of the samples could have become imprecise (Table 8.4). However, despite of the existing errors, it is possible to confirm that the swelling capacity of the hydrogels prepared by SARA ATRP is at least two times higher than the one of the commercial BAS Colesevelam. Considering the final application, one could expect that the hydrogels could form a softer gel in the intestine environment, which can contribute to better patient compliance (less constipation). The results also show that for the two crosslinkers used, their structure had no influence on the swelling capacity of the hydrogels.

8.5.3. Cholic acid sodium salt equilibrium binding by amphiphilic star block copolymers

ITC was used for the preliminary investigation of the binding thermodynamics between the NaCA molecules and the amphiphilic block copolymers. This technique has been employed for the study of the binding of bile salts by several receptors.[32-34] Contrary to the determination of the binding isotherms by HPLC, ITC can provide valuable information about the binding process, such as the number of binding sites in the polymer and the binding enthalpy change.[35] The preliminary ITC experiments were conducted using an initial concentration of NaCA below the critical micelle concentration (cmc) to avoid the formation of micelles, which could difficult the analysis of the titration results. However, in those conditions, all the samples showed to have low affinity towards the NaCA molecules (Figure D.2 in Appendix D). Therefore, unfortunately, the titration curves did not allow the determination of the binding parameters. Nevertheless, it was possible to observe that the enthalpy of binding was positive (endothermic process), meaning that the binding process was mainly governed by hydrophobic interactions. Additionally, the heat involved in the binding was strongly dependent on the buffer ionization enthalpy indicating changes on the ionization of the NaCA upon binding, corresponding to an increase in the NaCA neutral form (Figure D.3 in Appendix D). This further supports the prevalence of hydrophobic interactions under the conditions investigated.

Alternatively, the equilibrium binding of NaCA by the amphiphilic star block copolymers was investigated using HPLC and the experiments were conducted under the same conditions used for the hydrogels (section 8.5.2). The Hill model fitted very well the experimental data for all the samples investigated ($R^2 \geq 0.98$, Table D.1 in Appendix D) suggesting that the NaCA binding was cooperative, similarly to what was observed for the PAMPTMA-based hydrogels. These results were in agreement with those obtained from ITC (low affinity for NaCA initial concentrations below 5 mM). Despite having K values (Table D.1 in Appendix D) similar to those of Colesevelam and PAMPTMA-based hydrogels, generally the star block copolymers presented lower NaCA binding capacity (compare with Figure 8.4). These results suggest that polymer networks could be more beneficial for the binding process, in comparison to some nanoassembled polymer structures, probably due to the fact that the swollen hydrogels could facilitate the diffusion of the bile salt molecules and their access to the polymer binding sites. Nevertheless, the results also highlight the importance of fine-tuning the polymers composition, since it was possible to greatly increase the maximum binding capacity by changing, for instance, the size of the hydrophobic core of the star (e.g., red and pink symbols in Figure 8.5). Such control over the polymers features is only possible using RDRP techniques, as the one investigated in this work (SARA ATRP).

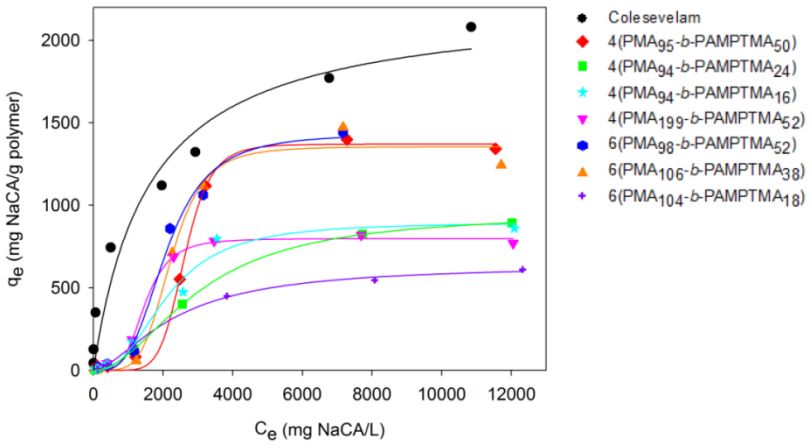

Figure 8.5. Isotherms for the binding of NaCA by the Colesevelam and the amphiphilic star block copolymers prepared by SARA ATRP. Binding conditions: 50 mM phosphate buffer (pH 6.8) at 37 °C. The lines represent the fitting to Langmuir or Hill models for the Colesevelam and amphiphilic star block copolymers, respectively.

As previously mentioned, the library of block copolymers synthesized in this work was designed to allow the investigation of the polymers structure/sequestration performance relationship. Figure 8.6 shows the variation of the binding parameters values with the increase of the hydrophilic cationic arm length, for both 4-arm and 6-arm star block copolymers with a fixed core size (MA DP/arm = 100). Regardless of the number of arms of the star, the increase of the hydrophilic cationic arm length led to an increase of the maximum binding capacity (black symbols in Figure 8.6), confirming that the electrostatic interactions play an important role in the binding process. The same trend was also observed by other authors[11] for BAS candidates based on cationic micelles. Generally, it seems that the variation of the number of arms from 4 to 6 did not have a significant impact in the NaCA sequestration, since the binding parameters were relatively in the same range (Figure 8.6 (a) and (b)).

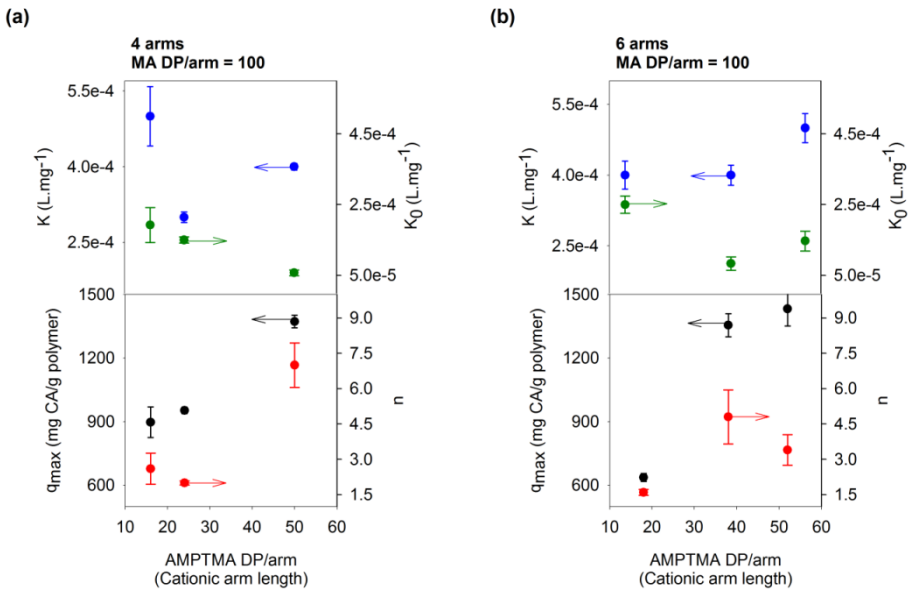

Figure 8.6. Variation of the binding parameters with the increase in the cationic arm length of the amphiphilic star block copolymers, for a fixed hydrophobic core size (MA DP/arm = 100): (a) 4-arm star and (b) 6-arm star.

The influence of the hydrophobic core size on the binding parameters was also investigated for samples of 4-arm star PMA-*b*-PAMPTMA block copolymers (Figure 8.7). The increase of the hydrophobic character of the polymer led to a decrease in the maximum NaCA binding capacity. In addition, there was an increase of both the polymer-NaCA ionic complex formation and the overall stability of the binding process (green and blue symbols in Figure 8.7, respectively). This behavior was also observed for

other polymeric materials and was attributed to the increase of the hydrophobic interactions between polymer and NaCA, for polymers with higher hydrophobic character.[9, 10, 36] In this case, the cooperative parameter decreased (red symbols in Figure 8.7) indicating that the contribution of the cooperative effect among the NaCA molecules to the overall binding process was less significant.

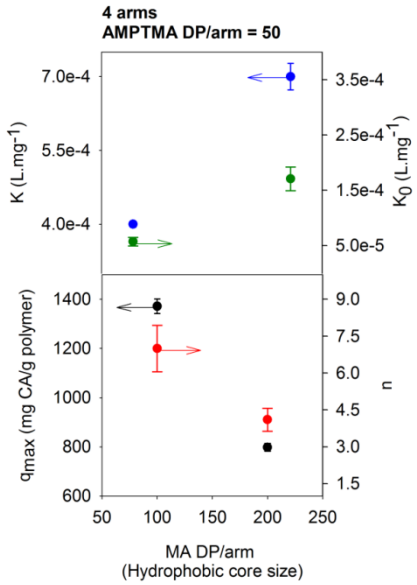

Figure 8.7. Variation of the binding parameters with the increase in the hydrophobic core size of 4-arm amphiphilic star block copolymers, for a fixed length of cationic arms (AMPTMA DP/arm = 50).

Nevertheless, it is worth to mention that the binding parameters might not have a linear variation with the polymers features.[9, 10, 13] Therefore, the interpretation of the results should be done with caution. This work represents the first approach towards the design of BAS based on new polymeric structures (amphiphilic star block copolymers). For a deeper understanding of the influence of the polymer features in the sequestration properties, further investigations covering a wider range of parameters (e.g., length of the cationic arm) are needed. In addition, it will be interesting to perform ITC analysis using a concentration of NaCA above its cmc, to study the high affinity region.

8.5.4. Insight into the binding mechanism

The results on the binding of NaCA by both hydrogels and amphiphilic star block copolymers suggested the existence of cooperative binding. One of the parameters that could influence this behavior is the starting concentration of both polymer and NaCA,

which ultimately will affect their conformation in solution (e.g., formation of micelles) and their affinity towards each other. To test this hypothesis, different initial concentrations of a selected hydrogel sample were used for the equilibrium binding assays (Figure 8.8).

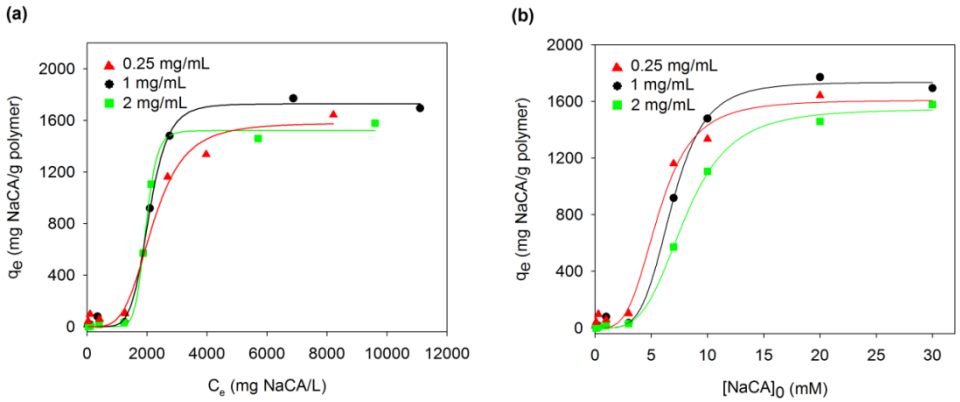

Figure 8.8. Isotherms for the binding of NaCA by a PAMPTMA-based cationic hydrogel (AB 100/10) prepared by SARA ATRP, using different starting concentrations of hydrogel for the binding assays. Binding conditions: 50 mM phosphate buffer (pH 6.8) at 37 °C. The lines represent the fitting to the Hill model.

The cooperative binding effect showed to be dependent on the concentration of polymer used in the binding assay (Figure 8.8 (b)). However, it was possible to observe that the abrupt increase of the binding capacity (q_e) of the hydrogel occurred for the same concentration of free NaCA in the solution (C_e) (Figure 8.8 (a)), irrespectively of the polymer concentration. The region of high affinity was observed for starting concentrations of NaCA above 3-7 mM (Figure 8.8 (b)), which is above its cmc.[37] Therefore, the results obtained suggest that instead of the existence of a cooperative binding process, the behavior observed could be in fact the result of a stronger interaction between the PAMPTMA-based materials and NaCA micelles (electrostatic interaction), than with NaCA unimers (both hydrophobic and electrostatic interactions). This aspect could be advantageous considering BAS applications, since the bile salts are usually present in the intestine at concentrations above their cmc.[38] Based on these results, it seems that the cooperative mechanism proposed in the literature[9, 10] is not the most suitable one to describe the binding of NaCA by the AMPTMA-based materials prepared by SARA ATRP. In this case, one might consider the existence of two different binding mechanisms corresponding to NaCA concentrations below and above the bile salt cmc.

As previously mentioned, the star block copolymers prepared by SARA ATRP present a PMA-based hydrophobic core and hydrophilic cationic arms, with high charge density (one charge per each AMPTMA repeating unit). The NaCA is an amphiphilic molecule that possesses both nonpolar (steroid skeleton) and polar (negatively charged) regions. In this case, one might consider that the NaCA unimers (concentration below the cmc) can interact either with the hydrophobic part of the polymer, which is less accessible, or/and with the cationic arms of the polymer by electrostatic interactions. On this matter, the ITC results (see section 8.5.3) suggested that the binding of NaCA unimers by the star block copolymers is relatively weak (low affinity constant K_1) and it is mainly governed by hydrophobic interactions with the nonpolar region of the polymer. This hypothesis was also confirmed by the low binding capacity obtained in the equilibrium binding experiments using $[NaCA]_0 < NaCA_{cmc}$ (e.g., Figure 8.8 (b)). In addition, data reported in the literature[13] indicates that the binding of NaCA unimers can be suppressed in the presence of small electrolytes (e.g., NaCl). This fact might have also contributed for the low affinity showed by the PAMPTMA-based materials towards NaCA molecules below the cmc, due to the intrinsic high concentration of Cl^- anions from the PAMPTMA segment. On the other hand, for initial concentrations of NaCA above its cmc, the NaCA micelles/aggregates formed will be able to compete with small Cl^- anions and establish electrostatic interactions with the polymer, since the nonpolar segment of the NaCA will be in the micelles core. In this case the binding process will be characterized by an affinity constant K_2, higher than K_1, and could be described by the Langmuir isotherm. In order to confirm this hypothesis, it will be necessary to obtain a more defined binding isotherm by increasing the number of data points analyzed for initial NaCA concentrations between 3 mM and 7 mM. Additionally, it will be interesting to perform ITC binding experiments using $[NaCA]_0 >$ cmc (high affinity region) to confirm the prevalence of electrostatic interactions.

The investigation of the binding process should then proceed with the evaluation of the binding kinetics, since the small intestine transit time for pharmaceutical dosages is around 3 ± 1h.[39] It is also important to study the competitive binding of different conjugated bile salts in the same starting solution, in order to check the polymer´s binding capacity/affinity in an intestine-mimicking environment.

8.5.5. *In vitro* degradation studies

Considering that polymeric BAS are administered orally, it is important to evaluate the stability of the synthesized materials under conditions that could simulate the GI tract environment. The determination of the molecular weight and the confirmation of the polymers chemical structure, after being subjected to the mentioned conditions, are effective tools to quantify any possible degradation. Due to the lack of proper solvents to analyze the amphiphilic star block copolymers by either SEC or ^{1}H NMR spectroscopy, the degradation of the materials was evaluated by analyzing each polymeric segment separately (linear PAMPMTA and star-shaped PMA). Therefore, it is assumed that the degradation mechanism of the block copolymer will be similar to that of the constituent parts. The degradation studies were carried out in triplicate at 37 °C in SGF at pH 1.2 for 2 h and in SIF at pH 6.8 for 3 h.[40, 41] Table 8.5 summarizes the molecular weights and dispersity of the polymers before and after degradation.

Table 8.5. Molecular weight and dispersity of linear PAMPTMA and star-shaped PMA before and after exposure to the degradation solutions at 37 °C.

Sample	Medium	Degradation time (h)	M_n^{SEC} x 10^{-3}	*Đ*
PAMPTMA	SGF	0	19.6	1.09
	(pH = 1.2)	2	19.6 ± 0.1	1.09 ± 0.01
PMA	SGF	0	51.7	1.07
	(pH = 1.2)	2	51.3 ± 0.7	1.07 ± 0.01
PAMPTMA	SIF	0	19.6	1.09
	(pH = 6.8)	3	19.4 ± 0.1	1.08 ± 0.01
PMA	SIF	0	51.7	1.07
	(pH = 6.8)	3	51.7 ± 0.8	1.08 ± 0.01

The results obtained by SEC suggest that there was no degradation of the polymers backbones, since there was no significant variation on the molecular weight values. However, one must be careful in the interpretation of the SEC results, since degradation of some polymer side chains (amide and ester linkages) could have minimal influence in the polymers molecular weight value. Therefore, additional ^{1}H NMR spectroscopy

analyses were performed. The results showed that there was no degradation of the side chains of both PMA and PAMPTMA, since the ratio between the integral of the protons of the backbone and the protons of the side chains was constant for the samples studied (Figure D.2 and Figure D.3 in Appendix D).

8.6. Conclusions

The SARA ATRP method was used for the synthesis of BAS candidates based on novel PAMPMTA-based hydrogels and amphiphilic star block copolymers. NaCA was used as the model bile salt for the study of the *in vitro* equilibrium binding. Both stars and hydrogels exhibited higher affinity towards NaCA micelles rather than NaCA unimers. This behavior was explained by the high density of cationic charges in the polymer and by the suppression of the NaCA binding, for low initial NaCA concentration, due to the presence of competing Cl^- anions from the AMPTMA monomer. The cationic hydrogels proved to be promising materials with similar performance to the commercial BAS Colesevelam hydrochloride, concerning both the binding affinity and the maximum binding capacity. Regarding the amphiphilic star block copolymers, it was possible to conclude that the binding parameters could be adjusted by small changes on the polymers targeted composition. Typically, longer cationic hydrophilic arms lead to higher binding capacity. The polymers prepared proved to be stable in degradation solutions mimicking the GI tract conditions.

8.7. References

1. Insull, W., Clinical utility of bile acid sequestrants in the treatment of dyslipidemia: A scientific review. *South Med. J.* **2006,** 99, (3), 257-273.

2. Dhal, P. K.; Polomoscanik, S. C.; Avila, L. Z.; Holmes-Farley, S. R.; Miller, R. J., Functional polymers as therapeutic agents: Concept to market place. *Adv. Drug Deliv. Rev.* **2009,** 61, (13), 1121-1130.

3. Dhal, P. K.; Huval, C. C.; Holmes-Farley, S. R., Biologically active polymeric sequestrants: Design, synthesis, and therapeutic applications. *Pure Appl. Chem.* **2007,** 79, (9), 1521-1530.

4. Reiner, Ž.; Catapano, A. L.; De Backer, G.; Graham, I.; Taskinen, M.-R.; Wiklund, O.; Agewall, S.; Alegria, E.; Chapman, M. J.; Durrington, P.; Erdine, S.; Halcox, J.; Hobbs, R.; Kjekshus, J.; Filardi, P. P.; Riccardi, G.; Storey, R. F.; Wood, D., ESC/EAS Guidelines for the management of dyslipidaemias. *Eur. Heart J.* **2011,** 32, (14), 1769-1818.

5. Hou, R.; Goldberg, A. C., Lowering Low-Density Lipoprotein Cholesterol: Statins, Ezetimibe, Bile Acid Sequestrants, and Combinations: Comparative Efficacy and Safety. *Clin. Endocrinol. Metab.* **2009,** 38, (1), 79-97.

6. Alberto, C.; Eberhard, W.; Michel, F., Colesevelam hydrochloride: usefulness of a specifically engineered bile acid sequestrant for lowering LDL-cholesterol. *Eur. J. Cardiovasc. Prev. Rehabil.* **2009,** 16, (1), 1-9.

7. Zarras, P.; Vogl, O., Polycationic salts as bile acid sequestering agents. *Prog. Polym. Sci.* **1999,** 24, (4), 485-516.

8. Synytsya, A.; Fesslová, L.; Marounek, M.; Čopíková, J., Sodium cholate sorption on N-octadecylpectinamide in comparison with cholestyramine. *Czech J. Food Sci.* **2007,** 25, 32-38.

9. Nichifor, M.; Zhu, X. X.; Cristea, D.; Carpov, A., Interaction of hydrophobically modified cationic dextran hydrogels with biological surfactants. *J. Phys. Chem. B* **2001,** 105, (12), 2314-2321.

10. Nichifor, M.; Zhu, X. X.; Baille, W.; Cristea, D.; Carpov, A., Bile acid sequestrants based on cationic dextran hydrogel microspheres. 2. Influence of the length of alkyl substituents at the amino groups of the sorbents on the sorption of bile salts. *J. Pharm. Sci.* **2001,** 90, (6), 681-689.

11. Cameron, N. S.; Eisenberg, A.; Brown, G. R., Amphiphilic block copolymers as bile acid sorbents: 2. Polystyrene-b-poly(N,N,N-trimethylammoniumethylene acrylamide

chloride): Self-assembly and application to serum cholesterol reduction. *Biomacromolecules* **2002,** 3, (1), 124-132.

12. Baille, W. E.; Huang, W. Q.; Nichifor, M.; Zhu, X. X., Functionalized beta-cyclodextrin polymers for the sorption of bile salts. *J. Macromol. Sci., Pure Appl. Chem.* **2000,** 37, (7), 677-690.

13. Nichifor, M.; Cristea, D.; Carpov, A., Sodium cholate sorption on cationic dextran hydrogel microspheres. 1. Influence of the chemical structure of functional groups. *Int. J. Biol. Macromol.* **2000,** 28, (1), 15-21.

14. Dhal, P.; Holmes-Farley, S.; Huval, C.; Jozefiak, T., Polymers as Drugs. In *Polymer Therapeutics I*, Satchi-Fainaro, R.; Duncan, R., Eds. Springer Berlin / Heidelberg: 2006; Vol. 192, pp 9-58.

15. Mandeville, W. H.; Goldberg, D. I., The sequestration of bile acids, a non-absorbed method for cholesterol reduction. A review. In *Current pharmaceutical design*, Sliskovic, D. R., Ed. Bentham science publishers: Hilversum, 1997; Vol. 3, pp 15-26.

16. Cameron, N. S.; Eisenberg, A.; Brown, G. R., Amphiphilic block copolymers as bile acid sorbents: 1. Synthesis of polystyrene-b-poly(N,N,N-trimethylammoniumethylene acrylamide chloride). *Biomacromolecules* **2002,** 3, (1), 116-123.

17. Matyjaszewski, K.; Miller, P. J.; Pyun, J.; Kickelbick, G.; Diamanti, S., Synthesis and Characterization of Star Polymers with Varying Arm Number, Length, and Composition from Organic and Hybrid Inorganic/Organic Multifunctional Initiators. *Macromolecules* **1999,** 32, (20), 6526-6535.

18. Ciampolini, M.; Nardi, N., Five-Coordinated High-Spin Complexes of Bivalent Cobalt, Nickel, andCopper with Tris(2-dimethylaminoethyl)amine. *Inorg. Chem.* **1966,** 5, (1), 41-44.

19. Zhang, Y.; Wang, Y.; Peng, C.-h.; Zhong, M.; Zhu, W.; Konkolewicz, D.; Matyjaszewski, K., Copper-Mediated CRP of Methyl Acrylate in the Presence of Metallic

Copper: Effect of Ligand Structure on Reaction Kinetics. *Macromolecules* **2011,** 45, (1), 78-86.

20. Ni, C.; Wu, G.; Zhu, C.; Yao, B., The Preparation and Characterization of Amphiphilic Star Block Copolymer Nano Micelles Using Silsesquioxane As the Core. *J. Phys. Chem. C* **2010,** 114, (32), 13471-13476.

21. Abreu, C. M. R.; Mendonça, P. V.; Serra, A. C.; Coelho, J. F. J.; Popov, A. V.; Guliashvili, T., Accelerated Ambient-Temperature ATRP of Methyl Acrylate in Alcohol–Water Solutions with a Mixed Transition-Metal Catalyst System. *Macromol. Chem. Phys.* **2012,** 213, (16), 1677-1687.

22. Mendonca, P. V.; Konkolewicz, D.; Averick, S. E.; Serra, A. C.; Popov, A. V.; Guliashvili, T.; Matyjaszewski, K.; Coelho, J. F. J., Synthesis of cationic poly((3-acrylamidopropyl)trimethylammonium chloride) by SARA ATRP in ecofriendly solvent mixtures. *Polym. Chem.* **2014,** 5, (19), 5829-5836.

23. Constantin, M.; Mihalcea, I.; Oanea, I.; Harabagiu, V.; Fundueanu, G., Studies on graft copolymerization of 3-acrylamidopropyl trimethylammonium chloride on pullulan. *Carbohydr. Polym.* **2011,** 84, (3), 926-932.

24. Gao, H.; Chan, N.; Oh, J.; Matyjaszewski, K., Designing Hydrogels by ATRP. In *In-Situ Gelling Polymers*, Loh, X. J., Ed. Springer Singapore: 2015; pp 69-105.

25. Jiang, C.; Shen, Y.; Zhu, S.; Hunkeler, D., Gel formation in atom transfer radical polymerization of 2-(N,N-dimethylamino)ethyl methacrylate and ethylene glycol dimethacrylate. *J. Polym. Sci., Part A: Polym. Chem.* **2001,** 39, (21), 3780-3788.

26. Gao, H.; Min, K.; Matyjaszewski, K., Determination of Gel Point during Atom Transfer Radical Copolymerization with Cross-Linker. *Macromolecules* **2007,** 40, (22), 7763-7770.

27. Gao, H.; Li, W.; Matyjaszewski, K., Synthesis of Polyacrylate Networks by ATRP: Parameters Influencing Experimental Gel Points. *Macromolecules* **2008,** 41, (7), 2335-2340.

28. Flory, P. J., *Principles of Polymer Chemistry: Paul J. Flory*. Cornell University: 1953.

29. Einarsson, K.; Ericsson, S.; Ewerth, S.; Reihnér, E.; Rudling, M.; Ståhlberg, D.; Angelin, B., Bile acid sequestrants: Mechanisms of action on bile acid and cholesterol metabolism. *Eur. J. Clin. Pharmacol.* **1991,** 40, (1), S53-S58.

30. Huval, C. C.; Bailey, M. J.; Braunlin, W. H.; Holmes-Farley, S. R.; Mandeville, W. H.; Petersen, J. S.; Polomoscanik, S. C.; Sacchiro, R. J.; Chen, X.; Dhal, P. K., Novel cholesterol lowering polymeric drugs obtained by molecular imprinting. *Macromolecules* **2001,** 34, (6), 1548-1550.

31. Hanus, M.; Zhorov, E., Bile acid salt binding with colesevelam HCl is not affected by suspension in common beverages. *J. Pharm. Sci.* **2006,** 95, (12), 2751-2759.

32. Awino, J. K.; Zhao, Y., Protein-Mimetic, Molecularly Imprinted Nanoparticles for Selective Binding of Bile Salt Derivatives in Water. *J. Am. Chem. Soc.* **2013**.

33. Zhang, Y. M.; Wang, Z.; Chen, Y.; Chen, H. Z.; Ding, F.; Liu, Y., Molecular binding behavior of a bispyridinium-containing bis(beta-cyclodextrin) and its corresponding [2]rotaxane towards bile salts. *Org. Biomol. Chem.* **2014,** 12, (16), 2559-67.

34. Létourneau, D.; Lorin, A.; Lefebvre, A.; Cabana, J.; Lavigne, P.; LeHoux, J.-G., Thermodynamic and solution state NMR characterization of the binding of secondary and conjugated bile acids to STARD5. *Biochim. Biophys. Acta* **2013,** 1831, (11), 1589-1599.

35. Freyer, M. W.; Lewis, E. A., Isothermal Titration Calorimetry: Experimental Design, Data Analysis, and Probing Macromolecule/Ligand Binding and Kinetic Interactions. In *Methods in Cell Biology*, Dr. John, J. C.; Dr. H. William Detrich, III, Eds. Academic Press: 2008; Vol. Volume 84, pp 79-113.

36. Benrraou, M.; Zana, R.; Varoqui, R.; Pefferkorn, E., Study of the interaction between dodecyltrimethylammonium bromide and poly(maleic acid-co-alkyl vinyl ether) in aqueous solution by potentiometry and fluorescence probing. *J. Phys. Chem.* **1992,** 96, (3), 1468-1475.

37. Navas Díaz, A.; García Sánchez, F.; García Pareja, A., Cholic acid behavior in water and organic solvent: study of normal and inverted aggregates. *Colloids Surf., A* **1998,** 142, (1), 27-34.

38. Brockman, H., Pancreatic Lipase. In *Intestinal Lipid Metabolism*, Mansbach, C., II; Tso, P.; Kuksis, A., Eds. Springer US: 2001; pp 61-79.

39. Lee, J. K.; Kim, S. Y.; Kim, S. U.; Kim, J. H., Synthesis of cationic polysaccharide derivatives and their hypocholesterolaemic capacity. *Biotechnol. Appl. Biochem.* **2002,** 35, 181-189.

40. Chellat, F.; Tabrizian, M.; Dumitriu, S.; Chornet, E.; Rivard, C. H.; Yahia, L. H., Study of biodegradation behavior of chitosan–xanthan microspheres in simulated physiological media. *J. Biomed. Mater. Res.* **2000,** 53, (5), 592-599.

41. Godge, G. R.; Hiremath, S. N., An Investigation into the Characteristics of Natural Polysaccharide: Polymer Metoprolol Succinate Tablets for Colonic Drug Delivery. *MU J. Pharm.* **2014,** 41, (2), 7-21.

Chapter 9

Final remarks

9.1. Overall conclusions

The metal-catalyzed reversible deactivation radical polymerization (RDRP) is a robust and versatile technique that allows the preparation of tailor-made polymers with controlled molecular weight, dispersity, composition, architecture and functionality. Along with the developments in the metal-catalyzed RDRP field, there has been an intense debate in the literature regarding the reaction mechanism of the Cu(0)-catalyzed RDRP, with two different mechanistic standpoints: supplemental activator and reducing agent atom transfer radical polymerization (SARA ATRP) and single electron transfer living radical polymerization (SET-LRP). The results obtained from the mechanistic studies on the Cu(0)-catalyzed RDRP of methyl acrylate (MA) (Chapter 2) revealed that there is no disproportionation of the catalytic complex CuBr/Me_6TREN (Me_6TREN: tris[2-(dimethylamino)ethyl]amine)) during the polymerization. Therefore, it was concluded that the CuBr/Me_6TREN is the most probable activator, being Cu(0) a supplemental activator and reducing agent of $CuBr_2$/Me_6TREN

The major issues associated with the ATRP method are the use of metal catalysts, which can contaminate the final product, and sometimes the inevitable use of harmful organic solvents. Current research trends aim to reduce the amount of catalyst used as well as to replace harmful organics solvents. The work described in Chapter 3 allowed the synthesis of well-defined poly(methyl acrylate) (PMA) by Fe(0)/$CuBr_2$/Me_6TREN-catalyzed SARA ATRP using a low concentration of soluble $CuBr_2$ (50 ppm) in an ecofriendly solvent (ethanol/water mixture) near room temperature (30 °C). The conditions developed in this work represent a considerable improvement of the ATRP of MA available in the literature and can contribute for the future scale-up of the SARA ATRP technique using an affordable technology. The same environmentally attractive SARA ATRP catalytic system was used for the polymerization of the relevant hydrophobic monomer styrene (Sty) (Chapter 4). It was possible to decrease the reaction temperature and increase the rate of polymerization in comparison to the normal ATRP of Sty, using dimethylformamide (DMF) as the solvent. The SARA ATRP system proved to be useful for the preparation of telechelic polystyrene (PS) that could react by "click" chemistry to produce well-defined PS-based block copolymers.

The work described in both Chapters 5 and 6 present the development of ATRP variation techniques for the preparation of biomedical-relevant polymers in alcohol/water mixtures or even aqueous medium, which is considered to be a very challenging solvent for ATRP. Well-defined cationic poly((3-acrylamidopropyl)trimethylammonium chloride) (PAMPTMA) was prepared by Cu(0)/$CuCl_2$/Me_6TREN-catalyzed SARA ATRP at room temperature and used for the preparation of different hydrophilic block copolymers (Chapter 5). Additionally, alkyne-functionalized PAMPTMA was successfully reacted with an azido-functionalized coumarin derivative, using "click" chemistry, to produce a fluorescent PAMPTMA molecule. A new activators regenerated by electron transfer (ARGET) ATRP, using slow feed of ascorbic acid in combination with $CuBr_2$/TPMA (TPMA: tris(2-pyridylmethyl)-amine)) was developed for the polymerization of 2-aminoethyl methacrylate hydrochloride (AMA) at 35 °C (Chapter 6). Very encouraging results were obtained since, for the first time, poly-AMA prepared by ATRP techniques retained high chain-end functionality, allowing the preparation of a well-defined hydrophilic block copolymer. Besides the good control over the molecular structure of the polymers, the reaction conditions developed for the polymerization of both PAMA and PAMPTMA are very attractive considering the preparation of complex macromolecular structures for biomedical applications.

Chapter 7 presents a different RDRP technique, namely the reversible addition-fragmentation chain transfer (RAFT) for the polymerization of functional *N*-(3-aminopropyl)methacrylamide hydrochloride (APMA) since, after several attempts, it was not possible to polymerize the referred monomer by ATRP techniques. APMA is commonly used for biomedical applications and it was of great interest to develop the RAFT system for the synthesis of well-defined azide- and alkyne-functionalized poly-APMA ($Đ \leq 1.1$) that can be used for the preparation of complex structures by "click" chemistry. The results showed that it was possible to use unprotected functional chain transfer agents, avoiding troublesome protection/deprotection steps, which can contribute to the expansion of the range of application of poly-APMA.

To prove the potential of the developed SARA ATRP method for the preparation of tailor-made materials for biomedical applications, new polymeric bile acid sequestrants (BAS) were designed (Chapter 8). The BAS candidates were based on PAMPTMA

hydrogels and amphiphilic PMA-*b*-PAMPTMA star block copolymers. Very promising results were obtained, with the PAMPTMA-based hydrogels showing similar binding parameters to the commercial BAS Colesevelam hydrochloride in the *in vitro* binding experiments using sodium cholate (NaCA) as the model bile salt. Additionally, it was possible to confirm the advantage of using RDRP methods in the preparation of new BAS, as the binding parameters of the PMA-*b*-PAMPTMA stars could be adjusted by fine-tuning the block copolymers composition.

Overall, this projected has contributed for the development of new ecofriendly ATRP systems for the polymerization of both hydrophobic and functional cationic hydrophilic monomers, which could be used to prepare tailor-made candidate materials for biomedical applications.

9.2. Recommendations for future work

This work has contributed for the development of new ATRP systems that present attractive reaction conditions (e.g., room temperature, ecofriendly solvents, etc.) for the further scale-up of the technique. However, there is certainly still room from improvement especially on the catalyst design field, since some of the commercial ligands available for ATRP could be relatively expensive (e.g., Me_6TREN). The creation of new inexpensive and active ligands is a current demand and should be consider as future work.

Based on the monomers investigated in this work, there is a vast range of molecular structures that could be designed to act as BAS. The results obtained considering the preparation of novel PAMPTMA-based hydrogels and PMA-*b*-PAMPTMA stars represent just the first step towards the development of a new generation of tailor-made BAS. On this matter, there are several relevant *in vitro* experiments that could be suggested as future work, including:

- Kinetic studies of the binding of NaCA by both PAMPTMA-based hydrogels and PMA-*b*-PAMPTMA stars in order to determine the time required to reach the equilibrium. The results will allow to understand if the polymers are able to bind the bile salts during the intestine transit time;

- Analysis of the binding of NaCA by the PMA-*b*-PAMPTMA stars in the high affinity region (using $[NaCA]_0$ > cmc) by isothermal titration calorimetry (ITC), in order to determine the enthalpy variation during the binding process and the number of binding sites in the polymer. This information will allow improving the understanding of the structure/performance relationship of the block copolymers.

- Competitive equilibrium binding using different conjugated bile salts in the initial solution. This study is of extreme importance since it will provide information about the affinity of the polymers for the different bile salts in an intestine-mimicking environment.

- Equilibrium binding studies with acidic pre-treatment of the polymers. This study will allow to confirm if the polymers are able to maintain their binding capacity after being subjected to a stomach-mimicking environment.

Appendices

Appendix A

Supporting information for Chapter 5. Synthesis of cationic poly(3-acrylamidopropyl trimethylammonium chloride) by SARA ATRP in ecofriendly solvent mixtures

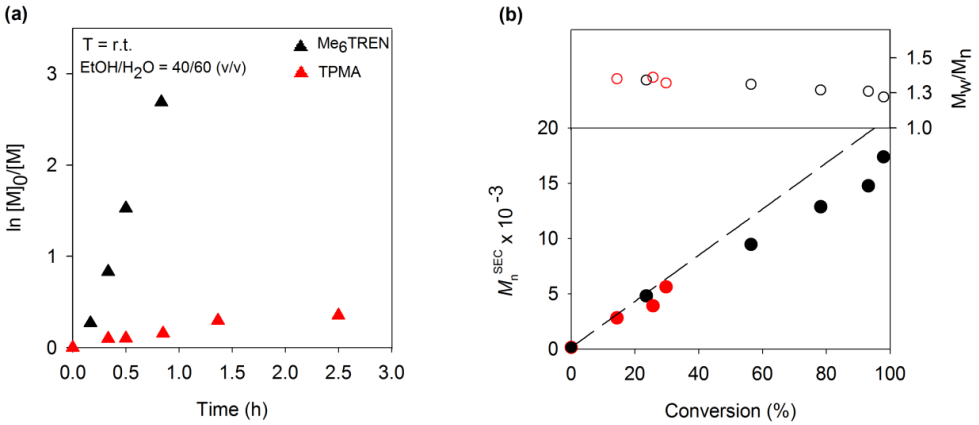

Figure A.1. (a) Kinetic plots of $\ln[M]_0/[M]$ *vs.* time and (b) plot of number–average molecular weights (M_n^{SEC}) and $Đ$ (M_w/M_n) *vs.* monomer conversion (the dashed line represents theoretical molecular weight at a given conversion) for the SARA ATRP of AMPTMA initiated by ECP, using Me_6TREN or TPMA as ligand. Conditions: $[AMPTMA]_0/[ECP]_0/[CuCl_2]_0/[ligand]_0/Cu(0)$ wire = 100/1/0.5/1.0/Cu(0) wire; $[AMPTMA]_0$ = 1.45 M; Cu(0) wire: l = 10 cm; d = 1 mm; $V_{solvent}$ = 5 mL.

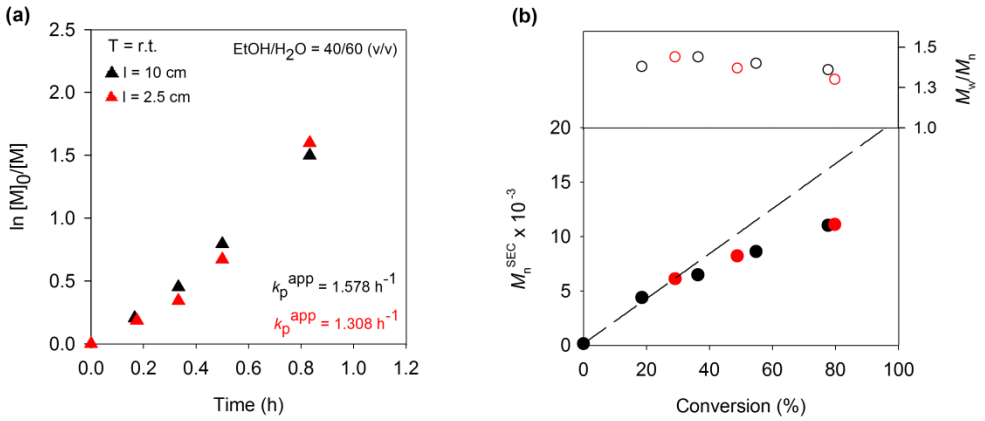

Figure A.2. (a) Kinetic plots of $\ln[M]_0/[M]$ *vs.* time and (b) plot of number–average molecular weights (M_n^{SEC}) and $Đ$ (M_w/M_n) *vs.* monomer conversion (the dashed line represents theoretical molecular weight at a given conversion) for the SARA ATRP of AMPTMA using different lengths of Cu(0) wire. Conditions: $[AMPTMA]_0/[ECP]_0/[CuCl_2]_0/[Me_6TREN]_0$/Cu(0) wire = 100/1/0.3/0.6/Cu(0) wire $[AMPTMA]_0$ = 1.45 M; Cu(0) wire: d = 1 mm; $V_{solvent}$ = 5 mL.

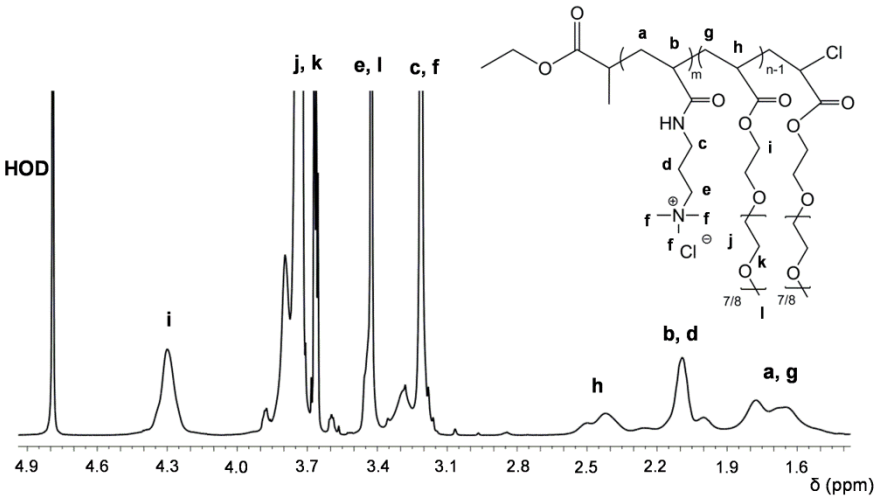

Figure A.3. 500 MHz ^{1}H NMR spectrum of the $PAMPTMA_{24}$-*b*-$POEOA_{39}$, in D_2O, obtained by "one-pot" SARA ATRP in $EtOH/H_2O$ = 50/50 at room temperature. Reaction conditions: first block - $[AMPTMA]_0/[ECP]_0/[CuCl_2]_0/[Me_6TREN]_0$/Cu(0) wire = 25/1/0.5/1.0; Cu(0) wire: l = 5 cm; d = 1 mm; $[AMPTMA]_0$ = 1.45 M; conversion = 97%; $V_{solvent}$ = 1.25 mL; second block - $[OEOA_{480}]_0$ = 0.4 M; $[OEOA]_0/[ECP]_0$ = 50; conversion = 90%.

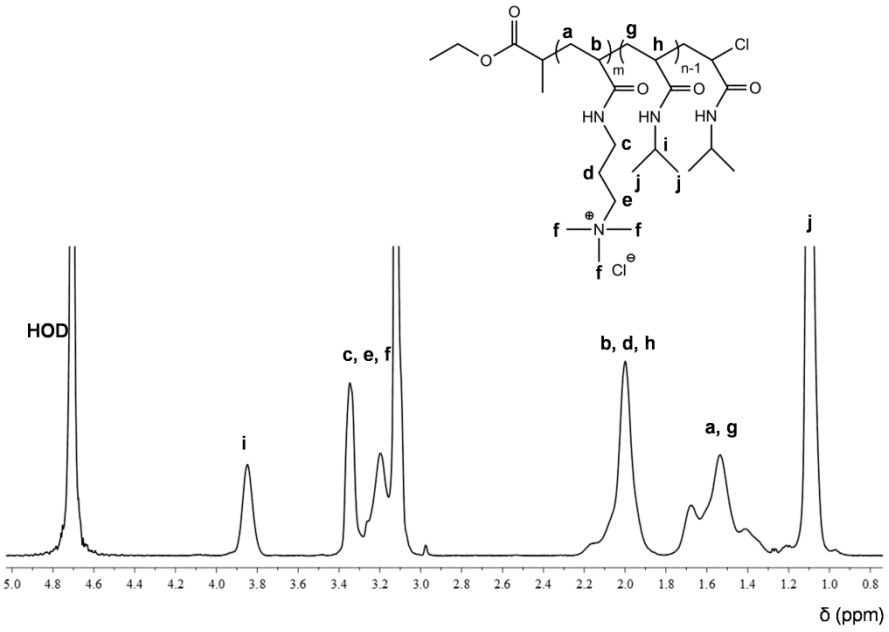

Figure A.4. 500 MHz ^{1}H NMR spectrum of the PAMPTMA$_{50}$-*b*-PNIPAAm$_{61}$, in D_2O, obtained by "one-pot" SARA ATRP in EtOH/H_2O = 50/50 (v/v) at room temperature. Reaction conditions: first block - $[AMPTMA]_0/[ECP]_0/[CuCl_2]_0/[Me_6TREN]_0$/Cu(0) wire = 50/1/0.5/1.0; Cu(0) wire: l = 5 cm; d = 1 mm; $[AMPTMA]_0$ = 1.45 M; conversion = 95%; $V_{solvent}$ = 1.25 mL; T = 25 °C; second block - $[NIPAAm]_0$ = 2 M; $[NIPAAm]_0/[ECP]_0$ = 150; T = 4 °C; conversion = 41%.

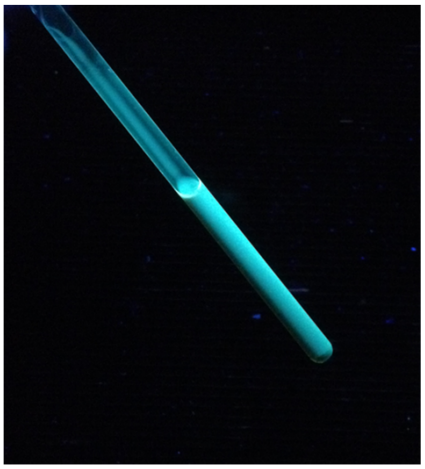

Figure A.5. UV light (λ = 366 nm) irradiated NMR tube containing a solution of fluorescent coumarin-functionalized PAMPTMA in CD_3OD, obtained by a "click" reaction.

Appendix B

Supporting information for Chapter 6. Straightforward ARGET ATRP for the synthesis of primary amine polymethacrylate with improved chain-end functionality under mild reaction conditions

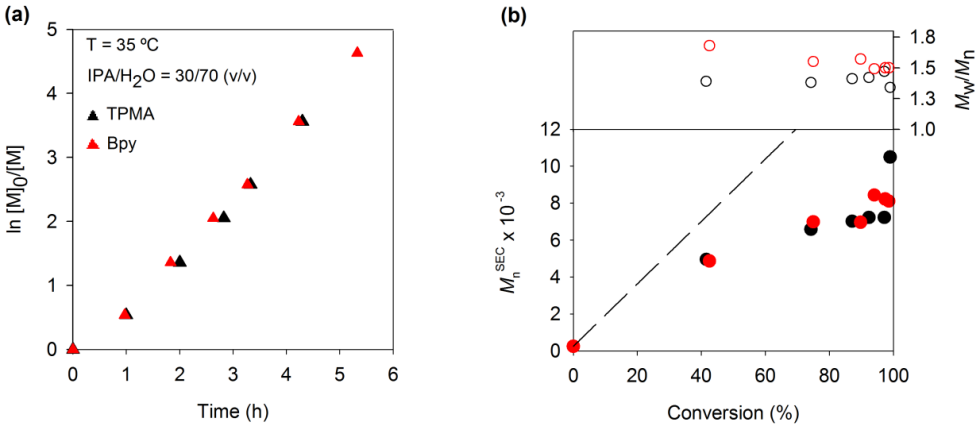

Figure B.1. (a) Kinetic plots of conversion and $\ln[M]_0/[M]$ vs. time and (b) plot of number-average molecular weights (M_n^{SEC}) and $Đ$ (M_w/M_n) *vs.* monomer conversion for the ARGET ATRP of AMA in IPA/H_2O = 30/70 (v/v) at 35 °C, using TPMA (black symbols) or bpy (red symbols) as a ligand. Reaction conditions: $[AMA]_0/[EBPA]_0/[CuBr_2]_0/[ligand]_0$ = 100/1/0.5/2.0; FR_{AscA} = 43 nmol/min; $[AMA]_0$ = 2 M; V_{total} = 1.72 mL.

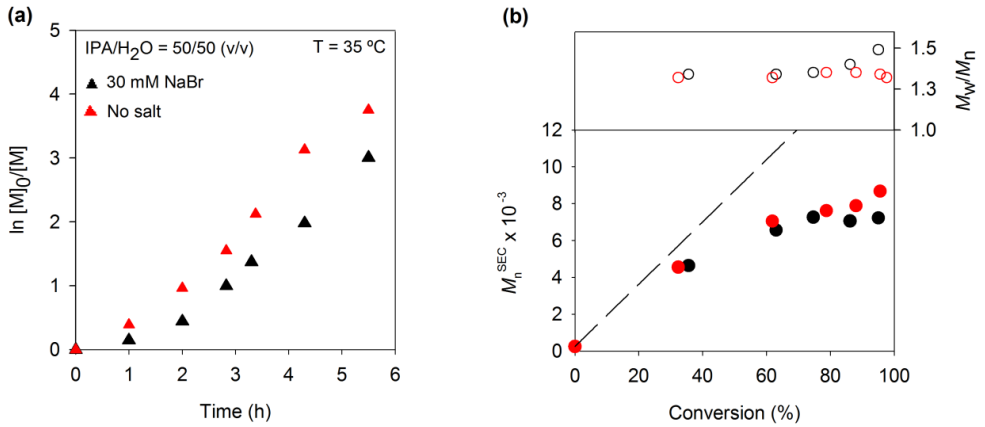

Figure B.2. (a) Kinetic plots of conversion and $\ln[M]_0/[M]$ vs. time and (b) plot of number-average molecular weights (M_n^{SEC}) and $Đ$ (M_w/M_n) *vs.* monomer conversion for the ARGET ATRP of AMA in IPA/H_2O = 50/70 (v/v) at 35 °C, with and without the addition of halide salt (30 mM of NaBr). Reaction conditions: $[AMA]_0/[EBPA]_0/[CuBr_2]_0/[TPMA]_0$ = 100/1/0.5/2.0; FR_{AscA} = 43 nmol/min; $[AMA]_0$ = 2 M; V_{total} = 1.72 mL.

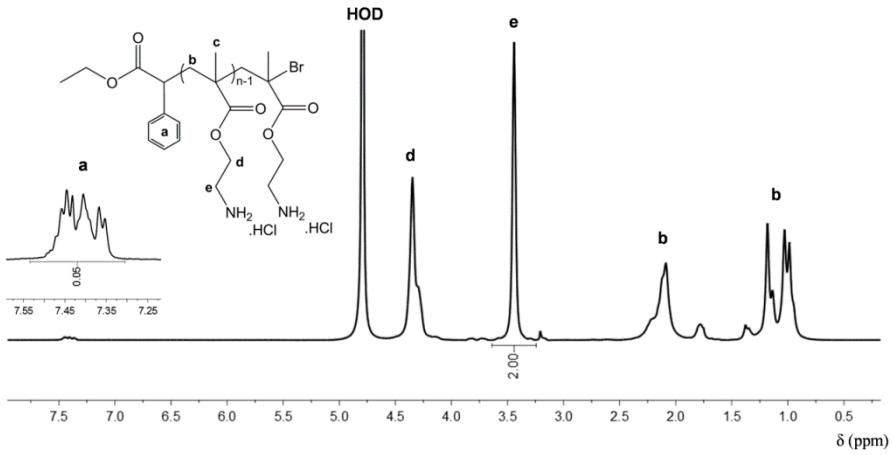

Figure B.3. 400 MHz ^{1}H NMR spectrum, in D_2O, of a purified PAMA sample obtained at 86% of monomer conversion by ARGET ATRP. Reaction conditions: $[AMA]_0/[EBPA]_0/[CuBr_2]_0/[TPMA]_0/[AscA]$ = 100/1/0.5/2.0/10 nmol/min; IPA/H_2O = 30/70 (v/v); T = 35 °C; time = 5.5 h; M_n^{NMR} = 17 x 10^3; M_n^{th} = 15 x 10^3.

The PAMA NMR molecular weight was calculated using the equation M_n^{NMR} = [(I(**e**)/2)/(I(**a**)/5)] x MW_{AMA} + MW_{EBPA} , where I(**e**) is the integral of the PAMA side chain CH_2 protons –CH_2-C**H$_2$**-NH_2 and I(**a**) is the integral of the aromatic ring fragment from the initiator.

Figure B.4. Reaction mixture of the normal ATRP of AMA, at 91% monomer conversion, showing the precipitation of the polymer. Conditions: $[AMA]_0/[EBiB]_0/[CuCl]_0/[bpy]_0$ = 30/1/1/2/; T = 50 °C; $[AMA]_0$ = 2 M; V_{total} = 2 mL

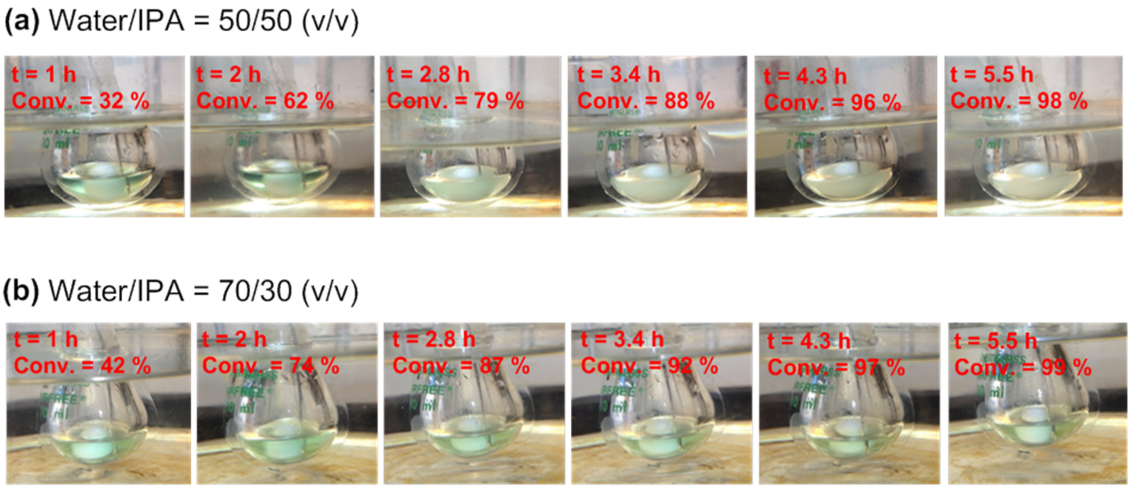

Figure B.5. Pictures of the Schlenk flask during the ARGET ATRP of AMA in (a) IPA/H_2O = 50/50 (v/v) and (b) IPA/H_2O = 30/70 (v/v), showing the differences in the polymer´s solubility. Conditions: $[AMA]_0/[EBPA]_0/[CuBr_2]_0/[TPMA]_0$ = 100/1/0.5/2.0; FR_{AscA} = 43 nmol/min; T = 35 °C; $[AMA]_0$ = 2 M; V_{total} = 1.72 mL.

Appendix C

Supporting information for Chapter 7. Efficient RAFT polymerization of *N*-(3-aminopropyl)methacrylamide hydrochloride using unprotected "clickable" chain transfer agents

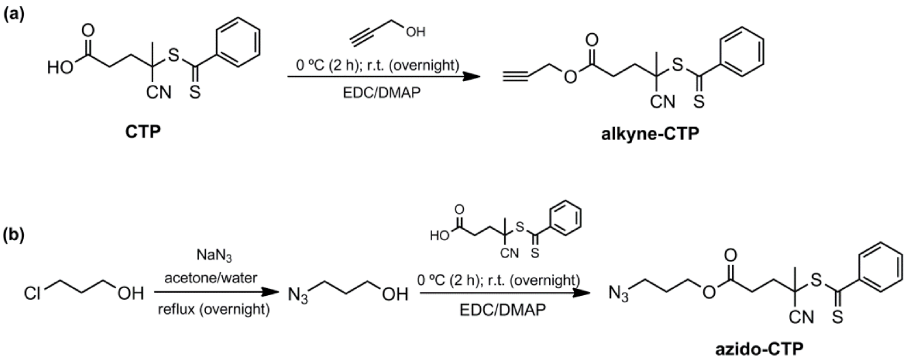

Figure C.1. Synthesis of the (a) alkyne-terminated CTP (alkyne-CTP) and (b) azide-terminated CTP (azido-CTP).

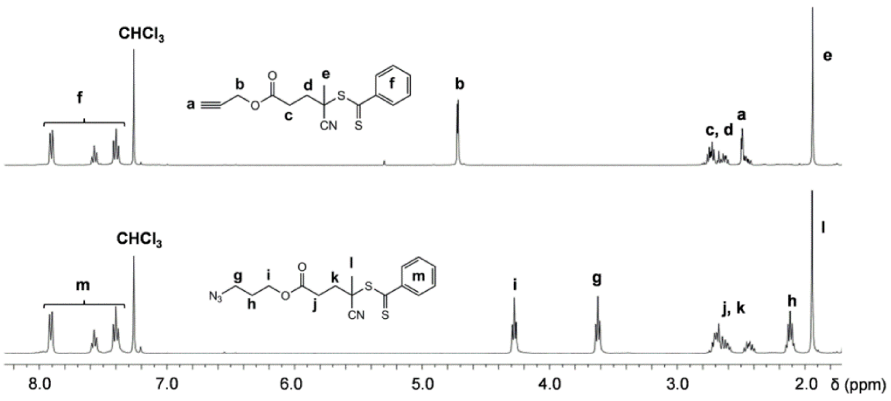

Figure C.2. 500 MHz ^{1}H NMR, in $CDCl_3$, of both alkyne-CTP and azido-CTP.

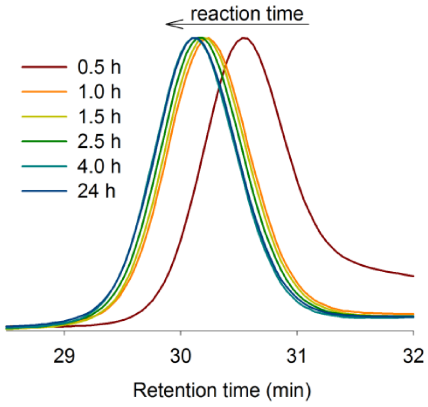

Figure C.3. SEC chromatograms of PAPMA samples during the RAFT polymerization at 70 °C in water:1,4-dioxane = 2/1 (v/v) mixture. Conditions: $[APMA]_0/[CTP]_0/[ACVA]_0$ = 100/1/0.5; $[APMA]_0$= 1.87 M.

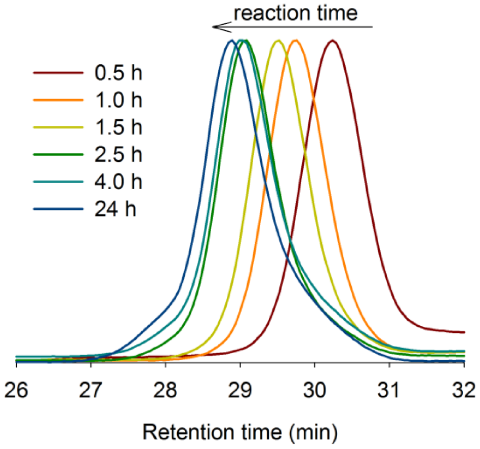

Figure C.4. SEC chromatograms of PAPMA samples during the RAFT polymerization at 70 °C in water:1,4-dioxane = 2/1 (v/v) mixture. Conditions: $[APMA]_0/[alkyne\text{-}CTP]_0/[ACVA]_0$ = 100/1/0.5; $[APMA]_0$= 1.87 M.

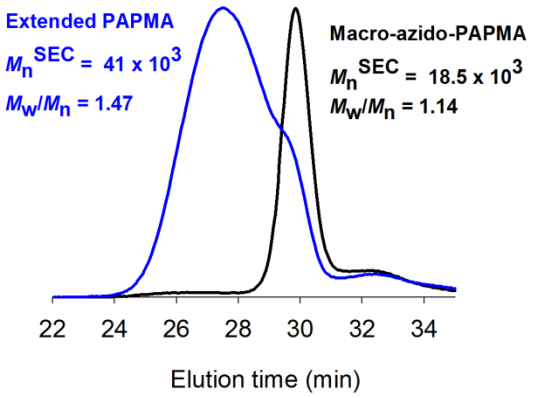

Figure C.5. SEC traces of the macro-PAPMA (azide-terminated) and extended PAPMA obtained in a RAFT polymerization at 70 °C in water:1,4-dioxane = 2/1 (v/v).

Appendix D

Supporting information for Chapter 8. Synthesis of new bile acid sequestrants by supplemental activator and reducing agent atom transfer radical polymerization

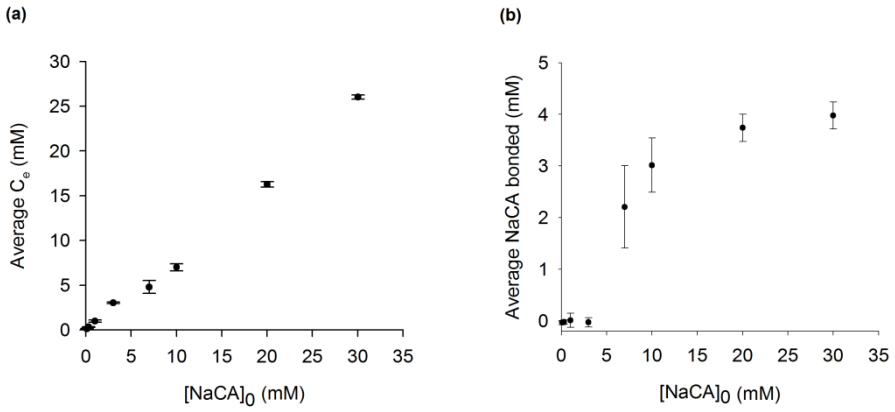

Figure D.1. Error (triplicate samples) in the determination of the binding parameters by HPLC for the cationic hydrogel AB 100/10: (a) concentration of free NaCA concentration in solution (C_e) and (b) concentration of NaCA bonded to the hydrogel.

Table D.1. Binding parameters of the amphiphilic star block copolymers prepared by SARA ATRP and the commercial BAS Colesevelam. The errors presented were obtained from the model fitting using the SigmaPlot software.

Sample code	R^2	K ($L.mg^{-1}$) x 10^4	n	K_0 ($L.mg^{-1}$) x 10^4	q_{max} $(mg/g)^a$ x 10^{-3}
Colesevelam	0.9771	6.0 ± 2.0	1.0	-	2.2 ± 0.24
4(PMA_{95}-*b*-$PAMPTMA_{50}$)	0.9968	4.0 ± 0.1	7.0 ± 0.9	0.6 ± 0.1	1.4 ± 0.03
4(PMA_{94}-*b*-$PAMPTMA_{24}$)	0.9997	3.0 ± 0.1	2.0 ± 0.1	1.5 ± 0.1	1.0 ± 0.02
4(PMA_{94}-*b*-$PAMPTMA_{16}$)	0.9791	5.0 ± 0.6	2.6 ± 0.6	1.9 ± 0.5	0.9 ± 0.07
4(PMA_{199}-*b*-$PAMPTMA_{52}$)	0.9971	7.0 ± 0.3	4.1 ± 0.5	1.7 ± 0.2	0.8 ± 0.02
6(PMA_{98}-*b*-$PAMPTMA_{52}$)	0.9905	5.0 ± 0.3	3.4 ± 0.6	1.5 ± 0.3	1.4 ± 0.08
6(PMA_{106}-*b*-$PAMPTMA_{38}$)	0.9896	4.0 ± 0.2	4.8 ± 1.1	0.8 ± 0.2	1.4 ± 0.05
6(PMA_{104}-*b*-$PAMPTMA_{18}$)	0.9987	4.0 ± 0.3	1.6 ± 0.1	2.5 ± 0.2	0.6 ± 0.02

[a] mg NaCA/g polymer.

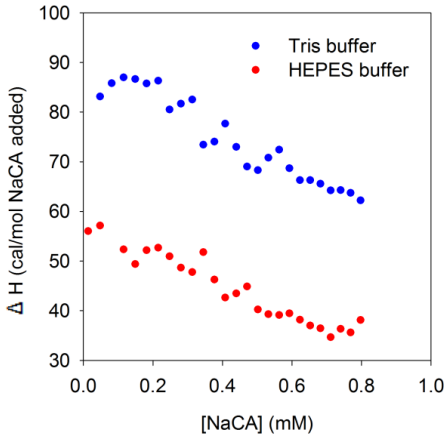

Figure D.2. ITC titration curves obtained at 37 °C for the binding of NaCA by an amphiphilic star block copolymer sample (4(PMA_{95}-*b*-$PAMPTMA_{50}$) in Tris buffer (blue symbols) or HEPES buffer (red symbols). The buffers contained 150 mM of NaCl.

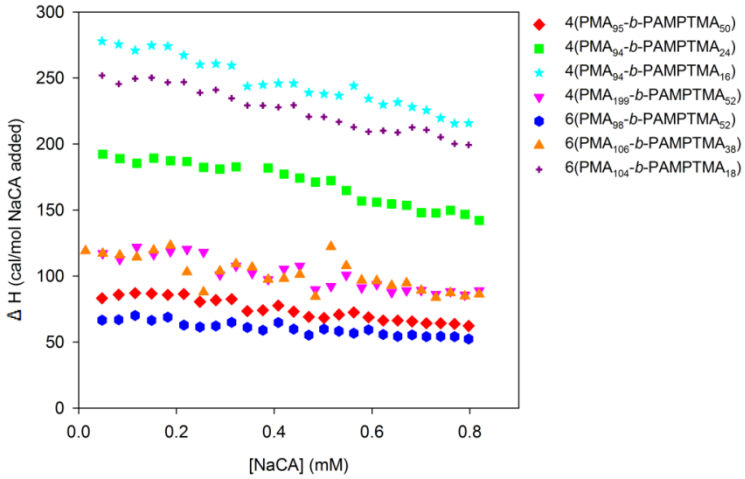

Figure D.3. ITC titration curves obtained at 37 °C for the binding of NaCA by amphiphilic star block copolymers in Tris buffer (with 150 mM of NaCl).

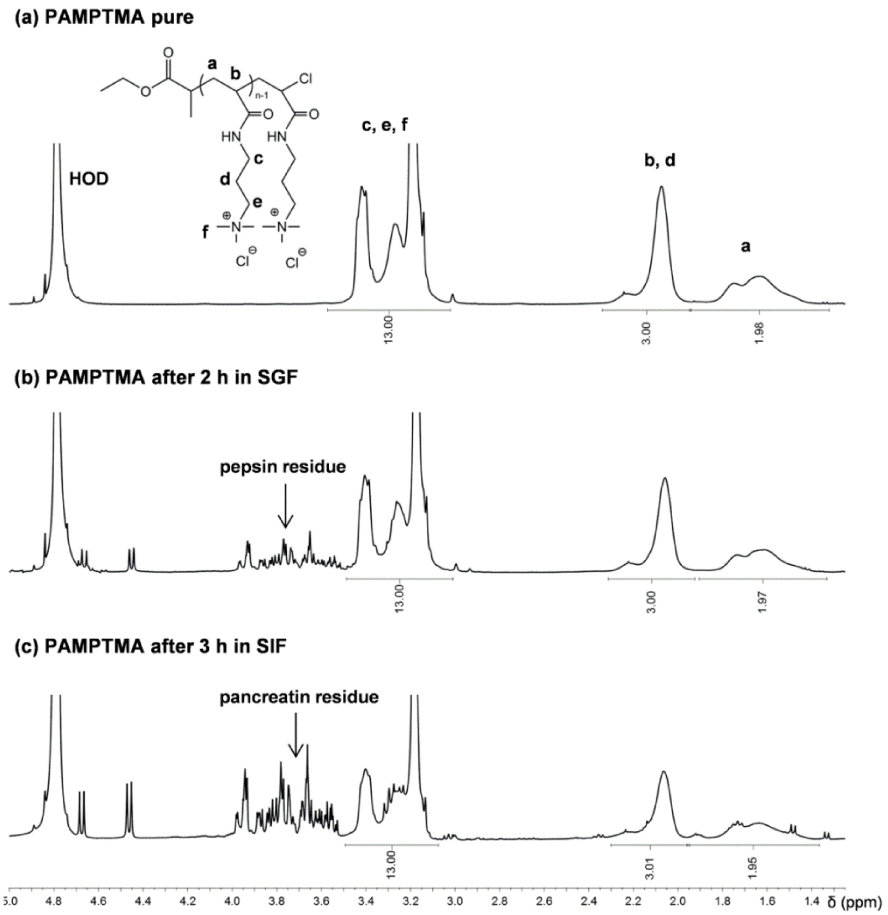

Figure D.4. ^{1}H NMR spectra, in D_2O, of the linear PAMPTMA before and after degradation in SIF or SGF at 37 ºC.

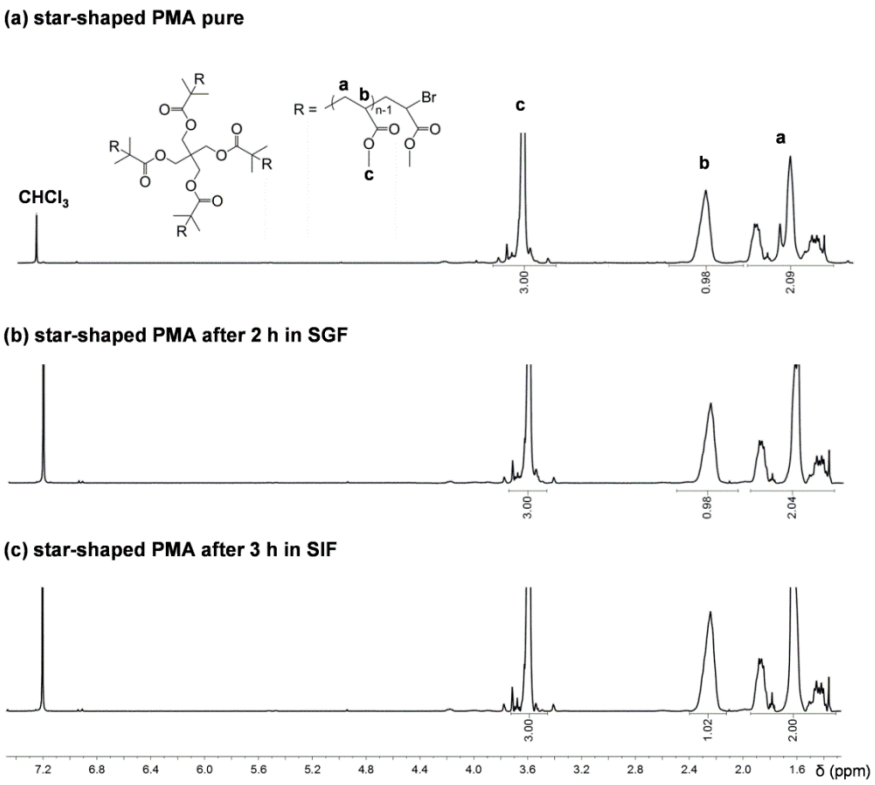

Figure D.5. ^{1}H NMR spectra, in $CDCl_3$, of the star-shaped PMA before and after degradation in SIF or SGF at 37 ºC.